PROCEEDINGS OF THE IRE®

Published Monthly by

The Institute of Radio Engineers, Inc.

VOLUME 44 — *July, 1956* — NUMBER 7

CONTENTS

ADVERTISING SECTION

THE COVER—The marked progress that has been made in the recent past in the miniaturization and automatic assembly of electronic equipment has received much of its impetus from the development of printed circuits. The widespread use of these circuits has brought about the redesign of many standard components for printed circuit applications. A number of such components are pictured on this month's cover. Changes ranging from simple modifications (resistor at top) to completely redesigned components (variable resistor next to bottom) may be found, for example, in the television receiver shown at the bottom.

Photos—*Chicago Telephone Supply Corp.*

Scanning the Issue

International Cooperation in Radio Research—URSI and IRE (Dellinger, p. 866)—At specified times every day a number of radio stations in widely separated countries broadcast extensive data regarding ionospheric, solar, geomagnetic and cosmic-ray conditions, using special five-letter codes. These daily "Ursigrams" are used in many parts of the world by transmitting organizations to aid in the selection of frequencies, times and paths of transmission and by researchers in their studies of radio propagation and of geophysical and cosmic phenomena. This is but one example of the valuable work which the International Scientific Radio Union (URSI) is doing to promote basic research and the exchange of information among radio scientists on an international scale. Another example is the URSI General Assembly, an international meeting of radio scientists which is held every three years or so. The next such meeting will be held in August of next year at Boulder, Colorado, marking the first time in thirty years that the United States has played host to this important conference. Most IRE members are not fully aware of how URSI is organized, what it accomplishes, nor of the close and important ties between URSI and the IRE. They will be interested to learn what the Honorary President of URSI has to say about these matters.

Tantalum Solid Electrolytic Capacitors (McLean and Power, p. 872)—A new type of electrolytic capacitor has been developed which contains no liquids of any kind. Instead of the usual aqueous electrolyte, it uses a solid semiconductor, manganese dioxide, which together with a tantalum anode gives substantial improvements in electrical quality and reliability and opens up important new fields of applications for electrolytic capacitors. Because the materials are all inorganic nonvolatile solids, no hermetic seal is required for ordinary applications. Moreover, this new capacitor has indefinitely long shelf life and much better low-temperature characteristics than previous electrolytics. Perhaps of greatest interest is the extremely small volume required by these capacitors, a factor which will make them of major importance in miniaturized transistor circuits. This development is regarded as the beginning of a completely new class of product which will be of great basic importance to component and circuit design engineers.

Theory of the Transverse-Current Traveling-Wave Tube (Dunn, *et al*, p. 879)—This paper analyzes the operation of a type of traveling-wave tube in which the electron beam approaches the helix at an angle from one side rather than head on. Thus each electron, instead of traveling the full length of the helix, cuts across it and interacts with it for only a small portion of its total length. At the same time, the beam is spread out so that all parts of the helix are crossed by some of the electrons. This arrangement gives, in effect, a system in which elements of the electron beam are continuously entering and leaving the interaction space throughout the entire length of the interaction space. The authors find that this results in three forward growing waves instead of one—one growing exponentially as in a conventional traveling-wave tube, one growing linearly, and one growing as the square of the distance. Although the device behaves much like a conventional traveling-wave tube in many respects, there are a number of differences. Perhaps the most notable of these is the fact that the power output is dependent on the saturation of individual elements of the beam rather than on the beam as a whole. As a result, as the input power is raised and passes the saturation point, the power output curve levels off and remains level instead of dropping off. How well this theoretical analysis is borne out by experiment is reported in the following paper.

An Experimental Transverse-Current Traveling-Wave Tube (Dunn and Harman, p. 888)—In the preceding paper the authors theorized on the behavior of a traveling-wave tube with a transverse electron beam which crosses the helix instead of traveling parallel to its axis. In this paper they describe an experimental tube of this type which they tested both as a forward wave amplifier and as a backward wave oscillator. Their experiments verify the theoretical predictions of the first paper and also yield some additional interesting information on the operating characteristics of this tube. For example, the usual null in the output power versus beam voltage curve, which in conventional traveling-wave tubes is very sharp and occurs only at a particular combination of voltage and current, is found in this tube to be surprisingly flattened out under certain conditions so as to produce a broad range of voltages and currents over which the output power is much lower than the level obtained with the beam turned off. This attenuating action opens up the possibility of building traveling-wave tubes with two beams, one beam for obtaining gain and power in the forward direction and a transverse beam adjusted to this null condition to provide attenuation in the backward direction. Other possible applications of this tube may suggest themselves to the reader. The flat output curve under saturation conditions might indicate that the tube could be used as a limiter, although the phase characteristics would have to be taken into account. The relatively short path of the electron beam suggests that it would be easier to focus. The applications of the tube remain to be explored further. The primary purpose here has been to investigate the operation of a device which is of interest in itself because it is significantly different.

Some Effects of Magnetic Field Strength on Space-Charge-Wave Propagation (Brewer, p. 896)—A general analysis of the propagation of space-charge waves in a magnetically focused electron beam is presented which ties together the different approaches that have been made to this problem in the past and fills in important areas between them. Prior analyses have worked out cases representing either the maximum or minimum extremes in magnetic field intensity for use in focusing an electron beam. This paper treats in one sweep these two limiting cases plus the vast array of physically realizable cases that lie between. Moreover it summarizes a field which has been argued back and forth in regard to many fine points by many workers in the field and includes the proper statements on which all have agreed. In so doing, it makes convenient to all a unified picture of a fundamentally important phenomenon.

Some General Properties of Nonlinear Elements—Part I. General Energy Relations (Manley and Rowe, p. 904)—In this paper the authors set out to investigate some general power relations which govern nonlinear reactor modulators, i.e., modulators whose nonlinear element is an inductor or capacitor, and succeed in deriving two equations of far-reaching significance. These equations make it possible to relate the powers at the different frequencies in a nonlinear element without requiring a knowledge of the detailed shape of the nonlinear characteristic of the element or of the external circuit to which it is connected. This information is very valuable in considering the gain and stability of nonlinear reactor modulators and demodulators, including such devices as magnetic and dielectric amplifiers. For example, it can be shown which sidebands in a nonlinear reactor tend to make the device stable and which tend to make it unstable, and in the latter case in which generator circuit the negative resistance will appear. These and other findings mark this as an important contribution to our understanding of the difficult subject of nonlinear circuits.

A Solution to the Approximation Problem for RC Low-Pass Filters (Su and Dasher, p. 914)—In studying the characteristics of networks it is often very helpful to locate the zeros and poles of the transfer function of the network on a graph drawn in the complex-frequency or s-plane. The zeros and poles represent the roots of the numerator and denominator of the transfer function in terms of the complex frequency s, and hence their positions on the graph reveal a great deal about the behavior of the network. In the case of RC networks the conditions which govern the positions of the poles are such that it is quite difficult to manipulate them and to analyze the transfer function. In this paper the author presents a technique involving elliptic functions which transforms the s-plane into a totally different graphical arrangement especially suited to the study of low-pass RC filters. The effect of this is to change the spatial relationships in such a way that the zeros and poles fall on the graph in a simple symmetrical fashion which is more readily visualized and easier to work with. As a result it is possible to design the passband tolerance, the stopband-passband ratio and the stopband attenuation by adjusting the geometrical dimensions in the transformed plane and the transformation equations. This mapping technique eliminates the painful job of finding the roots of polynomials and provides an interesting and useful method for designing filters.

Feedback Theory—Further Properties of Signal Flow Graphs (Mason, p. 920)—In September, 1953 the author published in the PROCEEDINGS a new and powerful method of circuit analysis which employed what he called "signal flow graphs." These graphs consist of simplified single-line representations of the relationships of the various electrical paths in a circuit. They are extremely helpful in visualizing what goes on in a circuit and greatly simplify the solution of certain circuit problems. The originality and simplicity of these techniques have attracted great interest and consequently the methods appear to be coming into wide use. This paper is a continuation of the 1953 paper. It indicates how one proceeds to evaluate from the flow graph certain characteristics, such as gain, of networks containing feedback loops, adding an important link in the development of flow-graph topology in circuit analysis. It is interesting to note in passing that the next paper in the issue considers network topology of another sort.

Topological Properties of Telecommunication Networks (Prihar, p. 927)—The previous paper presented a method of analyzing the topology of a circuit where our main interest was the input-output relations of a network containing feedback loops. In this paper a different type of network is considered, namely, a telecommunications network, such as a telephone exchange or a radio network. Here we are not concerned with such characteristics as gain or impedance of the network as a whole, but rather with the connectivity between the various points within the network. The author describes a method of matrix analysis previously developed for the study of relationships between social groups and applies it to the problem at hand, producing traffic matrices which make it possible to obtain quantitative indications of the traffic-handling capabilities of the network. For example, in a system comprised of an assortment of one- and two-way communication links, the matrices yield information on the number of stations in the network that are in direct contact and the number that must work through one, two, three, etc., intermediate stations to establish contact. The method presented here is of interest, not because it solves problems that are insoluble by other methods, but because it suggests a new direction of attack on certain practical problems involving the flexibility and economy of communication systems.

IRE Standards on Letter Symbols for Semiconductor Devices (p. 934)—This standard fills an important void in letter symbol standardization for the electronics field by providing a uniform system of identifying electrical quantities and parameters associated with semiconductor devices in much the same way as previous standards have provided symbols for electron tubes. Reprints of this standard may be purchased from IRE headquarters as indicated in the footnote on page 934.

Edward W. Herold

DIRECTOR, 1956–1958

Edward W. Herold was born in New York City on October 15, 1907. He received a B.S. degree in physics from the University of Virginia in 1930 and a M.S. degree from the Polytechnic Institute of Brooklyn in 1942. His start in radio was as an amateur while in high school in Newark, New Jersey. From 1924 to 1926 he was employed as a technical assistant in a picture-transmission research group at the Bell Telephone Laboratories in New York City. In 1927, and during the summers of 1928 and 1929, Mr. Herold worked on electron tubes for E. T. Cunningham, Incorporated. In 1930 he entered the research and development laboratories of the RCA Radiotron Company at Harrison, New Jersey, where he was responsible for the development of many new types of electron tubes, particularly converters, mixers and audio output tubes. In 1938 he transferred to a research group of RCA at Harrison, where he specialized in vhf and uhf problems, particularly fluctuation noise phenomena and signal-to-noise ratio.

After the formation of the RCA Laboratories Division in 1942, Mr. Herold moved with it to its present location at Princeton, New Jersey. During World War II, his work was again concerned with signal-to-noise ratio problems and research on beam-deflection tubes for superheterodyne mixing. From 1946 on, he became concerned with a broad variety of tube problems, among which was the coordination of RCA's work on color kinescopes during 1949–1950. He is now Director of the Electronic Research Laboratory which does research on electron tubes and semiconductor devices.

Mr. Herold is a member of Phi Beta Kappa and Sigma Xi. He is the author of many technical papers, a contributor to the Encyclopaedia Britannica, and holder of approximately forty patents.

Mr. Herold was Chairman of the Papers Committee for the 1945 Winter Technical Meeting of the IRE, and was one of the organizers of the Princeton Subsection of the IRE, which later became the Princeton Section. He was Vice-Chairman of the Princeton Section in 1948 and Chairman in 1949. He served on the Board of Editors between 1946 and 1953, on the Editorial Administrative Committee from 1946 to 1951, on the Membership Committee in 1942, and is now on the Editorial Board. He is a Fellow of the IRE.

Poles and Zeros

Special. Since 1951 it has been our custom to publish, twice or three times a year, issues of the PROCEEDINGS having a dominant technical theme. Two of these "special issues" have centered on color television, one each on transistors, ultra-high-frequency techniques, computers, scatter propagation, and the physics of the solid state. Last month's issue, while not completely given over to a single subject, was nevertheless heavily committed to the techniques of launching and observing artificial satellites. Ahead of us are five more one-subject issues, with plans for publication through the latter part of 1957, on such widely diverse subjects as ferrites, radio astronomy, single-sideband techniques, medical electronics, and the International Geophysical Year.

Plans for such single-minded publications have to be worked out with moderation, since those members who have an active disinterest in, say, radio astronomy will find the issue devoted to that subject almost a total loss. So the objective at present is to locate each year at least two, but not more than four, subjects calculated to hit home with a large fraction of the IRE readership.

The response to the special issues published to date has been uniformly favorable. As always in the editorial world, the indication of approval or disapproval comes from a distressingly small sample and hence is quite possibly misleading. But the almost complete lack of objection to the idea has encouraged the Editorial Board to proceed with a substantial special-issue program. Such issues are particularly convenient for reference to the subject they cover, since they bring together in one place at least one general review and a variety of specific treatments of the latest advances in a particular art. The special issue on transistors is, as a result of heavy reference demand, the only 1952 issue now out of stock.

Putting a special issue together is no cinch. The two essentials are an organization to provide the material and an individual to coordinate the project and arrange the papers in a coherent whole. Among the organizations supplying the drive are the IRE Professional Groups and such industry committees as NTSC and JTAC. One interesting example is the forthcoming issue on single-sideband transmission methods. This arose as a result of a JTAC study, initiated at the request of the FCC, of single-sideband as a technique of spectrum economy. Something like twenty different aspects of this subject have thus far turned up in as many papers, which goes to show that there's plenty of life in the radio business. Another example is the group of papers on the satellite program printed here last month. The Professional Group on Military Electronics, a new group thus far without a TRANSACTIONS of its own, put a lot of steam into that special-issue project and thus served the whole membership with vigor beyond reasonable expectations.

Special issues, it must be remembered, *are* special in the sense that they interrupt the planned course of balanced publication described here last month. But within moderate limits, two or three a year, they seem entirely justified.

We would like to base our judgment in this area on a larger sample of our readers. So, let us know if past special issues have hit the mark, if you would welcome others and, if so, on what subjects.

Policy. Two actions recently taken by the IRE Board of Directors are worthy of special attention by the membership at large. The first reflects the conviction that the grade of Fellow should be bestowed only when the candidate has shown active interest in IRE affairs for some time prior to his candidacy. Accordingly, the Bylaws are currently being amended to provide that nominations of United States residents for Fellow will be considered only if the nominee has attained the grade of Senior Member and has held membership in the Institute, in the Senior Member or some lower grade, for at least five years. Since election to Fellow is an honor to which all members aspire, this change puts new force behind upgrading of membership. Every member who has ambitions in respect to the Fellow grade, either to achieve it himself or to nominate a colleague, should now be on notice that upgrading to Senior Member is a necessary preliminary. The effective date of the change will be set by the Board at its August meeting.

The second action relates to the stability of the IRE as represented in its monetary reserves. The Auditor's Report for 1955 reveals that the IRE has an earned surplus of approximately one million dollars. This sounds like a lot of money to the individual member but, on a dollars-per-member basis, it's not as encouraging as it sounds. Our membership is currently over 49,000 strong, and by the time this appears in print it may well have passed 50,000. The reserve represents roughly \$20 per member, whereas the cost of operating the Institute is now about \$40 per member per year, so the reserve would cover only six months' operations.

We have a well-filled sock, but it won't go far if we are called on to maintain our present services under conditions less favorable to the electronics industry than those provided by the present government-supported boom. So the Board took the prudent step of directing the Treasurer and his staff to continue accumulation of earned surplus (not counting real estate) until a sum sufficient for one year's operation is reached. This policy is not merely prudent; it also acknowledges past growth and anticipates a continued upward trend.—D.G.F.

International Cooperation in Radio Research—URSI and IRE*

J. H. DELLINGER†, FELLOW, IRE

On August 22, 1957, the XIIth General Assembly of URSI will convene for a two week meeting in Boulder, Colorado, marking the first time in thirty years that the United States has played host to this scientific event. The following article presents a timely description of the activities of this important international body and their relation to IRE.

—*The Editor*

Summary—**After an introductory account of how the URSI and IRE began, almost simultaneously, in their respective fields of science and engineering, the paper describes how URSI functions. The system of National Committees is described and in particular the USA National Committee. Examples of URSI accomplishments are given. URSI-CCIR relations and URSI-IRE relations are explained. Future prospects are discussed.**

Introduction

INTERNATIONAL cooperation has been a large factor in the extraordinary development of radio. "Extraordinary" is not too strong a word for the process which led from the faint letter S transmitted across the Atlantic by Marconi, to the multibillion-dollar radio and electronics industries of today, all within the lifetime of many of us. Nor is the word "international" out of place, even for that very moment of birth of radio achievement in 1901. For Italy, England, Canada, and the USA were involved in that historic experiment. We shall see how international cooperation has played a role in progress ever since. This cooperation, moreover, has been a significant ingredient in that process of building trust and friendship between nations which the world so seriously needs.

This account will deal mainly with the URSI (International Scientific Radio Union) since its field is essentially science and research. The IRE (Institute of Radio Engineers) deals primarily with engineering and development but it has always kept close to their roots in science, and has had a beneficial relationship with the URSI.

We shall look at the purpose, mode of working, and accomplishments of the URSI, and also at the interrelated activities of the IRE and URSI. We shall also bring into the picture the CCIR (International Radio Consultative Committee), a body having the duty of implementing the findings of research and of engineering and thus substantially aided by the URSI and IRE.

From the beginning of radio it was apparent that progress depended upon large-scale research and development, both in respect to the association of many men for its accomplishment and in the use of great areas for experimentation. By 1912 this led to actions by men of distinction and foresight, both in America and in Europe, to set up organizations for these purposes. In the USA the IRE was established in that year, by consolidation of two small groups, Wireless Institute and Society of Wireless Telegraph Engineers; the leaders in this were Dr. Alfred N. Goldsmith, John V. L. Hogan, and Robert H. Marriott; the latter became the first President. In Europe in the same year a group of scientists began the establishment of what they called the International Commission of Scientific Wireless Telegraphy, abbreviated TSFS (from the French, Télégraphie Sans Fil Scientifique); the leaders were Dr. Robert B. Goldschmidt of Belgium, Col. (later Général) Gustave Ferrié and Prof. Henri Abraham of France, Dr. William Duddell of England, and Professor Vanni of Italy. The organization had not begun to function when World War I intervened but after the end of the war, in 1919, this group reorganized as the URSI, called at first the International Union of Scientific Radio Telegraphy. It was organized, as were similar Unions in other sciences (astronomy, geophysics, chemistry, etc.), under the auspices of the International Research Council (which later became the International Council of Scientific Unions).

The first president of the URSI was General Gustave Ferrié and the first Secretary General was Dr. Robert B. Goldschmidt. The principal backer of the Union in its early years, spiritually and financially, was Dr. Goldschmidt. He established the secretariat in his own office; it has remained in Brussels ever since and its accounts are rendered in Belgian francs. This gives the organization the appearance of substantial wealth, as the value of the Belgian franc is two American cents. Since the early period of financing by one dedicated individual, the Union (like the others) has been financed by official contributions assessed against the participating governments. Since the time of Dr. Goldschmidt, the office of Secretary General has been held by Dr. M. Philippson, Professor A. Dorsimont, and Col. E. Herbays, all Belgians. The present incumbent, Col.

* Original manuscript received by the IRE, February 2, 1956. Address given at WESCON August 25, 1955, San Francisco, Calif.

† Honorary President, URSI; Radio Consultant, Washington, D. C.

Herbays, is, as Dr. Goldschmidt was, a devoted, wise, and efficient officer.

The presidents of the URSI have been:

Gen. G. Ferrié (France), 1919–1932
Dr. L. W. Austin (USA), 1932
Prof. A. E. Kennelly (USA), 1932–1934
Dr. E. V. Appleton (England), 1934–1952
Dr. P. Lejay (France), 1952–to date

How URSI Functions

The aims of the URSI are: 1) to promote international cooperation in the scientific study of radio, 2) to encourage and aid in the organization of radio researches requiring cooperation on a large scale, 3) to promote the establishment and use of common methods and standards of radio measurement, 4) to encourage and aid in the discussion and dissemination of the results of these activities.

These objectives are pursued on both the international and the national levels. Internationally, the Union holds meetings, called General Assemblies, usually at three-year intervals. These last about two weeks, are attended by about 300 people, and are devoted principally to papers and symposiums in which the latest developments in radio science are reviewed. Committees consider various fields of research and recommendations are made on future projects. The General Assemblies are very stimulating to those so fortunate as to attend. Not only do the participants get a birdseye view of world activity in their specialties; but also the unique opportunity to promote personal acquaintance with those of like interest in other countries helps greatly in subsequent collaboration across national borderlines.

The General Assemblies of the URSI have been:

First —Brussels, Belgium; 1922
Second —Washington, D.C. USA; 1927
Third —Brussels, Belgium; 1928
Fourth —Copenhagen, Denmark; 1931
Fifth —London, England; 1934
Sixth —Venice, Italy; 1938
Seventh —Paris, France; 1946
Eighth —Stockholm, Sweden; 1948
Ninth —Zurich, Switzerland; 1950
Tenth —Sydney, Australia; 1952
Eleventh—The Hague, Netherlands; 1954

The USA had 51 delegates in attendance at the Eleventh General Assembly. The Twelfth General Assembly is to be in Boulder, Colo., in 1957.

The URSI also has permanent bodies, called Commissions, conducting continuous studies of the major fields of radio research. At the inception of URSI, in 1919, the Commissions were:

I. Radio Measurements and Standards
II. Radio Wave Propagation
III. Radio Atmospherics
IV. Cooperation with Radio Amateurs

These have been altered from time to time and are at present:

I. Radio Measurements and Standards
II. Tropospheric Radio Propagation
III. Ionospheric Radio Propagation
IV. Radio Noise of Terrestrial Origin
V. Radio Astronomy
VI. Radio Waves and Circuits
VII. Radio Electronics

The Commissions function through correspondence and the holding of symposiums and discussion and planning sessions at the General Assemblies. All of their activities reinforce the personal contacts at General Assemblies in the fructification of research and the accomplishment of mutual objectives in international projects. Examples of the latter are described below.

The URSI is financed by assessments paid by the governments of the member nations and by grants from UNESCO. The annual assessment paid by the United States is about $700. A paid secretariat of two people is maintained in Brussels, Belgium. Other expenses are for correspondence with the Commissions and National Committees and for the publications. The costs of the General Assemblies are paid, not by URSI, but by the National Committee of the country acting as host.

The National Committees

The national branches of the URSI constitute its third mode of working, the first two being the triennial General Assemblies and the international Commissions for the seven technical fields. The following 24 countries have national sections of the URSI, so-called "National Committees": Australia, Belgium, Canada, Czechoslovakia, Denmark, Finland, France, Germany, Great Britain, India, Italy, Japan, Morocco, Netherlands, New Zealand, Norway, Poland, Portugal, Spain, Sweden, Switzerland, Union of South Africa, United States of America, and Yugoslavia. The National Committees usually comprise from 10 to 30 people, who in many cases are a sort of Executive Committee for administering the activities of a much larger group engaged in promoting the technical objectives of the URSI in their country. These activities, nationally, include the holding of national meetings for the discussion and promotion of radio science, the operation of technical groups called Commissions similar to the international ones, and the handling of the national phases of URSI business such as the designation of national delegates to the triennial General Assemblies.

The National Committees are formed under the authority of each country's National Research Council or some similar body having governmental status. Through that body the financial support for the URSI is obtained from governmental sources. That body in each country formally appoints or approves the membership and the procedures of that country's National Committee.

THE USA NATIONAL COMMITTEE

The USA was the first to form a National Committee of the URSI. A plan of organization for the URSI was established in 1919 at Brussels but it did not have its first meeting until 1922. In 1920 the eminent French General, Ferrié, who became the first president of URSI, was visiting in Washington. To a small group at the National Research Council he explained how the URSI had been set up and how he had tried, without success as yet, to get National Committees organized in France and in England, although those countries had had National Committees under the old TSFS. The 8 persons at this meeting included Dr. L. W. Austin, great pioneer in radio wave propagation, General G. O. Squier, the first USA Chief Signal Officer, and Prof. A. E. Kennelly, the scientist who first envisioned the stratified ionosphere and explained long-distance propagation thereby. Three months later, on January 19, 1921, an organization meeting was held and the "American Section" of the URSI began. A constitution was adopted, which largely survives today, and technical Commissions were established on radio propagation, "static," physics of the electron tube, and radio interference. The first three continue to the present and the fourth has been replaced by others. The name was later changed from "American Section" to "USA National Committee" for uniformity with other countries.

The USA National Committee has 37 members. These include a number of representatives designated by various USA organizations, as follows: One representative each from the Institute of Radio Engineers, USA Department of Commerce, Federal Communications Commission, Division of Physical Sciences of the National Research Council; two representatives each from the Office of the Secretary of Defense, the Army, the Navy, the Air Force; officers and Commission chairmen of the URSI resident in the USA; the chairmen of the USA Commissions; the officers and junior past chairman; and 12 members-at-large. Three members-at-large are elected each year for four-year terms. The USA National Committee meets twice a year for planning the public technical meetings which it sponsors, for election of Commission members and officers, and for arranging for delegates, papers, resolutions, etc. for the international General Assemblies.

The USA Commissions are the counterparts of the international ones except that VI, Radio Waves and Circuits, is extended in the USA to two Commissions: 6A, Antennas and Waveguides, and 6B, Radio Waves and Circuits including General Theory. The chairman of each USA Commission is the Official Member from this country on the corresponding international Commission. USA Commission 1 has 14 members; Commission 2, 30; Commission 3, 46; Commission 4, 15; Commission 5, 33; Commission 6A, 21; Commission 6B, 15, and Commission 7 has 4 members. These Commissions plan for papers and symposiums at meetings held in the USA and at the international General Assemblies; they also prepare reports on the status of research in their fields and prepare resolutions on topics calling for action at the General Assemblies.

Technical meetings for the reading of papers are held by the USA National Committee, usually twice annually, in cooperation with the IRE. These began in 1926; they are attended by some 300 to 600 people. They are usually in Washington, D.C., but have been held also in Ithaca, N. Y.; Ottawa, Canada; San Diego, Calif.; Gainesville, Fla., and a future one is planned for Berkeley, Calif. These meetings are the principal USA meetings on the more scientific aspects of radio. They are a valuable aid to coordination of USA research effort, an effective opportunity for radio scientists to increase their acquaintance with one another's personalities as well as work, and also a main source of technical ideas and contributions for the international General Assemblies.

USA participation in URSI has always been vigorous. It has initiated a number of the valuable international activities. One of the early ones in which American leadership played a prominent part was the "Ursigrams," coded daily bulletins of geomagnetic, ionospheric, and cosmic data broadcast by radio. The system of Ursigrams was evolved through steps taken by the French and American National Committees, especially by General Ferrié and Professor Kennelly. The beginning was a service of plain-language daily bulletins of geophysical and solar data from the Eiffel Tower in Paris, starting Dec. 1, 1928. Then came coded daily bulletins from high-power stations of the U.S. Navy, starting Aug. 1, 1930. These were called Ursigrams and, through the use of special five-digit codes, compressed a large amount of information into a short message. Later, English, Philippine, and Japanese stations were added to the American and French stations to make the dissemination more nearly worldwide. Observing stations of many organizations provided data. In the USA the National Bureau of Standards and Science Service collaborated in the collection and forwarding of data. The purpose of the Ursigrams was to place useful data in the hands of radio transmitting organizations soon enough to aid in the selection of frequencies, times, and paths of transmission, and also to make widely available collections of data to research students of radio propagation and of geophysical and cosmic phenomena.

The Ursigram service continues to the present. The data broadcast include ionospheric (critical frequencies, sudden disturbances, radio noise enhancements), solar (flares, corona, sunspots, radio noise), geomagnetic, and cosmic-ray data. They are transmitted daily at specified times from radio stations in France, Germany, Japan, and India. Most are by radio telegraph, a few by radio telephone. As the data are broadcast in special five-letter codes, there is no difficulty over language in the various countries. The warnings of radio disturbance conditions broadcast every day by the National Bureau of Standards are based, in part, on data utilizing the Ursigrams. Similar use of them is made in other countries.

Some URSI Accomplishments

Beyond all comparison, the great accomplishments of this international body are two: 1) the interchange of information and ideas among the scientists of the world, richly fertilizing the growth of radio everywhere, and 2) the concomitant building of the habit of consultation and cooperation among men of different nations, the indispensable and well-nigh the only real basis of permanent international peace. The interchange of ideas among the scientists of different countries is extremely stimulating and fruitful. Many of the new developments in radio circuits and theory and electronics, thus disseminated, lead directly to improved devices and methods in radio communication and electronic techniques.

However, a few examples may be mentioned of the many specific projects evolved and carried on by the URSI or under its auspices. One such is the Ursigrams, already mentioned. Another, which also had its origin in the USA National Committee, is the Third International Geophysical Year of 1957–58. The word "Third" is interesting. The First International Polar Year, for intensification of geophysical research in polar regions, occurred in 1882–83, the Second in 1932–33 (50 years later). The URSI was active in the planning and the conduct of the Second Polar Year. In 1950, USA members of URSI evolved the idea that 25 years, rather than 50, would be a suitable interval nowadays, and also that such an undertaking should be worldwide and not limited to polar regions (hence the name should be "Geophysical"). They submitted these ideas to the international Joint Commission on the Ionosphere. Then the URSI at its 1950 General Assembly endorsed the idea and in 1951 the International Council of Scientific Unions appointed an international committee to make a go of it. The potency of the 1957-58 project is somewhat indicated by the fact that for the USA share of the work Congress has already appropriated $12,000,000 and the President has requested a supplemental $28,000,000 this year (1956). By contrast, in 1932 the USA National Committee donated its treasury balance, $118.07, for use in the Second Polar Year. The stepped-up program all over the world, with emphasis in polar regions, will include work on aurora and airglow, cosmic rays, geomagnetism, glaciology, ionospheric physics, meterology, seismology and gravity, solar activity, latitude and longitude, oceanography, and rocket exploration of the upper atmosphere.

A "Joint Commission" has just been mentioned. This is another of the mechanisms by which the International Scientific Unions accomplish their purposes. Where a subject overlaps the domain of two or more Unions, a Joint Commission is set up to carry on the necessary studies. Thus, the URSI and International Geophysical Union together have a Joint Commission on Radio-Meteorology. These two, plus the International Unions of Astronomy and of Physics, have a Joint Commission on the Ionosphere. The International Unions of Astronomy and of Geophysics and the URSI have one on Solar and Terrestrial Relationships. The Joint Commissions, with appointed members from each Union, meet usually just before a General Assembly of one of the Unions. They produce research plans, resolutions, and publications describing the status of research in their fields. A good example of the latter is the series of reports summarizing the current results of research on solar and terrestrial relationships put out by the Joint Commission on that subject; these reports clarify existing knowledge and aid the planning of future research on the effects of solar events upon our radio, geomagnetic, meteorological, and other domains. Examples of accomplishment by the Joint Commission on the Ionosphere are its survey and coordination of the ionosphere observing stations throughout the world, and its recommendations of specific types of ionospheric measurements to be made during the IGY (International Geophysical Year) of 1957–58.

The URSI is the principal body which promotes and coordinates systematic observations of ionosphere characteristics and predictions and warnings of radio transmission conditions based thereon. The practical value of the radio predictions services is, of itself alone, more than justification for all the effort and substance expended upon the URSI.

Before the advent of radio, the determination of longitudes depended upon the stability of clocks carried from one place to another. The advent of radio time signals permitted a great advance in the accuracy of longitude determined by simultaneous astronomical measurements. International measurement programs to realize these possibilities have been organized by the URSI; the first was in 1933, the next will be in the IGY of 1957-58. Extensive worldwide measurements will be made of the propagation time of time signals from transmitters in a number of countries.

One of the most striking developments of science in the past ten years has been the emergence of radio astronomy. Stars, the sun, and other heavenly sources emit radiations at radio as well as optical frequencies. Techniques have been developed to detect and measure their intensity and whole new chapters of astronomical knowledge are opening up. Many things are being revealed to which optical telescopes are blind. Some astronomers consider that new knowledge is now coming faster from radio telescopes than from optical telescopes. The URSI established a Commission to study radio astronomy in 1948. Its activities and the symposiums at the General Assemblies have been a major guiding and coordinating force in this rapidly moving field. The most advantageous location of observatories is aided by the URSI studies and the URSI has established a program of observation by these stations to assure coverage at all times.

The studies of longitude, ionosphere characteristics, and radio astronomy are examples of the special adaptability of radio to large-scale international collaboration. Where the whole world must be used as the laboratory, an international body such as the URSI has a significant role. This is one of the most vigorous of the International Scientific Unions.

The URSI has been particularly active in originating and supporting programs for observations during solar eclipses. It was not uncommon for eclipse expeditions in the old days to return empty-handed because clouds prevented seeing the eclipse. Radio observations are not affected by clouds. Eclipses give unique information about the ionosphere, because of the very rapid changes of ionization as compared with the slow change of day to night. They also give information about the location of radiating sources on the sun's disk, because radio telescopes are precise enough to detect the changes in radiation as successive radiating spots on the sun's disk are covered and uncovered. Much is being learned about the sun's corona from the eclipse radio studies.

While there has been much imaginative talk about earth satellites, there was, prior to President Eisenhower's announcement of July 29, 1955, little indication that serious work on such a thing was imminent. It is worthy of note that, at its General Assembly in August 1954, the URSI adopted the following resolution in connection with its planning for upper-atmosphere observations during the IGY: "URSI therefore draws attention to the fact that an extension of present isolated rocket observations by means of instrument earth satellite vehicles would allow the continuous monitoring of solar ultraviolet and X-radiation intensity and its effects on the ionosphere, particularly during solar flares, thereby greatly enhancing our scientific knowledge of the outer atmosphere."

The URSI promotes understanding and information through its publications. These include the *Proceedings of the General Assemblies*, a bimonthly printed Information Bulletin issued by the secretariat in Brussels, and Special Reports. The latter are surveys of the findings and status of particular fields. Ones issued in recent years include: "Solar and Galactic Radio Noise," "Tidal Phenomena in the Ionosphere," "Discrete Sources of Extra-Terrestrial Noise," "The Distribution of Radio Brightness on the Solar Disk," and "Interstellar Hydrogen." Others are in preparation on such subjects as radio propagation beyond and within the horizon, world distribution of ionosphere storms, radio detection of meteors, etc.

URSI–CCIR Relations

The CCIR (International Radio Consultative Committee) is an official body, one of the agencies of the ITU (International Telecommunication Union). To it are referred for solution the more technical radio problems arising in the various international conferences and other activities of the ITU, especially those affecting the allocation of the radio frequencies. It works through triennial Plenary Assemblies and through 14 international Study Groups working continuously, principally by correspondence. The fields of these Study Groups are: Radio Transmitters, Radio Receivers, Complete Radio Systems, Ground-Wave Propagation, Tropospheric Propagation, Ionospheric Propagation, Radio Time Signals and Standard Frequencies, International Monitoring, General Technical Questions, Broadcasting, Television, Tropical Broadcasting, Operating Questions, and Vocabulary.

As both are international radio organizations, it has often been asked whether they might be combined in some way. A proposal to designate URSI as the scientific branch of CCIR was considered by URSI in 1930 and rejected. URSI operates more appropriately as one of the family of International Scientific Unions, and it would perhaps not be advantageous to CCIR to segregate all its scientific problems in one group. Instead, a satisfactory mutual relation has developed. Each organization is represented by delegates in meetings of the other. The CCIR refers to URSI, for consideration and proposals, the more scientific aspects of the topics on which it works. The URSI includes these questions in its program and makes comments on them for the CCIR from time to time.

The topics referred to the URSI by various Study Groups (SG) of the CCIR at its London 1953 Plenary Assembly, on which the URSI supplied comments to the CCIR were as follows:

Studied by URSI Commission Radio Measurements and Standards

Recommendation 122. (SG VII). Standard frequency transmissions and time signals.

Studied by URSI Commission on Tropospheric Radio Propagation

Question 85. (SG V). Propagation data required for wide-band radio systems.

Study Program 56. (SG V). Tropospheric wave propagation.

Studied by URSI Commission on Ionospheric Radio Propagation

Recommendation 59. (SG VI). Exchange of information for short-term forecasts and ionospheric disturbance warnings.

Recommendation 115. (SG VI). Absorption in the ionosphere.

Resolution 12. (SG VI). Usage and meaning of MUF.

Resolution 14. (SG VI). Investigation of circularly polarized emitted waves propagated via the ionosphere.

Study Program 58. (SG VI). Choice of a basic solar index for ionospheric propagation.
Study Program 59. (SG VI). Identification of precursors indicative of short-term variations of ionospheric conditions.
Study Program 60. (SG VI). Basic prediction information for ionospheric propagation.
Study Program 63. (SG VI). Radio propagation at frequencies below 1,500 kc.
Study Program 66. (SG VI). Study of fading.
Study Program 67. (SG VI). Pulse transmission tests at oblique incidence.

Studied by URSI Commission on Terrestrial Atmospheric Radio Noise of Terrestrial Origin

Recommendation 120. (SG VI). Revision of atmospheric radio noise data.
Question 79. (SG II). Responses of radio receivers to quasi-impulsive interference.
Study Program 65. (SG VI). Measurement of atmospheric radio noise.

Studied by URSI Commission on Radio Astronomy

Recommendation 118. (SG VI). Protection of frequencies used for radio-astronomical measurements.

Studied by URSI Commission on Radio Waves and Circuits

Recommendation 107, Study Program 47, and Question 44. (SG III). Communication theory.

URSI–IRE Relations

By means of cross-memberships in the URSI and IRE there is constant interplay of ideas and information between them. The meetings of each lead to proposals of papers for presentation, or activities to pursue, in the other. By IRE representation on the USA National Committee of URSI there is a formal link.

There is, however, additional active relationship. Ever since the USA national meetings of URSI began, they have been held jointly with the IRE, or in recent years, with one or more of the Professional Groups. These have been the Professional Groups on Antennas and Propagation, Circuit Theory, Instrumentation, and Microwave Theory and Techniques. Certain Professional Groups have co-sponsored special meetings together with certain of the USA Commissions of URSI, *e.g.*, the Professional Group on Circuit Theory with the URSI–USA Commission 6B in group sessions at the 1954 IRE Convention.

The IRE has established a significant role for itself standardizing terminology, definitions, and symbols. In such a strictly scientific field, however, as the symbols, definitions, and practices of ionospheric data production and reduction, this work is done by URSI.

The relation of IRE to URSI is quite like the relation of CCIR to URSI. Both of those organizations depend upon URSI to handle the more fundamental or scientific, as well as the international, aspects of radio. If it were not for the existence of URSI, and for IRE's satisfactory relations to it, IRE would be more active in direct scheduling of meetings on basic scientific radio and in direct international promotion of research.

The 1955 Wescon performed a useful liaison function in scheduling a session for report on the accomplishments of the last General Assembly of URSI. This may well set a useful precedent, to be followed by the IRE after each General Assembly. In this connection, it should not be forgotten that IRE is itself an international organization. While its headquarters and principal activities are in the USA, it has branches and activities and members in other countries as well. It has ten active Sections in Canada, one in Israel, one in Egypt, one in Argentina, and one in Japan, besides those in the USA. It has some 4,000 members in 76 other countries besides 43,000 in the USA. It is the leading organization in radio and electronics of the world, not merely of the USA.

The Future

The structure and functioning of the URSI are time-tested and appear suitable for the growth assured by the ever widening role of radio, telecommunication, and electronics. The same can be said of the relations of the URSI with the IRE and the CCIR. As far as we can foresee, the development and the uses of radio will depend upon and be guided by scientific research. As the world becomes more closely knit together, the international coordination of such research will become ever more vital. The URSI will play a major role in the basic phases of this, as will the IRE and the CCIR in its adaptation to practical human needs.

The United States has a major assignment in the immediate future of the URSI. At the 1954 General Assembly the URSI accepted the USA invitation to hold the next General Assembly in Boulder, Colo., in 1957. The meeting will occupy August 22–September 5. The Boulder Laboratories of the National Bureau of Standards and the University of Colorado will be the local hosts in Colorado. Meetings of the Joint Commissions on the Ionosphere and on Radio-Meteorology will be held on August 14–16 in New York City. This is the first General Assembly of URSI in this country since 1927. The other countries which have acted as hosts have provided exceedingly fine programs, services, entertainment, and facilities. They are a distinct challenge to this country for the 1957 event; we must not fail to make it a memorable occasion for those who attend. Mention has been made that the General Assemblies are financed by the National Committee of the country in which held. In most other countries the National Committee is able to obtain the necessary funds from the government. In this country the government does not provide money for such purposes; funds are being raised from industry and others by subscription.

This paper has necessarily presented a great amount of detail in order to give those unfamiliar with the URSI a knowledge of how international radio research is coordinated. It is difficult to take a sufficiently detached view to appraise this activity as one of the components of our civilization. We do know that to the world at large radio, or electronics, is the very symbol of progress. Much less well known is the fact that by the very nature of its world-wide effects, radio lends itself ideally to international collaboration. In the scientific work of URSI and in the far-flung engineering activities with which the IRE deals, it is the habit of many men to deal day by day with men of other countries. Radio simply could not operate without world collaboration in the control of interference. In radio we are continuously proving that men of all nations can work out together the most complicated and difficult problems. Although we devote ourselves to a purely technical field, we are making a real contribution to those currents of good will and international friendliness which must grow mightily to give this world a happier future.

Tantalum Solid Electrolytic Capacitors*

D. A. McLEAN† AND F. S. POWER†

Summary—A new type of electrolytic capacitor has been developed which provides a valuable supplement to the capacitors previously available to the circuit designer. In these new capacitors, a solid semi-conductor replaces the usual aqueous electrolyte. Because the materials are all inorganic nonvolatile solids, no hermetic seal is required for ordinary applications. Compared to other electrolytics, these capacitors are superior in low temperature characteristics and in shelf-aging. Their small size makes them especially suitable for transistor circuitry. They are in limited commercial production and are being used in a new rural carrier system.

Introduction

ELECTROLYTIC capacitors are the first to be considered when large blocks of capacitance are needed in electrical circuits. No other capacitors offer such large capacitance per unit volume at a low cost. Electrolytic capacitors are deservedly popular in by-pass, blocking, and power-supply filter applications and for motor starting purposes. Unfortunately, their relatively low electrical quality in some respects limits the scope of their application in electronic circuitry and the user is often forced to resort to more bulky and more costly types. Although electrolytic capacitors are quite satisfactory for the applications listed above, any improvement in electrical quality and reliability will open new fields to these capacitors and will further enhance their standing among circuit designers. An important advance in recent years has been the introduction of the tantalum anode as a supplement to the classical aluminum anode, aiding miniaturization and improving the shelf-life obtainable. These improvements result from the high dielectric constant of tantalum oxide and the chemical stability of both tantalum and its oxide. Operating temperature range has been increased, especially in the sintered porous tantalum type employing electrolytic solutions of high conductivity and low freezing point, which solutions are not compatible with aluminum anodes. While the tantalum anode constitutes a laudable advance, these capacitors still suffer to a degree certain limitations associated with other electrolytic capacitors.

In our laboratory, H. E. Haring and R. L. Taylor have discovered a new type of electrolytic capacitor referred to here as the tantalum solid electrolytic capacitor. This capacitor has been the subject of active development for several years and has reached the point where commercial production is being undertaken. It is the purpose of this paper to discuss the principal structural features and properties of these new capacitors.

The tantalum solid electrolytic capacitor is fundamentally different from any previous electrolytic in that it contains no water or other liquids, but consists solely of stable, inorganic, nonvolatile materials. This results in important advantages, including small volume, absence of the necessity for an hermetic seal, flexibility as to shape, superior temperature characteristics, relatively low power factor, and indefinitely long shelf life. Present indications are that, compared with other tantalum electrolytics, they will be high in reliability and reasonable in cost. In their present state of development, these new capacitors also possess certain limitations, particularly with regard to maximum recommended operating potential. This limitation has not proved serious in most applications, especially in transistor circuits where their principal future may be.

* Original manuscript received by the IRE, March 19, 1956; revised manuscript received May 9, 1956. To be published in 1956 IRE Convention Record, part 6.

† Bell Telephone Labs., Murray Hill, N. J.

Structural Features

The basic structure, method of fabrication, and certain theoretical considerations will be discussed by Taylor and Haring[1] and will therefore be presented here in a more general manner. While capacitors have been made with both porous and dense tantalum anodes, the description here will be in terms of the porous type, which is most highly developed and the one which is being manufactured in greater quantities at present.

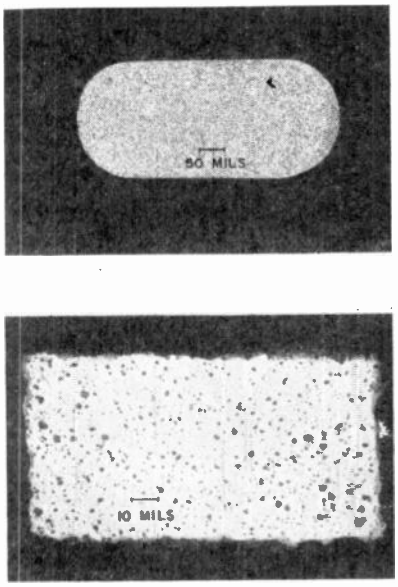

Fig. 1—Top: Photograph of a typical porous tantalum anode used for making solid electrolytic capacitors. Bottom: Cross section photomicrograph of a porous tantalum anode.

Fig. 1 is a photograph of a porous tantalum pellet of the type employed, and a photomicrograph of a cross section. This pellet is formed by pressing tantalum powder to shape in a die and sintering at high temperature under vacuum to weld the particles together. Some of the important factors are the purity of the tantalum powder, the distribution of particle sizes, and the conditions of sintering. The sintered pellets used in this work have a density ratio of about 60 per cent. The resulting high internal surface affords a large area and consequent high capacitance. For a formation voltage of 100 volts, one obtains approximately 10 microfarads per gram of tantalum.

Fig. 2 is a schematic cross section of a porous tantalum solid electrolytic capacitor. An anode lead of dense tantalum is attached to the porous tantalum body either by embedding it in the porous block during pressing or by subsequent welding. A layer of dielectric tantalum oxide is formed on the tantalum surfaces electrochemically by making the tantalum the anode in an electrolytic bath. The thickness of the oxide, which constitutes the dielectric in the ultimate capacitor is controlled by the forming voltage, to which it is proportional. Up to this point, both materials and process are similar to those employed in making conventional porous tantalum electrolytic capacitors. However, instead of the usual working electrolyte, a layer of semiconductor is deposited over all of the dielectric surface. Manganese dioxide, formed by the pyrolysis of manganous nitrate is used for this purpose and is applied in the following way. The pellet is saturated with an aqueous solution of manganous nitrate of 50 per cent or greater concentration. It is then placed in a furnace until the water evaporates and the decomposition of manganous nitrate is complete as evidenced by cessation of evolution of nitrogen oxides. The temperature of the furnace is adjusted so that this occurs in about one minute. Several coats of MnO_2 are applied in this way. It has been found that improved capacitors are obtained if at one or more points between coats of MnO_2, the units are replaced in an electrolytic bath and *re-formed* for a short time.

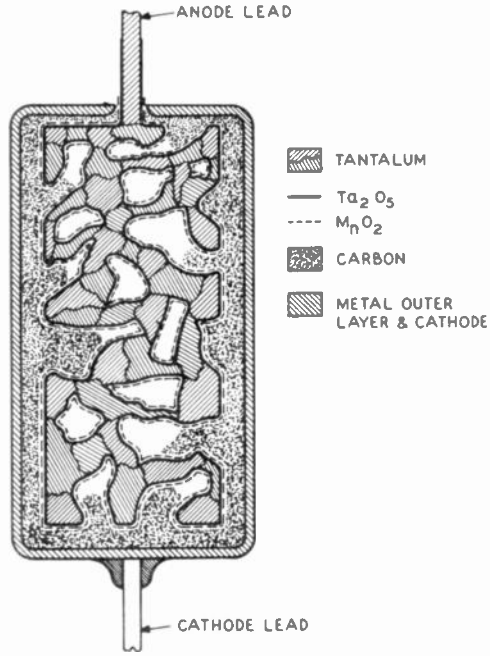

Fig. 2—Schematic cross section of a tantalum solid electrolytic capacitor.

The unit is then coated with a layer of carbon from a graphite dispersion. This coating makes intimate electrical contact with the MnO_2 and guards against excessive thermal and mechanical shock of the underlying layers in subsequent operations. At this point, the unit is ready for application of a metallic cathode encasement, which is conveniently applied by *Schooping* or metal spraying with a coating of lead-tin alloy. An alternative method which has been used in the laboratory to a limited extent is to plunge the unit into a metallic can containing molten solder or other conducting material. Other cathodes such as silver pastes and copper have also been employed successfully. A sprayed metal coating is low in cost and convenient to apply and results in minimum size of finished capacitor.

[1] R. L. Taylor and H. E. Haring, *Trans. Electrochem. Soc.* To be published.

From Fig. 2, it will be noted that near the anode terminal, each successive coating ends a little short of the underlying coat. This may be accomplished by masking and other suitable means.

Anode termination is completed by cutting the tantalum lead short and welding on a solderable nickel terminal. A tinned copper wire is soldered to the metallic cathode coat to provide a cathode terminal.

The final step is an electrical aging, in which a dc voltage is applied to the capacitors for 24 hours or more. This voltage is somewhat in excess of the ultimate working voltage. The units may be given a suitable finish or may be molded in plastic either before or after the aging step. They are now ready for testing and use.

In the following discussion, many comparisons are made with electrolytic capacitors of commercial types. It is not known that in every case these commercial capacitors tested represent the best available in their class. However, a much larger number of types has been studied than described, so much so that a full presentation would be cumbersome. An attempt has been made to include enough results to illustrate the range of properties observed, including the groups exhibiting the best characteristics with respect to the property being discussed. With regard to the solid electrolytics, likewise, only data on typical groups are shown. In all instances where curves are plotted or tables of data given, each point or value represents the average result for form four to ten capacitors unless otherwise stated.

Size and Shape Considerations

Inasmuch as the anode and the dielectric film are identical in essential structure and size to those used in commercial porous tantalum capacitors for equivalent capacitance and voltage rating, no size advantage can be attributed to these items alone. In fact, it is believed that at least for early applications which will be made before extensive reliability studies can be completed, a slightly wider margin between forming and working voltage will be desired. This works to the disadvantage of the solid type. However, this is more than compensated by the size advantage that results from the fact that it is necessary to add very little material to the anode to complete the capacitor. In previous commercial miniature types, on the other hand, most of the volume is occupied by the electrolyte between anode and cathode, by the container and by the seal.

Fig. 3 is a photograph of solid electrolytics. These have been finished with a fairly heavy elastomer coat for mechanical protection, and with a cellulosic lacquer. The maximum finished volumes of the capacitors illustrated are as follows for a 35 volt rating.

Capacitance μf	Volume cu in (max)	μf/cu in (min)
1	0.0045	220
5	0.0120	420
20	0.0410	490

Based on anode volume alone, the capacitance per unit volume obtained is constant for the various sizes at approximately 1,500 μf/cu in. The remainder of the volume in the table is made up of outer layers of MnO_2, carbon, cathode metal, and finish coats, all of which consume relatively more space in the smaller than in the larger physical sizes. For 20 volts working, the figures in the last column can be multiplied by two, and for 8 volts working by five.

An interesting aspect of the solid electrolytics is that their shape is unrestricted, whereas the shape of electrolytics containing electrolytes with volatile constituents is usually cylindrical for ease in making the seal. Considerable development of tantalum solid electrolytics has been on anodes of rectangular, disk, and oval shapes.

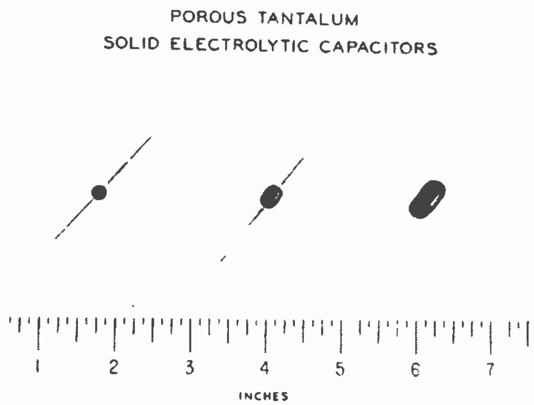

Fig. 3—Photograph of three typical tantalum solid electrolytic capacitors.

Temperature Characteristics

Temperature characteristics of conventional electrolytic capacitors are about as numerous as the types of capacitors. They all have in common, however, low temperature limitations resulting from increasing viscosity or actual solidification of the aqueous electrolyte. In this paper, comparison of the characteristics of tantalum solid electrolytics is made only with commercial tantalum types, which have in general somewhat better characteristics than coresponding aluminum electrolytic capacitors. In Fig. 4 are shown capacitance-temperature curves for various tantalum electrolytics. Above room temperature, the characteristics are very similar, representing a temperature variation which may be assumed tentatively to be that of the dielectric tantalum oxide film. Below room temperature, the capacitors of commercial types have characteristics which fall off along a variety of curves.

The best performance in the conventional types is shown by the capacitors of lowest capacitance values. This is to be expected, for in a given structure, the lower the capacitance, the less influence extraneous series resistance and series capacitance will have. The capacitance of the structure is, of course, inversely related to the formation voltage. The capacitances of the solid types continue on a gradual downward trend as the temperature is lowered, with a slight indication of an even smaller slope below room temperature. It is of interest that in the solid types even the 80 μf capacitors have excellent low temperature behavior, which is an indication of insignificant increase in series capacitance. The average temperature coefficient of the solid type from $-75°C$ to $+85°C$ calculated from the curves shown is $+0.05$ per cent/°C, based on the 25°C value. Extensive measurements of characteristics of capacitors of this type indicate that this value is somewhat lower than the average observed value which is about $+0.07$ per cent/°C. The temperature coefficient of these capacitors is quite reproducible and may be assumed to be that of tantalum oxide over the complete temperature range studied.

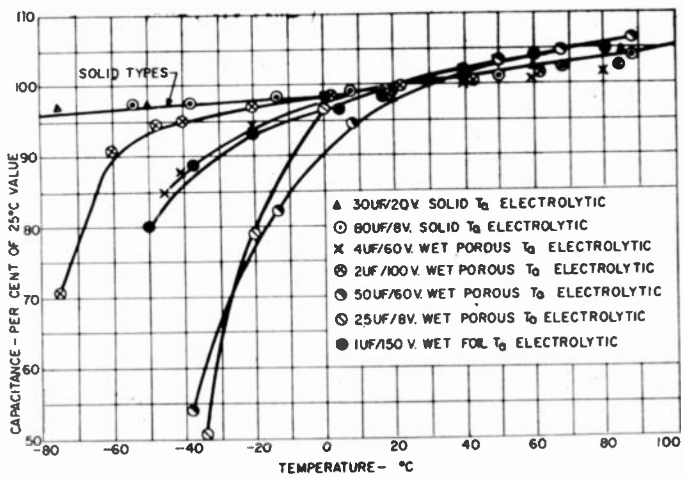

Fig. 4—Comparison of capacitance—temperature characteristics of typical tantalum wet and solid electrolytic capacitors.

One of the remarkable properties of tantalum solid electrolytics is the maintenance of low electrical losses down to very low temperatures. This reflects the retention of sufficiently high conductivity by MnO_2 even at low temperatures. This is illustrated in Fig. 5 which discloses no important change in power factor measured at 1,000 cycles down to $-75°C$. Other types, on the other hand, exhibit very large increases at low temperature, and these increases as well as capacitance change limit the use of the usual electrolytic capacitors for low temperature work.

The leakage current of these capacitors is on the average somewhat higher than for those employing aqueous electrolytes. However, these values are observed immediately upon application of voltage and, as will be shown later, do not degrade during shelf aging. Fig. 6 is a plot of data showing leakage current vs temperature at rated voltage for four typical capacitors. The fact that in this case the 5 μf and 20μf capacitors have almost identical leakage currents is a coincidence.

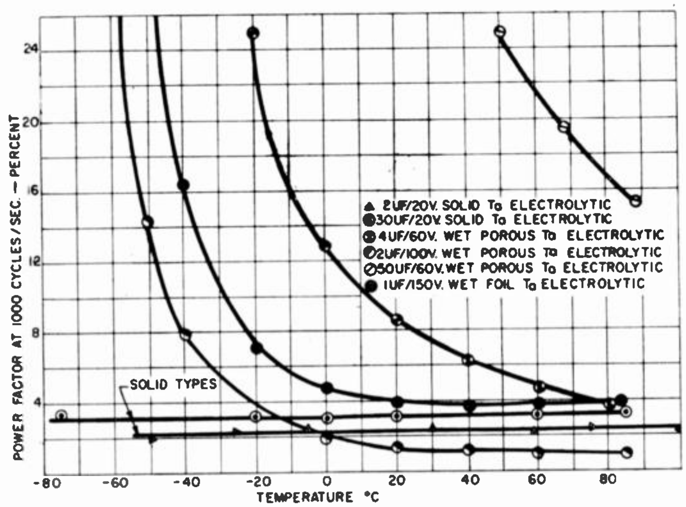

Fig. 5—Comparison of power factor—temperature characteristics of typical tantalum wet and solid electrolytic capacitors.

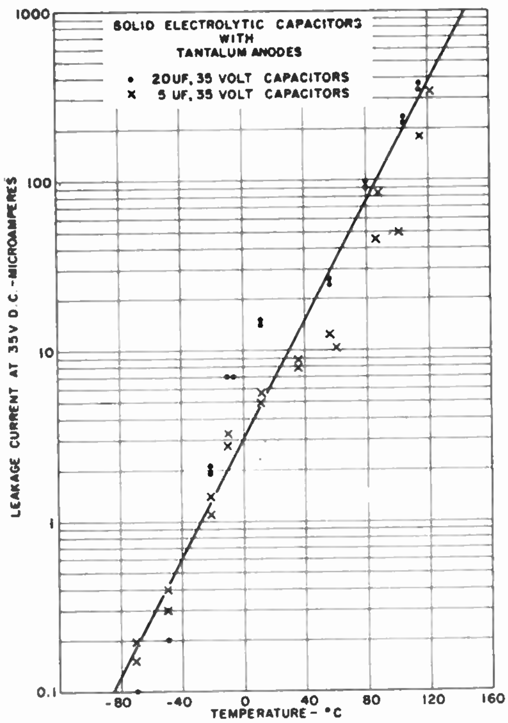

Fig. 6—Leakage current—temperature relationship for typical tantalum solid electrolytic capacitors.

Fig. 7 consists of a plot of the room temperature leakage vs test potential for four typical porous tantalum solid electrolytic capacitors. Further development work is continuing to decrease the leakage current of these capacitors through improvements in materials and processes.

Frequency Characteristics

The high-frequency limitations of electrolytic capacitors are less pronounced for solid electrolytic capacitors than for those employing aqueous electrolytes. This is

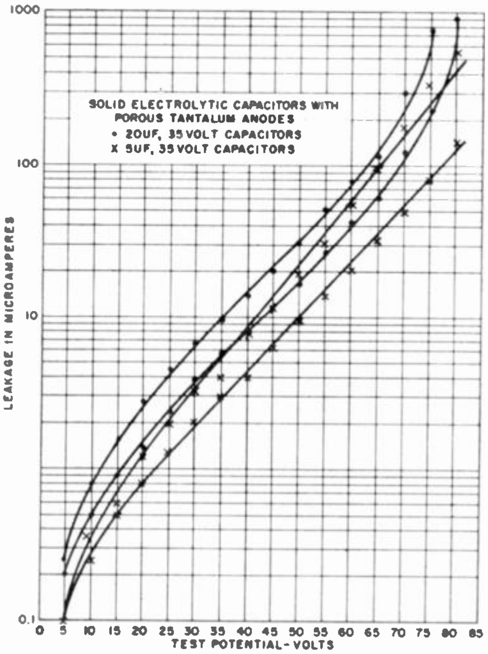

Fig. 7—Leakage current—test potential relationship for typical porous tantalum solid electrolytic capacitors.

illustrated by the curves of Figs. 8 to 11. Fig. 8 shows the capacitance-frequency curves for a number of porous tantalum capacitors. Here again, as might be expected, the low capacitance, higher voltage types have the best characteristics. At a given capacitance and voltage rating, the solid types are considerably superior to those containing aqueous electrolytes. It has been found that a slight etch of the tantalum anode with a hydro-fluoric-nitric acid solution prior to anodizing improves the high frequency characteristics. This is seen by comparing curve 7 with curve 1 and curve 8 with curve 2. Fig. 9 shows the relationship between Q and frequency. There is a general parallel between these results and those for capacitance.

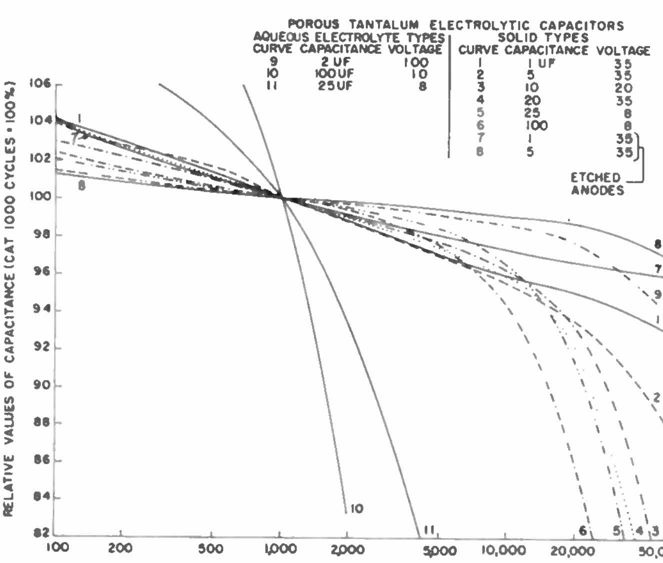

Fig. 8—Comparison of capacitance—frequency characteristics for typical tantalum wet and solid electrolytic capacitors.

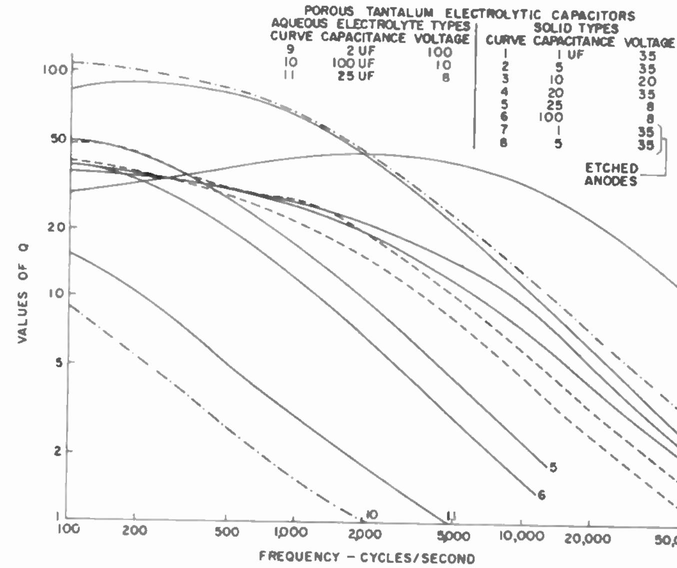

Fig. 9—Comparison of Q—frequency characteristics of typical tantalum wet and solid electrolytic capacitors.

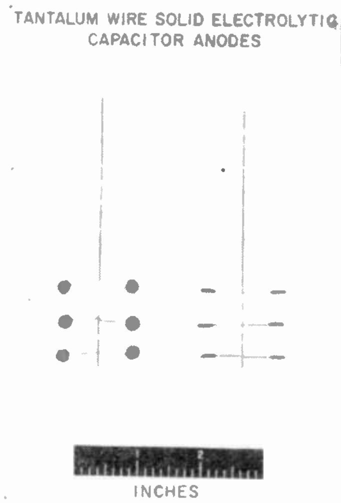

Fig. 10—Tantalum wire anodes ready for forming. Left: spirals; right: helices.

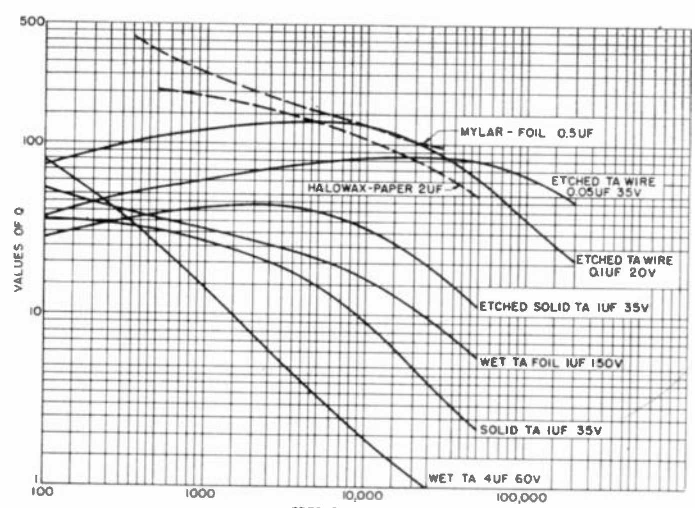

Fig. 11—Comparison of Q—frequency characteristics of porous tantalum wet and solid types, tantalum wire solid types, Mylar-foil capacitors, and paper capacitors.

In terms of effective series resistance, R_e, $Q = 1/\omega C R_e$ and, over most of the range, is for practical purposes the reciprocal of the power factor. In this equation, R_e is expressed in ohms, C in farads, and $\omega = 2\pi f$.

In Fig. 8 and 9, curves 5 and 11 are useful for comparing directly solid and wet type capacitors of identical capacitance and voltage rating. Curves 10 and 6 also represent almost identical ratings. It is seen that the Q values of the solid electrolytics fall off at about a decade higher frequency than the wet type.

Shelf Life

A number of samples of tantalum solid electrolytic capacitors in which porous anodes were employed have been shelf-aged by maintaining them at fixed temperatures without applied voltage and making periodic electrical measurements. The results are summarized in Table I. Capacitance and power factor values were measured at 1,000 cycles and the leakage current determined at the rated voltages of the capacitors. Besides these measurements, which were made at room temperature, leakage current values were obtained on the 65°C and 85°C samples at the aging temperature. In making all of the leakage current measurements, voltage was applied and the reading taken at the end of one minute, although the meter came almost immediately to a stable value. Inasmuch as the changes were small and gradual, only the initial and final values are presented. Many of these samples were placed on test well over a year ago, during which time active development has been underway. For this reason, the capacitors are not representative in all respects of the current product. In particular, some of the leakage current values are higher than those now obtained. However, the results are deemed to demonstrate adequately the stability of these capacitors under shelf-aging conditions. It will be noted that the small changes in capacitance and leakage current are predominantly negative and in power factor predominantly positive.

TABLE I

Shelf-Aging of Porous Tantalum Solid Electrolytic Capacitors

Type	N*	t, °C	Aging Time Days	Capacitance, µf		Leakage µa, Room Temp.		Leakage µa, Aging Temp.		Power Factor %, 1,000 Cycles	
				Initial	Final	Initial	Final	Initial	Final	Initial	Final
1.8 µf, 20V	6	rt	525	1.89	1.90	18	6.4			3.07	3.15
4 µf, 20v	9	rt	525	4.21	4.43	9.1	5.2			2.98	3.30
7 µf, 20v	5	rt	540	6.77	6.76	5.1	4.4			3.44	3.07
15 µf, 20v	2	rt	510	14.72	14.62	5.2	3.2			2.68	2.88
25 µf, 20v	2	rt	587	24.58	24.48	37.5	21.6			3.40	3.72
10 µf, 8v	2	rt	558	9.04	9.04	4.9	4.4			3.77	4.30
40 µf, 8v	7	rt	510	43.65	43.55	43.0	45.5			6.80	7.60
70 µf, 8v	2	rt	579	71.29	71.14	39.5	26.4			9.40	12.5
1.8 µf, 20v	9	65	407	1.77	1.74	7.9	4.5	16.1	19.1	3.73	2.96
1.8 µf, 20v	10	65	407	1.84	1.84	6.7	3.4	82.9	64.7	2.60	2.66
1.8 µf, 20v	10	85	54	1.86	1.84	5.2	6.7	50.5	82.9	3.07	2.60
6 µf, 35v	6	110	54	6.24	6.22	45.0	37.9			4.05	4.08

* N = number of samples.

Life Tests

It is difficult to collect life test data on components during the period of active laboratory development. Life tests on electrolytic capacitors are of long duration since methods of test giving large acceleration factors have not so far been successful. Therefore, during a period of rapid improvement, samples used for life tests are obsolete before the tests are complete. Nevertheless, a substantial number of samples have been life-tested under voltage stress at temperatures from room temperature up to 85°C. However, they represent such a variety of stages of development that it has been decided to defer detailed presentation. Rather, the general indications are given. As with other capacitors, performance depreciates at elevated temperatures. If aging under voltage stress is carried on employing conditions which are too severe, a progressive increase in leakage current is observed. This can be avoided with either lower voltage or lower temperature. Tests of this sort form the basis for logical voltage and temperature ratings. To date in the Bell System it has been found desirable to take full advantage of the potentialities of these capacitors by giving them voltage ratings appropriate for moderate temperatures, and then suitably derating above 65°C. Many additional life tests must be performed on samples incorporating all recent improvements in materials and processing. Such tests are being started at the present time. For the time being, it is recommended that these capacitors not be employed for operating temperatures above 65°C without voltage derating.

Dense Tantalum Anodes

Although the bulk of the work done to date has employed porous anodes, many capacitors have been produced with dense anodes, such as foil and wire. These are somewhat more bulky, but in specific cases offsetting advantages are realized. The properties of solid electrolytic capacitors with dense anodes will be discussed in terms of results obtained with tantalum wire, which constitutes a convenient form of dense tantalum. The advantages achieved are as follows: 1) Low capacitance units, *e.g.*, in the fractional microfarad range can be made which are extremely small. 2) Small quantities of capacitors with special capacitance values can be produced quickly and economically by employing suitable lengths of precalibrated wire, without the need for special dies for each size. 3) High-frequency losses are reduced to a point where relatively good values of Q can be realized up to 200 kc. 4) Preliminary indications are that higher voltage types are more readily made with dense than with porous tantalum. (However, the voltage limits have not been determined accurately and require further study.)

Typical anodes used in this study are shown in Fig. 10. Illustrated are spirals and helices wound from 20 mil wire and welded to a central stem for forming. One end of the wire is brought out to form the anode lead. The process used is identical with that used for the porous elements.

Fig. 11 shows average values of Q of a number of tantalum electrolytic types plotted against frequency. The particular 0.05 μf, 35 volt etched wire solid capacitors studied are remarkable for electrolytic capacitors in exhibiting a high Q over a large part of the frequency range and a value of 45 even at 200 kc. The 0.1 μf, 20 volt capacitors exhibit a Q exceeding 100 (power factor <1 per cent) from 350 cycles to 50 kc. These capacitors compare favorably in this respect with capacitors employing impregnated paper and Mylar films with aluminum foil electrodes for which curves are also shown. These properties open the possibility of using these capacitors in circuit situations where losses in conventional electrolytics would be intolerable.

Leakage current vs voltage curves for three tantalum wire solid electrolytics are shown in Fig. 12. These curves illustrate the ability of these capacitors to take moderately high instantaneous voltages without excessive leakage currents.

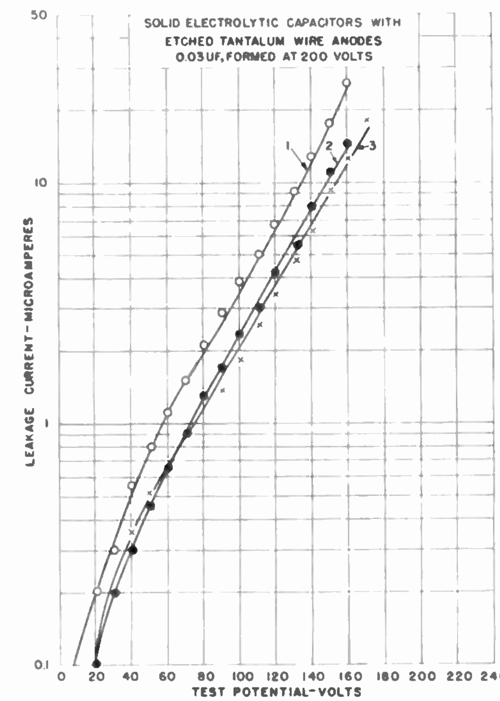

Fig. 12—Room temperature leakage current-voltage characteristics of tantalum wire solid electrolytic capacitors.

Acknowledgment

The authors wish to express their appreciation for the aid given by many associates during this work. For an appreciable part of the experimental work, we are indebted to Miss Jean Bowden, Miss Beatrice Jungblut, and Mr. Earl Smith. Many helpful discussions have been held with Messrs. H. E. Haring, R. L. Taylor, C. C. Houtz, M. Whitehead, and N. Fuss.

Theory of the Transverse-Current Traveling-Wave Tube*

D. A. DUNN†, ASSOCIATE MEMBER, IRE, W. A. HARMAN‡, ASSOCIATE MEMBER, IRE, L. M. FIELD§, FELLOW, IRE, AND G. S. KINO||, ASSOCIATE MEMBER, IRE

Summary—**An analysis is presented of a traveling-wave tube in which unmodulated dc current is continuously introduced along the length of the tube and is removed after traveling a fixed distance in the presence of the circuit field. This change in the dc current distribution as compared with that of a conventional traveling-wave tube results in three forward growing waves instead of one, one growing exponentially as in the conventional tube, one growing linearly, and one growing as the square of distance. Expressions for the over-all gain of a forward-wave amplifier of this type are derived as a function of the usual parameters plus an additional parameter related to the distance traveled by electrons in the interaction space. The power output of this device is found to depend on saturation of individual current elements rather than of the beam as a whole, with the result that, after saturation is once reached, the power output is independent of input power. An estimate of the value of the saturation power level is obtained from the linear analysis.**

Introduction

It is possible to construct a traveling-wave tube in which a beam of electrons is passed near a helix or other slow-wave circuit in such a fashion that elements of the beam continuously enter and leave the interaction space throughout the entire length of the interaction space. Each electron is only permitted to travel a distance through the interaction space that is small in comparison with the total length of the interaction space. In a practical traveling-wave tube, this end may be achieved either by skewing the elements of the circuit and passing the beam at a right angle to the direction of power flow on the circuit, or by skewing the beam so that it passes over the circuit at an acute angle to the direction of the power flow. The skew circuit form of the transverse current traveling-wave tube is shown in Fig. 1(a); the skew-beam tube is shown in Fig. 1(b).

In many respects the behavior of this device is similar to that of a conventional traveling-wave tube having a beam that travels the entire length of the interaction space. The properties of the transverse current tube that are different from those of the traveling-wave tube having the usual dc current distribution have primarily to do with the new variable, the length of the path of the individual elements of dc current in the interaction space, L in Fig. 1. When this length is below some critical value, the gain per unit length of the growing wave is much lower than that of the corresponding wave in an equivalent conventional tube and the gain varies more rapidly with current and frequency. Saturation power increases as this length falls below the critical value. Total efficiency, however, decreases.

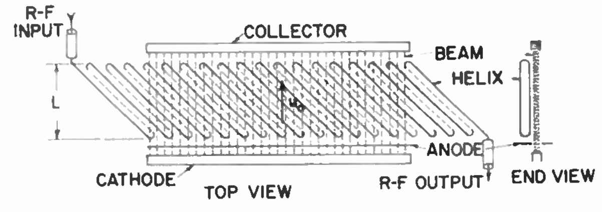

(a)

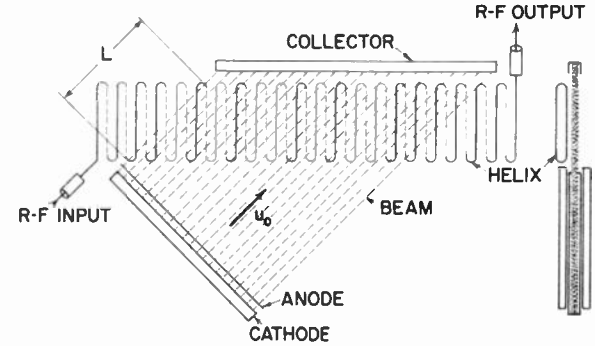

(b)

Fig. 1—(a) The skew circuit form of the transverse-current traveling-wave tube. A flat helix circuit having its wires skewed with respect to the direction of power flow is used in combination with a beam that travels over the circuit at a right angle to the direction of power flow on the circuit. (b) The skew beam form of the transverse-current traveling-wave tube. A flat helix circuit having its wires essentially perpendicular to the direction of power flow is used in combination with a beam that travels over the circuit at an acute angle to the direction of power flow on the circuit.

Perhaps of greater significance is the shape of the power output vs power input curve for a tube with an interaction space having a length many times the length of a single element of the beam. For such a tube, each element saturates in conventional fashion, reaching an equilibrium condition in which as much energy has been absorbed from the circuit by the element as was previously delivered to the circuit by the element. The maximum output power of the device is determined by the power level corresponding to this equilibrium condition for individual elements of the beam. When this condition is first reached at the output end of the tube, maximum output will occur. For higher input powers the output power is unchanged. The point at which saturation of a single element is first reached simply moves up and down the length of the tube as the input level is varied, all current elements beyond this point being in

* Original manuscript received by the IRE, December 1, 1955; revised manuscript received, February 13, 1956.
† Stanford University, Stanford, Calif.
‡ General Electric Microwave Lab., Palo Alto, Calif. Formerly at Stanford University, Stanford, Calif.
§ Hughes Aircraft Co., Culver City, Calif. Formerly at Stanford University, Stanford, Calif.
|| Bell Telephone Labs., Murray Hill, N. J. Formerly at Stanford University, Stanford, Calif.

equilibrium. The power output is completely independent of the input power in this region of operation. Other nonlinear behavior aspects of the device are similarly uniform after a certain critical input level has been reached, because the tendency of the beam elements is to reach an equilibrium condition individually.

The gain of a forward-wave amplifier having the dc current distribution of the transverse current tube can be expressed as a function of the usual variables plus the dc current per unit length introduced and the length of the path of the current element. First, the values of the propagation constants of the waves of the system are derived in terms of these variables. Then the appropriate wave amplitudes are evaluated at the boundaries of the system. The gain for a sufficiently long forward-wave tube, uniform in the z direction, may be expressed in terms of the gain of a growing wave in the form used by Pierce;[1] *i.e.*, gain in db $=A+BCN$. A suitable definition for C in the present case involves the total dc current passing a given z position, which is the current per unit length introduced times the length of the current elements. If M is the number of wavelengths in the length of an element of current, A and B can be expressed as functions of the usual variables plus the single additional variable CM.

Some earlier work on the transverse current tube by two of the authors[2,3] appeared briefly in the publications noted and in a survey article by Kompfner.[4] Some related material appears in a thesis by Rockwell.[5]

Waves of the System

Derivation of Equations for Propagation Constants

The solution of this problem may be obtained by the same general method that Pierce has employed in solving the problem of the "one-dimensional" conventional tube. An electronic equation for the ac current induced by a specified circuit field is combined with a circuit equation expressing the field induced on the circuit by a specified ac current in the beam, and a self-consistent solution for the propagation constants of the waves of the combined system is obtained.

The transverse current tube analysis can be reduced to an essentially one-dimensional problem by consideration of a model in which current elements starting at successive points along the z direction share the space with other elements, rather than being distributed in another dimension. Fig. 2 shows such a model suggested to the authors by J. R. Pierce. Here there are no variations of relevant quantities in the x direction. Electrons are considered to originate by some unspecified means in a uniform fashion along the z direction of the device; each electron is allowed to travel a distance L and then it is removed. In the side view of Fig. 2 electrons are shown entering and leaving by paths that originate and terminate above the interaction space, as a possible visualization of this model.

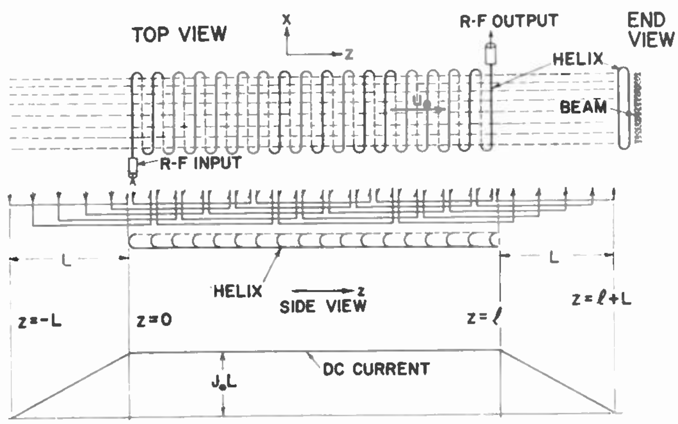

Fig. 2—A transverse-current traveling-wave tube in which the beam travels in the direction of power flow on the circuit. Elements of beam current are introduced and removed by an unspecified means via paths that terminate above the helix. Over the length of the helix, l, the dc beam current has a constant value equal to the product of the dc beam current per unit length introduced, J_0, and the length of travel of any electron, L.

A further simplification has been introduced in the Fig. 2 model. At $z=0$ and $z=l$ the circuit is considered to end abruptly, with dc current distribution extending at each end a distance L beyond both ends of the circuit. This model then has a constant dc current throughout its length. It is as if a beam, infinite in the z-direction, were placed near a circuit of length l. However, in a beam of this type, only those portions within L of the ends of the circuit can be coupled to the circuit, so the portions beyond this region can be eliminated, leaving the Fig. 2 configuration. A more accurate model of the Fig. 1 devices would have a varying dc current at the ends. Such a model can be imagined by simply extending the circuit of Fig. 2 to a length equal to the full length of the beam shown in Fig. 2. This article is limited to an analysis of the constant dc current model.

An analysis of the Fig. 2 model can be conveniently carried out by finding an equation for the ac current in a single element of the beam in terms of the circuit field, and then adding the currents in all the elements passing a given z position to find the total current at z. By this means an electronic equation for the total current at any z may be found in terms of the circuit field. The circuit equation for this device is exactly the same as that for the conventional traveling-wave tube.

Fig. 3 shows a portion of the Fig. 2 model near a point z. Elements of current are shown entering the interaction space near the helix at several values of ξ, between $\xi=z-L$ and $\xi=z$, ξ being a variable in the same direc-

[1] J. R. Pierce, "Traveling-Wave Tubes," D. Van Nostrand & Co. Inc., New York, N. Y.; 1950. Subsequent references to Pierce and Pierce's equations refer to items in this reference, and it will not be repeated hereafter.

[2] D. A. Dunn, "Higher power traveling-wave tubes," thesis, Dept. of Elec. Engrg., Stanford University; 1950.

[3] L. M. Field, "Recent developments in traveling-wave tubes," *Electronics*, vol. 23, pp. 100–104; January, 1950.

[4] R. Kompfner, "Traveling-wave tubes," *Reports on Progress in Physics*, vol. 15, pp. 275–327; 1952.

[5] R. G. Rockwell, "Transverse current traveling-wave tube for high power output," thesis, Dept. of Elect. Engrg., Stanford University; 1949.

tion as z. The usual force equation, definition of current, and continuity equation apply to any single element of the beam. An integral equation may be derived from the usual differential form of these equations which expresses the ac current at z in a beam which has been subjected to a prescribed field $E(\zeta)$ over a specified distance from $\zeta=0$ to $\zeta=z$. The derivation is carried out in the Appendix; the result is as follows.

$$i(z) = \frac{jI_0}{2V_0}\int_0^z E(\zeta)\beta_e(z-\zeta)e^{-j\beta_e(z-\zeta)}d\zeta. \tag{1}$$

In this equation I_0 and V_0 are the dc beam current and voltage, respectively, and $\beta_e=\omega/u_0$ is the beam phase constant, where ω is the angular frequency of the ac field $E(\zeta)$, and u_0 is the dc electron velocity. As written, (1) applies to a beam entering the interaction space at $\zeta=0$ with zero ac current and velocity.

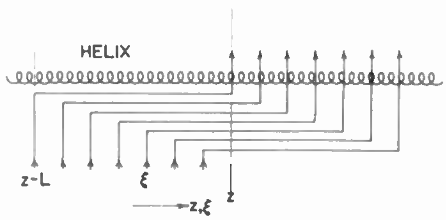

Fig. 3—A portion of the tube of Fig. 2 near a point z. The variable ξ specifies the point of entrance into the interaction space of a dc current element.

For an element of dc current starting at $\zeta=\xi$ in Fig. 3 with zero ac current and velocity, and having a total dc current of $J_0 d\xi$, where J_0 is the current per unit length introduced, and $d\xi$ is a length element in the ξ direction, (1) may be modified to give the ac current in this element at z as follows:

$$di(z,\xi) = \frac{jJ_0 d\xi}{2V_0}\int_\xi^z E(\zeta)\beta_e(z-\zeta)e^{-j\beta_e(z-\zeta)}d\zeta. \tag{2}$$

To find the total current at z, it is necessary to sum the di originating at ξ between $\xi=z-L$ and $\xi=z$. It is not necessary to include ξ outside this range, because such elements do not cross the z plane.

$$i(z) = \frac{jJ_0}{2V_0}\int_{z-L}^z\int_\xi^z E(\zeta)\beta_e(z-\zeta)e^{-j\beta_e(z-\zeta)}d\zeta d\xi. \tag{3}$$

By differentiating (3) with respect to z, the following electronic equation is obtained.

$$\begin{aligned}&\frac{d^3 i}{dz^3} + 3j\beta_e\frac{d^2 i}{dz^2} - 3\beta_e^2\frac{di}{dz} - j\beta_e^3 i\\ &= \frac{j\beta_e J_0}{2V_0}\left\{L\frac{dE(z)}{dz} + (j\beta_e L - 2)E(z)\right.\\ &\left.+\left[L\frac{dE(z-L)}{dz} + (j\beta_e L + 2)E(z-L)\right]e^{-j\beta_e L}\right\}.\end{aligned} \tag{4}$$

Eq. (4) is seen to be third order in current and to involve not only $E(z)$ and its derivative, but also $E(z-L)$ and its derivative, and the distance $\beta_e L$ explicitly.

The circuit equation for this device is no different from that of the conventional traveling-wave tube, because this equation is derived without reference to how the ac driving current arises. A differential equation form of Pierce's eq. (2.10) or his eq. (7.1), with zero space charge assumed, is as follows:

$$\frac{d^2E}{dz^2} - \gamma^2 E = -\gamma K\frac{d^2 i}{dz^2}, \tag{5}$$

where the circuit propagates waves in the absence of the beam as $\exp(-\gamma z)$, and where K is the circuit-beam coupling impedance, $E^2/2\beta^2 P$, E being the electric field in the z direction at the beam, β being the imaginary part of γ, and P the power transmitted by the circuit. (γ is the same as Pierce's Γ_1).

Solution of the Equations

A solution to (4) and (5) may be obtained by means of the Laplace transform method. The transformed variable is called $(-\Gamma)$ in the following, so as to conform to Pierce's notation. The transforms of (4) and (5), when combined, yield the following equation for $E(-\Gamma)$.

$$E(-\Gamma) = \frac{A(-\Gamma)}{B(-\Gamma)} \tag{6}$$

where

$$\begin{aligned}A(-\Gamma) = &-\gamma\Gamma^2 K[(\Gamma^2 - j3\beta_e\Gamma - 3\beta_e^2)i(0)\\ &+ (j3\beta_e - \Gamma)i'(0) + i''(0)]\\ &+ (j\beta_e - \Gamma)^3\{-\Gamma E(0) + E'(0)\\ &+ \gamma K[-\Gamma i(0) + i'(0)]\}\\ &+ j2\beta_e\gamma C^3\Gamma^2\left\{(1 + e^{-(j\beta_e-\Gamma)L})E(0)\right.\\ &- e^{-j\beta_e L}\left[\int_0^L E'(z-L)e^{\Gamma z}dz\right.\\ &\left.\left.+\frac{(j\beta_e L + 2)}{L}\int_0^L E(z-L)e^{\Gamma z}dz\right]\right\}\end{aligned} \tag{6a}$$

and

$$\begin{aligned}B(-\Gamma) = &(j\beta_e - \Gamma)^3(\Gamma^2 - \gamma^2) + \frac{j2\beta_e\gamma C^3}{L}\Gamma^2[(j\beta_e - \Gamma)L\\ &- 2 + (2 + (j\beta_e - \Gamma)L)e^{-(j\beta_e-\Gamma)L}]\end{aligned} \tag{6b}$$

and where

$$C^3 = \frac{KJ_0L}{4V_0} \tag{7}$$

and the primes mean derivatives with respect to z.

Before proceeding further it is worth noting the principal assumptions involved in arriving at (6). First, of course, it is assumed that the one-dimensional model of Fig. 2 will satisfactorily exhibit the essential properties of the Fig. 1 devices. Second, the boundary conditions of zero ac current and velocity have already been applied to all the individual current elements at their points of entrance into the interaction space. Third, zero space charge has been assumed. Other assumptions are those implicit in Pierce's conventional traveling-wave tube analysis. The small C assumption has not yet been made.

The roots of the characteristic equation, $B(-\Gamma)$ in (6), are the propagation constants of the waves in the combined circuit-beam system; *i.e.*, the waves that could be set up on an infinite system of the sort shown in Fig. 2. The amplitudes of these waves for typical boundary conditions, namely those associated with breaking off the circuit at $z=0$, as in Fig. 2, will be discussed in the next section. To find the roots of the characteristic equation, Pierce's definitions of δ, b, and d in his eqs. (7.11) and (7.12), and the definition of θ given below, will be used for the forward waves

$$-\Gamma = -j\beta_e + \beta_e C\delta \tag{8}$$

$$-\gamma = -j\beta_e[1 + C(b - jd)] \tag{9}$$

$$\theta = \beta_e CL. \tag{10}$$

By substituting (8), (9), and (10) into the characteristic equation, as it appears in (6), and assuming $C \ll 1$, the following equation is obtained.

$$\delta^3\left[b - jd - j\delta + \frac{1}{\theta\delta^3}(\theta\delta - 2 + (\theta\delta + 2)e^{-\theta\delta})\right] = 0. \tag{11}$$

If the exponential in (11) is expanded in series form, this equation may be rewritten as follows, after some algebra.

$$\delta^3\left[b - jd - j\delta + \frac{\theta^2}{6}\left(1 - \frac{\theta\delta}{2} + \frac{3(\theta\delta)^2}{20} - \cdots\right)\right] = 0. \tag{11a}$$

Written in this form it is evident that there is a triple root at $\delta=0$ or $-\Gamma = -j\beta_e$. Since the exponential term is not affected by the limitation to small C made in obtaining (11), this root is also a root of the characteristic equation as written in (6) before making the small C approximation.

After dividing through by δ, (11) may be rewritten in the same form used for the conventional traveling-wave tube in Pierce's eq. (7.14).

$$\delta^2(b - jd - j\delta) + 1 = \frac{2}{\theta\delta} - \left(\frac{2}{\theta\delta} + 1\right)e^{-\theta\delta}. \tag{12}$$

For Re $\theta\delta \gg 1$, the right-hand side of (12) approaches zero, leaving the equation of the conventional traveling-wave tube. Thus, as might have been expected, the gain of the growing wave in a transverse current tube approaches that of a conventional tube when the current elements are permitted to stay in the interaction space a sufficiently long distance. The only root that satisfies the condition that the real part of δ is positive is the growing-wave root, so the other two roots of the conventional tube equation are without meaning in connection with the transverse tube, even though the growing-wave roots for the two types of tube become equal for large $\theta\delta$.

For $\theta\delta \ll 1$, only the first two terms of the series in (11a) are required, yielding the following approximate equation for the δ of the growing wave.

$$b - jd - j\delta \approx -\frac{\theta^2}{6}\left(1 - \frac{\theta\delta}{2}\right) \tag{13}$$

Solving for δ in (13) using the subscript 1 to refer to the growing wave, yields

$$\delta_1 \approx \frac{1}{1 + \theta^6/144}\left[(\theta^5/72 + \theta^3 b/12 - d) + j(-\theta^2/6 - b - \theta^3 d/12)\right]. \tag{14}$$

It will be seen that for this condition, the imaginary part of δ_1 is much larger than the real part, and the real part of δ_1 is linearly proportional to b, implying a maximum growing wave gain at a voltage higher than synchronous voltage, and in fact, so much higher that the approximation made in obtaining this equation is no longer valid.

Another important aspect of (14) is the result for the effect of loss for small $\theta\delta$. The value of the real part of δ_1 with loss ($d \neq 0$) is smaller than the value of δ_1 without loss by the full value of d, rather than by $\frac{1}{3}d$, as in the case of the conventional tube. The meaning of this statement is that a small $\theta\delta$ tube with gain equal to that of the growing wave cannot be made short-circuit stable by the addition of distributed loss, because the loss decreases the gain by exactly the amount of the loss. This effect is similar to that of adding loss to a conventional tube very near the input where the signal is hardly increasing at all, even without loss, and the addition of loss actually causes the signal to decrease as a function of distance.

The gain of the growing wave may be expressed in the form used by Pierce as

$$\text{Gain in db} = BCN \tag{15}$$

where C is defined in (7) and

$$N = \frac{\beta_e l}{2\pi} \tag{16}$$

$$B = 54.5\,(Re\,\delta_1). \tag{17}$$

It is of interest to obtain the variation of B with the length of the current element path L, and this may be best shown by defining another quantity

$$M = \frac{\beta_e L}{2\pi}, \tag{18}$$

the number of wavelengths in a length L. For $b=d=0$, from (14) and (17), for small $\theta\delta$

$$B \approx 54.5 \frac{\theta^5}{72} = [5.94(CM)]^5. \tag{19}$$

For small CM, BCN, which is approximately the net gain in a high gain tube, is thus proportional to C^6, and hence proportional to the square of the dc beam current instead of the cube root of the current, as in the conventional tube. For this statement to be true, the tube must be very long; there must be high net gain and small CM. The gain vs frequency curve is also drastically narrowed for this condition, as compared with that of a conventional tube having equal midband gain (neglecting dispersion of the circuit in both cases; *i.e.*, $b=0$ for all frequencies). It is interesting that the shape of the curve is not altered. For large CM, B is not a function of CM, so gain is proportional to CN. For small CM, B is proportional to C^5M^5, and gain is proportional to C^6M^5N. Since both M and N are linearly proportional to frequency, gain is proportional to C^6N^6. Thus the gain vs frequency curve for the transverse current tube for small CM is simply the usual curve to the sixth power.

It has been noted that for large CM, the right-hand side of (12) approaches zero, so the solution for large CM is the same as for the conventional tube; *i.e.*, $B=47.3$. For values of Re $\theta\delta$ greater than about 3, the right-hand side of (12) is approximately $2/\theta\delta$. In this case, for $b=d=0$.

$$\delta(\delta^3 + j) = j\frac{2}{\theta}\cdot \tag{20}$$

Values of δ that are solutions of (20) and which give Re $\theta\delta>3$, have meaning, and, from these, B may be plotted as a function of CM for this range of values.

Fig. 4 shows B as a function of CM for $b=d=0$, from (14) and (20). Curves are drawn showing the value of B for the three approximations discussed above; *i.e.*, $\theta\delta\ll 1$, Re $\theta\delta>3$, Re $\theta\delta$ very large. A dotted line has been drawn in to indicate an estimated curve for intermediate values of $\theta\delta$.

It will be noted that for CM greater than 0.5 or thereabouts, B is not greatly different from that of a conventional tube. Fig. 5 is a plot of δ as a function of θ in the δ plane, also for $b=d=0$, obtained from (14) and (20). It is seen that for small θ, δ is almost purely imaginary.

The backward wave in this tube has a propagation constant that may be found conveniently by substituting in the characteristic equation for $-\Gamma$

$$-\Gamma_2 = +j\beta_e - \beta_e C\delta_2$$

and assuming small C. This process yields

$$-\Gamma_2=\gamma\left[1-\frac{C^3}{4}\left(1-\frac{1}{j\beta_e L}+\left(1+\frac{1}{j\beta_e L}\right)e^{-2j\beta_e L}\right)\right]. \tag{21}$$

The subscript 2 will be used in the following to refer to the backward wave. The term in brackets following

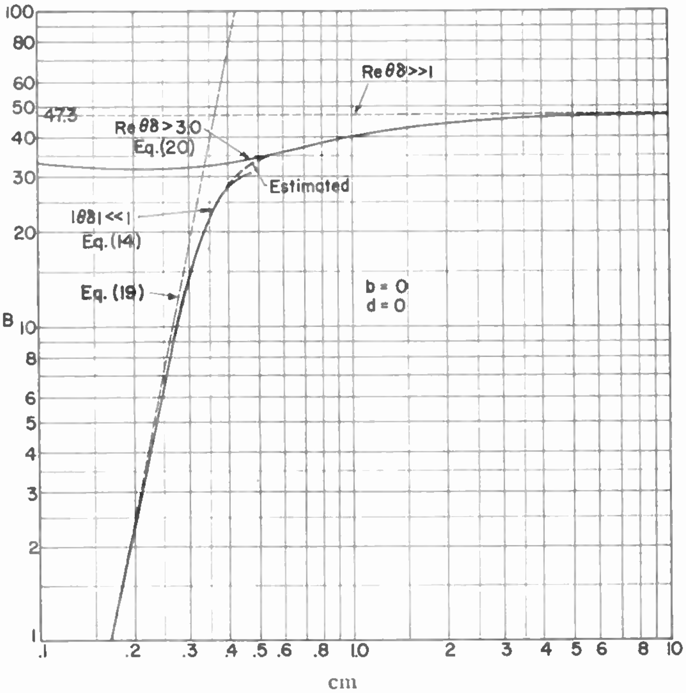

Fig. 4—The value of B, the gain in db per wavelength per unit C of the exponentially increasing wave, in a transverse-current traveling-wave tube as a function of the normalized length of the electron paths, CM, for $b=d=0$. For large values of CM, the value of B approaches 47.3, its value in the conventional traveling-wave tube.

$C^3/4$ is equal to unity in the conventional tube. Here this small perturbation from the unperturbed circuit propagation constant can be complex and have either a positive or a negative real part, but in any case it is negligible for small C.

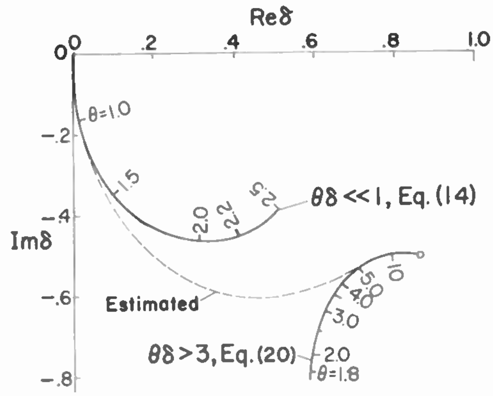

Fig. 5—The value of the real and imaginary parts of δ for the exponentially increasing wave as a function of the normalized length of the electron paths, $\theta=2\pi CM$, for $b=d=0$. The growing wave varies in the z direction as exp $(-j\beta_e+\beta_e C\delta)z$. For large values of θ (and CM) the value of δ approaches $0.866-j\,0.5$, its value in the conventional traveling-wave tube.

The five roots discussed thus far are then, in summary: three identical roots at $-j\beta_e$, which, as will be shown, lead to a constant amplitude wave, one growing linearly with z, and one growing as z^2; a growing wave near $-j\beta_e$ that has a propagation constant approaching the value for the conventional tube when the normalized length of the current elements, CM, is large enough;

and a backward wave very near $+\gamma$, the unperturbed circuit propagation constant. Fig. 6 is a plot of the Γ plane with these roots indicated.

In addition to these five waves that would be expected from the fifth order differential equation obtained by combining (4) and (5), there appear to be an infinite number of additional roots with large negative real parts resulting from the exponential term in the characteristic equation, (6) or (11). If $-\Gamma$ has a negative real part, and both real and imaginary parts are much greater than β_e, then the characteristic equation as it appears in (6) can be written approximately as

$$\Gamma^2 + 2j\beta_e\gamma C^3 e^{\Gamma L} \approx 0. \tag{22}$$

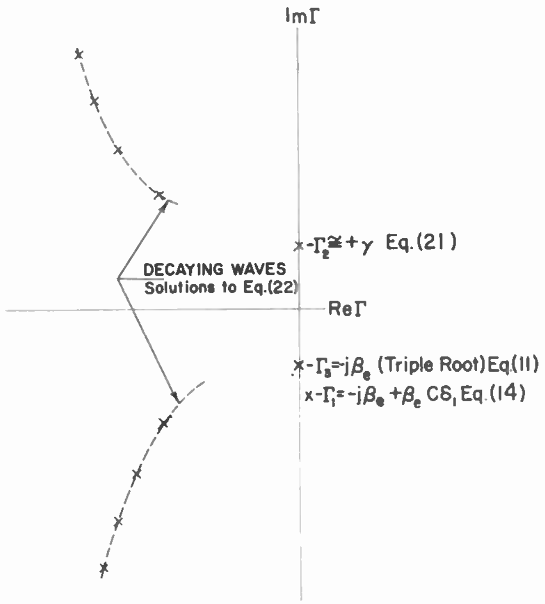

Fig. 6—The propagation constants of the waves of the transverse-current traveling-wave tube. There are five waves of interest near Re $\Gamma=0$, three waves having identical propagation constants corresponding to propagation at exactly the electron velocity.

For the absolute values of these two terms to be equal, the imaginary part of Γ must increase much faster than the real part, along the locus of the roots of this equation, as indicated in Fig. 6. It will be shown in the next section that at least most of these waves are excited with very small amplitudes and that the sum of all of them is small at the input of the tube. They will all be decaying very rapidly and hence, even if some are large at the input, they would be very small at any reasonable distance from the input. These waves thus do not appear to be of any physical significance, but the authors do not feel that they have made a complete disposition of this phase of the problem.

Boundary Conditions

This section is concerned with finding the amplitudes with which the various waves described in the previous section are excited by an applied field at $z=0$ in a forward wave amplifier. The total field as a function of z can then be computed by adding the amplitudes of these waves at any z, taking into account their original excitation and their rates of growth or decay between $z=0$ and the point in question. The model is that of Fig. 2, in which the following quantities may be defined from the physical characteristics of this model, for an applied field E_0 at $z=0$.

$$E(0) = E_0 \tag{23}$$

$$E(z) = 0 \text{ from } z = -L \text{ to } z = 0 \tag{24}$$

$$E'(z) = 0 \text{ from } z = -L \text{ to } z = 0 \tag{25}$$

$$E(-L) = E'(-L) = 0. \tag{26}$$

If the field E_0 is only a forward traveling wave with the beam on; *i.e.*, if there is no backward wave,

$$E'(0) = -\gamma E_0. \tag{27}$$

Eq. (6a) requires a knowledge of $i(0)$, $i'(0)$, and $i''(0)$. These quantities may be obtained from a knowledge of the fields given by (23) through (26), when it has already been specified that ac current and velocity are zero for all current elements as they enter the interaction space. The current and its derivatives are obtainable by differentiating (3) directly, and substituting $z=0$ in the results. This same procedure was used originally in the derivation of (6).

$$i(z) = \frac{jJ_0}{2V_0}\int_{z-L}^{z}\int_{\xi}^{z} E(\zeta)\beta_e(z-\zeta)e^{-j\beta_e(z-\zeta)}d\zeta d\xi \tag{28}$$

$$i'(z) = \frac{jJ_0}{2V_0}\left[\int_{z-L}^{z}\int_{\xi}^{z}\beta_e E(\zeta)e^{-j\beta_e(z-\zeta)}d\zeta d\xi - \int_{z-L}^{z} E(\zeta)\beta_e(z-\zeta)e^{-j\beta_e(z-\zeta)}d\zeta\right] - j\beta_e i(z) \tag{29}$$

$$i''(z) = \frac{jJ_0}{2V_0}\left[\beta_e L E(z) - 2\beta_e\int_{z-L}^{z} E(\zeta)e^{-j\beta_e(z-\zeta)}d\zeta + \beta_e L E(z-L)e^{-j\beta_e L}\right] - 2j\beta_e i'(z) + \beta_e^2 i(z). \tag{30}$$

Substitution of $z=0$ and (23) through (26) into (28), (29), and (30) yields the following:

$$i(0) = 0 \tag{31}$$

$$i'(0) = 0 \tag{32}$$

$$i''(0) = \frac{jJ_0 L\beta_e}{2V_0}E(0). \tag{33}$$

The two integrals in (6a) can be seen to be zero, if $E(z-L)$ and $E'(z-L)$ are zero from $z=0$ to $z=L$; *i.e.*, if $E(z)$ and $E'(z)$ are zero from $z=-L$ to $z=0$, as prescribed by (24) and (25). Setting these integrals equal to zero and substituting (23), (27), (31), (32), and (33) into (6) yields the following equation for $E(-\Gamma)$.

$$E(-\Gamma) = \frac{C(-\Gamma)}{B(-\Gamma)} \tag{34}$$

where

$$C(-\Gamma)=E_0\left[-(j\beta_e-\Gamma)^3(\Gamma+\gamma)+j2\beta_e\gamma C^3\Gamma^2e^{-(j\beta_e-\Gamma)L}\right] \quad (34a)$$

and where $B(-\Gamma)$ is the same as $B(-\Gamma)$ in (6b).

The inverse transform of (34) will yield the amplitudes of the waves of interest. An evaluation of the residues of the five poles of (34) (corresponding to the five roots of the denominator discussed in the previous section) may be carried out by the following procedure.[6] Let

$$E(-\Gamma)=\frac{E_1}{(\Gamma_1-\Gamma)}+\frac{E_2}{(\Gamma_2-\Gamma)}+\frac{E_3}{(\Gamma_3-\Gamma)}+\frac{E_4}{(\Gamma_3-\Gamma)^2}+\frac{E_5}{(\Gamma_3-\Gamma)^3}\sum_{n=6}^{\infty}\frac{E_n}{(\Gamma_n-\Gamma)}. \quad (35)$$

Then

$$E(z)=E_1e^{-\Gamma_1z}+E_2e^{-\Gamma_2z}+(E_3+E_4z+E_5z^2)e^{-\Gamma_3z}+\sum_{n=6}^{\infty}E_ne^{-\Gamma_nz} \quad (36)$$

where

$$E_1=\left\{(\Gamma_1-\Gamma)E(-\Gamma)\right\}_{\Gamma=\Gamma_1} \quad (37)$$

$$E_2=\left\{(\Gamma_2-\Gamma)E(-\Gamma)\right\}_{\Gamma=\Gamma_2} \quad (38)$$

$$E_3=\left\{\frac{1}{2}\frac{d^2}{d\Gamma^2}\left[(\Gamma_3-\Gamma)^3E(-\Gamma)\right]\right\}_{\Gamma=\Gamma} \quad (39)$$

$$E_4=\left\{\frac{d}{d\Gamma}\left[(\Gamma_3-\Gamma)^3E(-\Gamma)\right]\right\}_{\Gamma=\Gamma} \quad (40)$$

$$E_5=\left\{(\Gamma_3-\Gamma)^3E(-\Gamma)\right\}_{\Gamma=\Gamma_3} \quad (41)$$

and

$$-\Gamma_1=-j\beta_e+\beta_eC\delta_1 \quad (42)$$

$$-\Gamma_2=+j\beta_e-\beta_eC\delta_2 \quad (43)$$

$$-\Gamma_3=-j\beta_e \quad (44)$$

and where δ_1 and δ_2 are obtained from (11) and (21). Eq. (36) indicates that there are three growing waves in this type of tube: one growing linearly, another as z^2, and the usual exponentially increasing wave.

Performing the operations indicated in (37) through (41) yields, for small C and $d=0$:

$$E_1\cong E_0\frac{(\delta_1^3+je^{-\theta\delta_1})}{\delta_1^3+j\left[\frac{6}{\theta\delta_1}-2-\left(4+\theta\delta_1+\frac{6}{\theta\delta_1}\right)e^{-\theta\delta_1}\right]} \quad (45)$$

$$E_2\cong 0 \quad (46)$$

$$E_3\cong E_0\left[\frac{\frac{\theta^2}{2}}{\left(b+\frac{\theta^2}{6}\right)}-\frac{\frac{\theta^4}{12}+j\theta}{\left(b+\frac{\theta^2}{6}\right)^2}+\frac{\frac{\theta^6}{144}-\frac{\theta^4}{40}\left(b+\frac{\theta^2}{6}\right)+j\frac{\theta^3}{6}-1}{\left(b+\frac{\theta^2}{6}\right)^3}\right] \quad (47)$$

$$E_4\cong\frac{E_0}{L}\left[-\frac{\theta^2}{\left(b+\frac{\theta^2}{6}\right)}+\frac{\frac{\theta^4}{12}+j\theta}{\left(b+\frac{\theta^2}{6}\right)^2}\right] \quad (48)$$

$$E_5\cong\frac{E_0}{L^2}\left[\frac{\theta^2}{\left(b+\frac{\theta^2}{6}\right)}\right]. \quad (49)$$

To include loss, $(b-jd)$ may be substituted for b in the above equations.

It may be shown from (45) through (49) that, for $\theta\delta\ll1$ and for $\theta\delta\gg1$, the sum of the waves E_1 through E_5 at $z=0$ has a value within a few per cent of E_0. Since the sum of all the waves at $z=0$ must be E_0, this calculation indicates that the sum of all E_ns for $n>5$ must be very small. Since all of these waves with $n>5$ must decay rapidly beyond $z=0$, the only situation in which their neglect could introduce serious error would be if the amplitudes of several were very large and their phases were such as to cancel at the input. It can be shown, by taking both real and imaginary parts of Γ to be much greater than β_e in (34) that, for this condition

$$E(-\Gamma)\cong\frac{1}{\Gamma} \quad (50)$$

which is to say the numerator and denominator of (34) are equal except for the factor Γ^{-1}. So, for large Γ, there are zeros of the numerator of (34) very near all the zeros of the denominator. This result means that, as the values of the Γ's for these other roots approach infinity, their amplitudes approach zero, because for this condition

$$E_n=\left[\frac{\Gamma_n-\Gamma}{-\Gamma}\right]^{\Gamma=\Gamma_n}=0. \quad (51)$$

Hence, the only waves of this sort that can have appreciable amplitude are those relatively close to the origin of the Γ plane. The authors do not know whether or not there are any roots of (34) close enough to the origin to be significant.

In order to compute the gain according to the usual $A+BCN$ formula, it is necessary to know the value of A for the growing wave as given by

$$A=20\log_{10}\left|\frac{E_1}{E_0}\right|. \quad (52)$$

The value of A, for $b=d=0$, has been calculated from (45) and the result is plotted as a function of CM in Fig. 7.

It is also desirable to know how long the tube must be in terms of CN in order for the $A+BCN$ formula to

[6] M. F. Gardner and J. L. Barnes, "Transients in Linear Systems," John Wiley and Sons, New York, N. Y., chs. 6, 8; 1942.

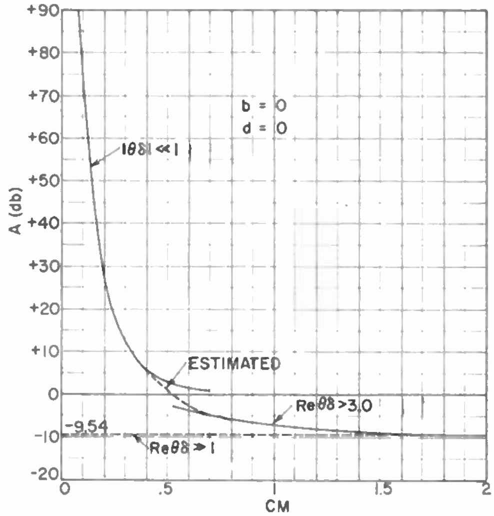

Fig. 7—The value of A, the initial loss or gain of the exponentially increasing wave, in a transverse-current traveling-wave tube as a function of CM for $b=d=0$. For large values of CM, the value of A approaches -9.54 db, its value in the conventional traveling-wave tube.

be reasonably accurate. By computing the total field as a function of CN from (36), and (45) through (49), for a typical small θ case, as has been done in Fig. 8, it can

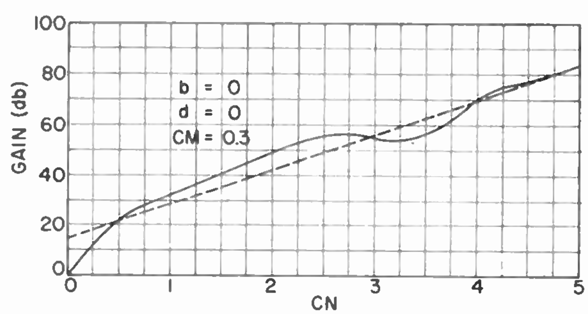

Fig. 8—How the signal level varies along a transverse-current traveling-wave tube for the special case of $b=d=0$ and $CM=0.3$ (solid curve). The dashed curve is the level of the exponentially increasing wave alone, which starts off with an apparent gain of 15 db. The value of CN must be greater than 0.4 before the $A+BCN$ equation is an accurate expression for the gain of a tube with this value of CM.

be seen that in this case the additional growing waves in the transverse tube remain of some importance out to $CN=4$, but at least an approximate answer can be obtained from the asymptotic formula for CN greater than the value at the crossover at $CN=0.5$. For smaller values of CM, greater values of CN are required before the asymptotic curve is a useful approximation. Both the value of CN for the first crossover and the amount of departure from the asymptotic curve are greater. For example, for $CM=0.159$, $b=d=0$, the crossover occurs at $CN=1.4$, the curve rises above the asymptotic curve by more than 30 db, and a close approximation is not reached until CN is greater than 75. It is evident then, that for small CM, it is desirable to compute the gain including all of the growing waves, rather than just the exponentially increasing wave.

Power Output

An estimate of maximum power output can be made from the linear analysis by solving for the power on the circuit corresponding to some estimated maximum value of ac current in the beam. The mechanism of beam saturation in the transverse tube, however, is different from that of the conventional tube because the beam cannot saturate as a whole. Instead, individual current elements reach maximum ac current in progression along the length of the tube. This process is easiest to visualize in one of the two-dimensional forms of the device. Fig. 9 is a top view of the Fig. 1(a) tube in which

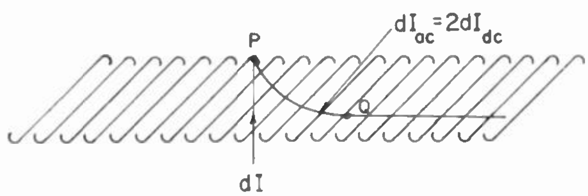

Fig. 9—A portion of the tube of Fig. 1(a) showing the general form of beam saturation in this type of tube. A contour of constant ac current equal to twice dc current is indicated for heavily overdriven conditions.

a current element dI first becomes fully bunched at point P as it is just leaving the tube. The wave is visualized as growing to the right in this figure, so elements to the right of dI will reach maximum current closer to the respective points of entrance than P, with the result that a line of maximum ac current takes the form shown. It seems reasonable to postulate that eventually a point will be reached at which an element of the beam will extract as much energy from the circuit beyond its point of maximum current as it gave up to the circuit in reaching the condition of maximum current. The point Q is indicated as such a point in Fig. 9. Beyond Q to the right the system is in equilibrium, with each element contributing no net energy to the fields on the circuit. As input power is varied, the points P and Q maintain their relationship to each other but move back and forth along the circuit to left or right. If this is a correct picture of the saturation mechanism, it is to be expected that the output power will be independent of the input power over a range of input powers sufficient to move the points P and Q from one end of the tube to the other. This is the observed result.

To obtain an estimate of the value of the maximum power to be expected, it is evident from the above that it is necessary to solve for the condition of saturation of a single element of current. Following Pierce's approach to the conventional tube, it will be assumed that the maximum value of ac current in a single element is equal to twice the dc current in that element and that only the exponentially increasing wave has significant amplitude.

An expression for the ac current in a single element can be obtained by substituting $Ee^{-\Gamma z}$ for $E(\zeta)$ in (2) and integrating. The result is

$$di(z, \xi) = \frac{jJ_0 d\xi \beta_e E_e^{-\Gamma z}}{2V_0(j\beta_e - \Gamma)^2}\left[1 - e^{-(j\beta_e - \Gamma)L}(1 + (j\beta_e - \Gamma)L)\right]. \quad (53)$$

Setting ac current equal to twice dc current

$$di(z, \xi) = 2J_0 d\xi \quad (54)$$

and solving for $|E|$, using (7) and (10)

$$E = \frac{4V_0\beta_e C^2\delta^2}{\left[1 - e^{-\theta\delta}(1 + \theta\delta)\right]}. \quad (55)$$

Using the definitions of K and C

$$P = \frac{J_0 L}{8V_0}\frac{E^2}{\beta^2 C^3} \quad (56)$$

and substituting (55) in (56)

$$P = kCJ_0 L V_0 \quad (57)$$

where

$$k = \frac{2\delta^4}{\left[1 - e^{-\theta\delta}(1 + \theta\delta)\right]^2}. \quad (58)$$

As before, it is interesting to consider the cases of large and small $\theta\delta$. For Re $\theta\delta$ large, the denominator of (58) approaches unity and k approaches $2\delta^4$, its value for the conventional tube. For small $\theta\delta$, it is easily shown that

$$k \approx \frac{8}{\theta^4} \approx \left[\frac{.268}{CM}\right]^4. \quad (59)$$

A plot of k vs CM is given in Fig. 10. One fact brought out by (59) is that for small $\theta\delta$, power and efficiency are independent of the velocity parameter b and the loss parameter d, unlike the result for the conventional tube. Also, (59) shows an apparently increasing power and efficiency as θ is decreased. However, it is important to note that J_0L is the dc current passing a given z plane, not the total dc current in a physical tube. As CM is decreased, the tube length must be increased to provide the same gain, and hence the total current must be increased. Since gain is proportional to $(CM)^6$ and k is proportional to $(CM)^{-4}$, the over-all efficiency of a tube with a constant gain, but variable CM, will be proportional to $(CM)^2$. In other words, the increase of dc current required to maintain a constant gain, as CM is reduced, more than compensates for the increase in efficiency due to decreasing CM and increasing k in (59); so that the over-all efficiency approaches zero as $(CM)^2$ as CM is reduced. Thus, the power output does increase as CM is decreased, but the over-all efficiency decreases. It is important to note that this entire discussion applies only to a tube in which the exponentially growing wave is dominant, a condition difficult to realize for small CM, as seen in connection with Fig. 8. In a short small CM tube, the saturation level will depend on the saturation of several waves of current rather than only one, so Fig. 10 is not applicable. The dependence of power output on power input should, however, remain the same for this case.

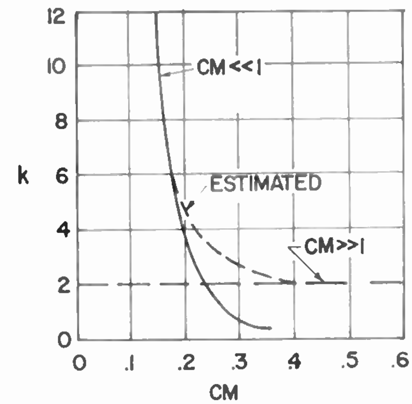

Fig. 10—The efficiency parameter k as a function of CM for $b=d=0$, calculated by taking the power as that given by linear theory for an ac current with a peak value twice the dc current in a single current element and for conditions in which only the exponentially increasing wave has significant amplitude. For large values of CM, the value of k approaches 2, its value for the conventional traveling-wave tube.

Appendix

Starting from the force equation, definition of current, and the continuity equation, Pierce's eqs. (2.11), (2.17), and (2.19), a differential equation form of Pierce's eq. (2.22) may be derived. It takes the form

$$\frac{d^2 i}{dz^2} + j2\beta_e\frac{di}{dz} - \beta_e^2 i = \frac{j\beta_e I_0}{2V_0}E. \quad (60)$$

If the Laplace transform of this equation is taken, again using $-\Gamma$ as the transform variable, it yields

$$i(-\Gamma) = \frac{j\beta_e I_0}{2V_0}\frac{E(-\Gamma)}{(j\beta_e - \Gamma)^2} + \frac{i(0)(j2\beta_e - \Gamma) + i'(0)}{(j\beta_e - \Gamma)^2}. \quad (61)$$

The inverse transform of (61) gives

$$i(z) = \frac{jI_0}{2V_0}\int_0^z E(\zeta)\beta_e(z - \zeta)e^{-j\beta_e(z-\zeta)}d\zeta + e^{-j\beta_e z}\left[i(0)(1 + j\beta_e z) + z i'(0)\right] \quad (62)$$

or expressing $i'(0)$ in terms of the ac velocity v, and the dc charge density ρ_0

$$i(z) = \frac{jI_0}{2V_0}\int_0^z E(\zeta)\beta_e(z - \zeta)e^{-j\beta_e(z-\zeta)}d\zeta + e^{-j\beta_e z}\left[i(0) + j\beta_e z\rho_0 v(0)\right]. \quad (63)$$

A similar equation, originally derived by Petrie, Strachey, and Wallis, appears in an article by Pierce and Shepherd.[7]

Acknowledgment

The early work on this tube was supported jointly by the Air Force, Army, and Navy, under contract with Stanford University. Later work was supported by the General Electric Company, also under contract with Stanford University. The authors are indebted to J. W. Christie for the calculation of the curve in Fig. 8.

[7] J. R. Pierce and W. G. Shepherd, "Reflex oscillators," *Bell. Sys. Tech. J.*, vol. 26, pp. 460–681; July, 1947. Eqs. (h7)–(h10), p. 664.

An Experimental Transverse-Current Traveling-Wave Tube*

D. A. DUNN†, ASSOCIATE MEMBER, IRE, AND W. A. HARMAN‡, ASSOCIATE MEMBER, IRE

Summary—**A transverse current traveling-wave tube employing a flat helix and a skew beam has been built and tested both as a forward wave amplifier and as a backward wave oscillator. The tube operates as an amplifier over the frequency range from 1 to 2 kmc with a power output of the order of 30 milliwatts. Tests on the tube indicated a gain vs voltage characteristic markedly different from that obtained with a conventional traveling-wave tube, particularly with respect to the wide range of current and voltage over which a large amount of attenuation in excess of the cold insertion loss of the circuit was observed. The general shapes of the curves of gain vs current and the gain and saturation power level vs frequency are as predicted from theory and display significant differences from calculated curves for an equivalent conventional tube. The nonlinear behavior of the tube, as a function of input signal level, follows the general pattern predicted from qualitative arguments. The output power is constant to within 0.05 db over an input power range of 20 to 30 db. With two signals of different frequencies supplied to the input of the tube, a region of operation was observed in which, with the input amplitude of one signal fixed, the output amplitudes of both signals were independent of the amplitude of the other (variable) input signal.**

Introduction

EXPERIMENTAL RESULTS on a transverse current traveling-wave tube employing a flat sheet beam passing over the surface of a flat helix will be described. This is the skew beam type of tube described in a companion paper.[1] A transverse current tube built in 1949, in which the circuit elements were skewed with respect to the direction of power flow on the circuit, has been described previously by one of the authors[2] and by Field[3] and Kompfner.[4] The results on this early tube were somewhat incomplete, partly because the tube was put together without an attenuator, and hence could only be operated under restricted conditions of current and voltage without oscillation. In the tube to be described, attenuation was provided by the losses of the circuit, which amounted to around 30 db of loss at the frequency for which maximum gain was obtained. In the early tube the corresponding loss was less than 2 db. It has been found that the limiting property of the tube; *i.e.*, its property of providing an output power independent of input power, was not changed by the presence of distributed loss. Over a range of input powers of 20 to 30 db, the output power did not vary, within the accuracy of the power meters used; *i.e.*, within about 1 per cent. A number of other unusual characteristics of the tube will be described, the most unexpected being the broad-band "Kompfner dip" condition and the two-signal nonlinear performance.

The next section will describe the construction of the tube and the electrical properties of the circuit. The following section includes the calculation of the usual parameters of the tube, such as C, N, etc., and the overall gain and power output of an equivalent conventional tube. The performance of this equivalent tube is compared with the measured small signal performance of the experimental transverse current tube. A comparison is also made of the theoretical transverse current tube characteristics for zero space charge with the measured results and with zero space charge performance of the equivalent conventional tube. The last section describes the measured nonlinear performance of that tube.

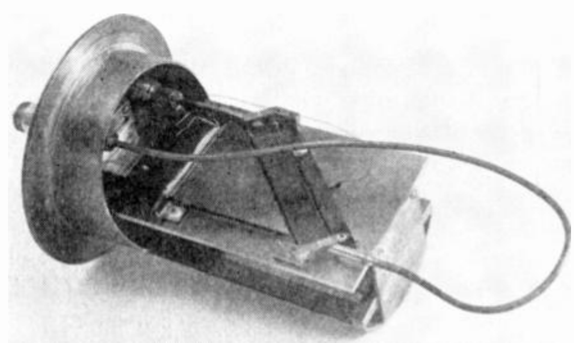

Fig. 1—The experimental transverse current traveling-wave tube. The flat sheet beam passes under the helix.

Tube Construction and Cold Circuit Properties

A photograph of the experimental tube is shown in Fig. 1. The rf input connection is made through the coax line at the far end of the helix and the rf output connection is made through the coax line at the near end that loops over the helix to the N-connector visible at the left. The beam passes between the triangular shaped plates, under the helix, to the collector plate which has its dc lead looping over the output coax. The picture will be made clearer by reference to Figs. 2(a) and 2(b) which are, respectively, a plan view and an end view along the axis of the helix of the tube shown in Fig. 1. A stop-band plate was used in operating the tube as an amplifier and is indicated in Figs. 2(a) and 2(b); it was removed for the photograph in Fig. 1. It was simply a conducting metal plate spaced above the upper surface

* Original manuscript received by the IRE, December 1, 1955; revised manuscript received, February 13, 1956.

† Stanford University, Stanford, Calif.
‡ Formerly at Stanford University, Stanford, Calif., now at General Electric Microwave Lab., Palo Alto, Calif.

[1] D. A. Dunn, W. A. Harman, L. M. Field, and G. S. Kino, "Theory of the transverse current traveling-wave tube," this issue.
[2] D. A. Dunn, "Higher power traveling-wave tubes," thesis, Stanford University; 1950.
[3] L. M. Field, "Recent developments in traveling-wave tubes," *Electronics*, vol. 23, pp. 100–104; January, 1950.
[4] R. Kompfner, "Traveling-wave tubes," *Reports on Progress in Physics*, vol. 15, pp. 275–327; 1952.

of the helix by 0.001-inch thick mica strips. The beam was focused by a very strong magnetic field perpendicular to the cathode. The beam was defined by a 0.015-inch slit at the edge of the drift tube nearest the helix.

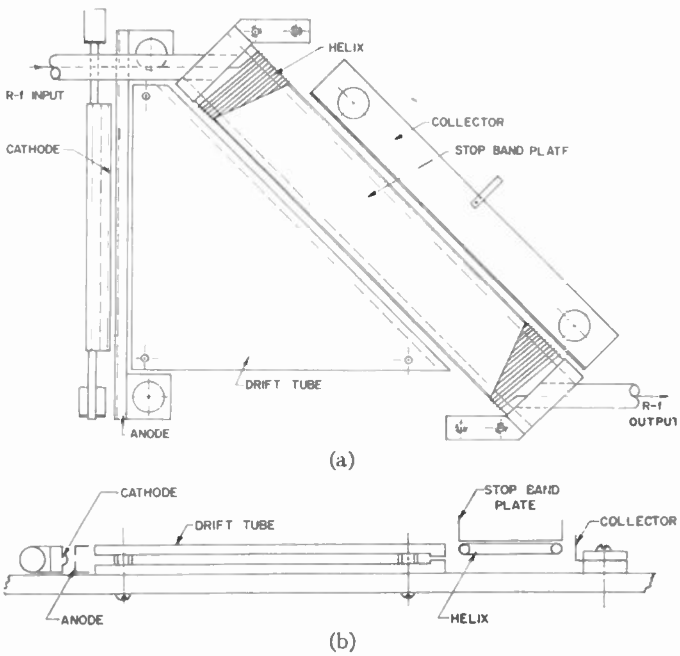

Fig. 2—(a) A plan view of the experimental tube; (b) an end view of the experimental tube looking down the axis of the helix.

The helix-beam configuration is as shown in Fig. 3, with dimensions in inches indicated. The helix is supported by two sapphire rods separated by a stainless steel support plate. The coaxial line input and output connectors have their outer conductors grounded to this plate. The plate was sufficiently far from the helix wires that it had no significant effect in the operating band of frequencies.

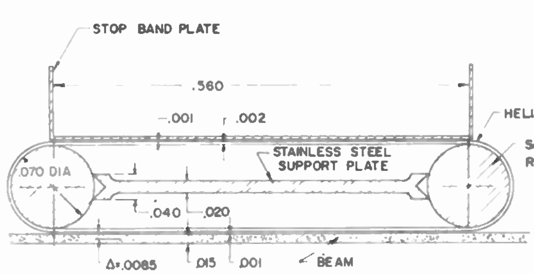

Fig. 3—An end view of the helix-beam configuration showing the stop-band plate used when operating the tube as a forward wave amplifier.

A list of the critical dimensions in inches of the circuit and beam is given in Table I.

TABLE I

Helix tape width	0.010
Helix tape thickness	0.002
Helix pitch	0.0238
Helix width between rod centers	0.560
Helix circumference	1.340
Helix length over-all	3.5
Cathode width	2.0
Beam thickness	0.015
Beam to helix spacing	0.001
Beam to helix angle	45°

The measured electrical properties of the circuit with the beam off and the stop band plate in position are listed in Table II.

TABLE II

Input and output vswr	Less than 2 to 1 from 1.6 kmc to 3.0 kmc. Considerably higher below 1.6 kmc.
Phase velocity	Constant, independent of frequency above 0.8 kmc, corresponding to a DLF of 0.76; *i.e.*, to a reduction in phase velocity of 0.76 as a result of dielectric loading.
Loss	Total loss essentially linearly proportional to frequency below 2.5 kmc, and having a value of approximately 0.4 db per guide wavelength.

Small Signal Performance

This section will present a comparison of the measured small signal performance of the transverse current tube with the theoretical performance of an equivalent conventional tube and with the zero space charge theory of the transverse current tube.

The calculation of the gain of the transverse current tube requires an expression for the impedance seen by a beam traveling above the surface of a helix at an angle. Expressions for this impedance and for C, d, M, and N as a function of the dimensions and measurable current and voltage are derived in the Appendix. A conventional traveling-wave tube having these values of C, d, and N has a theoretical gain vs frequency curve as indicated in Fig. 4, including the effects of space charge appropriate to the beam employed. The measured gain vs frequency curve for the transverse current tube is also shown in Fig. 4, and is seen to be both lower in magnitude and narrower. Both curves are for a value of beam voltage corresponding to maximum gain; in the measured curve only a few volts adjustment was necessary to obtain maximum gain at each frequency. Without a theory for the transverse current tube including space charge, it is difficult to say whether or not this shape could be predicted. An estimate can be made by comparing the theoretical gain vs frequency curves for zero space charge of the transverse current tube and the equivalent conventional tube based on the $A+BCN$ formulas. These are the two upper curves in Fig. 4. In order to compare the bandwidths of these four curves, which have different values of maximum gain, the bandwidths for which the gain has fallen by 10 per cent of the maximum number of db are computed. This is approximately the correct criterion for a comparison, because the BCN portion of the gain has the same shape on a db scale, regardless of the value of the peak, and A is not a rapidly varying function of QC, at least in a conventional tube. Making this comparison, it is seen from Fig. 4 that the ratio of the bandwidth of the transverse current tube to that of the equivalent conventional tube, first, theoretically, for $QC=0$, is

$$\frac{(f_{max}/f_{min})_{\text{transverse current tube}}}{(f_{max}/f_{min})_{\text{equivalent conventional tube}}} = \frac{1.83}{2.74} = .67.$$

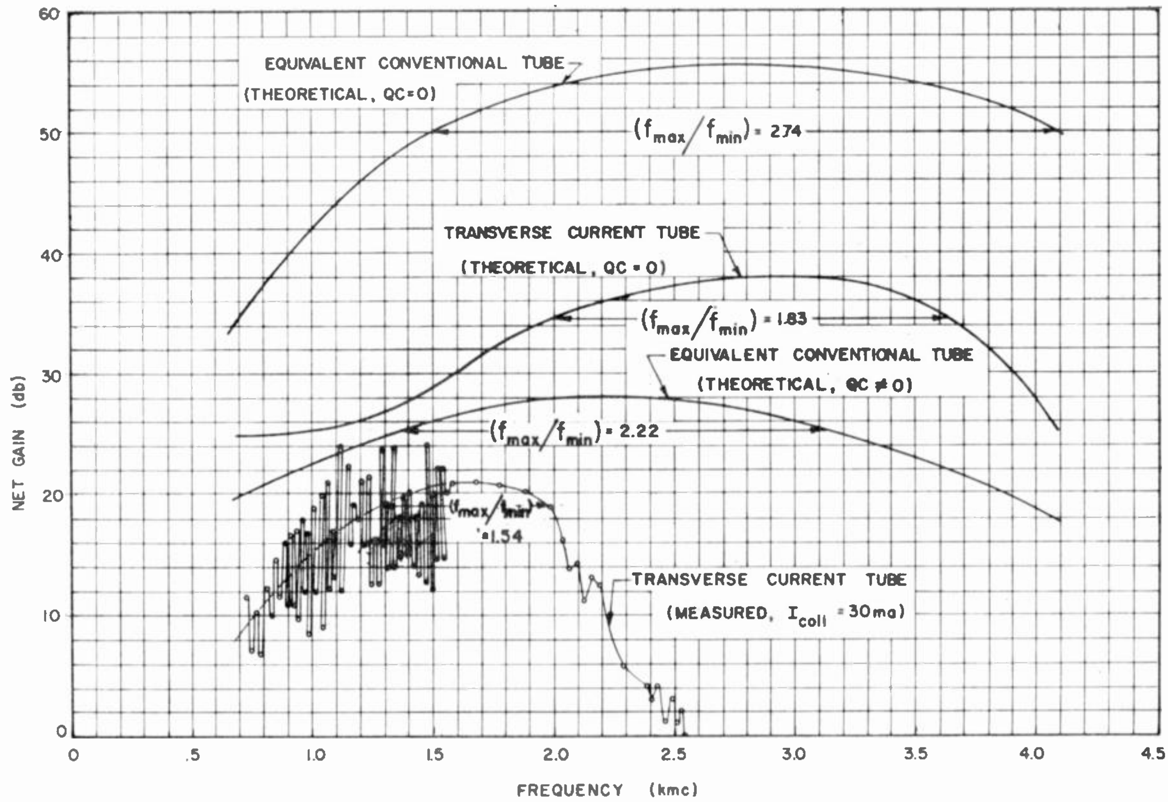

Fig. 4—A measured gain vs frequency curve for the experimental tube is compared with a theoretical curve for a transverse current tube with the parameters of the experimental tube, based on a zero-space charge theory. A conventional traveling-wave tube with the same C, N, and d as the transverse current tube has theoretical gain vs frequency curves as indicated.

This ratio may be compared with the ratio of the bandwidth of the measured curve for the transverse current tube to the theoretical bandwidth of the equivalent conventional tube including space charge.

$$\frac{(f_{\max}/f_{\min})_{\text{transverse current tube}}}{(f_{\max}/f_{\min})_{\text{equivalent conventional tube}}} = \frac{1.54}{2.22} = .69.$$

This comparison provides a partial explanation for the observed curve shape.

A measured curve of gain vs collector current for the transverse current tube is shown in Fig. 5. It is compared with a theoretical curve for the equivalent conventional tube including space charge. In this case, the calculation of the gain of the transverse current tube is a fairly elaborate procedure, because at low currents the amplitudes of several of the waves are important at the output. This calculation has not been performed. It is seen that the gain of the transverse current tube rises much more slowly than the gain of the equivalent conventional tube in the low current region, before the exponentially increasing wave becomes dominant. For very high currents the two curves should approach each other.

A measured set of curves of output power vs beam voltage, for a fixed value of input power at a fixed frequency, for several fixed values of beam current, is

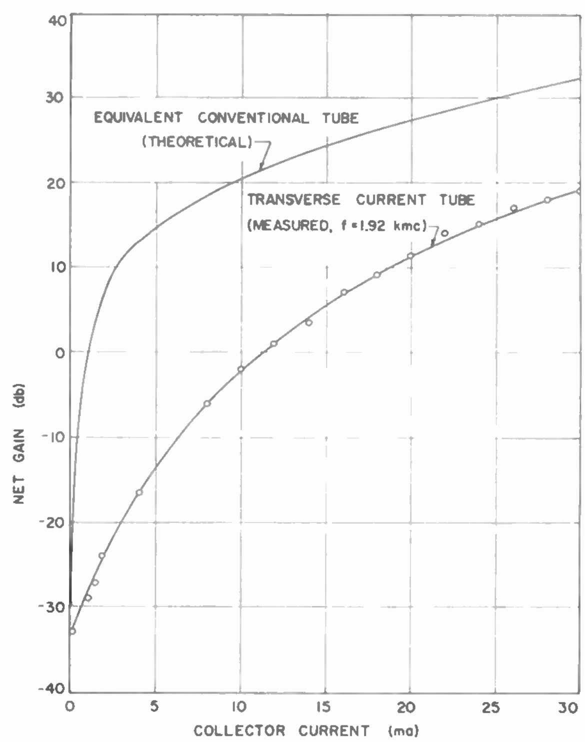

Fig. 5—Gain in db vs collector current for the experimental tube and a theoretical curve for the equivalent conventional tube.

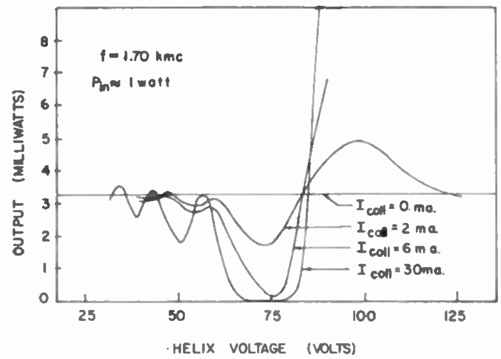

Fig. 6—Output power vs beam voltage for a fixed value of input power, for several values of collector current. At 30 ma there is a broad range of voltages over which the output is much lower than the level obtained with the beam turned off.

given in Fig. 6. The unusual feature of this set of data is that for all beam currents from about 10 ma to 30 ma the output was at least 30 db below the cold transmission level (the line for $I_{coll}=0$ ma in Fig. 6) at and for a a substantial range of voltages near 75 volts. It should be noted that the input level for this measurement was 30 db in excess of that necessary to saturate the tube at its gain peak. Similar patterns were obtained for smaller signals, but the detectable difference between the cold loss and the null was limited by crystal sensitivity, so that no definite statement can be made as to the depth of the null below the cold loss at very small signals. The comparable set of data for the conventional tube[5] shows a sharp null for a unique value of current and voltage; currents in excess of the correct value for cancellation do not cause a null. An application for this phenomenon is to be found as an attenuator for a traveling-wave tube in which one beam is employed to obtain gain and power and a transverse beam is adjusted for the null condition to provide attenuation in the backward direction. S. E. Webber in unpublished work has suggested the use of such an attenuator beam in a traveling-wave tube with two conventional beams traveling in opposite directions. The broad-band operation of such a tube is virtually impossible because of the requirement that the current and voltage in the attenuator beam both be correct for the null at all frequencies. L. M. Field[6] has attempted to operate a tube of this sort under narrow band conditions. The wide current and voltage range for large attenuation observed in the transverse current tube may make a broad-band tube of this sort possible.

One further piece of information predictable from a small signal analysis is the level of saturation power corresponding to an ac current in the beam equal to twice the dc current. Fig. 7 shows a plot of saturation power vs frequency for the experimental tube compared with theoretical curves for the transverse tube with zero space charge and for the equivalent conventional tube tube both with zero space charge and including space charge. The theoretical curves for the equivalent conventional tube include the effects of loss as a function of d according to Cutler and Brangaccio.[7] This estimate of the effect of loss is a more rapidly varying function of d than that of Pierce[8] and provides a curve as in Fig. 7 that drops more rapidly as frequency and d increase than would Pierce's estimate. It is seen, however, that the experimental curve still drops much more rapidly than either curve for the equivalent conventional tube. Using the estimated curve given in the companion paper for k as a function of CM and assuming, as a first approach, that the loss parameter, d, has the same effect here as in the conventional tube, so the Cutler and

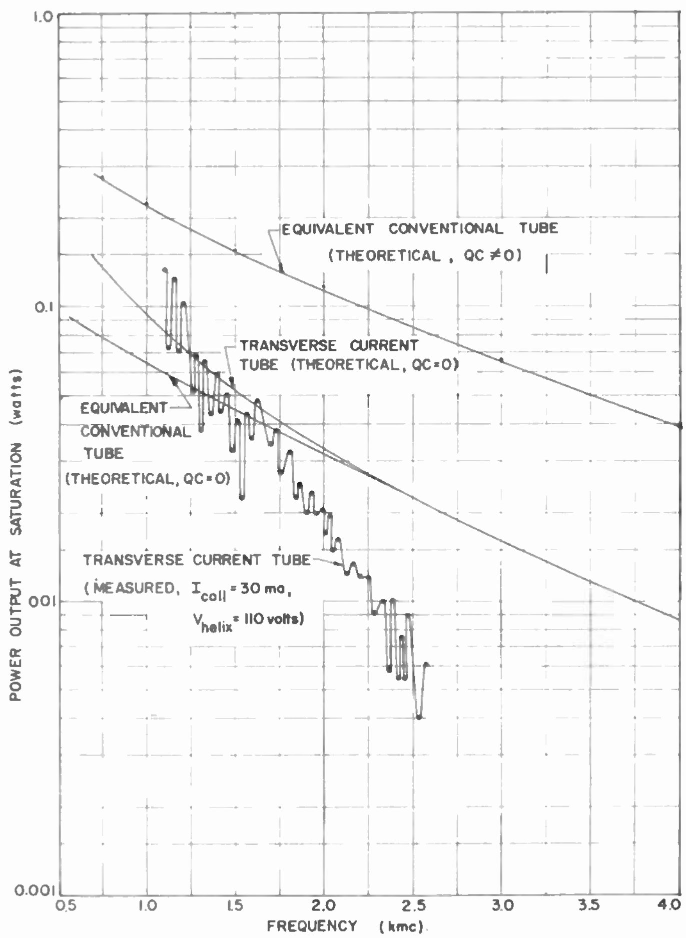

Fig. 7—Saturation power vs frequency for the experimental tube compared with theoretical curves for the transverse current tube and the equivalent conventional tube.

[5] R. Kompfner, "On the operation of the traveling-wave tube at low level," *J. Brit. IRE*, vol. 10, pp. 283–289; August–September, 1950.
H. R. Johnson, "Kompfner dip conditions," Proc. IRE, vol. 43, p. 874; July, 1955.
[6] L. M. Field, and C. C. Johnson, Quarterly Status Rept. Nos. 6, 7, and 8, Electron Tube Lab., California Instit. of Technology; 1954–1955.

[7] C. C. Cutler and D. J. Brangaccio, "Factors affecting traveling-wave tube power capacity," Trans. IRE vol. PGED-3, pp. 9–23; June, 1953.
[8] J. R. Pierce, "Traveling-Wave Tubes," D. Van Nostrand Co., Inc., New York, N. Y., p. 164; 1950.

Brangaccio curve may be used, the power output vs frequency curve given in Fig. 7 is obtained. It still does not vary as rapidly as the experimental curve. If, however, the effects of loss are taken into account more accurately, the curve rises more rapidly, because the effect of of loss is also a function of CM. The result would still have a different slope from the measured curve above 1.5 kmc. This difference may be a result of space charge effects, or it may have to do with the fact that the exponentially increasing wave is no longer dominant at these frequencies.

Measured curves of voltage vs frequency and starting current vs frequency for the experimental tube operated as a backward-wave oscillator are given in Figs. 8 and 9, respectively. The stop-band plate was removed for this measurement. Theoretical starting condition calculations for the transverse tube have not been carried out. Of interest, however, is the theoretical starting current curve, also shown in Fig. 9, for the equivalent conventional tube, calculated from theoretical curves of Johnson[9] and Watkins and Ash.[10] Actually what is plotted is 5.1 times the starting current of the equivalent tube, in order to compare equivalent currents. The equivalent conventional tube has a total beam current equal to J_0L, the current passing any cross section in the transverse tube, in order to give it the same C as the transverse tube. Since what is plotted for the transverse tube in Fig. 9 is the total beam current, or 5.1 times J_0L, the same constant has been used to multiply the current of the equivalent conventional tube.

Large Signal Performance

The most unusual feature of the transverse current tube is its large signal behavior. Typical power output vs power input curves take the form shown in Fig. 10 in which the output level does not change, within the accuracy of the measurement, over a 20 to 30 db range of power levels. It will be noted that, in this tube, this limiting behavior occurs for an input level sufficiently great to reduce the net gain to approximately zero db. In an earlier tube,[11] this region occurred with net gains of as great as 20 db. The principal difference between the two tubes was the amount of distributed loss. Here, as seen from Fig. 10, the loss was about 30 db at 1.98 kmc and about 40 db at 2.27 kmc, while in the early tube the loss was less than 2 db at the operating frequency. In both tubes, however, the shapes of the curves were about the same.

A related characteristic is the phase shift vs power input curve shown in Fig. 11 for a frequency of 2.0 kmc.

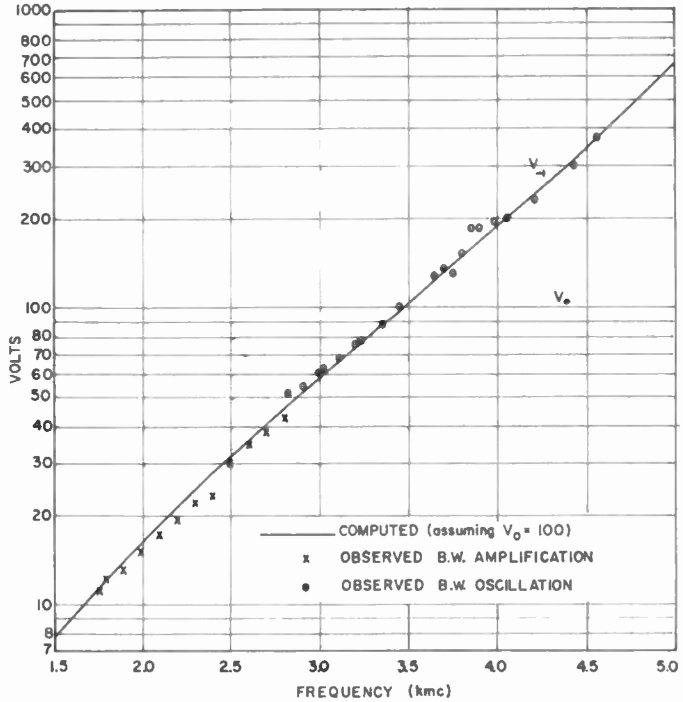

Fig. 8—A tuning curve for the experimental tube operated as a backward-wave oscillator.

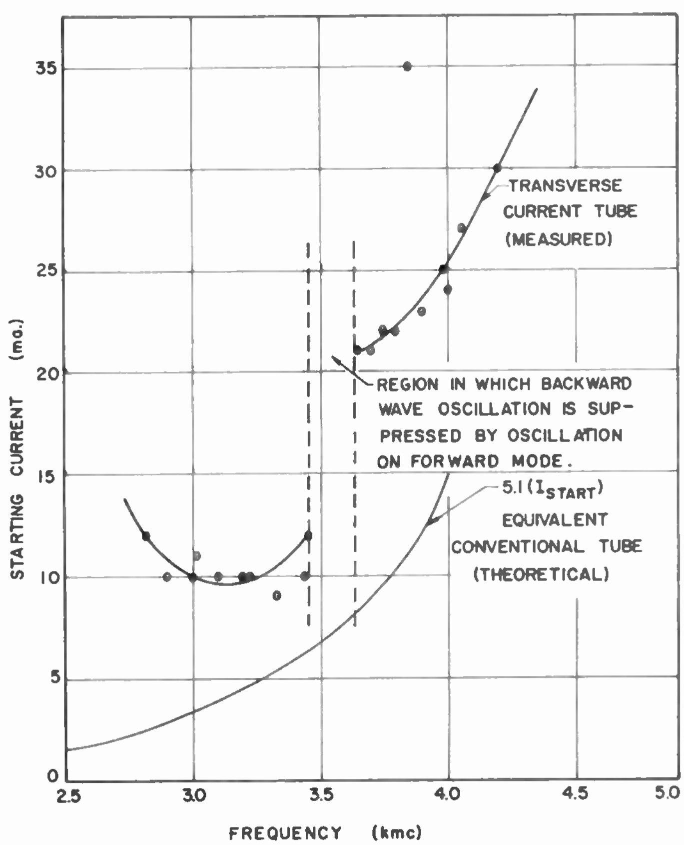

Fig. 9—Starting current vs frequency for the experimental tube operated as a backward-wave oscillator compared with a theoretical curve for the equivalent conventional tube.

[9] H. R. Johnson, "Backward-wave oscillators," Proc. IRE, vol. 43., pp. 684–697; June, 1955.
[10] D. A. Watkins and E. A. Ash, "The helix as a backward-wave structure," *J. Appl. Phys.*, vol. 25, pp. 782–790; June, 1954.
[11] D. A. Dunn, *loc. cit.*

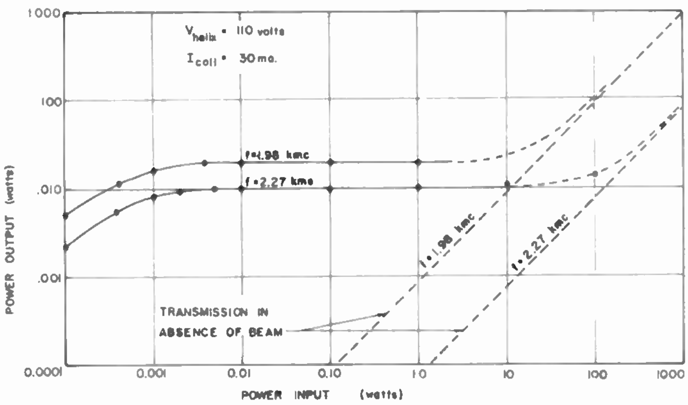

Fig. 10—Power output vs power input for the experimental tube at two frequencies. There is a wide range of input powers over which there was no measurable variation in output power.

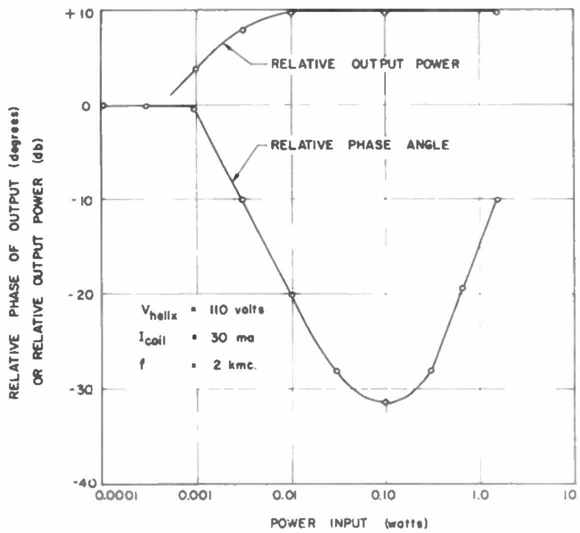

Fig. 11—Phase shift of the output signal relative to its small signal value vs power input and relative power output vs input at the same frequency.

A relative power output curve is shown in the same figure for the same frequency. The first onset of nonlinearity shows up in the phase shift characteristic as a sharp break, which occurs at an input level at which the output power is still increasing. The phase shift increases linearly over about a 15 db range of inputs; it then levels off, reaching a maximum excursion not far beyond the point of zero db net gain; it then decreases beyond this point.

A plausible qualitative explanation for this behavior may be given on the basis of the arguments given in the companion paper. Above some minimum power level, the tube may be considered to be divided into three sections: a first section nearest the input in which the behavior is linear; a second section in which the behavior is changing from linear to uniformly nonlinear; and a third section in which the behavior is uniformly nonlinear; *i.e.*, all currents elements in the third section follow the same curve of current vs distance along the direction of current travel, an equilibrium condition having been reached in this section. As the input level is varied, the relative amount of the tube given over to the first section in comparison with that given over to the third section varies, the second section being moved up and down the length of the tube. Under these conditions, the output power would be expected to remain constant as observed in Fig. 10. The phase angle of the output signal would be expected to change linearly in proportion to the db change in the input level, as in the section of the curve between the power inputs of 0.001 and 0.03 w in Fig. 11, because the gain in db is linearly proportional to tube length in the first section, and because the value of the phase shift per unit length in the linear section is presumably different from the value in the nonlinear section. A further explanation is required to account for the shape of the phase shift curve at higher input levels. A possible explanation may be made by considering the linear section of the tube to be made up of two regions, one with primarily an exponentially increasing wave near the output and another near the input in which the other growing waves are dominant. As the input level is increased, saturation will ultimately occur in the region in which the nonexponentially increasing waves are dominant. In this region, the gain in db is not linearly proportional to the length, so, as the input level is increased by a specified number of db, the length of the tube given over to uniformly nonlinear operation will not increase by the same number of centimeters as resulted from the same change in input level at lower signal levels. Hence, the output phase will no longer change linearly, when this condition is reached. An explanation of the fact that the phase change from linear conditions decreases above this point would require a detailed consideration of the phase shift in the region in which the nonexponentially increasing waves are dominant.

The two signal behavior of the transverse current tube at large signals is distinctly different from the behavior of a conventional tube. Typical characteristics are shown in Fig. 12, which is a plot of power output at 1.98 kmc and at 2.27 kmc as a function of power input at 1.98 kmc, for two values of power input at 2.27 kmc. The unusual feature of these characteristics is the fact that the power output at 2.27 kmc approaches a constant value as the power input at 1.98 kmc is increased above the level necessary to reach maximum output at 1.98 kmc. In a conventional tube, the variable amplitude signal (corresponding to 1.98 kmc in Fig. 12) reaches a maximum and decreases, while the fixed amplitude signal (corresponding to 2.27 kmc in Fig. 12) steadily decreases as the variable amplitude signal is increased. The smaller signal is suppressed by the larger (variable) signal; *i.e.*, the ratio of the amplitude of the large signal to the amplitude of the small signal is greater at the output of the tube than at the input. In the transverse tube, however, it is seen from Fig. 12 that the ratio of the large signal amplitude to the small signal amplitude at the output of the tube is a fixed value, once saturation by the variable signal is reached. It is quite possible for this ratio to be much smaller at the output of the transverse tube than at the input, depending on the relative signal levels. In particular, this will be so for very large values of the variable signal amplitude, as seen from Fig. 12.

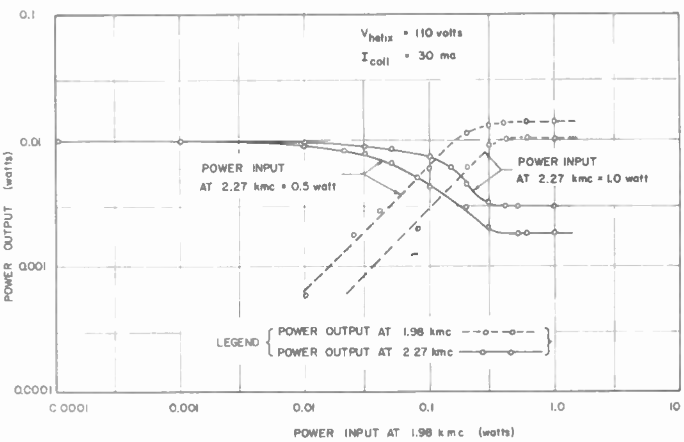

Fig. 12—When two signals at different frequencies are supplied to a transverse current tube, the power outputs at the two frequencies varies in the manner shown, as the input power levels of the two signals are varied.

In the two signal measurement of Fig. 12, the two frequencies used had saturation levels in the absence of each other differing by about 3 db. For this case, the curves as a function of the input amplitude of one of the signals will be different from the curves as a function of the input amplitude of the other signal. A complete family of curves of the type given in Fig. 12 is sufficient to determine curves of power output at both frequencies as a function of the power input at both frequencies; so, actually, only one set of curves is required even in this case. If the two signals in the absence of each other saturated at exactly the same power level, presumably the two sets of curves would be identical.

Appendix

Skew Beam Tube Parameters

Fig. 13 is a diagram of a skew beam tube viewed from above. The z direction is taken to coincide with the direction of beam travel; the z' direction is taken to coincide with the direction of electric field and power flow on the circuit. In the companion paper, the performance of a one-dimensional model of the transverse current tube was obtained in terms of the parameters C, M, and N defined for that model. Here it is desired to compute the values of these parameters in terms of the dimensions of the physical three-dimensional tube having the Fig. 13 configuration.

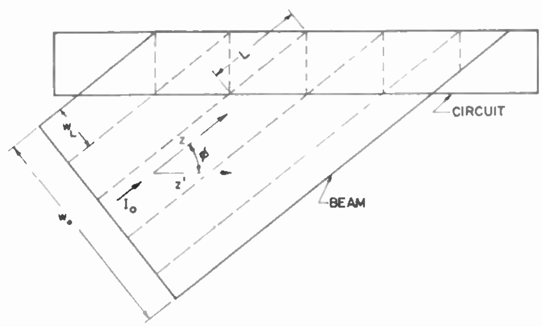

Fig. 13

First, assume that the value of the impedance of the circuit in terms of the field and β in the z' direction is given as

$$K_{z'} = \frac{E_{z'}^2}{2\beta_{z'}^2 P}$$

where

E_z' = field in z' direction

$\beta_{z'} = \dfrac{\omega}{v_{z'}}$

$v_{z'}$ = phase velocity in z' direction

P = total power flow in the z' direction for a field $E_{z'}$.

Now let

E_z = field in z direction

$\beta_z = \dfrac{\omega}{v_z}$

v_z = phase velocity in z direction.

Then from geometry

$$E_z = E_{z'} \cos \phi$$

$$v_z = \frac{v_{z'}}{\cos \phi}$$

$$\beta_z = \beta_{z'} \cos \phi.$$

So, the impedance of interest, in terms of field and β in the z direction, is exactly the same as the impedance in the z' direction.

$$K_z = \frac{E_z^2}{2\beta_z^2 P} = \frac{E_{z'}^2}{2\beta_{z'}^2 P}.$$

The value of C is defined for the one-dimensional model as

$$C^3 = \frac{KJ_0L}{4V_0}$$

where

K = impedance seen by the beam
J_0 = current per unit length in the direction of beam travel introduced into the interaction space
L = length of travel of a beam element
V_0 = beam voltage.

In terms of Fig. 13 quantities, L is as indicated, V_0 is the true beam voltage, K is K_z, as explained above, and J_0 may be defined in terms of the total current I_0 in a width w_0 as follows. The total current passing any cross section in the one-dimensional model is equal to J_0L. In Fig. 13, this current is the current in a width w_L. Then

$$J_0L = \frac{I_0}{w_0} w_L = \frac{I_0}{w_0} L \cos\phi \sin\phi.$$

The value of M in terms of Fig. 13 quantities is the same as in the one-dimensional model.

$$M = \frac{\beta_e L}{2\pi}$$

where

$$\beta_e = \frac{\omega}{u_0}$$

u_0 = electron velocity corresponding to V_0.

An approximation is required in the determination of N, because in Fig. 13 the circuit is not introduced abruptly at $z=0$ as in the one-dimensional model. One approximation is to calculate N as if the beam extended to infinity in both directions. In this case, the value of N corresponding to the width of beam w_0 is

$$\frac{N}{M} = \frac{w_0}{w_L} = \frac{w_0}{L \cos\phi \sin\phi}.$$

If, on the other hand, the two sections at each end are considered to have zero effect

$$\frac{N}{M} = \frac{w_0 - 2w_L}{w_L} = \frac{w_0}{L \cos\phi \sin\phi} - 2.$$

The best approximation lies between these extremes. For example, if the end sections are considered to each be half as effective as a section in the center of the tube

$$\frac{N}{M} = \frac{w_0 - w_L}{w_L} = \frac{w_0}{L \cos\phi \sin\phi} - 1.$$

In a long tube, where N/M is much greater than unity, the choice is, of course, unimportant.

It is of some interest to note the effect of varying the angle ϕ on CM, for a fixed width circuit; *i.e.*, if $L \sin\phi$ = const. It will be assumed that the axial phase velocity of the circuit, $v_{z'}$ is varied to maintain the beam voltage and v_z constant independent of ϕ, that γ times the spacing to the beam is held constant, and that the current per unit length, I_0/w_0, is constant.

$$CM = \left(\frac{KJ_0L}{4V_0}\right)^{1/3}\left(\frac{\beta_e L}{2\pi}\right)$$

$$= \left(\frac{\beta_e}{2\pi}\right)\left(\frac{K}{4V_0}\right)^{1/3} J_0^{1/3}L^{4/3}$$

$$= \left(\frac{\beta_e}{2\pi}\right)\left(\frac{K}{4V_0}\right)^{1/3}\left(\frac{I_0}{w_0} L \sin\phi\cos\phi\right)^{1/3}\left(\frac{L\sin\phi}{\sin\phi}\right)$$

$$= \text{constant} \times \frac{(\cos\phi)^{1/3}}{\sin\phi}$$

with the result that maximum CM is obtained with $\phi=0$. In a skew circuit tube, the maximum value of CM is obtained when $\phi=60°$, under the same assumptions.

The experimental tube employed a helix wound on a pair of ceramic rods separated by a metal plate as shown in Fig. 3 and discussed in connection with that figure. An estimate of the impedance of this circuit may be made from Pierce's developed helix theory.[12]

For a developed sheath helix having its axis aligned with the z direction, the impedance at the helix is given by

$$K_z = \frac{E_z^2}{2\beta^2 P} = \left(\frac{\gamma}{\beta}\right)^3 \frac{30}{ks}$$

where

p = helix pitch

$2\pi s$ = helix circumference when wrapped up

$$k = \frac{\omega}{c}$$

$$\beta = k\left(\frac{2\pi s}{p}\right)$$

$$\gamma^2 = \beta^2 - k^2.$$

Some question arises as to the proper reduction factors to apply to the above impedance formula to take into account the presence of dielectric loading and the effect of the stop-band plate. The authors have estimated the total reduction factor as a result of dielectric loading and the presence of the stop-band plate to be equal to the square of the dielectric loading factor. On this basis, the impedance at the helix is approximately

$$K_z = \frac{30}{ks}(\text{DLF})^2.$$

The impedance seen by the beam is approximately the value at the center of the beam. If Δ is the distance from the helix to the center of the beam, as indicated in Fig. 3,

$$K_z = \frac{30}{ks}(\text{DLF})^2 e^{-2\gamma\Delta}.$$

It has been shown that the impedance seen by a beam traveling at an angle ϕ to the axis of the helix is independent of the angle. The impedance of interest, then, using the dimensions listed in Fig. 3 and Table I, is, in terms of the frequency, f, in kmc

[12] J. R. Pierce, *op. cit.*, p. 31.

$$K \cong \frac{76.2}{f} e^{-.67f}.$$

A number of experimental measurements were made at a beam voltage of 110 v and a beam current of 30 ma. For this condition, using the expression for J_0 derived above

$$J_0 L = 5.85 \text{ ma}$$

$$C^3 = \frac{1.016 \times 10^{-3}}{f} e^{-.67f}.$$

The value of M at this beam voltage is, in terms of f

$$M = \frac{\beta_e L}{2\pi} = 3.47f.$$

Using the estimate discussed above that the two end sections of beam are half as effective as the central sections

$$\frac{N}{M} = \frac{w_0}{L \cos \phi \sin \phi} - 1$$

$$= 5.1 - 1 = 4.1.$$

So

$$N = 14.2f.$$

Acknowledgement

This work was supported by the General Electric Co. under a contract with Stanford University.

Some Effects of Magnetic Field Strength on Space-Charge-Wave Propagation*

GEORGE R. BREWER†, SENIOR MEMBER, IRE

Summary—An analysis is made of the propagation of space-charge waves in an axially symmetric electron beam originating at an emitting surface threaded by an arbitrary amount of magnetic flux. The propagation characteristics, for the fundamental radial mode with no azimuthal variations, are expressed in terms of the plasma-frequency reduction factor, graphs of which are shown. Approximate methods of evaluating the propagation characteristics of a beam in a helix are given, expressed in terms of the usual traveling-wave tube space-charge parameter Q and impedance parameter K.

Introduction

If a uniform electron plasma of infinite extent possesses a drift velocity u_0, it is possible for two space-charge waves to be propagated with phase constants $\gamma = \beta_e \pm \beta_p$. When a portion of this moving plasma is confined within a conducting cylinder, the charge accumulations corresponding to the bunches in the space-charge waves induce charges on the walls of the cylinder. These wall charges and the charge accumulations in the stream result in fields in the region of the space-charge flow which modify the debunching forces and thus change the frequency of oscillation of the moving electron plasma. The phase constants in this case are $\gamma = \beta_e \pm p\beta_p$ where p is called the plasma-frequency reduction factor.

Values of the plasma-frequency reduction factor for a cylindrical beam have been calculated for the case of an infinite confining magnetic field from the work of Hahn[1] or Ramo[2] and for a beam in "perfect" Brillouin flow by Rigrod and Lewis.[3] Since it is impossible to shield the emitting surface completely from the magnetic field, both of these focusing conditions are limiting values; the intensity of practical focusing fields lies between these extremes. Therefore, in this paper the characteristics of the space-charge waves which can be propagated along a cylindrical electron stream confined by a magnetic field of arbitrary intensity or with arbitrary magnetic flux threading the emitting surface will be determined. The results of the analysis will be applied to the case of an electron stream in a helix and approximate relations for the impedance parameter K and the space-charge parameter Q derived for a traveling-wave tube.

The procedure to be used here will generally follow that of Rigrod and Lewis. The magnitude of the electron perturbation from its steady-state trajectory will be determined from the equations of motion. This equation will then be combined with the field equations to determine the total field configuration inside of the stream;

* Original manuscript received by the IRE, March 12, 1956.
† Electron Tube Lab., Hughes Aircraft Co., Culver City, Calif.

[1] W. C. Hahn, "Small signal theory of velocity modulated electron beams," *GE Rev.*, vol. 42, p. 258; June, 1939.
[2] S. Ramo, "Space charge and field waves in an electron beam," *Phys. Rev.*, vol. 56, p. 276; August, 1939.
[3] W. W. Rigrod and J. A. Lewis, "Wave propagation along a magnetically focused cylindrical electron beam," *Bell Sys. Tech. J.*, vol. 33, p. 399; March, 1954.

applying the appropriate boundary conditions allows solution for the propagation constants.

The Equations of Motion

Using the Lagrangian formulation, the equations of motion can be written in component form as

$$\frac{\partial v_r}{\partial t} + v_r \frac{\partial v_r}{\partial r} + v_z \frac{\partial v_r}{\partial z} - r\dot{\theta}^2 = -\eta r\dot{\theta}B_0 - \eta E_r \quad (1)$$

$$\frac{\partial \dot{\theta}}{\partial t} + v_r \frac{\partial \dot{\theta}}{\partial r} + v_z \frac{\partial \dot{\theta}}{\partial z} + \frac{2v_r\dot{\theta}}{r} = \eta \frac{v_r}{r} B_0 \quad (2)$$

$$\frac{\partial v_z}{\partial t} + v_r \frac{\partial v_z}{\partial r} + v_z \frac{\partial v_z}{\partial z} = -\eta E_z. \quad (3)$$

Let[4]

$$\dot{\theta} = \dot{\theta}_0 + \dot{\tilde{\theta}} \qquad v_z = u_0 + \tilde{v}$$

and

$$r = r_0 + \tilde{r} \quad (4)$$

where the tilde denotes an ac term and the zero subscript a time-invariant term. The ac terms are assumed very small compared with the dc terms. It can be shown that for slow waves the contribution to the force equation of the ac magnetic fields and of E_θ are very small and can be neglected.

The total electron angular velocity can be expressed by means of Busch's theorem, which is essentially an integral of (2), as

$$\dot{\theta} = \omega_H - \frac{\eta\psi_c}{2\pi r^2} \quad \cdot \quad \omega_H = \eta B_0/2. \quad (5)$$

ψ_c is the total magnetic flux threading the cathode within the periphery of a stream line passing through r_0, the equilibrium radius of any electron in the beam. Using (4), this equation can be divided into a time-invariant part, giving the angular velocity of an unperturbed electron and a part due to the radius perturbation, with the result:

$$\dot{\theta}_0 = \omega_H - \Omega, \qquad \dot{\tilde{\theta}} = 2\frac{\tilde{r}}{r_0}\Omega \quad (6)$$

where $\Omega = \eta\psi_c/2\Pi r_0^2$.

The ac radial electric field E_r acting on an electron will consist of an ac term $\tilde{E}_r$ due to ac charges within and external to the beam plus a first-order ac term due to the motion of the electron through a region in which a dc electric field exists (the unperturbed beam). This latter term can be expressed as

$$\tilde{r}\left(\frac{\partial E_{r0}}{\partial r}\right)_{r_0} \quad (7)$$

where E_{r0} is the dc space-charge field. Considering the charge density, ρ_0, to be constant,

$$E_{r0} = \frac{\rho_0 r}{2\epsilon_0} \quad (8)$$

is the dc electric field at radius r. Using (8) and making use of the dc equilibrium conditions,[5]

$$\ddot{r}_0 = -\frac{\eta\rho_0 r_0}{2\epsilon_0} + r_0\dot{\theta}_0^2 - r_0\dot{\theta}_0\eta B = 0$$

Expression (7) becomes:

$$\eta\tilde{r}\left(\frac{\partial E_{r0}}{\partial r}\right)_{r_0} = \eta\tilde{r}\frac{\rho_0}{2\epsilon_0} = \tilde{r}(\dot{\theta}_0^2 - 2\omega_H\dot{\theta}_0). \quad (9)$$

The ac quantities are assumed to vary as exp $i\omega_b t$ with $\tilde{r} = \tilde{v}_r/i\omega_b$, $\omega_b = \omega - \gamma u_0$. Making these substitutions into (1), we obtain:

$$-\omega_b^2\tilde{r} - (r_0 + \tilde{r})(\dot{\theta}_0^2 + 2\dot{\theta}_0\dot{\tilde{\theta}}) + 2\omega_H(r_0 + \tilde{r})(\dot{\theta}_0 + \dot{\tilde{\theta}}) + \tilde{r}(\dot{\theta}_0^2 - 2\omega_H\dot{\theta}_0) = -\eta\tilde{E}_r \quad (10)$$

which becomes, keeping only first-order-ac terms:

$$\tilde{r} = \frac{\eta\tilde{E}_r}{\omega_b^2 - 4\Omega^2} \quad (11)$$

while (3) is reduced to

$$\tilde{z} = \frac{\eta\tilde{E}_z}{\omega_b^2}. \quad (12)$$

If the magnetic flux density threading the emitting surface is zero, (6) and (11) are reduced to the corresponding relations given by Rigrod and Lewis; while if $\omega_c = B_c\pi r_c^2$ and $B_c \to \infty$, they are reduced to the corresponding equations of Ramo.

Let us examine these comparisons briefly. The latter case can be understood easily, since an infinite value of magnetic field will constrain the electrons to rectilinear paths, preventing any transverse motion, which is the condition assumed by Ramo. In the case of a perfect Brillouin flow beam ($\psi_c = 0$, uniform charge density), the three forces acting on the electron in the dc state (centrifugal, space charge, and Lorentz) are in balance at all radii. Thus, a small perturbation from the steady-state condition will result in motion of the electron into a field region such that the force equilibrium condition is still maintained; that is, the inward Lorentz force and the outward space charge and centrifugal forces have the same functional variation with radius, so that a

[4] The z-directed dc velocity u_0 is assumed constant over the cross section of the beam. In the case of Brillouin flow with flux threading the cathode u_0 varies with r_0 as

$$\frac{u_0^2}{2\eta V_0} = 1 + \frac{2r_0^2\Omega(\omega_H - \Omega)}{2\eta V_0}.$$

Under usual conditions the second term is less than about 0.04. If the change in u_0 with r_0 is small compared with $(u_0/v) - 1 = p\omega_p/\omega = \omega_q/\omega$, where v is the phase velocity of the wave, the approximation of constant u_0 should be satisfactory. In typical cases ω_q/ω is greater than about 0.1, so that in both confined flow and Brillouin flow this is a reasonable approximation except for values of beam perveance in excess of about 5×10^{-6}.

[5] See, for example, J. R. Pierce, "Theory and Design of Electron Beams," D. Van Nostrand, New York, N. Y.; 1950. It is implicitly assumed here that the beam is substantially smooth so that $\ddot{r}_0 = 0$.

small perturbation does not upset the balance but merely results in a radial displacement of the perturbed electron. If a magnetic flux is now considered to thread the cathode, the above statements are no longer true. Eq. (5) shows that with $\psi_c \neq 0$, ω_H and $\dot{\theta}$ are no longer equal. Thus, while the steady-state equilibrium of forces can still be obtained, a small rf perturbation will bring the electron into fields varying with r in a manner other than directly, so that the force unbalance must result in the perturbed electron executing a motion including rotation (see Fig. 1). As a result of this rotation it is possible for a resonance to occur between the (Doppler) frequency of the signal as seen by the electron moving with the wave (ω_b) and the angular velocity of the perturbed electron ($\dot{\tilde{\theta}}$). This resonance is the physical cause of the singularity in (11).

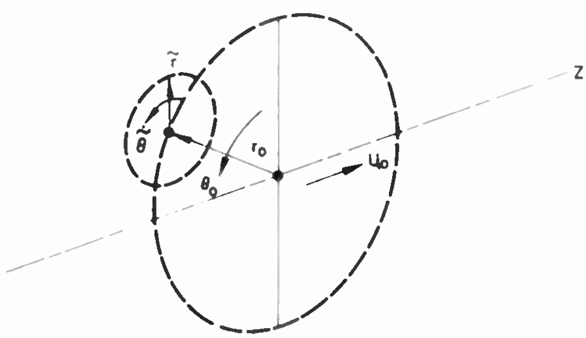

Fig. 1—Illustration of the perturbed electron motion. With flux threading the cathode the angular motion consists of the dc precession θ_0 plus ac rotation $\tilde{\theta}$.

The Field Equations

The field equations are:

$$\nabla_T^2 \tilde{E}_z - (\gamma^2 - k^2)\tilde{E}_z = \frac{1}{\epsilon_0} \nabla_z \tilde{\rho} + i\omega\mu_0 \tilde{J}_z \tag{13}$$

$$\tilde{H}_\theta = \frac{\omega\epsilon_0}{\gamma} \tilde{E}_r - \frac{j}{\gamma} \tilde{J}_r$$

$$\tilde{E}_r = \frac{j}{\gamma} \frac{\partial \tilde{E}_z}{\partial r} \tag{14}$$

where

$$k = \omega/c, \qquad \omega_p^2 = \frac{-\rho_0 \eta}{\epsilon_0}.$$

The ac charge density $\tilde{\rho}$ is found from

$$\nabla \cdot \tilde{J} = -i\omega\tilde{\rho}$$

and from (11) and (12) to be

$$\tilde{\rho} = \frac{i\rho_0}{\omega_b} \nabla \cdot \tilde{v} = \frac{i\rho_0}{\omega_b}\left[\frac{1}{r}\frac{\partial}{\partial r}(r\tilde{v}_r) + \frac{\partial \tilde{v}_z}{\partial z}\right]. \tag{15}$$

$$\tilde{\rho} = \frac{\omega_p^2 \epsilon_0}{\omega_0^2 \gamma} \frac{\partial^2 \tilde{E}_z}{\partial r^2} + \frac{\omega_p^2 \epsilon_0}{\omega_0^2 \gamma} \frac{1}{r} \frac{\partial \tilde{E}_z}{\partial r} - \frac{i\omega_p^2 \epsilon_0 \gamma}{\omega_b^2} \tilde{E}_z \tag{16}$$

where $\omega_0^2 = \omega_b^2 - 4\Omega^2$.

The convection current densities are:

$$\tilde{J}_r = \rho_0 \tilde{v}_r$$
$$\tilde{J}_\theta = \rho_0 \tilde{v}_\theta + \tilde{\rho} u_\theta$$
$$\tilde{J}_z = \rho_0 \tilde{v}_z + \tilde{\rho} u_0$$

from which (13) can be written

$$1/r \frac{\partial}{\partial r}\left(r \frac{\partial \tilde{E}_z}{\partial r}\right) - \left[\gamma^2 - k^2\left(1 - \frac{\omega_p^2}{\omega\omega_b}\right)\right]\tilde{E}_z = \frac{-i\gamma}{\epsilon_0} \tilde{\rho}\left[1 - k^2 \frac{u_0}{\gamma\omega}\right]. \tag{17}$$

It is assumed throughout that for the slow waves to be considered, $\gamma^2 \ll k^2$.

Using (14) and (16), (17) becomes:

$$\frac{\partial^2 \tilde{E}_z}{\partial r^2} + 1/r \frac{\partial \tilde{E}_z}{\partial r} - \gamma^2 \left[\frac{(\omega_p^2/\omega_b^2) - 1}{(\omega_p^2/\omega_0^2) - 1}\right]\tilde{E}_z = 0. \tag{18}$$

If

$$\tau^2 = \gamma^2 \left[\frac{(\omega_p^2/\omega_b^2) - 1}{(\omega_p^2/\omega_0^2) - 1}\right], \tag{19}$$

a solution to (18) is:

$$\tilde{E}_z = A I_0(\tau r), \tag{20}$$

which expresses the radial variation of rf electric field in the electron stream. It is seen that $A = \tilde{E}_z(r=0)$. Using (20), (17) becomes

$$\tilde{\rho} = \frac{i\omega_p^2 \epsilon_0 \gamma}{\omega_0^2}\left(\frac{\tau^2}{\gamma^2} - \frac{\omega_0^2}{\omega_b^2}\right)\tilde{E}_z \tag{21}$$

and $\tilde{H}_\theta$ can be written:

$$\tilde{H}_\theta = \frac{-j\omega\epsilon_0\tau}{\gamma^2}\left[1 - \frac{\omega_p^2 \omega_b}{\omega_0^2 \omega}\right] A I_1(\tau r). \tag{22}$$

The surface current resulting from the ac radius perturbations is

$$\tilde{G}_z = \rho_0 u_0 \tilde{r} = \frac{\rho_0 u_0 \eta \tilde{E}_r}{\omega_0^2}. \tag{23}$$

Using (12) and (21), the z-directed convection current density is

$$\tilde{J}_z = \frac{-i\omega_p^2 \epsilon_0}{\omega_b^2}\left(\omega - \gamma u_0 \frac{\omega_b^2}{\omega_0^2} \frac{\tau^2}{\gamma^2}\right) A I_0(\tau r)$$

so that the total body current is

$$\tilde{I}_B = 2\pi \int_0^b r\tilde{J}_z dr$$

$$= i\omega\epsilon_0 A 2\pi b^2 I_1(\tau b) \frac{\dfrac{4\Omega^2}{\omega_p^2} + p\dfrac{\omega_p}{\omega}(1 - p^2)}{p^2 \gamma b H} \tag{24}$$

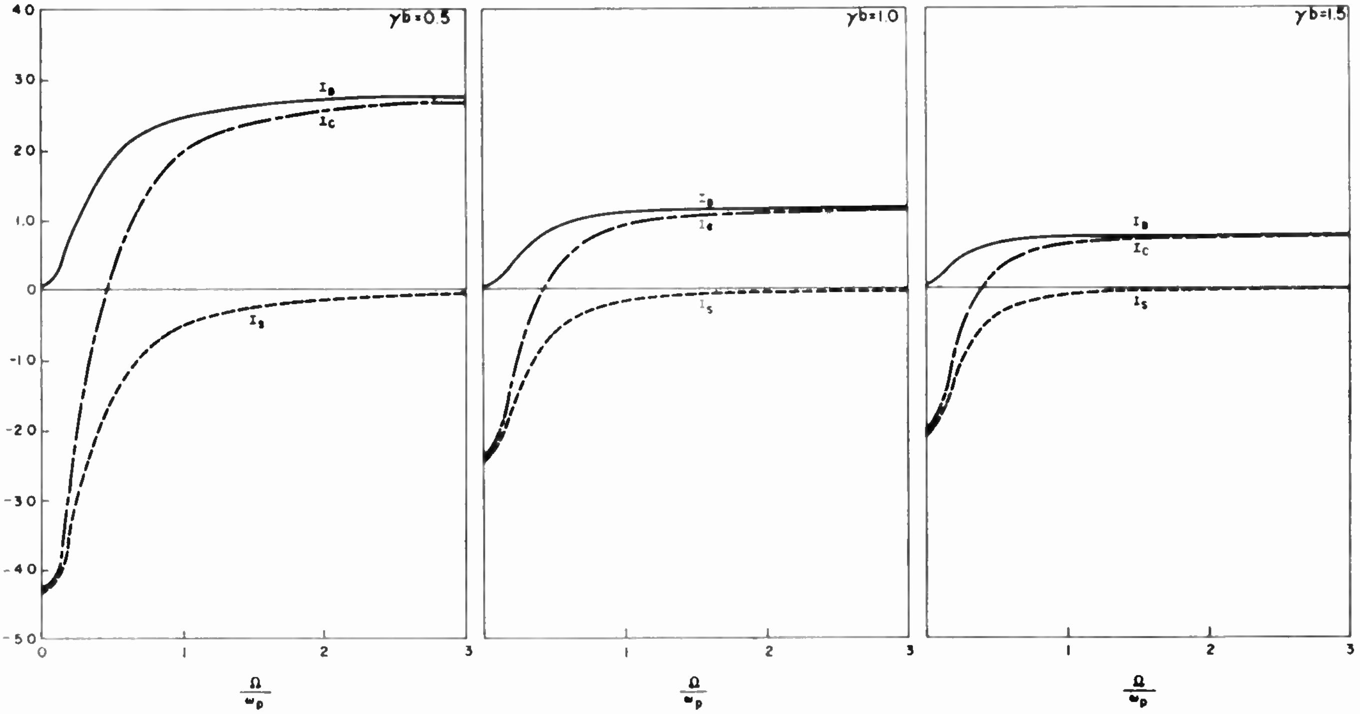

Fig. 2—Plot of the normalized beam convection currents. I_B denotes the body current, I_S the current carried by surface ripples, and I_c the total current. These curves show that for low values of Ω/ω_p the current is principally in the surface ripples while the body current predominates at large values of Ω/ω_p. The prime denotes that each current equation has been divided by $i\omega\epsilon_0 E_z(0)2\pi b^2 \cdot \omega_p/\omega \approx 0.1$.

where

$$H = \sqrt{\left(1 - p^2 + \frac{4\Omega^2}{\omega_p^2}\right)\left(\frac{1}{p^2} - 1\right)\left(p^2 - \frac{4\Omega^2}{\omega_p^2}\right)}$$

and from (23) the surface current density is

$$\tilde{G}_z = \frac{-i\omega_p^2\epsilon_0}{\omega_0^2}\,\frac{\tau u_0}{\gamma}\,A I_1(\tau r)$$

from which the total surface current is

$$\begin{aligned}\tilde{I}_S &= 2\pi b\tilde{G}_z \\ &= -\,i\omega\epsilon_0 A 2\pi b^2 I_1(\tau b)\,\frac{\left(\frac{1}{p^2} - 1\right)\left(1 - p\frac{\omega_p}{\omega}\right)}{H\gamma b}. \qquad (25)\end{aligned}$$

The total convection current in the beam is then

$$\begin{aligned}\tilde{I}_c &= 2\pi\int_0^b r\tilde{J}_z dr + 2\pi b\tilde{G}_z \\ &= i\omega\epsilon_0 A 2\pi b^2 I_1(\tau b)\,\frac{\frac{4\Omega^2}{\omega_p^2} - (1 - p^2)}{Hp^2\gamma b}. \qquad (26)\end{aligned}$$

Values of the body, surface, and total current are plotted in Fig. 2 as a function of the magnetic field parameter Ω/ω_p. It is seen that for small values of Ω/ω_p, the total current is principally in the surface perturbations while at large values of Ω/ω_p the body current is predominant.

Beam in a Drift Tube

The electronic admittance looking radially in at the beam boundary ($r = b$) is:

$$Y_e = \frac{\tilde{H}_\theta + \tilde{G}_z}{\tilde{E}_z} = \frac{-i\omega\tau\epsilon_0}{\gamma^2}\left[1 - \frac{\omega_p^2}{\omega_0^2}\right]\frac{I_1(\tau b)}{I_0(\tau b)} \qquad (27)$$

and the wall admittance evaluated at $r = b$ is[6]

$$Y_w = -\frac{\tilde{H}_\theta}{\tilde{E}_z} = \frac{-i\omega\epsilon_0}{\gamma}\left[\frac{I_1(\gamma b) - \delta K_1(\gamma b)}{I_0(\gamma b) + \delta K_0(\gamma b)}\right] \qquad (28)$$

where for a drift tube,

$$\delta = -\frac{I_0(\gamma a)}{K_0(\gamma a)}. \qquad (29)$$

Equating (27) and (28) we can determine values of the plasma-frequency reduction factor $p \equiv \omega_b/\omega_p$ (the notation $p = \omega_q/\omega_p$ is used by some writers) as functions of Ω/ω_p, γa, and b/a. Figs. 3 through 9 show, for example, that the present equation reduces to that of Rigrod and Lewis for $\Omega = 0$ and of Ramo for $\Omega \to \infty$; that for large values of Ω/ω_p the effect of the finite size of the stream (expressed by γb) is greater than that of the proximity of the wall, while for low values of Ω/ω_p the two effects are more comparable; that the total range in p from $\Omega = 0$ to $\Omega = \infty$, for typical values of parameters γb and b/a is about 40 per cent, and largest changes in p occur for Ω/ω_p between zero and one and one-half.

[6] See, for example, J. R. Pierce, "Traveling-Wave Tubes," D. Van Nostrand Co., New York, N. Y., p. 242; 1950.

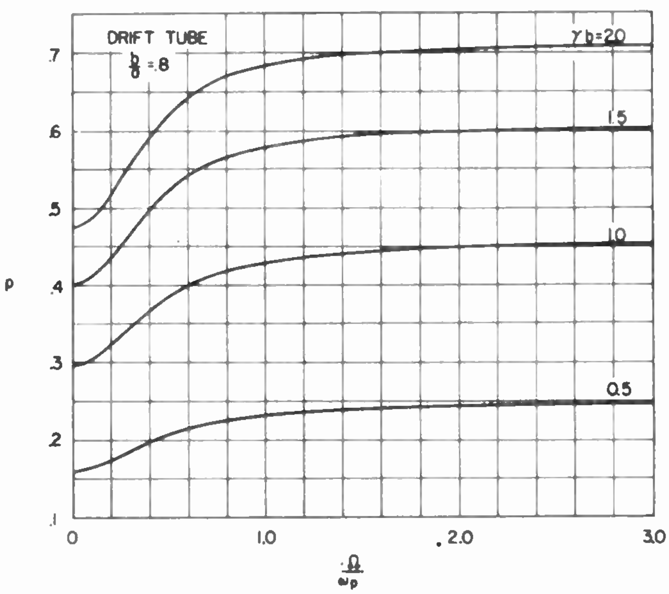

Fig. 3—Plot of the plasma-frequency reduction factor $p=\omega_b/\omega_p$ as a function of the magnetic field parameter Ω/ω_p, with γb as parameter, for a solid cylindrical electron beam in a conducting drift tube; $b/a=0.8$, $\Omega=\eta\psi_c/2\pi r_0^2$.

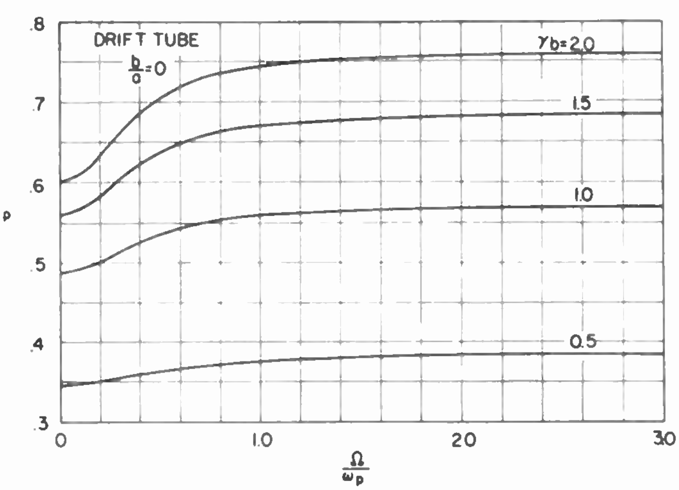

Fig. 4—Plot of the plasma-frequency reduction factor $p=\omega_b/\omega_p$ as a function of the magnetic field parameter Ω/ω_p, with γb as parameter, for a solid cylindrical electron beam in a conducting drift tube; $b/a=0$, $\Omega=\eta\psi_c/2\pi r_0^2$.

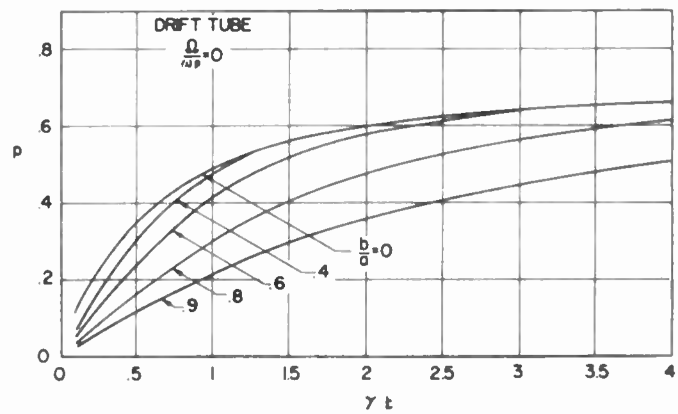

Fig. 5—Plot of the plasma-frequency reduction factor as a function of γb with b/a as parameter, for a solid cylindrical electron beam in a conducting drift tube with $\Omega/\omega_p=0$.

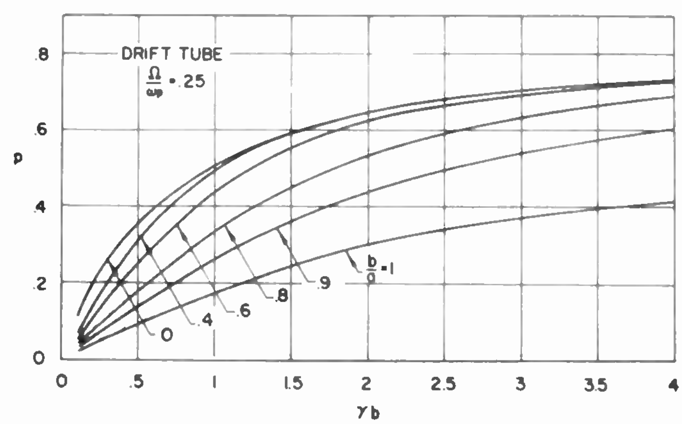

Fig. 6—Plot of the plasma-frequency reduction factor as a function of γb with b/a as parameter, for a solid cylindrical electron beam in a conducting drift tube with $\Omega/\omega_p=0.25$.

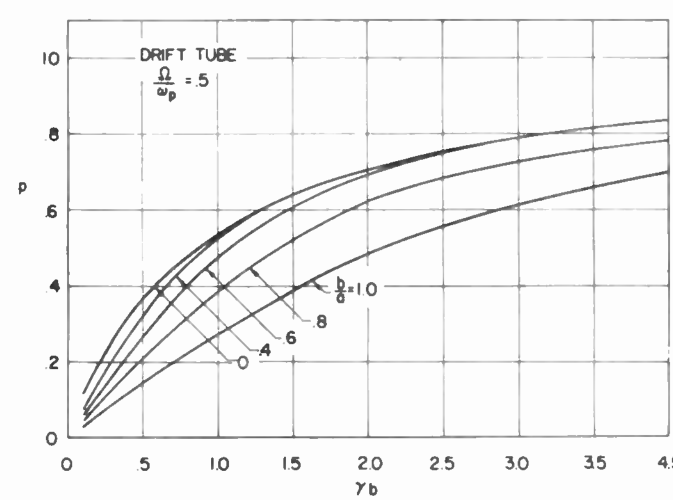

Fig. 7—Plot of the plasma-frequency reduction factor as a function of γb with b/a as parameter, for a solid cylindrical electron beam in a conducting drift tube with $\Omega/\omega_p=0.50$.

For a beam in Brillouin flow $\psi_c=\pi r_c^2 B_c$, where B_c is the flux density at the cathode of radius r_c, if B_c is uniform over the area of the cathode. In this case the dc equilibrium conditions used in (9) are correct (if the beam is injected properly so that no dc scollops are present) so that the results of the analysis are applicable. With immersed or confined flow focusing, $\psi_c=\pi r_c^2 B$ so that $\Omega/\omega_p=\omega_H/\omega_p$ if $r_c=r_0$, and the beam will always exhibit dc scollops. One could solve the dc beam equations and, including a dc radial velocity term, presumably solve (1) exactly. However, let us assume that the confined flow beam can be considered essentially smooth. The present theory is then an approximate representation of confined flow for ω_H/ω_p greater than about two, where the dc beam scollops are relatively small. The main effect of the stationary dc scollops would be to cause the electrons to move in a periodically varying field, which would not appear to cause a first-order change in the propagation characteristics.

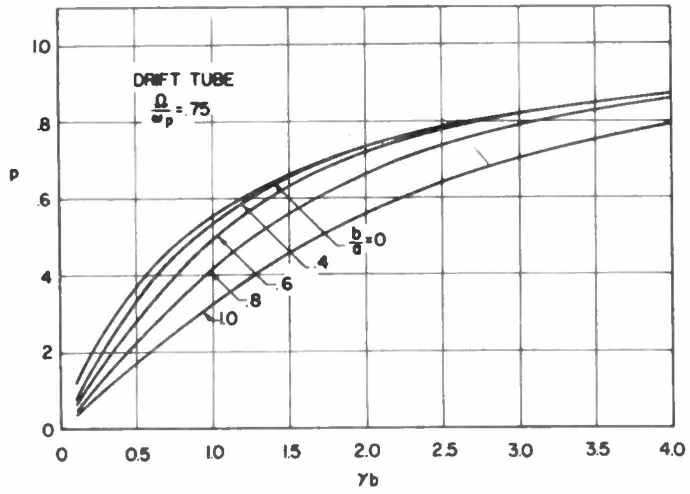

Fig. 8—Plot of the plasma-frequency reduction factor as a function of γb with b/a as parameter, for a solid cylindrical electron beam in a conducting drift tube with $\Omega/\omega_p = 0.75$.

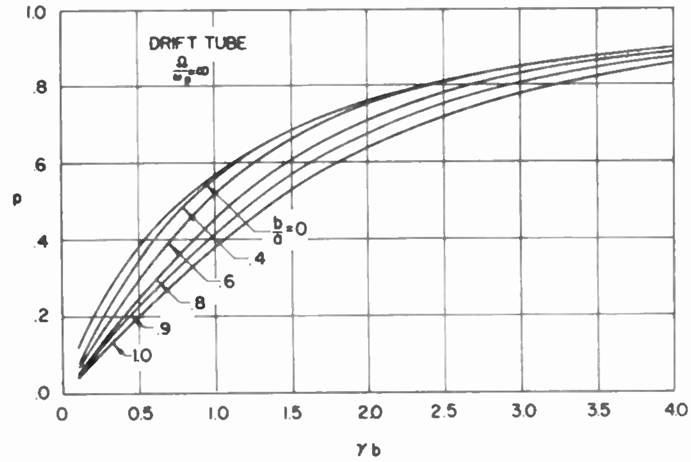

Fig. 9—Plot of the plasma-frequency reduction factor as a function of γb with b/a as parameter, for a solid cylindrical electron beam in a conducting drift tube with $\Omega/\omega_p = \infty$.

It is of interest to examine a few points concerning the relation between the present analysis and previous theories together with a description of some of the physical processes involved.

The equations representing the space-charge-wave propagation characteristics in a cylindrical stream in which an infinitely strong magnetic field prevents any transverse electron motion were given by Ramo. The corresponding relations for a Brillouin flow beam were given by Rigrod and Lewis. These two analyses represent the high and low extremes in magnetic field intensity for use in focusing an electron beam. In the former case the ac charge density was found to be

$$\tilde{\rho} = \frac{-i\omega_p^2\epsilon_0\gamma}{\omega_b^2}\tilde{E}_z \tag{30}$$

and the variation of $\tilde{E}_z$ with radius expressed by a $J_0(\tau r)$ function, admitting of solutions involving eigenvalues when the beam fills the drift tube and exhibiting an imaginary radial propagation constant. In the latter case the ac charge density is found to be zero[7] and the E_z field follows an $I_0(\tau r)$ variation with a real radial propagation constant, so that space-charge-wave propagation cannot occur in this case if the beam fills the drift tube. The propagation characteristics thus are divided into two regimes, separated by the singularity of (19), *viz*:

$$\omega_b^2 - 4\Omega^2 = \omega_p^2. \tag{31}$$

The ac charge density (21) is thus always negative and increases monotonically from zero at $\Omega = 0$ to the Ramo value (30) at $\Omega = \infty$. The physical reason for this condition can be seen by examination of (11), (12), and (15). When $\Omega = 0$ the electrons in the beam execute radial and axial ac displacements but with no ac rotation; in this peristaltic-type motion the net z-directed electron flux into a small volume of the beam is just equal to the net r-directed electron flux out of the same volume, resulting in no electron accumulations. When $\Omega \neq 0$, the electrons execute ac rotations in addition to the radial motion; thus the radial electron velocity is modified but the axial velocity is not, and the unbalance results in the formation of bunches ($\tilde{\rho} \neq 0$). After a 90-degree phase displacement of the rf wave, the electron radial velocity will result in a perturbation in the radius of the electron trajectory. As $\Omega \rightarrow \infty$, the radial velocity is reduced to zero and one obtains the familiar picture of electron bunching in a smooth confined electron stream.

The change in plasma frequency with beam size and magnetic field can be understood physically as follows. In a plasma of infinite extent ($\gamma b = \infty$) the electric flux lines connecting regions of charge accumulations follow along the direction of oscillation of these charge accumulations. As the beam is made of finite size, some of these flux lines can reach to the outside of the beam, reducing the net debunching forces and thus p. Likewise, as the magnetic field parameter Ω/ω_p is decreased, and the beam thus allowed to expand instead of accumulating charges in certain regions, the debunching forces are again weaker (that part of E_z due to ac charges decreases as Ω/ω_p decreases) resulting in a decreased value of p.

Beam in a Helix

It would be of interest to determine the effect of the intensity of the magnetic field on the operating characteristics of a traveling-wave tube. Such effects may be expressible in terms of the space-charge parameter QC and the impedance factor K,[8] which will be functions of

[7] Rigrod and Lewis also found $\tilde{\rho} = 0$ using both the continuity equation and the divergence equation, which are not independent. This method will yield $\tilde{\rho} = 0$ solutions for any case (including that of Ramo) in which each component of electron velocity is related to its appropriate component of electric field by the same constant, so that one must be careful in interpretation of the results.

[8] Pierce, *loc. cit.*

Ω/ω_p. Unfortunately, the equations which include an arbitrary value of magnetic field are considerably more involved than those appropriate to Brillouin flow or for an infinite magnetic field, so that only an approximate method of evaluation of QC and K will be given here.

Kino[9] has shown that values of the parameter QK for a thin hollow beam in a sheath helix determined by the normal mode expansion method and from consideration of the same beam in free space agree well within the region of most interest. He also states that further work indicates that a similar method is fairly accurate for a solid beam. We will assume that such is the case and evaluate the product QK from a knowledge of the plasma-frequency reduction factor for a solid beam in free space.

For small values of the gain parameter C, and with $\beta_e = \gamma$, the product QK can be expressed approximately in terms of the ratio ω_b/ω_p as:[10]

$$QK\frac{\beta_0}{\gamma_0} \approx 60\left(\frac{p}{\gamma b}\right)^2. \tag{32}$$

Values of p for a solid cylindrical beam in free space are found from (27) and (28) by letting $a \to \infty$ and are plotted in the figures as $b/a = 0$. The graph of Fig. 10 shows the QK product determined in this way, with the values given by Rigrod and Lewis ($\Omega = 0$) and by Fletcher[11] ($\Omega = \infty$) indicated by the arrows; it appears that this method is a reasonable approximation except for small values of γb and large values of b/a.

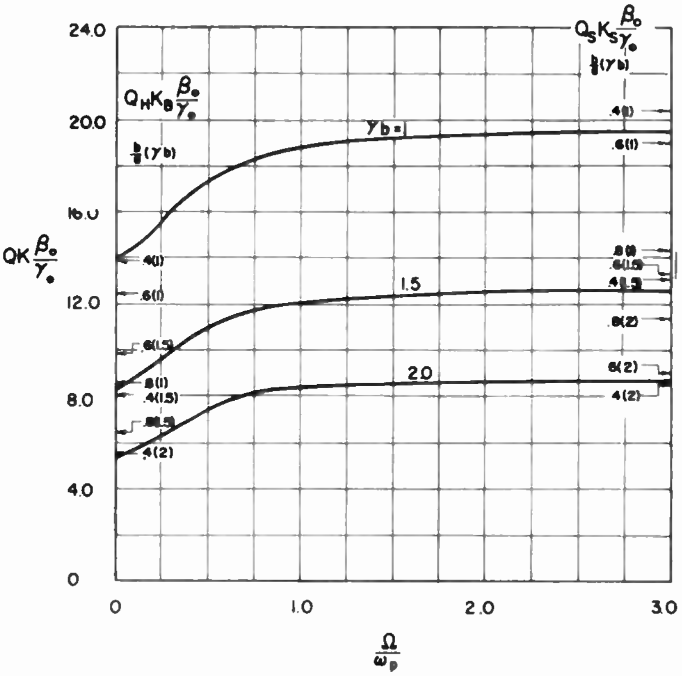

Fig. 10—Plot of the product QK vs Ω/ω_p for three values of γb, determined from the drift tube reduction factor values for $b/a = 0$ by making use of (32). The values of the QK product for the "perfect" Brillouin flow case ($Q_H K_B$) from Rigrod and Lewis and the values for an infinite magnetic field ($Q_S K_S$) from Fletcher are indicated by the arrows for the values of b/a and γb shown. It is seen that this approximate method of determining QK agrees with the existing theories as limiting values within the uncertainties of other quantities for $b/a = 0.6$ or less.

Let us use the following approximate, and perhaps somewhat arbitrary, method of evaluating the impedance parameter $E_z^2/\beta^2 P$, which can be used together with the value of QK determined from (32) to form an estimate of the value of Q as a function of Ω/ω_p.

It is noted from Fig. 2 that near $\Omega = 0$ the convection current in the stream is carried predominantly by the surface perturbations, while for large values of Ω/ω_p the surface current is negligible compared with the body current. This suggests that near $\Omega = 0$ the interaction between the convection current in the stream and the fields from the helix will be similar to that from a hollow beam of radius b. Pierce[12] points out that with a thin hollow beam the impedance parameter $2K$ can be evaluated by multiplying the value of the impedance on the axis by $I_0^2(\gamma b)$. Likewise, when the magnetic field is strong enough so that the electron motion is substantially rectilinear, we can use Pierce's approximation for a solid beam. In this case the impedance parameter $2K$ is found by multiplying the value on the axis by $I_0^2(\gamma b) - I_1^2(\gamma b)$. In order to interpolate between these two relations, we will use an arbitrary weighting factor, obtained by multiplying the former by the surface current and the latter by the body current, dividing the sum by the total current.

$$\begin{aligned} 2K &= \frac{E_z^2}{\beta^2 P} = \frac{\beta}{\beta_0} F^3(\gamma a)\left[\frac{I_0^2(\gamma b) I_S + (I_0^2(\gamma b) - I_1^2(\gamma b)) I_B}{I_c}\right] \\ &= \frac{\beta}{\beta_0} F^3(\gamma a)\left[\frac{-(1-p^2) I_0^2(\gamma b) + 4\Omega^2/\omega_p^2 (I_0^2(\gamma b) - I_1^2(\gamma b))}{p^2 - 1 + 4\Omega^2/\omega_p^2}\right] \end{aligned} \tag{33}$$

where $F(\gamma a) = 7.154 \exp(-0.6664\gamma a)$.

Graphs of (33) for several values of γb and b/a showed that for small values of $\Omega(\Omega < \omega_b/2)$ the Rigrod and Lewis

[9] G. S. Kino, "Normal Mode Theory in Perturbed Transmission Systems," Stanford Univ., ERL Tech. Rep. No. 84; May, 1955.

[10] See, for example, G. M. Branch, "Reduction of plasma frequency in electron beams by helices and drift tubes," PROC. IRE, vol. 43; p. 1018, August, 1955.

[11] R. C. Fletcher, "Helix parameters in traveling-wave tube theory," PROC. IRE, vol. 38, pp. 413–417; April, 1950.

[12] Pierce, *op. cit.*, Appendix 2 and p. 28.

value of impedance reduction factor could be used while for $\Omega > \omega_b/2$ the Fletcher values are appropriate. Except in the neighborhood of the singularity $\omega_b = 2\Omega$, where the theory is invalid, the impedance appears almost independent of Ω.

The impedance value for "perfect" Brillouin flow ($\Omega = 0$) is highest since the beam appears similar to a hollow beam for the interaction, the electrons on the average interacting with stronger circuit fields.

From Fig. 10 and the above considerations it is seen that the value of Q decreases as Ω/ω_p decreases. This is consistent with the change from a solid to a hollow stream behavior as Ω/ω_p decreases; the value of Q for a rectilinear hollow beam being less than that of a solid beam. Another way of looking at this effect is to observe, as in a previous section, that the debunching forces decrease with Ω/ω_p so that less energy is stored in the space-charge fields at low values of Ω/ω_p, resulting in more effective interaction between the electrons and the circuit fields and thus a lower value of Q.

Conclusion

The propagation constants for the space-charge waves in a cylindrical electron beam, expressed in terms of the plasma-frequency reduction factor $p = \omega_b/\omega_p$, have been determined in terms of the magnetic field parameter Ω. This quantity is a measure of the total magnetic flux threading the cathode within radius r_c and can be evaluated for both Brillouin flow and confined flow focusing methods, although its application to the latter is an approximation in that a smooth flow is assumed.

It is found, as in previous analyses of space-charge-wave propagation, that both the fields within the stream and those from external wall charges influence the space-charge oscillation. In addition, the strength of the magnetic field affects the electron trajectories, the ac charge density and through these the debunching forces and ω_b.

Approximate methods of determining the change with magnetic field of the traveling-wave tube parameters QC and K are given. The former quantity changes more with Ω and its effect on tube performance is significant. It is seen that these parameters do not change with Ω for values of Ω equal to or greater than about one, so that the Pierce or Fletcher values of QC and K and the Ramo values of p are valid for all usual immersed flow focusing situations. However, the change in Q, K, and p at low values of Ω, due to flux threading the cathode in Brillouin flow, is appreciable so that the effect of cathode flux in Brillouin flow cannot be ignored.

List of Symbols

$\beta_e = \omega/u_0$
u_0 = average electron velocity
ω = radian signal frequency
$\beta_p = \omega_p/u_0$
$\omega_p = -\eta\rho_0/\epsilon_0$ = plasma frequency evaluated at r_0
ρ_0 = average volume charge density
$\omega_H = \eta\beta_0/2$ = Larmar radian frequency
$\tilde{r}$ = instantaneous value of beam radium perturbation
r_0 = average beam radius
$\Omega = \eta\psi_c/2\pi r_0^2$
ψ_c = total magnetic flux threading the cathode within the periphery of a stream line passing through r_0
$\eta = e/m$ = magnitude of the electron charge to mass ratio
$\omega_b = \omega - \gamma u_0$
γ = axial wave propagation constant
B_c = cathode magnetic flux density
τ = defined by (19)
$p = \omega_b/\omega_p$ = plasma-frequency reduction factor
$\beta_0 = \omega/c$
c = velocity of light
β = [used only in (33)] is Pierce's notation—same as γ
b = effective beam radius (can be taken as r_0).
a = radius of helix or drift tube

Acknowledgment

The author wishes to express his appreciation to his co-workers in the Electron Tube Laboratory whose suggestions have contributed substantially to the content of this paper, and especially to Dr. R. W. Gould for many helpful discussions throughout the course of the work. He is also indebted to Mrs. Jeanne McLeod and to Dr. James Pachares under whose direction most of the computations were carried out.

Some General Properties of Nonlinear Elements—Part I. General Energy Relations*

J. M. MANLEY†, SENIOR MEMBER, IRE, AND H. E. ROWE‡, ASSOCIATE, IRE

Summary—**Two independent equations relating the average powers at the different frequencies in nonlinear inductors and capacitors are derived. These equations are a consequence only of the assumption of a single-valued characteristic for the nonlinear element. They are independent of the particular shape of this characteristic, of the power levels at the various frequencies, and of the external circuit in which the nonlinear reactor is connected.**

These general energy relations give information regarding the gain and stability of nonlinear reactor modulators and demodulators, and consequently of magnetic and dielectric amplifiers, without requiring detailed information about these devices. The utility of these equations is illustrated by discussing the gain and stability of the simplest types of nonlinear reactor modulators and demodulators and harmonic generators.

This analysis for nonlinear inductors and capacitors is extended to include the effects of hysteresis in the nonlinear characteristic in the special case where the operating hysteresis loop is no more than double-valued.

A similar analysis applied to nonlinear resistors yields two equations relating the reactive powers at the different frequencies, rather than the real powers as above. The interpretation of reactive power under these conditions is not clear.

Introduction

Any amplifier can be considered to be a modulator in that the input wave causes variations in the energy flowing from the amplifier's energy source. The modulator must deliver more power to an output load than the input wave delivers to the modulator if it is to provide useful gain.

If the energy source of a modulator is direct, for example a battery, the output wave is, ideally, a replica of the input wave. Examples are: the direct electron current in the plate-cathode path of a vacuum tube is varied by the field caused by applying a wave to the grid; the direct battery current in a carbon microphone is varied by mechanical motion of the diaphragm; the direct collector-emitter current in a transistor is varied by the base-emitter current, which is proportional to an applied wave. Depending on the nature of the modulator it may exhibit a gain or a loss.

On the other hand, if the energy source does not have zero frequency, but is an alternator, referred to as the local oscillator, the output is not a replica of the input, but occurs at a different frequency than the input, and consequently the device is called a modulator, demodulator, or a mixer. This shift in frequency occurs because new frequencies are generated when waves of two different frequencies, both different from zero, are applied to a nonlinear element. These frequencies are harmonics and sum and difference combinations of the applied frequencies. Again, some of these devices exhibit a modulating gain and some a loss, depending on their nature. Examples are: magnetic amplifiers,[1] dielectric amplifiers,[2] and copper oxide modulators.

Although modulators with ac energy sources are quite similar to the more conventional type of amplifier, whose energy is supplied by a dc source, their special properties are less widely known. The main purpose of Part I of this paper is to derive some general power relations which govern nonlinear reactor modulators; *i.e.*, modulators whose nonlinear element is a nonlinear inductor or capacitor. These relations consist of two independent equations relating the powers at the different frequencies in such an element; their only restriction is that the nonlinear characteristic, voltage-charge or flux-current for the nonlinear capacitor or inductor respectively, be single-valued. They do not depend on the detailed shape of this characteristic or on the external circuit in which the nonlinear element is connected. They are independent of the levels at the various frequencies; they are thus not confined to the small signal case, in which all signal levels are much lower than the local oscillator level, but hold true in general.

These results are useful in considering the gain and the stability of nonlinear reactor modulators and demodulators,[3] and hence of magnetic and dielectric amplifiers, which may be regarded as carrier systems using a nonlinear reactor modulator. The question of stability is similar to that which arises with conventional feedback amplifiers; *i.e.*, modulators with a dc carrier, which may oscillate under certain operating conditions. With nonlinear reactor modulators, instability corresponds to the production of additional frequencies, which may or may not be the normal signal frequencies, with only the local oscillator frequency applied. In general these new frequencies are incommensurable with the local oscillator frequency and may be greater or less than this frequency; but in special cases

* Original manuscript received by the IRE, January 31, 1956. A shortened version of this paper was presented at a symposium on nonlinear circuit analysis, sponsored by the Polytechnic Inst. of Brooklyn, N. Y., on April 25, 26, and 27, 1956.

† Bell Telephone Labs., Inc., Murray Hill, N. J.
‡ Bell Telephone Labs., Inc., Holmdel, N. J.

[1] J. M. Manley, "Some general properties of magnetic amplifiers," Proc. IRE, vol. 39, pp. 242–251; March, 1951.

[2] W. P. Mason and R. F. Wick, "Ferroelectrics and the dielectric amplifier," Proc. IRE, vol. 42, pp. 1606–1620; November, 1954.

[3] In the remainder of this paper the term *modulator* will be used to denote a device in which the output signal frequency is higher than the input signal frequency, while the term *demodulator* will denote a device in which the output signal frequency is lower than the input signal frequency, when specific devices are under consideration. The term *modulator* will also be used, as above, to denote the general class of devices in which new frequencies are produced.

these new frequencies may be rationally related to the local oscillator frequency, yielding frequencies that are subharmonics or multiples of subharmonics.

The utility of these results is illustrated by applying them to the simplest nonlinear reactor modulators and demodulators, in which only one of the principal sidebands of the applied signal frequency about the local oscillator frequency is allowed to carry a significant amount of power. Under these conditions the powers at the various frequencies will be directly proportional to the frequencies. There will be two different situations to consider, depending on the relative positions of the local oscillator and the signal frequencies. In the stable case the maximum available gain is equal to the ratio of the output frequency to input frequency; consequently, modulators have gain while demodulators have loss. In the potentially unstable case the gain is unlimited, any gain from 0 to ∞ being attainable for either the modulator or the demodulator; however, the gain as a modulator exceeds the gain as a demodulator, as in the stable case.

The remainder of Part I discusses certain related results. The analysis is extended to include the effects of hysteresis in the characteristic of nonlinear reactors under somewhat more restricted conditions, which insure that the operating hysteresis loop is no more than double-valued. Finally, a similar analysis applied to nonlinear resistors yields analogous relations among the reactive powers at the various frequencies. The interpretation of reactive power in this situation is not clear, and these results seem to be less important than those of the nonlinear reactor analysis.

Part II of this paper (to be submitted later) entitled "Small-Signal Theory," is concerned with the application of the well-known small signal analysis[4] to the determination of further properties of these devices.

Historical Note

To the best knowledge of the writers, the first calculations of the reactions of currents of different frequencies on one another in a reactance modulator was made by R. V. L. Hartley of the Bell Telephone Labs. in 1916. He assumed a simple cubic characteristic for a biased iron-cored inductance modulator, and assumed that the external circuit permitted currents at only four frequencies, the two applied frequencies and their sum and difference frequencies, to flow through the nonlinear inductance. There are two important results of his analysis:

1) The high and low frequency sources applied to the modulator supply power unequally, the ratio of these two powers being greater than the ratio of their corresponding frequencies. Thus, if one source has a much higher frequency than the other, it will supply most of the power to the modulator, the low-frequency source supplying very little power.

2) The flow of power out of the modulator at the sum frequency absorbs power from both generators; *i.e.*, introduces a positive resistance into both source circuits. However, the flow of power at the difference frequency introduces a positive resistance into the high frequency source circuit, a negative resistance into the low frequency source circuit.

The first result shows that a modulating gain is possible with this type of modulator when the local oscillator frequency is appreciably higher than the signal frequency. The second result shows that under certain conditions instability or oscillation is possible, with power emerging from all of the signal terminals with only the local oscillator applied to the modulator. These output frequencies will, in general, be incommensurable with the applied carrier frequency, but in special cases may be rationally related, being subharmonics or multiples of subharmonics. This suggests that by operating close to instability, very high gains may be obtained as either a modulator or as a demodulator.

The first application of these results was to the coil modulators being studied then for possible use in carrier telephone systems. The experiments bore out the analysis in that good modulating gains could be obtained and that instabilities resulted when attempts were made to operate a demodulator with gain. They were also used to explain the generation of subharmonics and other nonharmonic frequencies,[5,6] and the occurrence of gain and the source of occasional instability in magnetic amplifiers.[1] Later, Hartley analyzed a particular form of capacitance modulator and obtained similar results,[7] which were verified experimentally.[8] He suggested that similar processes could occur within atoms and thereby explain the Raman effect.[9,6]

These results were derived by J. M. Manley under much more general conditions.[10] His analysis assumes only that the characteristic of the nonlinear reactor is single-valued; *i.e.*, that there be no hysteresis; otherwise the shape of the nonlinear characteristic is arbitrary. The derivation includes an arbitrary number of sidebands and is valid for arbitrary power levels at the various frequencies.

This analysis is the principal topic of Part I of this paper. It is extended to include the effects of hysteresis in the nonlinear characteristic for the special case in which the operating hysteresis loop is no more than double-valued.

[4] W. R. Bennett, "A general review of linear varying parameter and non-linear circuit analysis," Proc. IRE, vol. 38, pp. 259–263; March, 1950.

[5] J. M. Manley and E. Peterson, "Negative resistance effects in saturable reactor circuits," *Trans. AIEE*, vol. 65, pp. 870–881; 1946.

[6] E. Peterson, "Atomic Physics and Circuit Theory," *Bell Labs., Record*, vol. 7, p. 231; February, 1929.

[7] R. V. L. Hartley, "Oscillations in systems with non-linear reactance," *B.S.T.J.*, vol. 15, pp. 424–440; July, 1936.

[8] L. W. Hussey and L. R. Wrathall, "Oscillations in an electromechanical system," *B.S.T.J.*, vol. 15, pp. 441–445; July, 1936.

[9] R. V. L. Hartley, "A wave mechanism of quantum phenomena," *Phys. Rev.*, vol. 33, p. 289; February, 1929.

[10] Unpublished memoranda; 1933–1935.

General Energy Relations in Nonlinear Reactors

In this section we derive J. M. Manley's power relations for hysteresisless nonlinear capacitors and inductors,[10] which relate the powers at the different frequencies in such an element. The analysis will be carried out for the nonlinear capacitor only, since the corresponding analysis for the nonlinear inductor is almost identical and yields identical final results.

The characteristic of the nonlinear capacitor is given by specifying the voltage as some arbitrary function of the charge:

$$v = f(q), \tag{1}$$

where q is the charge on the nonlinear capacitor and v is the voltage across it. In particular, for a linear capacitor (1) becomes

$$v = \frac{1}{C} \cdot q$$

where C is the capacitance. In the present section hysteresis is excluded and so $f(q)$ is a single-valued function, but otherwise its shape is arbitrary; there are no further restrictions on the analysis. In a later section hysteresis is considered in the special case for which $f(q)$ is at most a double-valued function. Note that the characteristic of the nonlinear capacitor could be given equally well by specifying the charge as some arbitrary but single-valued function of the voltage; the subsequent analysis would then be the dual of that presented below. In the corresponding nonlinear inductor analysis the flux and current must be similarly related by an arbitrary single-valued function.

In general, all of the frequencies $f_{mn} = mf_1 + nf_0$ will be present, where m and n take on all integral values, positive, negative, and zero. The two fundamental frequencies f_1 and f_0 are assumed to be incommensurable and positive. In later applications of these results f_1 and f_0 will be taken as the two applied frequencies, and the other frequencies as the resulting sidebands. However, this identification is not essential to the analysis, and others may be convenient.

For conceptual purposes, the nonlinear capacitor may be thought of as connected in the circuit of Fig. 1, in which each frequency flows in a separate external circuit. Each of these circuits contains in series a voltage generator of the appropriate frequency, a load impedance, and an ideal filter which presents a short circuit to the desired frequency and an open circuit to all other frequencies. The voltages of all generators in this equivalent circuit except those corresponding to the sources driving the nonlinear capacitor are, of course, set equal to zero. Thus, in the case discussed above where only two generators at the frequencies f_1 and f_0 are connected to the nonlinear capacitor, only these two branches in the equivalent circuit will contain voltage generators, all other branches containing passive load

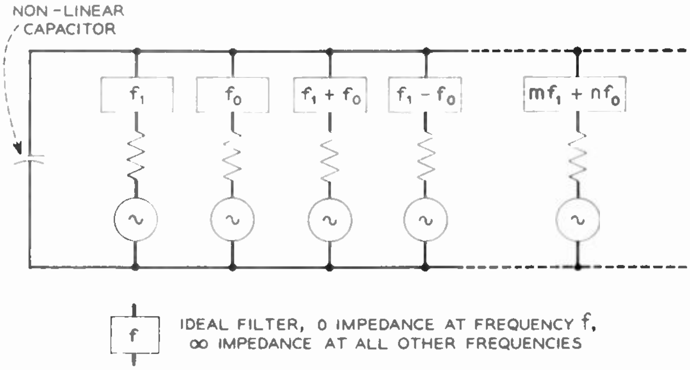

Fig. 1—Illustrative circuit with a nonlinear capacitor.

impedances. This circuit is only for purposes of illustration, and does not enter into the analysis in any way.

The charge q flowing into the nonlinear capacitor may be written as a double Fourier series,

$$q = \sum_{m=-\infty}^{\infty} \sum_{n=-\infty}^{\infty} Q_{m,n} e^{j(mx+ny)} \tag{2}$$

$$x = \omega_1 t \qquad \omega_1 = 2\pi f_1$$
$$y = \omega_0 t \qquad \omega_0 = 2\pi f_0. \tag{3}$$

Since q is real,

$$Q_{m,n} = Q_{-m,-n}^* \qquad Q_{-m,-n} = Q_{m,n}^{*}\text{[11]} \tag{4}$$

The variables x and y are initially considered as independent, taking on any values in the $x-y$-plane. They are subsequently replaced by the substitution of (3), so that only values along a straight line in the $x-y$ plane appear in the final results. This method was first used by W. R. Bennett in calculating modulation products.[12]

Taking the total derivative of (2) with respect to time, we obtain the current i flowing into the nonlinear capacitor.

$$i = \frac{dq}{dt} = \sum_{m=-\infty}^{\infty} \sum_{n=-\infty}^{\infty} I_{m,n} e^{j(mx+ny)} \tag{5}$$

$$I_{m,n} = j(m\omega_1 + n\omega_0) Q_{m,n} \tag{6}$$

$$I_{m,n} = I_{-m,-n}^* \qquad I_{-m,-n} = I_{m,n}^*. \tag{7}$$

Next, the voltage v is assumed to be a single-valued, periodic function of x and y, so that it may be represented by a double Fourier series similar to (2). In the present case where the characteristic $f(q)$ is single-valued, v will satisfy these conditions, in view of (2) for q. In the analysis of hysteresis in a later section it will be shown that under the restrictions which insure that $f(q)$ is at most double-valued, v will again satisfy these conditions. Thus,

$$v = f(q) = f[q(x, y)] = F(x, y) \tag{8}$$

where in both cases $F(x, y)$ is single-valued and periodic in x and y. Consequently v may be expanded in a double Fourier series.

[11] The * indicates the complex conjugate.

[12] W. R. Bennett, "New results in the calculation of modulation products," *B.S.T.J.*, vol. 12, pp. 228–243; April, 1933.

$$v = \sum_{m=-\infty}^{\infty} \sum_{n=-\infty}^{\infty} V_{m,n} e^{j(mx+ny)} \quad (9)$$

$$V_{m,n} = V_{-m,-n}^* \qquad V_{-m,-n} = V_{m,n}^*. \quad (10)$$

The coefficients are given by

$$V_{m,n} = \frac{1}{4\pi^2} \int_0^{2\pi} dy \int_0^{2\pi} dx \cdot F(x, y) e^{-j(mx+ny)}. \quad (11)$$

Let us multiply both sides of (11) by $jmQ_{m,n}^*$ and sum from $-\infty$ to $+\infty$ over m and n. Then, interchanging the order of integration and summation on the right-hand side, (11) becomes

$$\sum_{m=-\infty}^{\infty} \sum_{n=-\infty}^{\infty} jmQ_{m,n}^* V_{m,n} = \frac{1}{4\pi^2} \int_0^{2\pi} dy \int_0^{2\pi} dx F(x, y) \cdot \sum_{m=-\infty}^{\infty} \sum_{n=-\infty}^{\infty} jmQ_{m,n}^* e^{-j(mx+ny)}. \quad (12)$$

The double summation inside the integral may be easily identified. Taking (2) for q and differentiating with respect to x,

$$\frac{\partial q}{\partial x} = \sum_{m=-\infty}^{\infty} \sum_{n=-\infty}^{\infty} jmQ_{m,n} e^{j(mx+ny)}. \quad (13)$$

Using (4), this may be written as

$$\frac{\partial q}{\partial x} = -\sum_{m=-\infty}^{\infty} \sum_{n=-\infty}^{\infty} jmQ_{m,n}^* e^{-j(mx+ny)}, \quad (14)$$

which is just the negative of the double summation inside the integral of (12). Further, solving (6) for $Q_{m,n}$, taking the complex conjugate, and substituting into the left-hand side of (12), this latter equation may be written as

$$\sum_{m=-\infty}^{\infty} \sum_{n=-\infty}^{\infty} \frac{mV_{m,n}I_{m,n}^*}{mf_1 + nf_0} = \frac{1}{2\pi} \int_0^{2\pi} dy \int_0^{2\pi} dx \cdot \frac{\partial q}{\partial x} \cdot F(x, y). \quad (15)$$

Since $(\partial q/\partial x)dx$ is just dq with y held constant, the variable in the second integral in (15) may be changed from x to q. Referring to (8), (15) becomes

$$\sum_{m=-\infty}^{\infty} \sum_{n=-\infty}^{\infty} \frac{mV_{m,n}I_{m,n}^*}{mf_1 + nf_0} = \frac{1}{2\pi} \int_0^{2\pi} dy \int_{q(0,y)}^{q(2\pi,y)} f(q)dq. \quad (16)$$

The limits on the second integral indicate that the variation of q is determined by allowing x to vary from 0 to 2π, holding y constant.

A similar analysis may be performed in which the roles of x and y are interchanged. Both sides of (9) are multiplied by $jnQ_{m,n}^*$ and summed from $-\infty$ to $+\infty$ over m and n. Interchanging the order of summation and integration on the right-hand side, the resulting double summation is identified as $-(\partial q/\partial y)$; the remainder of the analysis is identical to that given above. Thus, the analog of (16) becomes

$$\sum_{m=-\infty}^{\infty} \sum_{n=-\infty}^{\infty} \frac{nV_{m,n}I_{m,n}^*}{mf_1 + nf_0} = \frac{1}{2\pi} \int_0^{2\pi} dx \int_{q(x,0)}^{q(x,2\pi)} f(q)dq, \quad (17)$$

where the limits on the second integral indicate that the variation of q is determined by allowing y to vary from 0 to 2π with x constant.

While all of the above equations have included both positive and negative frequencies, there can be no physical distinction between a positive and a negative frequency of the same magnitude. Therefore, we wish to combine appropriate pairs of terms on the left-hand sides of (16) and (17), relating the quantities $V_{m,n}I_{m,n}^*$ to the average powers associated with the various frequencies. Defining

$$S_{m,n} = W_{m,n} + jX_{m,n} = 2V_{m,n}I_{m,n}^* \quad (18)$$

$$S_{m,n} = S_{-m,-n}^* \qquad S_{-m,-n} = S_{m,n}^* \quad (19)$$

we have

$$W_{m,n} = V_{m,n}I_{m,n}^* + V_{m,n}^*I_{m,n} = W_{-m,-n} \quad (20)$$

$$X_{m,n} = j(V_{m,n}^*I_{m,n} - V_{m,n}I_{m,n}^*) = -X_{-m,-n}. \quad (21)$$

A particular frequency includes both the positive and the negative components $m'f_1+n'f_0$ and $-(m'f_1+n'f_0)$, where m' and n' have been chosen so that $m'f_1+n'f_0>0$ (the alternate choice would have been $-m'$, $-n'$). Then $S_{m',n'}$, $W_{m',n'}$, and $X_{m',n'}$ are respectively the vector, real, and reactive powers flowing into the nonlinear element at this frequency. While this choice of indexes is necessary in order for $S_{m,n}$ and $X_{m,n}$ to agree with the usual definitions of vector and reactive power, in view of (20), $W_{m,n}$ will be the real or average power flowing into the nonlinear element at this frequency for either choice of indexes.

Inspection of (16) and (17) shows that only the real powers $W_{m,n}$ will appear in the nonlinear reactor case, and consequently only (20) of the present discussion will be used in this section; the reactive powers will appear in the corresponding analysis of the nonlinear resistor. Eq. (20) for the real power may be easily derived by taking the time average of the product of (5) and (9).

Thus, combining pairs of terms corresponding to the positive and negative components of each frequency, taking care to include each term only once, and making use of (20), (16), and (17) become:

$$\sum_{m=0}^{\infty} \sum_{n=-\infty}^{\infty} \frac{mW_{m,n}}{mf_1 + nf_0} = \frac{1}{2\pi} \int_0^{2\pi} dy \int_{q(0,y)}^{q(2\pi,y)} f(q)dq \quad (22)$$

$$\sum_{m=-\infty}^{\infty} \sum_{n=0}^{\infty} \frac{nW_{m,n}}{mf_1 + nf_0} = \frac{1}{2\pi} \int_0^{2\pi} dx \int_{q(c,0)}^{q(x,2\pi)} f(q)dq, \quad (23)$$

where $W_{m,n}$ is the average power flowing into the nonlinear capacitor at the frequencies $\pm|mf_1+nf_0|$. Note that the summations extend over different ranges in these two equations. To obtain terms of a similar form on the left-hand sides of both equations, they may be rewritten so that positive frequencies always appear in the denominator and the corresponding values of m and

n appear as subscripts on W, making use of (20). For example, the term corresponding to the frequency $3f_1-2f_0$ (assuming $3f_1>2f_0$) in (22) is

$$\frac{3W_{+3,-2}}{3f_1-2f_0}.$$

The term corresponding to this frequency in (23) is written

$$\frac{2W_{-3,+2}}{-3f_1+2f_0}=-\frac{2W_{+3,-2}}{3f_1-2f_0}.$$

We next make use of the requirement that there be no hysteresis in the nonlinear characteristic, noting that since this assumption has not yet been introduced, (22) and (23) are valid for a more general type of characteristic. These equations provide the starting point for the treatment of hysteresis in a later section.

The limits on the second integrals in (22) and (23) indicate that the variation of q is determined by allowing x and y respectively to vary from 0 to 2π, holding the other variable constant. Since q is periodic in x and y and consequently returns to its initial value at the end of these integrations, and since $f(q)$ is single-valued, these two integrals on q will be identically zero for all values of y and x respectively. Consequently the right-hand sides of these equations are equal to zero if the nonlinear characteristic is single-valued, and they become

$$\sum_{m=0}^{\infty}\sum_{n=-\infty}^{\infty}\frac{mW_{m,n}}{mf_1+nf_0}=0. \tag{24}$$

$$\sum_{m=-\infty}^{\infty}\sum_{n=0}^{\infty}\frac{nW_{m,n}}{mf_1+nf_0}=0. \tag{25}$$

Eqs. (24) and (25) are the final results that have been sought. They provide two independent relations among the powers flowing into the nonlinear capacitor at the various frequencies; they apply equally well to the case of a nonlinear inductor, the analysis being almost identical to that given above. These results are a consequence only of the single-valuedness of the characteristic of the nonlinear capacitor or inductor. They are quite remarkable in that they are independent of the shape of this characteristic and of the power levels. We note that since they hold true in general, they must apply to a linear capacitor, in which no modulation effects take place. In this case $W_{m,n}=0$ for all m and n, and (24) and (25) remain satisfied.

Since, in the absence of hysteresis no power may be dissipated in the nonlinear reactor, the sum of all the powers flowing into it at the different frequencies must be zero. This result is readily obtained from (24) and (25) by multiplying (24) by f_1, (25) by f_0, and adding the two together.

Certain general properties of nonlinear reactor modulators and demodulators may be deduced from these relations. We assume that two generators are connected to the device at frequencies f_1 and f_0. Since power can enter the nonlinear element from only the two generators, all of the $W_{m,n}$ must be negative or zero except $W_{1,0}$ and $W_{0,1}$. Since (24) contains $W_{1,0}$ but not $W_{0,1}$ and (25) contains $W_{0,1}$ but not $W_{1,0}$, we may solve these two equations for the respective generator powers in terms of the sideband powers. Then, as Manley and Peterson[1,5] have pointed out, these equations show that the flow of a sum frequency (m and n both positive) yields a positive contribution to the power entering the nonlinear element from both generators, while the flow of a difference frequency (m and n of opposite sign) yields a positive contribution to one generator power and a negative contribution to the other. Stated differently, the flow of a sum frequency introduces positive resistances in both source circuits, while flow of a difference frequency introduces a positive resistance in one source circuit and a negative resistance in the other. Of course the values of the various powers in these equations can be determined only by a detailed circuit analysis of the nonlinear element and the external circuit.

While at least one of the generator powers $W_{1,0}$ and $W_{0,1}$ must be positive, (24) and (25) show that it is possible for one of them to be negative. There are consequently two possible situations: 1) $W_{1,0}$ and $W_{0,1}$ both positive. Power flows into the nonlinear element from both generators, and the device is said to be stable. 2) Either $W_{1,0}$ or $W_{0,1}$ negative. Power flows into the nonlinear element from one generator, but is returned to the other generator by the nonlinear element. The device is said to be potentially unstable.

The reason for these definitions is that if the external positive resistance in the generator circuit to which the nonlinear element presents a negative resistance is reduced until the net resistance of this circuit is zero, the generator can be removed and current of approximately the same frequency will continue to flow in this circuit, generating sidebands with the remaining generator, as before. The exact frequency of operation is determined by the tuning of the external circuits. Thus, new frequencies in general incommensurable with a single applied frequency can be generated by a nonlinear capacitor or inductor under these conditions, several different types of oscillation being possible.[5]

In considering the behavior of the device as a modulator or as a demodulator, one generator represents the local oscillator and the other the applied signal. One or more of the resulting sidebands may be taken as the useful signal output. The signal input and output terminals may thus be regarded as externally available while the local oscillator is regarded as an internal part of the modulator. Instability can arise as a result of negative resistance introduced in either the local oscillator circuit or in the applied signal circuit.

Consider first instability in the local oscillator circuit. Under normal conditions the applied signal level is so far below the local oscillator level that even though it introduces a negative resistance in the local oscillator circuit, the losses in this circuit are sufficient to prevent instability. However, under these conditions if the input signal level is raised until it becomes comparable with the local oscillator level, the total resistance in the local oscillator circuit can become negative, with the resulting instability and the production of new frequencies unrelated to the signal and local oscillator frequencies.

Our primary interest is in the case where the signal levels are small compared to the local oscillator level. Consequently instability in the local oscillator circuit is ignored, and the device is regarded as potentially unstable only if a negative resistance appears in the applied signal circuit, so that it is possible to have power emerging at all of the signal frequencies with only the local oscillator applied and passive impedances connected to the signal terminals; otherwise the device is considered to be stable. Regarding the local oscillator circuit as an internal part of the modulator, this definition of stability is in accord with the usual definition adopted for transducers. However, the possibility of instability caused by negative resistance introduced in the local oscillator circuit must be kept in mind for extreme operating conditions.

In order to simplify the analysis of modulation problems it is customary to assume that currents (or voltages) at only the most important frequencies are allowed to flow through (or exist across) the nonlinear element, all the other frequencies being suppressed by ideal filters. In the present analysis of nonlinear reactors it may be assumed that all frequencies except the ones of interest are terminated in an open circuit, short circuit, or pure reactance so that $W_{m,n}=0$ for all but the wanted frequencies. While this is a useful procedure, in practice it must be kept in mind that although the powers of all of the unwanted frequencies may be quite small, they are not likely to be strictly zero; and some of these unwanted components can cause regeneration or even oscillation under unfavorable conditions, greatly modifying the characteristics of the device. This method is adopted in the next section, where the simplest nonlinear reactor devices are discussed.

Nonlinear Reactor Modulators, Demodulators, and Harmonic Generators[1,10]

The general results of the previous section are best illustrated by some simple examples. Consider nonlinear reactor modulators and demodulators in which only one of the principal sidebands of the signal about the carrier is allowed to carry a significant amount of power; all other sidebands are assumed to be reactively terminated. Fig. 2 illustrates the frequencies involved in each of the two types of devices considered. Recalling that in the previous section f_1 and f_0 were taken as the two applied frequencies, the local oscillator frequency is designated as f_1. We have avoided using the symbol f_0 in order to eliminate confusion, because we wish to allow any of the signal frequencies to be the signal input in order to discuss the different modulators and demodu-

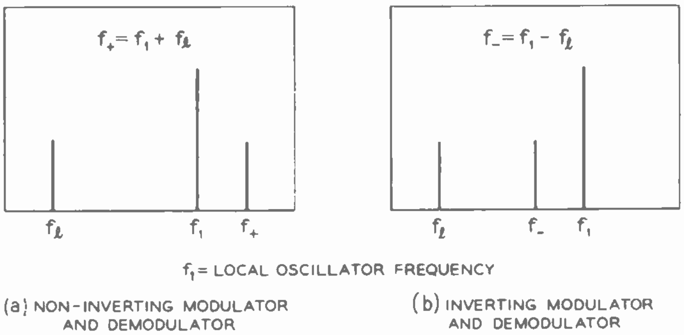

Fig. 2—Signal and local oscillator frequencies for modulators and demodulators.

lators. Consequently f_l indicates the lowest signal frequency, small compared to the local oscillator frequency, while f_+ and f_- are equal to $f_1 \pm f_l$ respectively. For the modulators the signal input is at f_l, the signal output at either f_+ or f_-; for the demodulators the signal input is at either f_+ or f_-, the signal output at f_l.

The two cases illustrated in Fig. 2 are distinguished by whether the local oscillator frequency lies between the two signal frequencies or whether it is greater than either of the signal frequencies. The choice of names *noninverting* and *inverting* is based on what the device does to the signal spectrum. This is best understood by considering not a single signal frequency as shown but a narrow band of signal frequencies. Then it is easily seen that the modulator and demodulator illustrated in Fig. 2(a) do not invert the signal spectrum, while those of Fig. 2(b) do invert the signal spectrum.

Taking the noninverting modulator and demodulator, whose signal and local oscillator frequencies are shown in Fig. 2(a), and assuming that the powers at all but the three frequencies shown are equal to zero, (24) and (25) become

$$\frac{W_1}{f_1} + \frac{W_+}{f_+} = 0, \tag{26}$$

$$\frac{W_l}{f_l} + \frac{W_+}{f_+} = 0, \tag{27}$$

where W_l, W_+, and W_1 represent the powers flowing into the nonlinear reactor at the frequencies f_l, f_+, and f_1 respectively. For the modulator W_l and W_1 are positive, representing power flowing into the nonlinear reactor, while W_+ is negative, representing the useful power output of the device. For the demodulator the situation is reversed, W_+ being positive and W_l and W_1 negative.

The power gain G_p is easily found from (27) for the noninverting modulator and demodulator. This gain is defined as the ratio of the power delivered to a specified load impedance to the power absorbed by the input of a transducer.[13] The two power gains are

$$G_{pl+} = \frac{f_+}{f_l}, \quad \text{noninverting modulator power gain} \tag{28}$$

[13] "American standard definitions of electrical terms," *ASA* C42; August, 1953.

$$G_{p+l} = \frac{f_l}{f_+}, \text{ noninverting demodulator power gain} \tag{29}$$

where the subscripts show the direction of travel of the signal, the first subscript indicating the input terminals, the second, the output terminals. The power gains are independent of the load impedances, which is not true for all transducers.

The power gain is seen to be simply the ratio of the output frequency to the input frequency; the modulator and demodulator gains are reciprocal. Thus a noninverting modulator operating between widely separated frequencies has a substantial power gain; a small amount of input power at the frequency f_l controls a large amount of local oscillator power at the frequency f_1, the sum of these powers appearing as useful output at the frequency f_+. In contrast a noninverting demodulator operating between widely separated frequencies has a corresponding loss; most of the input power at the frequency f_+ is wasted in the local oscillator circuit, very little of it emerging as useful output at the frequency f_l. These results hold true for any single-valued nonlinear characteristic and for any external circuit conditions, assuming that all unwanted frequencies are terminated in lossless circuits.

Since these power gains are positive the device must be stable, according to the discussion of the preceding section; that is, power cannot be delivered to purely passive terminations at both of the signal terminals (f_l and f_+) simultaneously with only the local oscillator applied to the nonlinear reactor. Consequently, the power gain of the noninverting modulator and demodulator is equal to the maximum available gain,[13] which is equal to the transducer gain,[13] defined as the ratio of the power delivered to the load impedance to the available power of the source, for a conjugate match at both source and load terminals. We note that the instability in the local oscillator circuit discussed in the preceding section can occur only in the demodulator, and then only if the input signal power at the frequency f_+ is not small compared to the local oscillator power.

Next, consider the inverting modulator and demodulator, whose signal and local oscillator frequencies are shown in Fig. 2(b). Assuming as before that the powers at all unwanted frequencies are equal to zero, (24) and (25) become

$$\frac{W_1}{f_1} + \frac{W_-}{f_-} = 0 \tag{30}$$

$$\frac{W_l}{f_l} - \frac{W_-}{f_-} = 0. \tag{31}$$

These differ from (26) and (27) for the noninverting device in the negative sign in the second equation. From (31) the power gains are

$$G_{pl-} = -\frac{f_-}{f_l}, \text{ inverting modulator power gain.} \tag{32}$$

$$G_{p-l} = -\frac{f_l}{f_-}, \text{ inverting demodulator power gain.} \tag{33}$$

The power gains are again reciprocal, but in this case are the negative of the ratio of the output frequency to input frequency, in contrast with (28) and (29) for the noninverting case. For both the inverting modulator and demodulator W_1 is positive, W_l and W_- negative; the input power from the local oscillator at the frequency f_1 flows out of the nonlinear reactor at the two signal frequencies, most of it appearing at the higher signal frequency f_-, only a small amount appearing at the lower signal frequency f_l. Thus the inverting device is potentially unstable and under certain conditions will oscillate, power emerging from both of the signal terminals into passive terminations with only the local oscillator applied.

Consequently, the transducer gain for either the inverting modulator or demodulator can take on any value between zero and infinity, depending on the external impedances at the signal terminals. The resistive component of input impedance at either signal frequency is negative, and so neither the source nor the load can be matched. Since, for the inverting device, most of the input power from the local oscillator appears at the high signal frequency, we would expect that for fixed terminal impedances the modulator gain will greatly exceed the demodulator gain, as with the noninverting device, although in contrast to this latter case these two gains can both be made arbitrarily large by operating close to the point of instability. Finally, we note that instability in the local oscillator circuit cannot arise in this case.

As a final example, consider the application of (24) and (25) to a nonlinear reactor harmonic generator. Assuming the power input $W_{1,0}$ at the fundamental frequency f_1 and the power output $-W_{m,0}$ at the harmonic frequencies mf_1, setting all other powers equal to zero,

$$W_{1,0} = \sum_{m=2}^{\infty} - W_{m,0}. \tag{34}$$

The total harmonic power output is equal to the fundamental power input, in agreement with the fact that the nonlinear reactor is assumed lossless. If the load impedances at the unwanted harmonic frequencies can be made zero, infinite, or purely reactive, the power gain to the desired harmonic can approach 1.

Hysteresis

In this section we extend the analysis of nonlinear reactors given in the third section to include the effects of hysteresis in the special case for which there are no departures from the principal single-frequency hysteresis loop established by the local oscillator alone. Thus, the path traversed in the q-v plane is assumed to be, at most, double-valued.

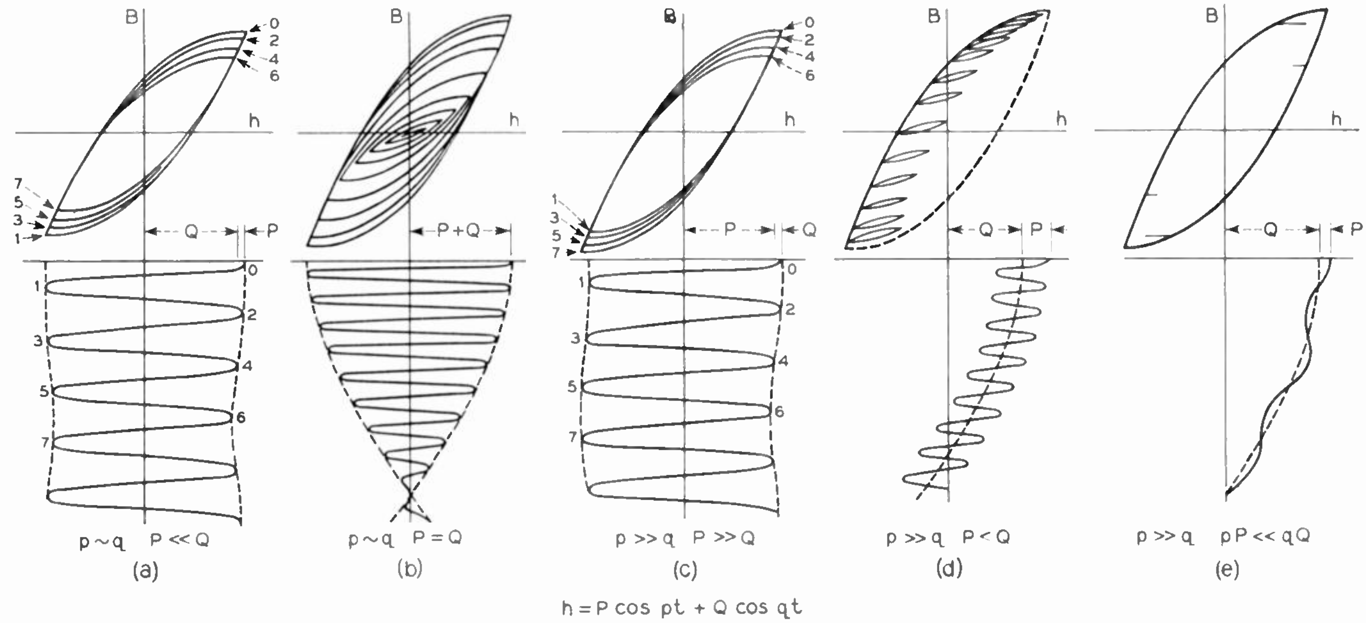

Fig. 3—Types of hysteresis loops characteristic of a two-frequency magnetizing force (taken from R. M. Kalb and W. R. Bennett,[14] Fig. 1).

R. M. Kalb and W. R. Bennett[14] have considered the problem of a nonlinear inductor with hysteresis when currents at only two frequencies flow in the element and when the operation is far from saturation. They give a detailed discussion of the various ways in which complex hysteresis loops can be formed and the corresponding effects on the operation of the device.

The present analysis differs from Kalb and Bennett's in three principal respects: 1) More than two driving frequencies are involved. 2) The level of the local oscillator at the frequency f_1 is assumed to be large enough to drive the nonlinear element well into saturation, so that the q-v characteristic will be single-valued over appreciable regions near its ends. The signal levels at the other frequencies are assumed to be small compared to the local oscillator level. 3) It is necessary to restrict this analysis by ruling out complex hysteresis loops and requiring the q-v characteristic to be at most double-valued in order to obtain any simple general results. The restrictions imposed in 2) and 3) above simplify the analysis in two ways: The voltage v, while a double-valued function of the charge q, is a single-valued function of x and y in (8), so that (22) and (23) remain valid in this case. The integrals on the right-hand sides of (22) and (23) may be simply evaluated in terms of the area of the hysteresis loop, as shown below.

The possible types of departure from the principal single-frequency hysteresis loop for the case of two applied frequencies and operation far from saturation are illustrated in Fig. 3, taken from a previous reference.[14] These show the general types of complex hysteresis loops which must be considered in the present analysis, although since many driving frequencies may be present, the corresponding complex hysteresis loops may be combinations of the types shown in Fig. 3.

Taking account of the fact that the local oscillator level far exceeds the other signal levels, there are two principal types of departure from the main hysteresis loop that must be considered. The first type, illustrated in Fig. 3(a) and (c), corresponds to a slow modulation of the single-frequency hysteresis loop. There are no reversals between successive maxima of the hysteresis loop, but the magnitudes of these maxima vary in a periodic manner. Consequently the successive branches of the complex hysteresis loop are all quite similar but are shifted a small amount from each other on each successive cycle of the local oscillator. This can occur either because of small high frequency components whose frequencies are near the local oscillator frequency f_1, which modulate the amplitude of the local oscillator at a slow rate, or because of small low frequency components, which shift the average value of the local oscillator waveform at a slow rate. Since in the present analysis the local oscillator is assumed to drive the nonlinear device well into saturation, and since the other signal levels are assumed to be small compared to the local oscillator, this type of departure from the main loop cannot occur and is eliminated from further consideration.

The second type of departure from the principal loop is illustrated in Fig. 3(d) and (e). Here there are small reversals between the principal maxima of the complex hysteresis loop, which result in the formation of many minor loops inside the principal loop; the principal maxima all have approximately the same magnitude. This phenomenon is caused by the presence of small

[14] R. M. Kalb and W. R. Bennett, "Ferromagnetic distortion of a two-frequency wave," *B.S.T.J.*, vol. 14, pp. 322–359; April, 1935.

components of much higher frequency than the local oscillator. This type of departure from the main loop must also be ruled out if the conditions of the present analysis are to be satisfied; this can be done in two ways:

1) The device may be assumed to have the property that small reversals in the direction of travel as the principal hysteresis loop is traversed do not cause departures from this principal loop, in the form of minor loops.

2) If the assumption, 1) above, is not tenable, then further restrictions must be placed on the signal levels so that such reversals cannot occur in the open portion of the principal hysteresis loop; *i.e.*, the part of the loop that is double-valued. This sort of restriction is illustrated in Fig. 3(e) for the case of only one high frequency component and the nature of the necessary restriction on levels is given for this case. The restrictions in the general case are similar, merely requiring that the sum of the maximum slopes of all of the high frequency components must be less than the slope of the local oscillator driving function at the ends of the open portion of the main loop. One special case of interest in which this restriction must be satisfied is that discussed in previous sections in which currents at only the local oscillator frequency f_1 and the three signal frequencies f_0 and $f_1 \pm f_0$ are allowed to flow in the nonlinear element (or the dual case where voltages at only these four frequencies are allowed to exist across it). Then none of the high frequency components exist, and no minor loops can be formed.

Subject to the above conditions, the q-v characteristic may be treated as, at most, a double-valued function. While the signal levels must be fairly small compared to the local oscillator to satisfy these conditions, they need not be vanishingly small, as in the small signal analysis of Part II. Consequently this might be called a quasi-small-signal analysis.

Returning to the analysis of the third section, in (1) we now regard v as a double-valued function of q. In the subsequent analysis the lower branch of this function must be chosen when the charge at the local oscillator frequency f_1 is increasing, the upper branch when it is decreasing. For example, if in (2) $Q_{1,0}=Q_{-1,0}$, so that both are real and the local oscillator charge at frequency f_1 is a cosine function, then for $0<x<\pi$ the upper branch of the q-v characteristic must be chosen, while for $\pi<x<2\pi$ the lower branch is selected. In (8) while v is a double-valued function of q, it is a single-valued function of x and y, as it must be if v is to be expanded into a double Fourier series. Thus, hysteresis does not alter the analysis leading up to (22) and (23).

The integrals on the right-hand sides of (22) and (23) were found to be identically equal to zero in the third section for the case of no hysteresis, $v=f(q)$ single-valued. The introduction of hysteresis, with $v=f(q)$ double-valued, requires reconsideration of these integrals.

Consider first the integral of (22). With $y=$constant, q will travel entirely around the hysteresis loop as x goes from 0 to 2π. Thus the integral on q yields a constant, independent of y, equal to the area of the hysteresis loop, which is called h. The integral on y cancels the factor $1/2\pi$, and (22) becomes

$$\sum_{m=0}^{\infty}\sum_{n=-\infty}^{\infty}\frac{mW_{m,n}}{mf_1+nf_0}=h \tag{35}$$

where

$$h=\oint f(q)dq,\ \text{area of hysteresis loop} \tag{36}$$

h is equal to the energy dissipated in the nonlinear reactor in one transit around the hysteresis loop, which occurs in a time equal to one period of the local oscillator frequency f_1. Therefore the average power H dissipated in the nonlinear reactor is

$$H=f_1\cdot h \tag{37}$$

and so (35) may be written

$$\sum_{m=0}^{\infty}\sum_{n=-\infty}^{\infty}\frac{mW_{m,n}}{mf_1+nf_0}=\frac{H}{f_1} \tag{38}$$

where H is the average power dissipated in hysteresis.

Next, consider the integral of (23). With x constant, q will travel back and forth along the same branch of the hysteresis loop, returning to its initial value without enclosing any area, as y goes from 0 to 2π. Thus, this integral on q is identically equal to zero for all x, and the right-hand side of (23) remains equal to zero, as in the case of no hysteresis, yielding

$$\sum_{m=-\infty}^{\infty}\sum_{n=0}^{\infty}\frac{nW_{m,n}}{mf_1+nf_0}=0. \tag{39}$$

Eqs. (38) and (39) give the general power relations in nonlinear reactors with hysteresis, subject to the restrictions discussed above, which insure that the hysteresis loop is no more than double-valued. We must remember that f_1 has been taken as the local oscillator frequency. Examining (38), we see that the hysteresis term may be transferred to the left-hand side and combined with the local oscillator term, $W_{1,0}/f_1$, to give $(W_{1,0}-H)/f_1$. Referring to (24) and (25), we see that the only difference from the results for the hysteresisless case is that the power lost in hysteresis is subtracted from the input power from the local oscillator. Thus, the power lost in hysteresis may be considered to come only from the local oscillator circuit, subject to the restriction that the hysteresis loop is no more than double-valued.

Consequently the power gains of the nonlinear reactor modulators and demodulators discussed above will remain the same while the power gain of the harmonic generator will be reduced in the presence of hysteresis.

The presence of complex hysteresis loops would complicate these calculations considerably, as illustrated by Kalb and Bennett's analysis.[14] Since no general results could be obtained, this case is not considered.

Nonlinear Resistor

A general analysis for the nonlinear resistor, similar to that given above for nonlinear reactors, may be carried out. However, the results of the nonlinear resistor analysis are relations among the reactive powers at the various frequencies, rather than among the real powers, as in the case of nonlinear reactors; further, the frequencies do not enter these equations.

The nonlinear resistor characteristic may be given by specifying the voltage v as some arbitrary single-valued function of the current i.

$$v = f(i). \tag{40}$$

As before, the current is written as a double Fourier series.

$$i = \sum_{m=-\infty}^{\infty} \sum_{n=-\infty}^{\infty} I_{m,n} e^{j(mx+ny)} \tag{41}$$

$$x = \omega_1 t \qquad \omega_1 = 2\pi f_1$$

$$y = \omega_0 t \qquad \omega_0 = 2\pi f_0 \tag{42}$$

$$I_{m,n} = I_{-m,-n}^* \qquad I_{-m,-n} = I_{m,n}^* \tag{43}$$

Since the characteristic is single-valued, v is also periodic in x and y and may be written

$$v = \sum_{m=-\infty}^{\infty} \sum_{n=-\infty}^{\infty} V_{m,n} e^{j(mx+ny)} \tag{44}$$

$$V_{m,n} = V_{-m,-n}^* \qquad V_{-m,-n} = V_{m,n}^*. \tag{45}$$

Proceeding as in the nonlinear reactor case, and making use of (18)–(21), the results corresponding to (24) and (25) are

$$\sum_{m=0}^{\infty} \sum_{n=-\infty}^{\infty} mX_{m,n} = 0 \tag{46}$$

$$\sum_{m=-\infty}^{\infty} \sum_{n=0}^{\infty} nX_{m,n} = 0 \tag{47}$$

with $X_{m,n}$ given by (21).

As with the nonlinear capacitor results, the summations in (45) and (46) extend over different ranges. Consequently, it is necessary to rewrite these results to obtain similar terms in the two equations, making use of (21) and making the choice of subscripts m,n that insures that $mf_1+nf_0>0$, so that the resulting X's will represent the reactive powers flowing into the nonlinear resistor at the various frequencies.

These relations among the reactive powers in a nonlinear resistor do not appear to be particularly useful. The interpretation of reactive power in this situation is not clear. Note that reactive power in a nonlinear resistor is not conserved, as was real power in the nonlinear capacitor.

Discussion

The general energy relations derived above provide two independent equations relating the powers at the different frequencies in nonlinear capacitors and inductors. These results are independent of the detailed shape of the nonlinear characteristic, of the levels at the various frequencies, and of the external circuits. They show which sidebands in a nonlinear reactor tend to make the device stable and which tend to make it unstable, and in the latter case in which generator circuit the negative resistance will appear. They thus provide useful information about the gain and stability of nonlinear reactor modulators, including such devices as magnetic and dielectric amplifiers, and indicate the conditions under which the production of subharmonic and other frequencies incommensurable with the applied frequency is possible in a nonlinear reactor. These equations would be useful in checking the results of detailed analysis of special nonlinear circuits.

The discussion of the two simplest types of nonlinear reactor modulators and demodulators, illustrated in Fig. 2, shows further properties of these devices. The noninverting device is stable and gives the best performance when matched; it has a high modulator gain and demodulator loss. The inverting device is potentially unstable, and so can not be matched; while the modulator gain again greatly exceeds the demodulator gain, either can become as large as desired by operating close enough to the point of instability. This suggests that although a reasonable modulator gain may be obtained with the inverting device, gain as a demodulator can be obtained only by operating so close to instability that the resulting bandwidth will be narrow and the sensitivity[15] of the gain to changes in the terminating impedances will be high.

In the small signal analysis of Part II (to be submitted later) the bandwidth, sensitivity, and the terminal impedances of these devices are determined for the special case in which the signal levels are much smaller than the local oscillator level.

[15] H. W. Bode, "Network Analysis and Feedback Amplifier Design," D. Van Nostrand Co., Inc., New York, N.Y.; 1945.

A Solution to the Approximation Problem for RC Low-Pass Filters*

K. L. SU† AND B. J. DASHER†, ASSOCIATE MEMBER, IRE

Summary—**This paper presents a method for investigating the transfer functions of RC low-pass networks. The procedure involves the use of the concept of potential analogy and the technique of conformal transformation. The poles and zeros are arranged in a certain symmetrical fashion in the transformed plane and on this plane the frequency characteristic may be written in closed form. The frequency characteristics obtained by this method have equal-ripple variation inside the pass band. By mathematical manipulations, the several quantities that are essential in describing the quality of each frequency characteristic; *i.e.*, the pass-band tolerance, the stopband-passband ratio and the stop-band attenuation, may be expressed in terms of several geometrical quantities in the transformed plane and the parameters of the transformation function. Thus, the design of this group of network functions may be accomplished by adjusting the geometric dimensions in the transformed plane and the transformation functions. The transformation used here is a function that involves elliptic functions. Some design charts which are helpful in the selections of these values are given.**

Introduction

THE PROBLEM of the synthesis of RC networks is of frequent interest chiefly because of their low cost, stable operation and practicality for low-frequency applications. Generally, a synthesis problem consists of two main steps: approximation and realization. Several methods have been devised for the realization of an RC network when a realizable transfer function is given.[1–7]

The approximation part of the problem is quite difficult because of the restrictions imposed on the location of the poles of the transfer functions of RC networks. An analog two-dimensional electrostatic field together with conformal transformations has been used by many[8–12] to facilitate the visualization of the effects of various locations of singularities on the frequency characteristic of a network function. A transformation especially suitable for locating poles and zeros of RC network functions to obtain low-pass frequency characteristics with equal-ripple variation inside the pass band is employed here. The manner in which the transformation is used is essentially the same as that used by Fano[12] to obtain equal ripple characteristics in the case of RLC networks. The present problem is more difficult because of the restrictions on the location of poles of RC networks. Matthaei[11] uses conformal transformation in a somewhat different way.

The selection of transformation parameters to obtain predetermined tolerances involves the inversion of rather complicated expressions. The use of precalculated design curves practically eliminates this difficulty. A brief consideration leads to the following correspondent quantities in the two domains: negative charges and zeros, positive charges and poles, complex potential and transmission function, potential and gain, etc. Actually these analog quantities need not be distinguished as they represent the same analytical variables. These quantities will be used interchangeably herein.

The Transformation

The transformation[13]

$$s = \frac{\operatorname{sn}(z, k)}{\sqrt{\dfrac{1}{k^2 \operatorname{sn}^2(aK, k)} - \operatorname{sn}^2(z, k)}} \tag{1}$$

* Original manuscript received by the IRE, October 13, 1955; revised manuscript received, March 2, 1956.

† Georgia Institute of Technology, Atlanta, Ga.

[1] E. A. Guillemin, "Synthesis of RC networks," *Jour. Math. Phys.*, vol. 28, pp. 22–42; 1949.

[2] A. Fialkow and I. Gerst, "The transfer function of general two terminal-pair RC networks," *Quart. Appl. Math.*, vol. 10, pp. 113–127; 1952.

[3] P. F. Ordung, G. S. Krauss, G. S. Axelby, and W. P. Yetter, "Synthesis of paralleled three-terminal RC networks to provide complex zeros in the transfer functions," Trans. AIEE, vol. 70, pp. 1861–1867; 1951.

[4] H. J. Orchard, "The synthesis of RC networks to have prescribed transfer functions," Proc. IRE, vol. 39, pp. 428–432; April, 1951.

[5] J. L. Bower and P. F. Ordung, "The synthesis of RC networks," Proc. IRE, vol. 38, pp. 263–269; March, 1950.

[6] J. T. Fleck and P. F. Ordung, "The realization of a transfer ratio by means of an RC ladder network," Proc. IRE, vol. 39, pp. 1069–1074; September, 1951.

[7] B. J. Dasher, "Synthesis of RC transfer functions as unbalanced two terminal-pair networks," Technical Report No. 215, Research Laboratory of Electronics, Massachusetts Institute of Technology, 1951.

[8] W. W. Hansen and O. C. Lundstrum, "Experimental determination of impedance functions by the use of electrolytic tank," Proc. IRE, vol. 33, pp. 528–534; August, 1945.

[9] W. H. Huggins, "A note on frequency transformations for use with the electrolytic tank," Proc. IRE, vol. 36, pp. 421–424; March, 1948.

[10] S. Darlington, "The potential analogue method of network synthesis," *B.S.T.J.*, vol. 30, pp. 315–365; 1951.

[11] G. L. Matthaei, "A general method for synthesis of filter transfer function as applied to LC and RC filter examples," Tech. Report No. 39, E.R.L., Stanford Univ.; 1951.

[12] R. M. Fano, "A note on the solution of certain approximation problems in network synthesis," *Franklin Inst. Jour.*, vol. 249, pp. 189–205; 1950.

[13] Transformation (1) may be derived from two simpler transformations

$$s = \frac{w}{\sqrt{A^2 - w^2}}$$

and $w = \operatorname{sn} z$, where

$$A = \frac{1}{k \operatorname{sn}(aK)}.$$

where $\mathrm{sn}(z, k)$ is the Jacobian elliptic function[14] of modulus k and K is its quarter-period in the real direction, maps the entire s-plane into a rectangle in the z-plane. The geometry of this transformation is depicted in Fig. 1.

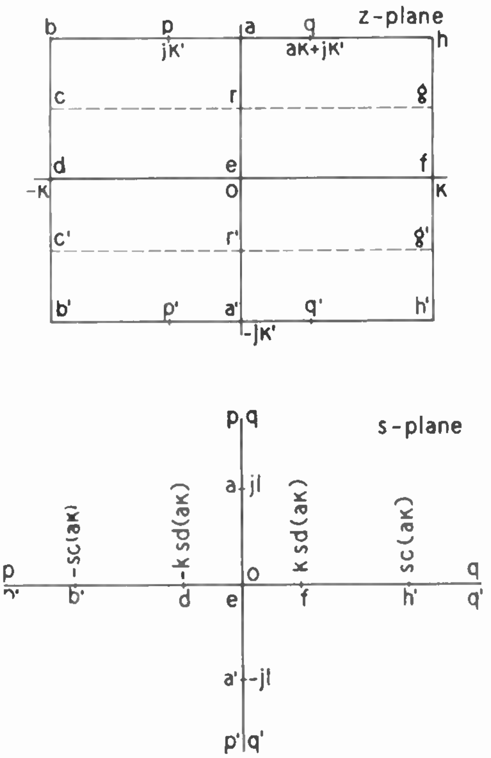

Fig. 1—The transformation of (1).

Fig. 2 suggests a process to aid the visualization of this transformation by considering the s-plane as being cut up and compressed into a rectangle. Since the axes of the s-plane are the most important regions in this synthesis problem, their images in the z-plane must be closely followed.

The transformed rectangle as shown in Fig. 1 repeats itself in both the x-direction and the y-direction. Therefore, this function is doubly periodic and the rectangle of Fig. 1 is merely a sample "cell" of the entire z-plane. Because of the symmetry possessed by this problem it is sufficient to show only one cell. However, the fact that there are an infinite number of rectangles should not be overlooked.

All realizable network functions must have their singularities located symmetrically about the real axis. If all the singularities in the left half-plane are also duplicated in the right half-plane, the potential along the imaginary axis will be exactly doubled. If this is

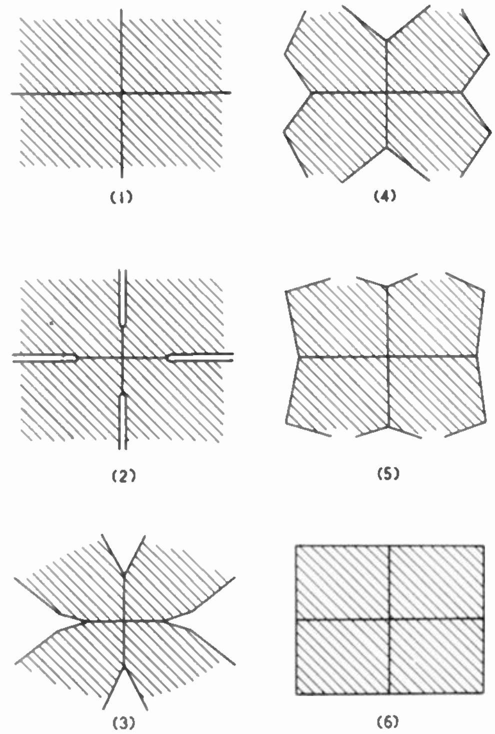

Fig. 2—The compression of the s-plane into a rectangle.

always done the analytical work is greatly simplified because of the resulting quadrantal symmetry. The right-half-plane singularities may be discarded at the end. This quadrantal symmetry will be used here and its validity is implied without being mentioned at every occasion. The following features that exist in the z-plane should be observed.

1) The total number of positive charges must equal that of negative charges inside a cell.

2) The point at infinity is split and mapped into four parts: points p, p', q, and q'.

3) The positive real-frequency axis is mapped onto e-a-p and regions of quadrantal symmetry.

4) Negative real axis is mapped onto e-d-b-p and regions of quadrantal symmetry.

In applying transformation (1), if the following rules are followed when charges are being arranged in the z-plane, the equal-ripple low-pass filter characteristics will be obtained.

1) Poles are distributed uniformly along b-b'.

2) Zeros are distributed uniformly along lines parallel to the y-axis.

3) Region e-a is considered as the pass band.

Several arrangements satisfying these conditions are shown in Fig. 3.

It can be shown mathematically that in all cases shown in Fig. 3 the potential will decrease monotonically between the origin, e, and the point, f, which is the first point on the imaginary axis nearest to any zero. The rest of the axis has a similar potential variation. Thus, the potential along the imaginary axis will vary in equal-

[14] For the definition of *elliptic functions* see, for instance, P. Franklin, "Methods of Advanced Calculus," McGraw-Hill Book Co., New York, N. Y.; 1944, L. M. Milne-Thomson, "Jacobian Elliptic Function Tables," Dover Publications, New York, N. Y.; 1950, or A. C. Dixon, "The Elementary Properties of the Elliptic Functions," Macmillan and Co.; London; 1894.

ripple manner with one complete cycle between two horizontal rows of zeros.

In considering the total charge contained in each cell, all charges located along the edges of each rectangle are shared by rectangles adjacent to it. Therefore, only half of each charge should be considered as lying in each cell. Taking this into consideration it is seen that there are as many positive charges as there are negative ones in each rectangle.

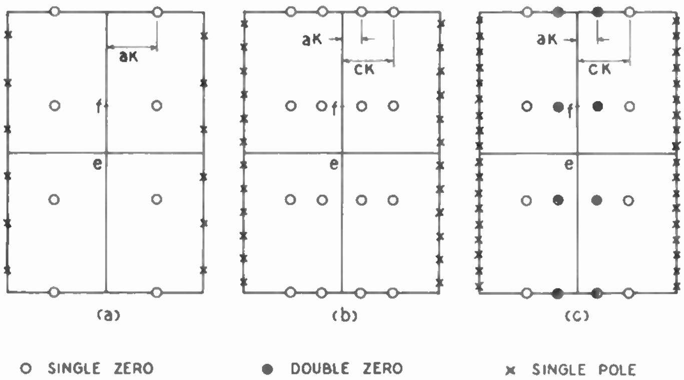

Fig. 3—Some singularity arrangements that produce low-pass RC network functions.

Networks Employing One Row of Simple Zeros in the z-Plane

The first arrangement to be considered is the one shown in Fig. 3(a) in which one row of zeros is included. Zeros must be spaced twice as far apart among themselves as positives charges. The corresponding singularity distribution in the s-plane takes the general form shown in Fig. 4. That the right-half-plane singularities

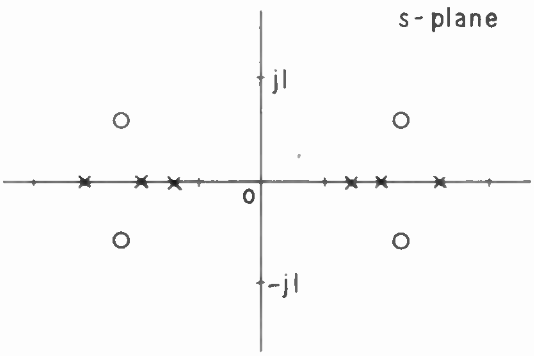

Fig. 4—Singularities in the s-plane for the arrangement of Fig. 3(a).

are to be discarded in the final network function is understood. The response of this group of networks takes the general shape shown in Fig. 5.

In order to arrive at an expression which will yield the singularities as shown in Fig. 3(a) one may observe that the expression

$$\mathrm{sn}^2 (C_1 z, k_1) - \mathrm{sn}^2(aK_1 + jK_1', k_1)$$

is equal to zero at $C_1 z = aK_1 + jK_1'$ and all its congruent points[15] and is equal to infinity at $C_1 z = jK_1'$ and all its

[15] For definition of the term *congruent*, see E. T. Whittaker and G. N. Watson, "Modern Analysis," Cambridge University Press, Cambridge, Eng., pp. 430; 1950.

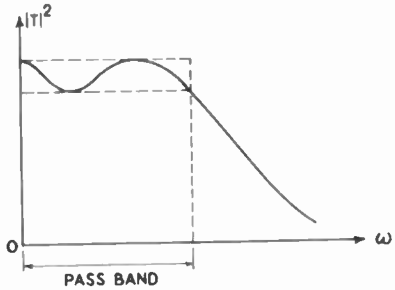

Fig. 5—Frequency characteristic for singularity arrangement of Fig. 3(a).

congruent points while the expression

$$\mathrm{sn}^2 (C_1 z, k_1) - \mathrm{sn}^2 \left(K_1 + j \frac{K_1'}{2}, k_1 \right)$$

is equal to zero at $C_1 z = K_1 + jK_1'/2$ and all its congruent points and is equal to infinity at $C_1 z = jK_1'$ and all its congruent points. Thus the expression

$$T[s(z)]T[-s(z)] = \frac{\mathrm{sn}^2 (C_1 z, k_1) - \mathrm{sn}^2 (aK_1 + jK_1', k_1)}{\mathrm{sn}^2 (C_1 z, k_1) - \mathrm{sn}^2 \left(K_1 + j \frac{K_1'}{2}, k_1 \right)} = \frac{\mathrm{sn}^2 (C_1 z, k_1) - \frac{1}{k_1^2} \mathrm{sn}^2(aK_1, k_1)}{\mathrm{sn}^2 (C_1 z, k_1) - \frac{1}{k_1}} \qquad (2)$$

will have zeros located at $aK_1 + jK_1'$ and all its congruent points and poles located at $K_1 + jK_1'/2$ and all its congruent points in the $C_1 z$-plane. The function has the desired quadrantal symmetry and represents $|T(j\omega)|^2$.

Now if k_1 is so chosen that the quarter-periods of modulus k, K and jK', and that of modulus k_1, K_1, and jK_1', are related by the equation

$$\frac{nK_1'}{K_1} = \frac{K'}{K}, \qquad (3)$$

where n is the number of zeros included in one half of a cell, and C_1 made to be equal to the ratio of K_1 to K, expression (2) has zeros and poles in the z-plane as shown in Fig. 3(a).

For the type of arrangement shown in Fig. 3(a), n is necessarily odd. If n is to be even, zeros must be placed away from the horizontal sides of each cell. A similar consideration in this case will yield the following expression to give the proper poles and zeros.

$$T[s(z)]T[-s(z)] = \frac{\mathrm{sn}^2 (C_1 z, k_1) - \mathrm{sn}^2(aK_1, k_1)}{\mathrm{sn}^2 (C_1 z, k_1) - \frac{1}{k_1}} \qquad (4)$$

where k_1 and C_1 have the same significance as before.

Along the y-axis a minimum of $|T|^2$ occurs whenever y is equal to the ordinate of a zero and a maximum occurs midway between every two adjacent minima. The

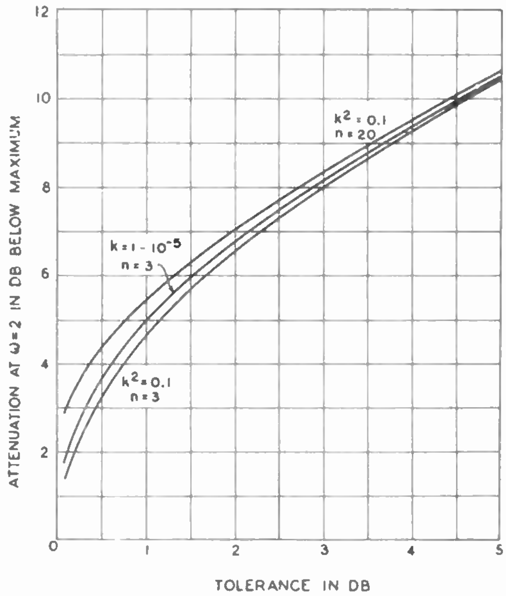

Fig. 6—Attentuation at $\omega=2$ for various values of n and k for singularity arrangement of Fig. 3(a).

variation between a minimum and the next maximum is monotonic. It is clear that at all maxima and at all minima $|T|^2$ assumes the same values. Thus, the equal ripple property is assured.

Quantitatively,

$$\frac{|T|^2 \max}{|T|^2 \min} = \frac{1}{k_1 \operatorname{sn}^2(aK_1)} \tag{5}$$

for either odd or even n. Thus, for this type of charge arrangement,

$$\text{tolerance} = 10 \log \left[\frac{1}{k_1 \operatorname{sn}^2(aK_1)}\right] db. \tag{6}$$

The location of any point outside the pass band where $s=j\omega_2$ in the C_1z-plane is bK_1+jK_1 where

$$\operatorname{sn}(bK) = \frac{\sqrt{\omega_2^2-1}}{\omega_2} \operatorname{sn}(aK). \tag{7}$$

The value of $|T|^2$ at this frequency may be calculated from (2) or (3).

By means of this analysis a group of varied arrangements of singularities may be compared and studied by (2) and (6) while the low-pass and equal-ripple features remain fixed.

An investigation of the effects of the modulus k of the transformation function shows that only a very small improvement in the rate of cutoff is gained by making k very large (approaching unity). This conclusion is evidenced by a comparison of the attenuation at a point outside the pass band where $\omega=2$ for a moderate value of k, 0.1, and a value very close to unity as shown by Fig. 6. A large value of k will make the poles in the s-plane cluster into a very narrow region and make the realization problem very difficult. Thus the value of k may be chosen for the best pole distribution without appreciable sacrifice in filter quality.

If the number of real-frequency zeros is held constant, an increase in the total number of zeros merely increases the number of ripples inside the pass band while the cutoff part of the filter characteristic is practically unaffected. This is also verified by a comparison of the attenuation at $\omega=2$ for two values of n, 3 and 20. It is seen from Fig. 6 that the attenuation at $\omega=2$ increases very slowly as n is increased. Thus, little is gained by increasing the complexity of the network in this direction.

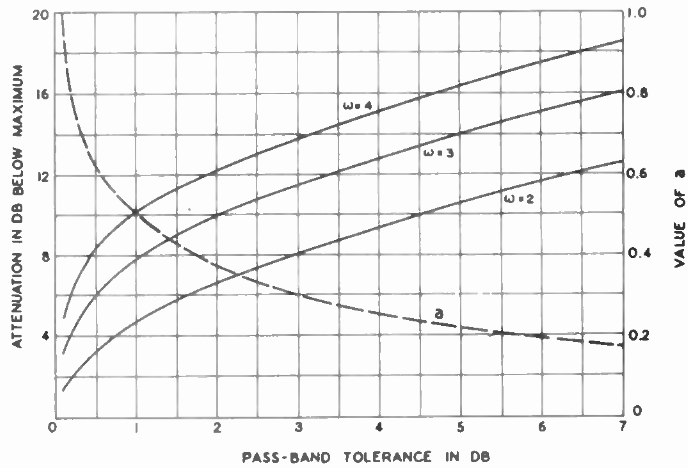

Fig. 7—Attenuation outside the pass band for singularity arrangement of Fig. 3(a) with $k^2=0.1$ and $n=3$.

Fig. 7 shows the attenuation at several points outside the pass band for various tolerances. The value of a which is necessary in locating all zeros in the s-plane corresponding to a given pass band tolerance may be found from the dashed curve.

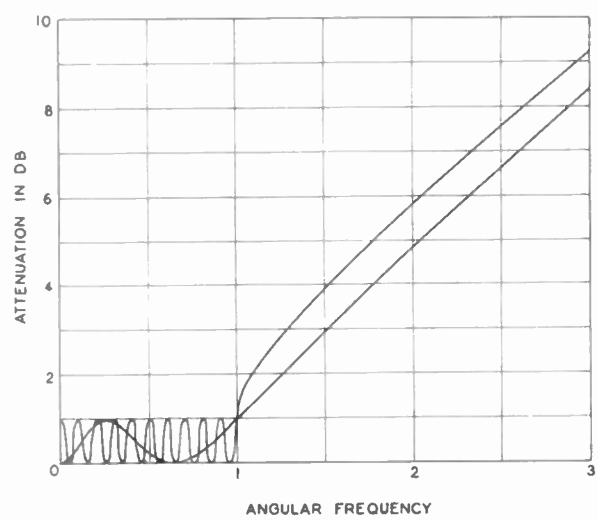

Fig. 8—Frequency characteristics for charge arrangement of Fig. 3(a) for $n=3$ and $n=20$, $k^2=0.1$.

Networks Employing Two Rows of Zeros in the z-Plane

The arrangement of Fig. 3(b) places a zero between the edge of the pass band and infinity. This improves the cutoff rate outside the pass band. The frequency characteristic will take the general form shown in Fig. 9.

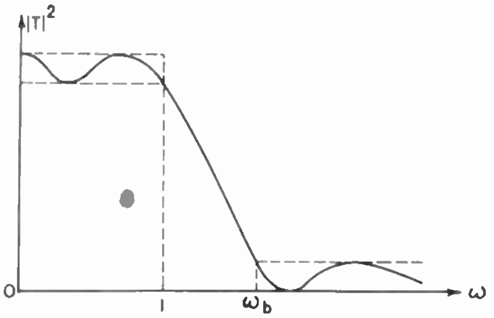

Fig. 9—Frequency characteristic for singularity arrangement of Fig. 3(b).

The arrangement of the positions of maxima and minima is very similar to the previous case. The frequency ω_b will be designated as the lower edge of the stop band. This is the lowest frequency at which the attenuation equals the minimum stop-band attenuation.

By a derivation similar to that by which (2) is arrived at, the function that gives the singularities shown in Fig. 3(b) may be found to be

$$T(-s)T(s) = \frac{[\text{sn}^2(C_1z, k_1) - \text{sn}^2(aK_1 + jK_1', k_1)][\text{sn}^2(C_1z, k_1) - \text{sn}^2(cK_1 + jK_1', k_1)]}{\left[\text{sn}^2(C_1z, k_1) - \text{sn}^2\left(K_1 + j\frac{K_1'}{4}, k_1\right)\right]\left[\text{sn}^2(C_1z, k_1) - \text{sn}^2\left(K_1 + j\frac{3K_1'}{4}, k_1\right)\right]} \tag{8}$$

for odd n, where n is still the number of ripples inside the pass band. The number of negative charges used in each quadrant in this case is $2n$. The numbers K, K', K_1, K_1', and C_1 have the same significance as described for (2) and (3).

The tolerance in this case is given by the expression

$$\text{Tolerance} = 10 \log \left[\frac{\text{dn}^2\left(\frac{K_1'}{4}, k_1'\right)\text{dn}^2\left(\frac{3K_1'}{4}, k_1'\right)}{k_1^4 \,\text{sn}^2(aK_1, k_1)\,\text{sn}^2(cK_1, k_1)}\right] db. \tag{9}$$

From (9) it is seen that for a given tolerance, a and c may assume different values as long as this equation is satisfied. The choice of values of a and c will affect the stop-band attenuation and the frequency at which the stop band begins. These are usually the deciding considerations. If expressions are derived to give these values they will only be implicit in nature and a cut-and-try process must be used. Therefore it is desirable to have these values precalculated and plotted as curves. By so doing the selection of values of a and c is greatly facilitated. Figs. 10 and 11 are examples of a set of such graphs. They are calculated for a value of k equal to $\sqrt{0.1}$ and $n=3$.

In the process of realizing this group of networks the right half-plane charges must be discarded. This leaves two half-unit charges on the $j\omega$-axis. Since such a function is not physically realizable it is necessary to double all charges and two networks must be constructed, connected in tandem and isolated by some device such as a vacuum tube.

Networks Employing One Row of Simple-Zeros and One Row of Double-Zeros

In order to eliminate the half-order zero on the imaginary axis caused by the necessary procedure of dropping the charges in the right half-plane, the row of zeros closer to the imaginary axis may be doubled. For this case the function that gives these singularities may be written as

$$T(s)T(-s) = \frac{\text{sn}^2(C_1z, k_1) - \text{sn}^2(aK_1 + jK_1', k_1)}{\text{sn}^2(C_1z, k_1) - \text{sn}^2\left(K_1 + j\frac{K_1'}{6}, k_1\right)} \times \frac{[\text{sn}^2(C_1z, k_1) - \text{sn}^2(cK_1 + jK_1', k_1)]^2}{\left(\text{sn}^2(C_1z, k_1) - \text{sn}^2\left(K_1 + j\frac{K_1'}{2}, k_1\right)\right)^1} \times \frac{1}{\text{sn}^2(C_1z, k_1) - \text{sn}^2\left(K_1 + j\frac{5K_1'}{6}, k_1\right)} \tag{10}$$

for an odd number of ripples.

The tolerance is given by

$$\text{Tolerance} = 10 \log \left[\frac{1}{\text{dn}^2\left(\frac{K_1'}{6}, k_1'\right)\text{dn}^2\left(\frac{K_1'}{2}, k_1'\right)\text{dn}^2\left(\frac{5K_1'}{6}, k_1'\right)\text{sn}^2(aK_1, k_1)\,\text{sn}^4(cK_1, k_1)}\right]. \tag{11}$$

A problem of choosing the proper values of a and c to give an acceptable compromise between tolerance and steepness of cutoff exists in this arrangement as in the previous case. Figs. 12 and 13 are examples of graphs that are useful for this purpose. They are prepared for a value of k equal to $\sqrt{0.1}$ and $n=3$.

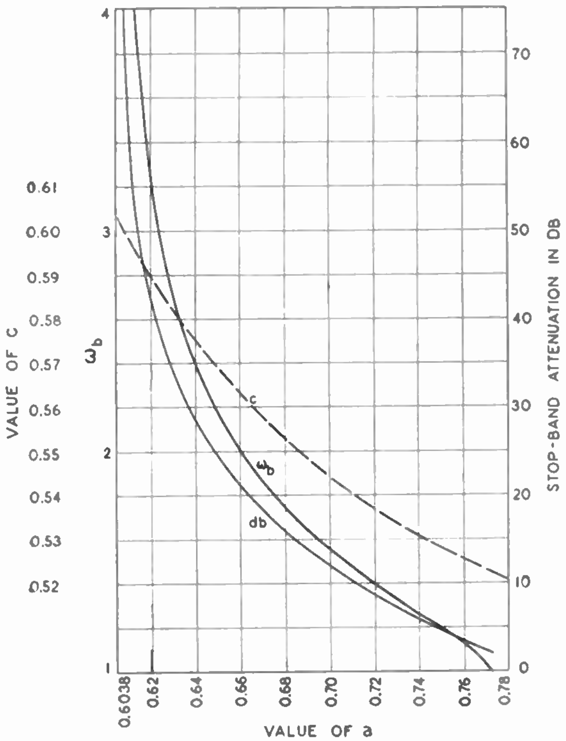

Fig. 10—Stop-band attenuation and ω_b for pass-band tolerance of 2 db, $n=3$ and $k^2=0.1$, for singularity arrangement of Fig. 3(b).

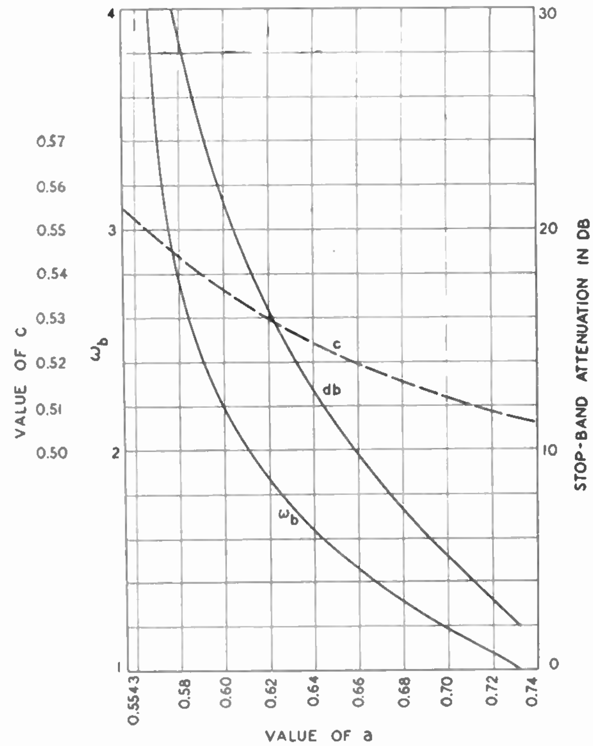

Fig. 12—Stop-band attenuation and ω_b for pass-band tolerance of 2 db, $n=3$ and $k^2=0.1$, for singularity arrangement of Fig. 3(c).

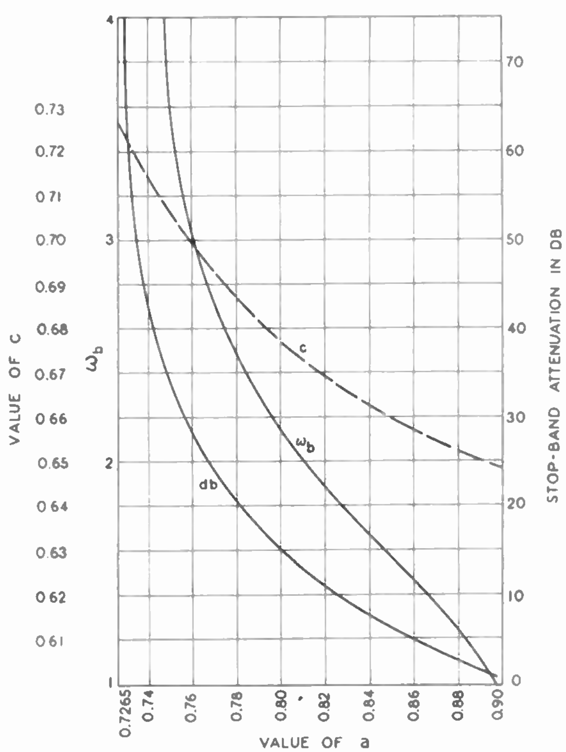

Fig. 11—Stop-band attenuation and ω_b for pass-band tolerance of 1 db, $n=3$ and $k^2=0.1$, for singularity arrangement of Fig. 3(b).

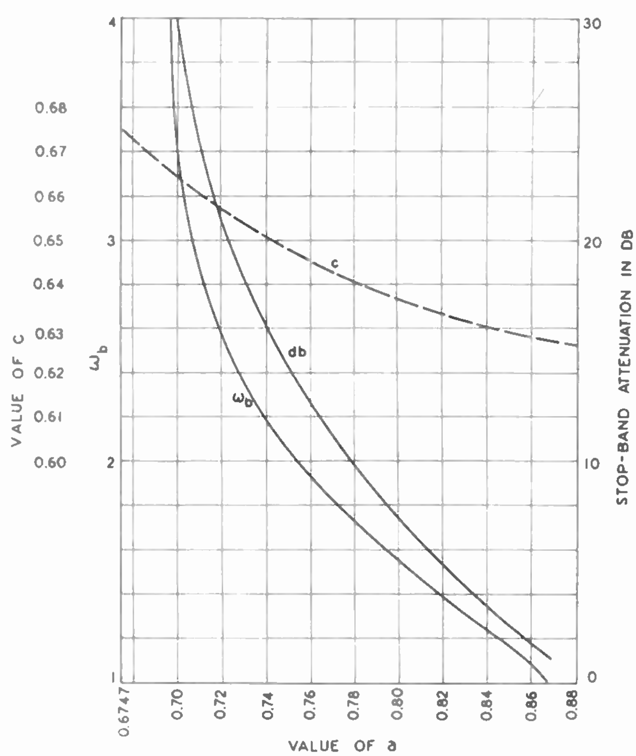

Fig. 13—Stop-band attenuation and ω_b for pass-band tolerance of 1 db, $n=3$ and $k^2=0.1$, for singularity arrangement of Fig. 3(c).

Conclusion

The elliptic function transformation (1). is used here for the purpose of locating zeros and poles of a low-pass filter network function. Charts of the type shown in Figs. 7 to 12 may be prepared for any range of application whenever desired. The compactness of the expressions that give the tolerance and other characteristic quantities makes the preparation of these charts which represent a whole group of network functions with many singularities a matter of evaluating only a few terms together with a few rational operations. These charts, after they are prepared, will be very helpful for design purposes. For instance, if a required attenuation beyond twice the cut-off frequency must be greater than 13 db, Fig. 10 indicates that a filter function with the charge arrangement of Fig. 3(b) and values of a and c of 0.810 and 0.673 respectively will satisfy the requirement. The locations of all poles and zeros of this filter are determined in the z-plane. The locations of zeros and poles in the s-plane may be found by applying the inverse transformation.

Feedback Theory—Further Properties of Signal Flow Graphs*

SAMUEL J. MASON†

***Summary*—A way to enhance**
Writing gain at a glance.
Dr. Tustin extended
Proof appended.
Examples illustrative
Pray not frustrative.

Background

THERE ARE many different paths to the solution of a set of linear equations. The formal method involves inversion of a matrix. We know, however, that there are many different ways of inverting a matrix: determinantal expansion in minors, systematic reduction of a matrix to diagonal form, partitioning into submatrices, and so forth, each of which has its particular interpretation as a sequence of algebraic manipulations within the original equations. A determinantal expansion of special interest is

$$D = \sum a_{1i}a_{2j}a_{3k} \cdots a_{nz} \tag{1}$$

where a_{mp} is the element in the mth row and pth column of a determinant having n rows, and the summation is taken over all possible permutations of the column subscripts. (The sign of each term is positive or negative in accord with an even or odd number of successive adjacent column-subscript interchanges required to produce a given permutation.) Since the solution of a set of linear equations involves ratios of determinantal quantities, (1) suggests the general idea that a linear system analysis problem should be interpretable as a search for all possible combinations of something or other, and that the solution should take the form of a sum of products of the somethings, whatever they are, divided by another such sum of products. Hence, instead of undertaking a sequence of operations, we can find the solution by looking for certain combinations of things. The method will be especially useful if these combinations have a simple interpretation in the context of the problem.

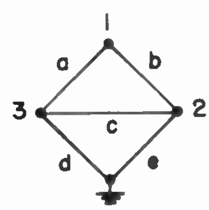

Fig. 1—An electrical network graph.

As a concrete illustration of the idea, consider the electrical network graph shown in Fig. 1. For simplicity, let the branch admittances be denoted by letters a, b, c, d, and e. This particular graph has *three* independent node-pairs. First locate all possible sets of *three* branches which *do not contain closed loops* and write the sum of their branch admittance products as the denominator of (2).

$$Z_{12} = \frac{ab + ac + bc + bd}{abd + abe + acd + ace + ade + bcd + bce + bde} \tag{2}$$

Now locate all sets of *two* branches which *do not form*

* Original manuscript received by the IRE, August 16, 1955; revised manuscript received, February 27, 1956. This work was supported in part by the Army (Signal Corps), the Air Force (Office of Scientific Research, Air Research and Development Command), and the Navy (Office of Naval Research).

† Dept. of Elect. Engrg. and Res. Lab. of Electronics, M.I.T., Cambridge, Mass.

closed loops and which also *do not contain any paths from node 1 to ground or from node 2 to ground*. Write the sum of their branch admittance products as the numerator of expression (2). The result is the transfer impedance between nodes 1 and 2, that is, the voltage at node 2 when a unit current is injected at node 1. Any impedance of a branch network can be found by this process.[1]

So much for electrical network graphs. Our main concern in this paper is with signal flow graphs,[2] whose branches are directed. Tustin[3] has suggested that the feedback factor for a flow graph of the form shown in Fig. 2 can be formulated by combining the feedback loop

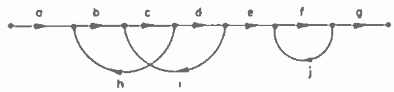

Fig. 2—The flow graph of an automatic control system.

gains in a certain way. The three loop gains are

$$T_1 = bch \tag{3a}$$

$$T_2 = cdi \tag{3b}$$

$$T_3 = fj \tag{3c}$$

and the forward path gain is

$$G_0 = abcdefg. \tag{4}$$

The gain of the complete system is found to be

$$G = \frac{G_0}{[1 - (T_1 + T_2)](1 - T_3)} \tag{5}$$

and expansion of the denominator yields

$$G = \frac{G_0}{1 - (T_1 + T_2 + T_3) + (T_1T_3 + T_2T_3)} \cdot \tag{6}$$

Tustin recognized the denominator as unity plus the sum of all possible products of loop gains taken one at a time $(T_1+T_2+T_3)$, two at a time, $(T_1T_3+T_2T_3)$, three at a time, and so forth, excluding products of loops that touch or partially coincide. The products T_1T_2 and $T_1T_2T_3$ are properly and accordingly missing in this particular example. The algebraic sign alternates, as shown, with each succeeding group of products.

Tustin did not take up the general case but gave a hint that a graph having several different forward paths could be handled by considering each path separately and superposing the effects. Detailed examination of the general problem shows, in fact, that the form of (6) must be modified to include possible feedback factors in the numerator. Otherwise (6) applies only to those graphs in which each loop touches all forward paths.

[1] Y. H. Ku, "Resume of Maxewll's and Kirchoff's rules for network analysis," *J. Frank. Inst.*, vol. 253, pp. 211–224; March, 1952.

[2] S. J. Mason, "Feedback theory—some properties of signal flow graphs," Proc. IRE, vol. 41, pp. 1144–1156; September, 1953.

[3] A. Tustin, "Direct Current Machines for Control Systems," The Macmillan Company, New York, pp. 45–46, 1952.

The purposes of this paper are: to extend the method to a general form applicable to any flow graph; to present a proof of the general result; and to illustrate the usefulness of such flow graph techniques by application to practical linear analysis problems. The proof will be given last. It is tempting to add, at this point, that a better understanding of linear analysis is a great aid in problems of nonlinear analysis and linear or nonlinear design.

A Brief Statement of Some Elementary Properties of Linear Signal Flow Graphs

A signal flow graph is a network of directed branches which connect at nodes. Branch jk originates at node j and terminates upon node k, the direction from j to k being indicated by an arrowhead on the branch. Each branch jk has associated with it a quantity called the branch gain g_{jk} and each node j has an associated quantity called the node signal x_j. The various node signals are related by the associated equations

$$\sum_j x_j g_{jk} = x_k, \qquad k = 1, 2, 3, \cdots \tag{7}$$

The graph shown in Fig. 3, for example, has equations

$$ax_1 + dx_3 = x_2 \tag{8a}$$

$$bx_2 + fx_4 = x_3 \tag{8b}$$

$$ex_2 + cx_3 = x_4 \tag{8c}$$

$$gx_3 + hx_4 = x_5. \tag{8d}$$

We shall need certain definitions. A *source* is a node having only outgoing branches (node 1 in Fig. 3). A *sink* is a node having only incoming branches. A *path* is any continuous succession of branches traversed in the indicated branch directions. A *forward path* is a path from source to sink along which no node is encountered more than once (*abch*, *aeh*, *aefg*, *abg*, in Fig. 3).

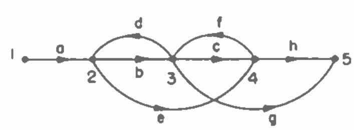

Fig. 3—A simple signal flow graph.

A *feedback loop* is a path that forms a closed cycle along which each node is encountered once per cycle (*bd*, *cf*, *def*, but not *bcfd*, in Fig. 3). A *path gain* is the product of the branch gains along that path. The *loop gain* of a feedback loop is the product of the gains of the branches forming that loop. The *gain of a flow graph* is the signal appearing at the sink per unit signal applied at the source. Only one source and one sink need be considered, since sources are superposable and sinks are independent of each other.

Additional terminology will be introduced as needed.

General Formulation of Flow Graph Gain

To begin with an example, consider the graph shown in Fig. 4. This graph exhibits three feedback loops, whose gains are

$$T_1 = h \tag{9a}$$

$$T_2 = fg \tag{9b}$$

$$T_3 = de \tag{9c}$$

and two forward paths, whose gains are

$$G_1 = ab \tag{10a}$$

$$G_2 = ceb. \tag{10b}$$

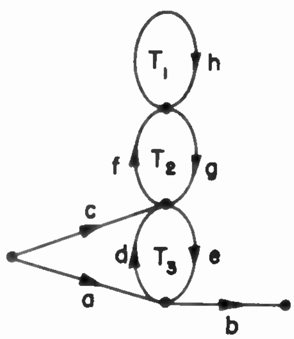

Fig. 4—A flow graph with three feedback loops.

To find the graph gain, first locate all possible *sets of nontouching loops* and write the algebraic sum of their gain products as the denominator of (11).

$$G = \frac{G_1(1 - T_1 - T_2) + G_2(1 - T_1)}{1 - T_1 - T_2 - T_3 + T_1T_3} \tag{11}$$

Each term of the denominator is the gain product of a set of nontouching loops. The algebraic sign of the term is plus (or minus) for an even (or odd) number of loops in the set. The graph of Fig. 4 has no sets of three or more nontouching loops. Taking the loops two at a time we find only one permissible set, T_1T_3. When the loops are taken one at a time the question of touching does not arise, so that each loop in the graph is itself an admissible "set." For completeness of form we may also consider the set of loops taken "none at a time" and, by analogy with the zeroth power of a number, interpret its gain product as the unity term in the denominator of (11). The numerator contains the sum of all forward path gains, each multiplied by a factor. The factor for a given forward path is made up of all possible sets of loops which *do not touch each other* and which also do *not touch that forward path*. The first forward path ($G_1 = ab$) touches the third loop, and T_3 is therefore absent from the first numerator factor. Since the second path ($G_2 = ceb$) touches both T_2 and T_3, only T_1 enters the second factor.

The general expression for graph gain may be written as

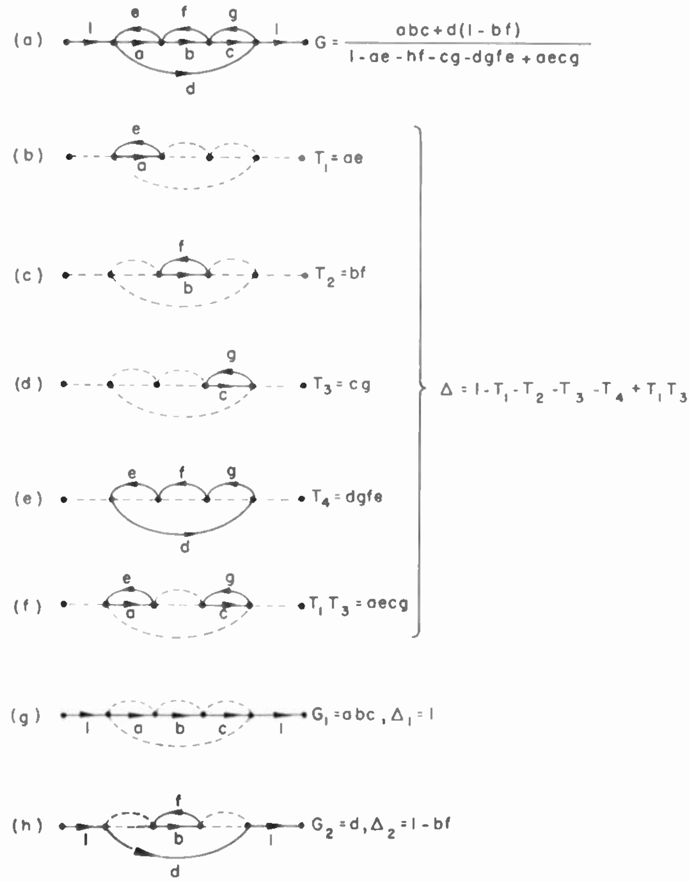

Fig. 5—Identification of paths and loop sets.

$$G = \frac{\sum_k G_k \Delta_k}{\Delta} \tag{12a}$$

wherein

$$G_k = \text{gain of the } k\text{th forward path} \tag{12b}$$

$$\Delta = 1 - \sum_m P_{m1} + \sum_m P_{m2} - \sum_m P_{m3} + \cdots \tag{12c}$$

P_{mr} = gain product of the mth possible combination of r nontouching loops (12d)

Δ_k = the value of Δ for that part of the graph not touching the kth forward path. (12e)

The form of (12a) suggests that we call Δ the *determinant* of the graph, and call Δ_k the *cofactor* of forward path k.

A subsidiary result of some interest has to do with graphs whose feedback loops form nontouching subgraphs. To find the *loop subgraph* of any flow graph, simply remove all of those branches *not* lying in feedback loops, leaving all of the feedback loops, and nothing but the feedback loops. In general, the loop subgraph may have a number of nontouching parts. The useful fact is that the *determinant of a complete flow graph is equal to the product of the determinants of each of the nontouching parts in its loop subgraph.*

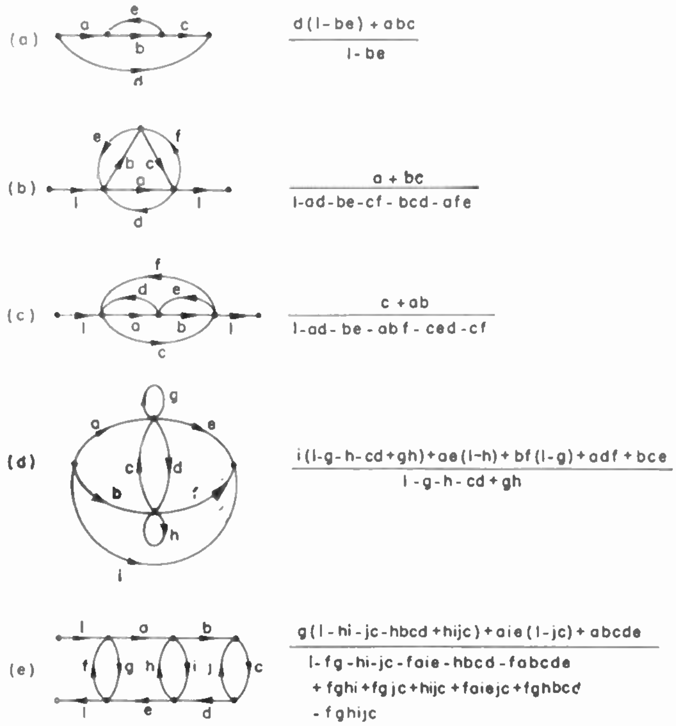

Fig. 6—Sample flow graphs and their gain expressions.

Illustrative Examples of Gain Evaluation by Inspection of Paths and Loop Sets

Eq. (12) is formidable at first sight but the idea is simple. More examples will help illustrate its simplicity. Fig. 5 (on the previous page) shows the first of these displayed in minute detail: (a) the graph to be solved; (b)–(f) the loop sets contributing to Δ; (g) and (h) the forward paths and their cofactors. Fig. 6 gives several additional examples on which you may wish to practice evaluating gains by inspection.

Illustrative Applications of Flow Graph Techniques to Practical Analysis Problems

The study of flow graphs is a fascinating topological game and therefore, from one viewpoint, worthwhile in its own right. Since the associated equations of a linear flow graph are in cause-and-effect form, each variable expressed explicitly in terms of others, and since physical problems are often very conveniently formulated in just this form, the study of flow graphs assumes practical significance.

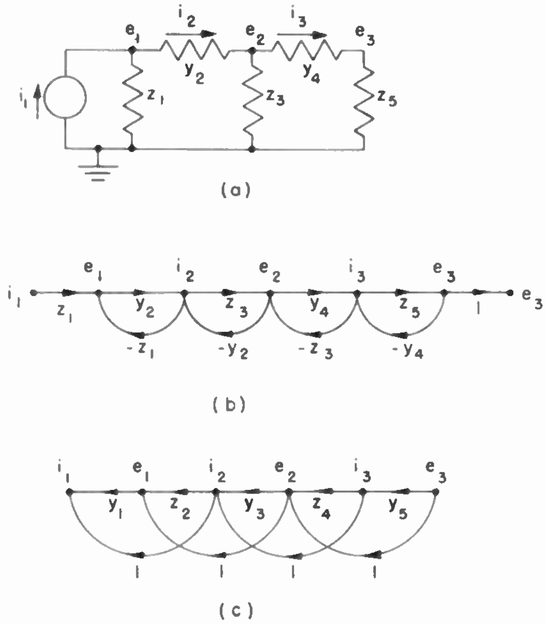

Fig. 7—The transfer impedance of a ladder.

Consider the ladder network shown in Fig. 7(a). The problem is to find the transfer impedance e_3/i_1. One possible formulation of the problem is indicated by the flow graph Fig. 7(b). The associated equations state that $e_1 = z_1(i_1 - i_2)$, $i_2 = y_2(e_1 - e_2)$, and so forth. By inspection of the graph,

$$\frac{e_3}{i_1} = \frac{z_1 y_2 z_3 y_4 z_5}{1 + z_1 y_2 + y_2 z_3 + z_3 y_4 + y_4 z_5 + z_1 y_2 z_3 y_4 + z_1 y_2 y_4 z_5 + y_2 z_3 y_4 z_5} \tag{13a}$$

or, with numerator and denominator multiplied by $y_1 y_3 y_5 = 1/z_1 z_3 z_5$,

$$\frac{e_3}{i_1} = \frac{y_2 y_4}{y_1 y_3 y_5 + y_2 y_3 y_5 + y_1 y_2 y_5 + y_1 y_4 y_5 + y_1 y_3 y_4 + y_2 y_4 y_5 + y_2 y_3 y_4 + y_1 y_2 y_4}. \tag{13b}$$

This result can be checked by the branch-combination method mentioned at the beginning of this paper.

A different formulation of the problem is indicated by the graph of Fig. 7(c), whose equations state that $i_3 = y_5 e_3$, $e_2 = e_3 + z_4 i_3$, $i_2 = i_3 + y_3 e_2$, and so forth. In the physical problem i_1 is the primary cause and e_3 the final effect. We may, however, *choose* a value of e_3 and then calculate the value of i_1 *required* to produce that e_3. The resulting equations will, from the analysis viewpoint, treat e_3 as a primary cause (source) and i_1 as the final effect (sink) *produced* by the chain of calculations. *This does not in any way alter the physical role of i_1.* The new graph (c) may appear simpler to solve than that of (b). Since graph (c) contains no feedback loops, the determinant and path cofactors are all equal to unity. There are many forward paths, however, and careful inspection is required to identify the sum of their gains as

$$\frac{i_1}{e_3} = y_1z_2y_3z_4y_5 + y_1z_2y_3 + y_1z_2y_5 + y_1z_4y_5 + y_3z_4y_5 + y_1 + y_3 + y_5 \tag{13c}$$

which proves to be, as it should, the reciprocal of (13b). Incidentally, graph (c) is obtainable directly from graph (b), as are all other possible cause-and-effect formulations involving the same variables, by the process of path inversion discussed in a previous paper.[2] This example points out the two very important facts: 1) the primary *physical* source does not *necessarily* appear as a source node in the graph, and 2) of two possible flow graph formulations of a problem, the one having fewer feedback loops is not necessarily simpler to solve by inspection, since it may also have a much more complicated set of forward paths.

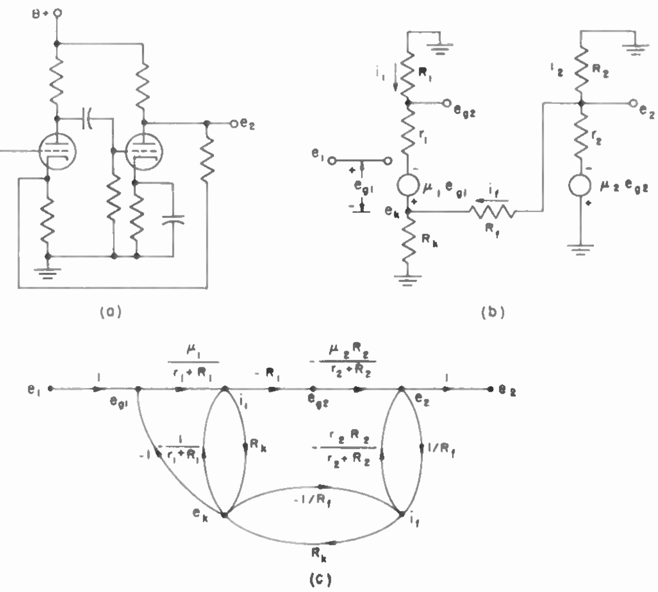

Fig. 8—Voltage gain of a feedback amplifier. (a) A feedback amplifier; (b) The midband linear incremental circuit model; (c) A possible flow graph.

Fig. 8(a) offers another sample analysis problem, determination of the voltage gain of a feedback amplifier. One possible chain of cause-and-effect reasoning, which leads from the circuit model, Fig. 8(b), to the flow graph formulation, Fig. 8(c), is the following. First notice that e_{g1} is the difference of e_1 and e_k. Next express i_1 as an effect due to causes e_{g1} and e_k, using superposition to write the gains of the two branches entering node i_1. The dependency of e_{g2} upon i_1 follows directly. Now, e_2 would be easy to evaluate in terms of either e_{g2} or i_f if the other were zero, so superpose the two effects as indicated by the two branches entering node e_2. At this point in the formulation e_k and i_f are as yet not explicitly specified in terms of other variables. It is a simple matter, however, to visualize e_k as the superposition of the voltages in R_k caused by i_1 and i_f, and to identify i_f as the superposition of two currents in R_f caused by e_k and e_2. This completes the graph.

The path from e_k to e_{g1} to i_1 may be lumped in parallel with the branch entering i_1 from e_k. This simplification, convenient but not necessary, yields the graph shown in Fig. 9. We could, of course, have expressed i_1 in terms of e_1 and e_k at the outset and arrived at Fig. 9 directly. All simplifications of a graph are themselves

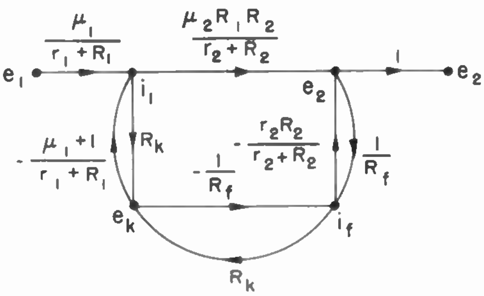

Fig. 9—Elimination of superfluous nodes e_{g1} and e_{g2}.

possible formulations. The better our perception of the workings of a circuit, the fewer variables will we need to introduce at the outset and the simpler will be the resulting flow graph structure.

In discussing the feedback amplifier of Fig. 8(a) it is common practice to neglect the loading effect of the feedback resistor R_f in parallel with R_k, the loading effect of R_f in parallel with R_2, and the leakage transmission from e_k to e_2 through R_f. Such an approximation is equivalent to the removal of the branches from e_k to i_f and i_f to e_2 in Fig. 9. It is sometimes dangerous to make early approximations, however, and in this case no appreciable labor is saved, since we can write the exact answer by inspection of Fig. 9:

$$\frac{e_2}{e_1} = \frac{\dfrac{\mu_1\mu_2R_1R_2}{(r_1+R_1)(r_2+R_2)}\left[1+\dfrac{R_k}{R_f}\right] + \dfrac{\mu_1R_kr_2R_2}{(r_1+R_1)(R_f)(r_2+R_2)}}{1 + \dfrac{(\mu_1+1)R_k}{r_1+R_1} + \dfrac{R_k}{R_f} + \dfrac{r_2R_2}{R_f(r_2+R_2)} + \dfrac{(\mu_1+1)\mu_2R_1R_kR_2}{R_f(r_1+R_1)(r_2+R_2)} + \dfrac{(\mu_1+1)R_kr_2R_2}{R_f(r_1+R_1)(r_2+R_2)}} \tag{14}$$

The two forward paths are $e_1i_1e_2$ and $e_1i_1e_ki_fe_2$, the first having a cofactor due to loop e_ki_f. The principal feedback loop is $i_1e_2i_fe_k$ and its gain is the fifth term of the denominator. Physical interpretations of the various paths and loops could be discussed but our main purpose, to illustrate the formulation of a graph and the evaluation of its gain by inspection, has been covered.

As a final example, consider the calculation of microwave reflection from a triple-layered dielectric sandwich. Fig. 10(a) shows the incident wave A, the reflection B, and the four interfaces between adjacent regions of different material. The first and fourth interfaces, of course, are those between air and solid. Let r_1 be the reflection coefficient of the first interface, relating the incident and reflected components of tangential electric field. It follows from the continuity of tangential E that the interface transmission coefficient is $1+r_1$, and from symmetry that the reflection coefficient from the opposite side of the interface is the negative of r_1. A suitable flow graph is sketched in Fig. 10(b). Node signals along the upper row are right-going waves just to the left or right of each interface, those on the lower row are left-going waves, and quantities d are exponential phase shift factors accounting for the delay in traversing each layer.

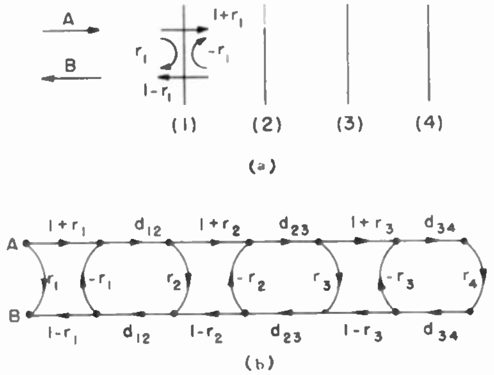

Fig. 10—A wave reflection problem. (a) Reflection of waves from a triple-layer; (b) A possible flow graph.

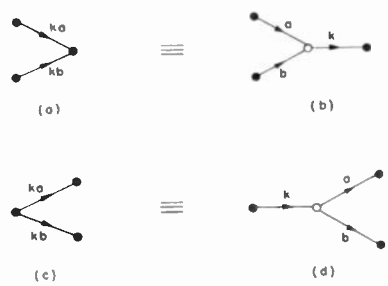

Fig. 11—Two touching paths.

Apart from the first branch r_1, the graph has the same structure as that of Fig. 6(e). Hence the reflectivity of the triple layer will be

$$\frac{B}{A} = r_1 + (1 + r_1)(1 - r_1)G \tag{15}$$

where G is in the same form as the gain of Fig. 6(e). We shall not expand it in detail. The point is that the answer can be written by inspection of the paths and loops in the graph.

Proof of the General Gain Expression

In an earlier paper[2] a quantity Δ was defined as

$$\Delta = (1 - T_1')(1 - T_2') \cdots (1 - T_n') \tag{16}$$

for a graph having n nodes, where

T_k' = loop gain of the kth node as computed with all higher-numbered nodes split.

Splitting a node divides that node into a new source and a new sink, all branches entering that node going with the new sink and all branches leaving that node going with the new source. The loop gain of a node was defined as the gain from the new source to the new sink, when that node is split. *It was also shown that Δ, as computed according to (16), is independent of the order in which the nodes are numbered, and that consequently Δ is a linear function of each branch gain in the graph. It follows that Δ is equal to unity plus the algebraic sum of various branch-gain products.*

We shall first show that each term of Δ, other than the unity term, is a product of the gains of nontouching feedback loops. This can be done by contradiction. Consider two branches which either enter the same node or leave the same node, as shown in Fig. 11(a) and (c). Imagine these branches imbedded in a larger graph, the remainder of which is not shown. Call the branch gains ka and kb. Now consider the equivalent replacements (b) and (d). The new node may be numbered zero, whence $T_0'=0$, the other T' quantities in (16) are unchanged, and Δ is therefore unaltered. If both branches ka and kb appear in a term of the Δ of graph (a) then the square of k must appear in a term of the Δ of graph (b). This is impossible since Δ must be a linear function of branch gain k. Hence no term of Δ can contain the gains of two touching paths.

Now suppose that of the several nontouching paths appearing in a given term of Δ, some are feedback loops and some are open paths. Destruction of all other branches eliminates some terms from Δ but leaves the given term unchanged. It follows from (16) and the definitions of T_k', however, that the Δ for the subgraph containing only these nontouching paths is just

$$\Delta = (1 - T_1)(1 - T_2) \cdots (1 - T_m) \tag{17}$$

where T_k is the gain of the kth feedback loop in the subgraph. Hence the open path gains cannot appear in the given term and it follows that each term of Δ is the product of gains of nontouching feedback loops. Moreover, it is clear from the structure of Δ that a term in any subgraph Δ must also appear as a term in the Δ of the complete graph, and conversely, every term of Δ is a term of some subgraph Δ. Hence, to identify all possible terms in Δ we must look for all possible subgraphs comprising sets of nontouching loops. Eq. (17) also shows that the algebraic sign of a term is plus or minus in accord with an even or odd number of loops in that term. This verifies the form of Δ as given in (12c) and (12d).

We shall next establish the general expression for graph gain (12a). The following notation will prove convenient. Consider the graph shown schematically in Fig. 12, with node $n+1$ given special attention. Let

Δ' = the Δ for the complete graph of $n+1$ nodes.

Δ = the value of Δ with node $n+1$ split or removed.

T = the loop gain of node $n+1$.

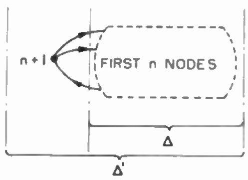

Fig. 12—A flow graph with one node placed strongly in evidence.

There will in general be several different feedback loops containing node $n+1$. Let

T_k = gain of the kth feedback loop containing node $n+1$,

Δ_k = the value of Δ for that part of the graph not touching loop T_k.

With the above notation, we have from (16) that

$$1 - T = \frac{\Delta'}{\Delta} \cdot \tag{18}$$

Remembering that any Δ is the algebraic sum of gain products of nontouching loops, we find it possible to write

$$\Delta' = \Delta - \sum_k T_k \Delta_k. \tag{19}$$

Eq. (19) represents the count of all possible nontouching loop sets in Δ'. The addition of node $n+1$ creates new loops T_k but the only new loop sets of Δ' not already in Δ are the nontouching sets $T_k\Delta_k$. The negative sign in (19) suffices to preserve the sign rule, since the product of T_k and a positive term of Δ_k will contain an odd number of loops.

Substitution of (19) into (18) yields the general result:

$$T = \frac{\sum_k T_k \Delta_k}{\Delta} \cdot \tag{20}$$

With node $n+1$ permanently split, T is just the source-to-sink gain of the graph and T_k is the kth forward path. This verifies (12a).

Acknowledgment

The writer is indebted to Prof. K. Wildes and also to J. Cruz, L. Boffi, G. Amster, and other students in his 1955 summer-term class in subject 6.633, Electronic Circuit Theory, M.I.T.; for helpful suggestions.

Correction

James R. Wait, author of the Correspondence item "The Radiation Pattern of an Antenna Mounted on a Surface of Large Radius of Curvature," which appeared on page 694 of the May, 1956 issue of PROCEEDINGS, has requested that the following text, modified in editing, be reinstated in its original form.

The last sentence in the first paragraph should read:

"It is the purpose of the present note to extend and apply the Van der Pol-Bremmer theory to calculate the radiation pattern of a dipole or a slot on a conducting sphere of large radius."

The last sentence of the article should read:

"It is interesting to compare this value with the 6 db field strength reduction in the tangent plane from a slot on a flat ground plane which is abruptly truncated."

Mr. Wait has also informed the editors that in (2), the second bracketed term should be $zh_\nu^{(1)}(z)$.

Topological Properties of Telecommunication Networks*

Z. PRIHAR†, SENIOR MEMBER, IRE

Summary—This paper describes a method of matrix analysis, developed by Luce and Perry for the study of sociometric group structures and cliques. These concepts are applied to telecommunication networks. Two new traffic matrices are also suggested which, in combination with the connectivity matrices, yield quantitative indications of the incoming and outgoing traffic. Various useful concepts are pointed out and a number of applications are illustrated by numerical examples.

Graphs and Matrices

THE GENERAL classical graph theory distinguishes two main types of graphs: finite and infinite. These, in turn, can be either of the oriented or nonoriented class, and each of these graphs is completely characterized by its set of links p terminated at the various vertices m.

According to this terminology of the graph theory, a telecommunication network would belong to the class of finite oriented graphs. The other corresponding analogical concepts in a telecommunication network would be as follows: a telephone exchange, a radio or relaying station, etc. would belong to a 0-dimensional region; *i.e.*, a point or vertex m. A communication link would correspond to a 1-dimensional region; *i.e.*, a link p.

Following other concepts of the linear graph theory, a local communication network could be defined as a bounded region and a general country-wide network as an unbounded region. A number of interconnected exchanges would then form a simply-connected structure. This would also apply to a number of interconnected radio or relaying stations, and a main station or exchange, connected to a number of satellite exchanges would form an n-fold connected structure.

Since topology investigates the nonmetrical aspects of space, and, in particular, the possible connections between different positions, properties of a qualitative nature, it would seem possible to apply usefully these relationships to the study of telecommunication networks.

One of the main problems in planning telecommunication networks is the connectivity between the above defined points m through certain links p; the general problem is to define through what regions the link must run in order that the required communication be attained with the minimum of connectivity.

Let Fig. 1 represent a simple oriented graph. Any link, say, P_1Q_1, would be fully defined by its vertix $m = P_1$ and link p = from P_1 to Q_1. A useful application to oriented graphs, expressing the various connections and their relationships, is the logical function of the binary relative R. The above link from P_1 to Q_1 would thus be defined as P_1RQ_1. In the case of an antimetry, a one-way link would be:

$$P_1RQ_1 \neq Q_1RP_1;$$

in the case of symmetry, two-way link,

$$P_1RQ_1 = Q_1RP_1.$$

Likewise, a transitivity would correspond to

$$P_2RP_1 + P_1RQ_1 = P_2RQ_2,$$

a connection from P_2 to Q_1 via an intermediate station P_1.

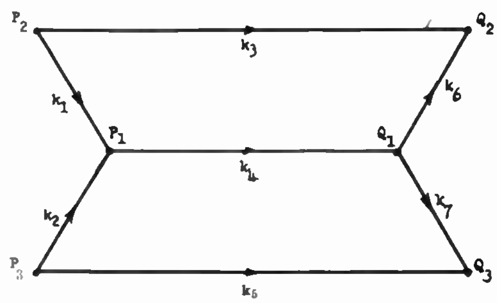

Fig. 1

Another class of the logical function is the relation P_1RP_1, corresponding to a case of reflexivity; *i.e.*, a point connected to itself. This class is outside the scope of this paper but it could interpret a case of feedback, for the problem by graph theory treated by Mason.[1]

As Luce and Perry have shown,[2,3] when presenting various relationships in diagram or graph forms, the analysis and presentation of the results may be greatly expedited by using matrix algebra. In their papers, Luce and Perry present a matrix method for the study of relationships between individuals and groups; with the aid of certain propertes of these matrices they develop various connectivity properties and concepts of n-chains and cliques. Their mathematical formulation is based on symbolism and nomenclature as used in point-set theory

* Original manuscript received by the IRE, October 20, 1955; revised manuscript received January 3, 1956.

† RCA International Division, New York, N. Y.

[1] S. J. Mason, "Feedback theory—some properties of signal flow graphs," Proc. IRE, vol. 41, p. 1144; September, 1953.

[2] R. D. Luce, and A. D. Perry, "A method of matrix analysis of group structure," *Psychometrika*, vol. 14, pp. 95–116; March, 1949.

[3] R. D., Luce, "Connectivity and generalized cliques in sociometric group structure," *Psychometrika*, vol. 15, pp. 169–190; June, 1950.

and general topology. The following concepts, as developed by Luce and Perry, will be applied to telecommunication networks. The mathematical formulation, given here in a limited form for a better understanding of the subject, will be made with the standard forms of matrix algebra with which engineers are more familiar.

The matrix of antimetries (one-way links) is formed by the following entries x_{ij}:

$x_{ij}=1$ if, and only if, there exists a link between i and j,

$x_{ij}=0$ if no link exists between i and j.

A matrix of symmetries is formed from the above matrix with entries s_{ij} defined as follows:

$s_{ij}=1$ if, and only if, $x_{ij}=x_{ji}$ a two-way link exists between i and j.

$s_{ij}=0$ otherwise, no two-way link exists between i and j.

To fix ideas, the oriented graph of Fig. 1 will have the following corresponding matrix of antimetries $X=(x_{ij})$

$$X=(x_{ij})=\begin{array}{c|cccccc} & P_1 & P_2 & P_3 & Q_1 & Q_2 & Q_3 \\ \hline P_1 & 0 & 0 & 0 & 1 & 0 & 0 \\ P_2 & 1 & 0 & 0 & 0 & 1 & 0 \\ P_3 & 1 & 0 & 0 & 0 & 0 & 1 \\ Q_1 & 0 & 0 & 0 & 0 & 1 & 1 \\ Q_2 & 0 & 0 & 0 & 0 & 0 & 0 \\ Q_3 & 0 & 0 & 0 & 0 & 0 & 0 \end{array}$$

Since Fig. 1 network has only one-way links, the corresponding $S=(s_{ij})$ matrix would have all its entries equal to 0. On the other hand, if all the links of Fig. 1 were two-way, the S matrix would have the same form as the above X matrix.

Though it would seem that in modern communication networks all links are always symmetrical; *i.e.*, two-way traffic, it will be shown here, in one numerical example, that in certain radio circuits there are possible antimetries in communication networks.

The application of matrices to graphs is not new. Nor need the entries be confined to a two-valued logic, with only 0 or 1 entries. In the Poincaré-Veblen matrix of a finite oriented graph, as quoted by König[4] if P_i are the vertices of the graph, with $i=1, 2, \cdots, a_0$ and k_j its links, with $j=1, 2, \cdots, a_1$, the t_{ij} values of the matrix are defined as follows:

$t_{ij}=1$ if P_i is the vertex of origin of link k_j,
$t_{ij}=-1$ if P_i is the end vertex of link k_j, and
$t_{ij}=0$ if P_1 has no link with k_j.

[4] D. König, "Theorie der endlichen und unendlichen Graphen," New York, N. Y., Chelsea Publishing Company, p. 141; 1950.

The matrix thus defined, with a 3-valued logic,

$$T=(t_{ij})(i=1, 2\cdots a_0; j=1, 2\cdots a_1)$$

with a_0 rows and a_1 columns, is termed the Incident-matrix of G, G being the finite oriented graph in question. For instance, to fix ideas, the corresponding Poincaré-Veblen matrix for Fig. 1 would have 6 rows corresponding to the six vertices and seven links corresponding to the seven columns $k_1, \cdots, k_7$ and will be of the following form:

$$T=(t_{ij})=\begin{array}{c|ccccccc} & k_1 & k_2 & k_3 & k_4 & k_5 & k_6 & k_7 \\ \hline P_1 & -1 & -1 & 0 & 1 & 0 & 0 & 0 \\ P_2 & 1 & 0 & 1 & 0 & 0 & 0 & 0 \\ P_3 & 0 & 1 & 0 & 0 & 1 & 0 & 0 \\ Q_1 & 0 & 0 & 0 & -1 & 0 & 1 & 1 \\ Q_2 & 0 & 0 & -1 & 0 & 0 & -1 & 0 \\ Q_3 & 0 & 0 & 0 & 0 & -1 & 0 & -1 \end{array}$$

As it is seen, each column of the incident-matrix has $+1$ and one -1 entries and a total sum of 0. The rank of an incident-matrix is always equal to a_0-v where v = number of meshes. Hence, the above matrix for Fig. 1 will have the rank $6-2=4$.

Further applications of matrices and their properties are given by König in his treatment of Poincaré-Veblen matrices and various other general properties and relations of matrices and determinants in their application to graphs are also given by König.[5]

Applications in Telecommunication Networks

The concepts developed by Luce and Perry have the following possible applications in telecommunication networks: If an $X^{(2)}$ matrix is formed from the matrix of antimetries X, its diagonal entries $x_{ii}^{(2)}$ will indicate at a glance the direct communication channels of station i with stations j of the network, with $j=1, 2, \cdots, n$. The proof that $x_{ii}^{(2)}=c$ as entry, c being a real value, if, and only if, there are c symetric lines; *i.e.*, relations, with i for the ith entry, is given by the definition of the main diagonal entry of a matrix

$$x_{ii}^{(2)}=\sum_{j=1}^{n} x_{ij}x_{ji} \qquad (i=j=1, 2, \cdots n)$$

and a two-way connection will exist if $x_{ij}=x_{ij}=1$. Otherwise, $x_{ij}=x_{ji}=0$ and their product $=0$. Since the summation is for $j=1$ to all n entries, the above expression will thus yield the total of direct connection between station i and station j of the network, with $j=1, 2, \cdots, n$.

[5] König, *ibid.*, p. 237.

If an $X^{(n)}$ matrix is formed from an X matrix, its entries $x_{ij}^{(n)}=h$, with h being a real number, will indicate that there are h possible ways in the network for station i to reach station j in n steps; *i.e.*, links, corresponding to passing through $n-1$ intermediate stations between i and j. Such a matrix would be of interest for the control of traffic flow and diversions in case of partial breakdowns of circuits forming part of the network.

The proof that the $x_{ij}^{(n)}$ entry of an $X^{(n)}$ matrix will have a value h if there are h distinct chains from i to j through n links or n_1-1 intermediate stations, can again be obtained from the definition of the matrix

$$x_{ij}^{(n)} = \sum_{q=1}^{n} \cdots \sum_{k=1}^{n} x_{ik}x_{k1}x_{1m} \cdots x_{pq}x_{qj}$$

since only if any of these individual links exist,

$$x_{ik} = x_{k1} = x_{1m} = \cdots = x_{pq} + x_{qj} = 1$$

and otherwise 0, each of these chains will be also equal to 1 and their summation will yield the total number of all the distinct n paths from i to j through $n-1$ intermediate stations. Fig. 2 will make the above clear in the case of simple example of $x_{ij}^{(2)}$ through one intermediate station. For $n=2$,

$$x_{ij}^{(n)} = x_{ij}^{(2)} = \sum_{k=1}^{n} x_{ik}x_{kj}$$

$$= x_{i1}x_{1j} + x_{i2}x_{2j} + \cdots + x_{in}x_{nj}.$$

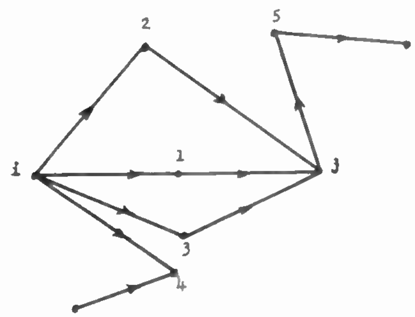

Fig. 2

For Fig. 2,

$$x_{ij}^{(2)} = \sum_{k=1}^{n} x_{ik}x_{kj}$$

$$= 1 \times 1 + 1 \times 1 + 1 \times 1 + 1 \times 0 + 1 \times 0 = 3.$$

Hence, the total number of available connections between i and j through an intermediate station will be $h=3$. Other numerical examples given later in the paper show the application of this matrix to more complex networks.

A general idea of a network's degree of connectivity and general importance, from the traffic point of view, can be obtained from the matrix

$$A(n) = X + X^{(2)} + X^{(3)} + \cdots + X^{(n)}.$$

If all entries of such an $A(n)$ matrix are filled, the matrix will then indicate that all stations forming the network will be able to intercommunicate in either direct or through 1, 2, or 3, etc. up to $n-1$ intermediate stations. 0 entries will show that no direct or indirect connections exist between the given stations. The application and usefulness of this matrix will be made clear by the numerical example given later in the paper.

A measure of connectivity of a network could be obtained by making use of some other concepts of the linear graph theory. If p = number of links of a network, m = its number of stations (vertices) then its maximum limit of connectivity, *i.e.*, the maximum possible number of connections of the network will be

$$p_{\max} = m(m-1),$$

its First Betti Number (Cyclomatic index)

$$\mu = p - m + 1,$$

and rank

$$R = m - 1 = p - \mu.$$

Given the actual degree of connectivity of a network, expressed by the number of its links p, p could be related to the maximum and minimum connectivities of the network by the following relations:

degree of maximum connectivity $p/m(m-1)$ and
degree of minimum connectivity $= p/(m-1)$ (for $\mu=0$).

The relation given by the First Betti Number

$$\mu = p - m + 1 = 0$$

could be used to determine minimal communication networks and would be of particular interest in automatic telephone systems. Before the advent of automatic telephony, when operation was mostly manual, it was neither feasible nor economical to establish a connection in a zonal network through more than 2–3 exchanges. Consequently, as many direct links as economically possible were provided. The following is a simple typical example. In a manually operated system, Fig. 1 would probably be the network provided for six exchanges. In an automatic system, where connection-paths are not apparent to the user, the probably most economical and sufficient connectivity would be, for the above system of Fig. 1, the network shown in Fig. 3. It will be understood that both, Fig. 1 and Fig. 2, will have two-way-links for this example.

Applying the above suggested measures of connectivity, for Fig. 1, $p=9$; $m=6$; and $\mu=4$; this would correspond to a maximum connectivity ratio of $9/30$ and a minimum connectivity ratio of $9/3$. For Fig. 3 $p=5$; $m=6$; and $\mu=0$; the maximum connectivity ratio will be $5/30=1/6$ and the minimum ratio of connectivity $=5/5=1$.

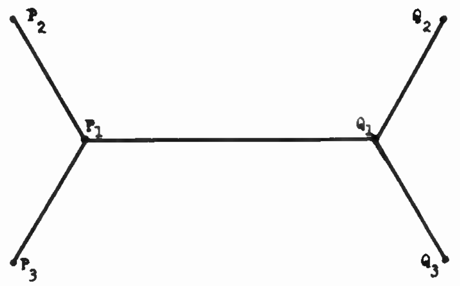

Fig. 3

Traffic Matrices

In the following a new matrix relation is suggested as a possible useful tool in the study of telecommunication networks.

Given a communication network with a connectivity matrix X, with each existing connectivity between any two stations i and j of the network defined in the X matrix by an entry $x_{ij}=1$ and an entry $x_{ij}=0$ if no such connectivity exists, and if each of these connectivities has t lines or traffic units, t being a real number, and a matrix T is formed with the corresponding t_{ij} entries, where t_{ij} = number of lines or traffic units between stations i and j, then a product of X and T matrices will give the following two new matrices:

Incoming traffic matrix $P=XT$
Outgoing traffic matrix $Q=TX$.

The main diagonal entries of matrix P will indicate the total number of incoming lines or traffic units to the station and the main diagonal entries of matrix Q will indicate the total number of outgoing lines or traffic units from the station.

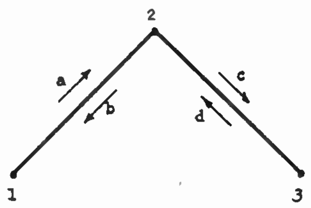

Fig. 4

The following illustration of an application in a simplified case of three exchanges will make the above more clear. Let Fig. 4 represent the connections between the three exchanges 1, 2, and 3 and let a, b, c, and d be the quantities in real numbers of either lines or traffic units between the three stations in the two directions. The corresponding connectivity matrix X of Fig. 4 is

$$X = \left| \begin{matrix} 0 & 1 & 0 \\ 1 & 0 & 1 \\ 0 & 1 & 0 \end{matrix} \right.$$

and the traffic matrix T

$$T = \left| \begin{matrix} 0 & a & 0 \\ b & 0 & c \\ 0 & d & 0 \end{matrix} \right.$$

From these two matrices, the incoming traffic matrix P

$$P = XT = \left| \begin{matrix} b & 0 & c \\ 0 & (a+d) & 0 \\ b & 0 & c \end{matrix} \right.$$

with the main-diagonal entries showing the incoming number of lines to stations 1, 2, and 3. Likewise, the outgoing traffic matrix Q

$$Q = TX = \left| \begin{matrix} a & 0 & a \\ 0 & (b+c) & 0 \\ d & 0 & d \end{matrix} \right.$$

where the main-diagonal entries indicate the outgoing traffic from the three stations.

A proof of the above is obtained from the definition of a product of two matrices. For any two matrices,

$$(x_{ij})(t_{ji}) = \sum_{j=1}^{n} x_{ij}t_{ji} = p_{ii}$$
$$= x_{i1}t_{1i} + x_{i2}t_{2i} + \cdots + x_{in}t_{ni},$$

since $x_{ij}=1$ if, and only if, there is a connectivity between i and j and $x_{ij}=0$ otherwise. Since the summation is for all values of j, the above expression of p_{ii}, with t_{ij} being real numbers, will yield the sum of all incoming lines to station i. Likewise, for the outgoing traffic.

$$(t_{ji})(x_{ij}) = \sum_{i=1}^{n} t_{ji}x_{ij} = q_{jj}$$

where again, if $x_{ij} \neq 0$ it can only be equal to 1. The sum of the member products will give the total number of the stations' outgoing lines, or traffic units, to all other stations of the network with which it has a direct connection.

The off-diagonal entries of the $P=XT$ and $Q=XT$ matrices are also of some interest. They are given by the following expressions:

$$(x_{ij})(t_{jk}) = \sum_{j=1}^{n} x_{ij}t_{jk}$$

and

$$(t_{jk})(x_{kj}) = \sum_{k=1}^{n} t_{jk}x_{kj}.$$

The P matrix off-diagonal entries are $p_{13}=c$ and $p_{31}=b$ and those of the Q matrix $q_{13}=a$ and $q_{31}=d$. This could be interpreted that an extension from 1 to 3 is provided by c and from 3 to 1 by b. Likewise, in the opposite direction, q_{13} indicates an available extension by a and q_{31} by d. These entries would also seem to provide an indication of possible interfering links in a system.

Illustrative Examples

The following is an illustration of a practical application of the above concepts to telecommunication networks. Let Fig. 5 represent the hypothetical network to be examined. Station A is assumed to be a very powerful radio transmitting station capable of contacting any other station of the network. As the oriented links indicate, while some of the stations would be in a position to respond to A by direct contacts, others would only be able to reach it in n-steps, through relaying stations, due to their transmitters' range limits. Hence, this would represent a case of antimetries (one-way connections) and symmetries (two-way connections).

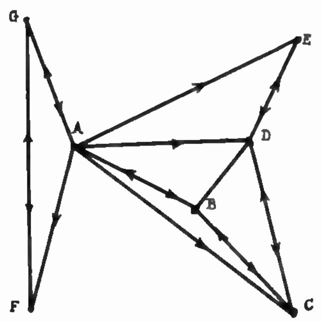

Fig. 5

The following is the X matrix for Fig. 5 network:

$$X = \begin{array}{c|ccccccc} & A & B & C & D & E & F & G \\ \hline A & & 1 & 1 & 1 & 1 & 1 & 1 \\ B & 1 & & 1 & 1 & & & \\ C & & 1 & & 1 & & & \\ D & & 1 & 1 & & 1 & & \\ E & & & & 1 & & & \\ F & & & & & & & 1 \\ G & 1 & & & & & 1 & \end{array}$$

The corresponding $X^{(2)}$ matrix is

$$X^{(2)} = \begin{array}{c|ccccccc} & A & B & C & D & E & F & G \\ \hline A & 2 & 2 & 2 & 3 & 1 & 1 & 1 \\ B & & 3 & 2 & 2 & 2 & 1 & 1 \\ C & 1 & 1 & 2 & 1 & 1 & & \\ D & 1 & 1 & 1 & 3 & & & \\ E & & 1 & 1 & & 1 & & \\ F & 1 & & & & & 1 & \\ G & & 1 & 1 & 1 & 1 & 1 & 2 \end{array}$$

The above matrix, as explained previously, contains the following information about the network: the diagonal entries x_{ii} indicate the total number of all possible direct two-way communication channels of the stations; *e.g.*, station A will have 2, station B 3, etc. up to station G which will have two direct two-way channels with the other stations of the network. All the other off-diagonal entries of the matrix indicate the number of possible 2-step connections between the stations indicated by the matrix; *i.e.*, the number of possibilities station i will have to reach station j through one relaying station. For instance, station A will be able to reach station D through three different stations acting as intermediate relaying stations, whereas station D will only have one possible 2-step link with station A.

The S matrix, derived from the X matrix, is

$$S = \begin{array}{c|ccccccc} & A & B & C & D & E & F & G \\ \hline A & & 1 & & & & & 1 \\ B & 1 & & 1 & 1 & & & \\ C & & 1 & & 1 & & & \\ D & & 1 & 1 & & 1 & & \\ E & & & & 1 & & & \\ F & & & & & & & 1 \\ G & 1 & & & & & 1 & \end{array}$$

The S matrix indicates all direct two-way communication channels. Hence, the sum of each row will be equal to the diagonal entry of the corresponding row in the $X^{(2)}$ matrix.

To check whether all stations will be able to intercommunicate in either one or two steps, the $A(n)=A(2)$ is formed, where $A(2)=X+X^{(2)}$.

$$A(2) = X + X^{(2)} = \begin{array}{c|ccccccc} & A & B & C & D & E & F & G \\ \hline A & 2 & 3 & 3 & 4 & 2 & 2 & 2 \\ B & 1 & 3 & 3 & 3 & 2 & 1 & 1 \\ C & 1 & 2 & 2 & 2 & 1 & & \\ D & 1 & 2 & 2 & 2 & 1 & & \\ E & & 1 & 1 & 1 & 1 & & \\ F & 1 & & & & & 1 & 1 \\ G & 1 & 1 & 1 & 1 & 1 & 2 & 2 \end{array}$$

The above $A(2)$ matrix shows that all stations will be able to intercommunicate in one or two steps with the exception of stations C, D and E, which will not be able to communicate with stations F and G. Also station E will not be able to communicate with station A and station F with stations B, C, D and E.

To check whether all stations will be able to intercommunicate in one, two, or three steps, through two intermediate relaying stations, the matrix $A(3)$ is formed where

$$A(3) = X + X^{(2)} + X^{(3)}$$

It will first be necessary to determine the $X^{(3)}$ matrix from the above $X^{(2)}$ and X matrices

$$X^{(3)} = \begin{array}{c|ccccccc} & A & B & C & D & E & F & G \\ \hline A & 3 & 7 & 7 & 7 & 5 & 3 & 3 \\ B & 4 & 4 & 5 & 7 & 2 & 1 & 1 \\ C & 1 & 4 & 3 & 5 & 2 & 1 & 1 \\ D & 1 & 5 & 5 & 3 & 4 & 1 & 1 \\ E & 1 & 1 & 1 & 3 & & & \\ F & & 1 & 1 & 1 & 1 & 1 & 2 \\ G & 3 & 2 & 2 & 3 & 1 & 2 & 1 \end{array}$$

The off-diagonal entries of this matrix indicate the number of ways any station i will reach the coresponding station j in three steps through two intermediate stations. The $A(3)$ matrix will be

$$A(3) = X + X^{(2)} + X^{(3)} = \begin{array}{c|ccccccc} & A & B & C & D & E & F & G \\ \hline A & 5 & 9 & 9 & 10 & 6 & 4 & 3 \\ B & 4 & 7 & 7 & 9 & 4 & 2 & 2 \\ C & 2 & 5 & 5 & 6 & 3 & 1 & 1 \\ D & 2 & 3 & 5 & 5 & 3 & 1 & 1 \\ E & 1 & 3 & 2 & 3 & 1 & & \\ F & 1 & 1 & 1 & 1 & 1 & 2 & 2 \\ G & 3 & 3 & 3 & 4 & 2 & 3 & 3 \end{array}$$

This matrix indicates that station E will be the only one unable to communicate with stations F and G even in three steps, and an $A(4)$ matrix will show that all entries have been filled. Hence, station E will have to use three intermediate stations to reach stations F and G or have the power of its transmitter increased.

Radio vs Cable Telecommunication Systems

The following example illustrates a possible application by which the relative degrees of flexibility of radio and cable systems for a given telecommunication network are compared. The network is to consist of 11 stations. Direct two-way channels are required between all stations. Hence, the corresponding connectivity matrix $X=S$ will have the maximum number of entries $m(m-1)$ with $m=11$. The following will be the matrix

$$X = S = \begin{array}{c|ccccccccccc} & a & b & c & d & e & f & g & h & i & j & k \\ \hline a & & 1 & 1 & 1 & 1 & 1 & 1 & 1 & 1 & 1 & 1 \\ b & 1 & & 1 & 1 & 1 & 1 & 1 & 1 & 1 & 1 & 1 \\ c & 1 & 1 & & 1 & 1 & 1 & 1 & 1 & 1 & 1 & 1 \\ d & 1 & 1 & 1 & & 1 & 1 & 1 & 1 & 1 & 1 & 1 \\ e & 1 & 1 & 1 & 1 & & 1 & 1 & 1 & 1 & 1 & 1 \\ f & 1 & 1 & 1 & 1 & 1 & & 1 & 1 & 1 & 1 & 1 \\ g & 1 & 1 & 1 & 1 & 1 & 1 & & 1 & 1 & 1 & 1 \\ h & 1 & 1 & 1 & 1 & 1 & 1 & 1 & & 1 & 1 & 1 \\ i & 1 & 1 & 1 & 1 & 1 & 1 & 1 & 1 & & 1 & 1 \\ j & 1 & 1 & 1 & 1 & 1 & 1 & 1 & 1 & 1 & & 1 \\ k & 1 & 1 & 1 & 1 & 1 & 1 & 1 & 1 & 1 & 1 & \end{array}$$

The number of the actual traffic channels, two-way, required between the different stations is given by the following traffic matrix T:

$$T = \begin{array}{c|ccccccccccc} & a & b & c & d & e & f & g & h & i & j & k \\ \hline a & & 192 & 24 & 12 & 36 & 24 & 12 & 24 & 24 & 24 & 24 \\ b & 192 & & 24 & 24 & 12 & 6 & 4 & 12 & 12 & 6 & 12 \\ c & 24 & 24 & & 12 & 12 & 6 & 4 & 4 & 4 & 4 & 12 \\ d & 12 & 24 & 12 & & 4 & 4 & 4 & 4 & 4 & 4 & 4 \\ e & 36 & 12 & 12 & 4 & & 12 & 12 & 4 & 6 & 4 & 4 \\ f & 24 & 6 & 6 & 4 & 12 & & 4 & 12 & 6 & 4 & 12 \\ g & 12 & 4 & 4 & 4 & 12 & 4 & & 4 & 12 & 4 & 4 \\ h & 24 & 12 & 4 & 4 & 4 & 12 & 4 & & & & \\ i & 24 & 12 & 4 & 4 & 6 & 6 & 12 & 12 & & & \\ j & 24 & 6 & 4 & 4 & 4 & 4 & 4 & 12 & 4 & & \\ k & 24 & 12 & 12 & 4 & 4 & 12 & 4 & 4 & 4 & 4 & \end{array}$$

Since all channels will carry two-way traffic

$$P = XT = TX = Q$$

and the following are main diagonal entries of the $P=Q$ matrix

$$P = Q = \begin{array}{c|ccccccccccc} & a & b & c & d & e & f & g & h & i & j & k \\ \hline a & 396 & & & & & & & & & & \\ b & & 304 & & & & & & & & & \\ c & & & 106 & & & & & & & & \\ d & & & & 76 & & & & & & & \\ e & & & & & 106 & & & & & & \\ f & & & & & & 90 & & & & & \\ g & & & & & & & 64 & & & & \\ h & & & & & & & & 92 & & & \\ i & & & & & & & & & 88 & & \\ j & & & & & & & & & & 70 & \\ k & & & & & & & & & & & 84 \end{array}$$

The above are the in- and out-going channels of each of the stations corresponding to the entries $p_{ii} = q_{ii}$.

For a cable system, the following will be the connectivity matrix $X_c = S_c$ of the cable network which would satisfy all the economic and technological requirements at minimum cost; *i.e.*, minimal network.

$$X_c = S_c = \begin{array}{c|ccccccccccc}
 & a & b & c & d & e & f & g & h & i & j & k \\
\hline
a & & & & & & & & & & & 1 \\
b & & & & 1 & & & & & & & \\
c & & & & 1 & 1 & & & & & & 1 \\
d & & 1 & 1 & & & & & & & & \\
e & & & 1 & & & & 1 & & & & \\
f & & & & & & & & 1 & & & 1 \\
g & & & & & 1 & & & & 1 & & \\
h & & & & & & 1 & & & 1 & & \\
i & & & & & & & 1 & 1 & & & \\
j & & & & & & & & 1 & & & \\
k & 1 & & 1 & & & 1 & & & & &
\end{array}$$

In the case of a radio system, where the distribution, or beamed transmission, need not follow the rigid cable system routing, the following connectivity matrix $X_r = S_r$ of a network would satisfy the corresponding economic and technological requirements of the system:

$$X_r = S_r = \begin{array}{c|ccccccccccc}
 & a & b & c & d & e & f & g & h & i & j & k \\
\hline
a & & & & & & 1 & & & & & 1 \\
b & & & & 1 & & & & & & & \\
c & & & & 1 & 1 & 1 & & & & & 1 \\
d & & 1 & 1 & & & & & & & & \\
e & & & 1 & & & 1 & 1 & & & & 1 \\
f & 1 & & 1 & & 1 & & & 1 & & & 1 \\
g & & & & & 1 & & & & 1 & & \\
h & & & & & & 1 & & & 1 & 1 & \\
i & & & & & & & 1 & 1 & & & \\
j & & & & & & & & 1 & & & \\
k & 1 & & 1 & & 1 & 1 & & & & &
\end{array}$$

The corresponding $X^{(2)} = S^{(2)}$ matrices for the two systems are as follows:

$$X_c^{(2)} = S_c^{(2)} = \begin{array}{c|ccccccccccc}
 & a & b & c & d & e & f & g & h & i & j & k \\
\hline
a & 1 & & 1 & & & 1 & & & & & \\
b & & 1 & 1 & & & & & & & & \\
c & 1 & 1 & 3 & & & 1 & 1 & & & & \\
d & & & & 2 & 1 & & & & & & 1 \\
e & & & & 1 & 2 & & & & 1 & & 1 \\
f & 1 & & 1 & & & 2 & & & 1 & 1 & \\
g & & & 1 & & & & 2 & 1 & & & \\
h & & & & & & & 1 & 3 & & & 1 \\
i & & & & & 1 & 1 & & & 2 & 1 & \\
j & & & & & & 1 & & & 1 & 1 & \\
k & & & & 1 & 1 & & & 1 & & & 3
\end{array}$$

and

$$X_r^{(2)} = S_r^{(2)} = \begin{array}{c|ccccccccccc}
 & a & b & c & d & e & f & g & h & i & j & k \\
\hline
a & 2 & & 2 & & 2 & 1 & & 1 & & & 1 \\
b & & 1 & 1 & & & & & & & & \\
c & 2 & 1 & 4 & & 2 & 2 & 1 & 1 & & & 2 \\
d & & & & 2 & 1 & 1 & & & & & 1 \\
e & 2 & & 2 & 1 & 4 & 2 & & 1 & 1 & & 2 \\
f & 1 & & 2 & 1 & 2 & 5 & 1 & & 1 & 1 & 3 \\
g & & & 1 & & & 1 & 2 & 1 & & & 1 \\
h & 1 & & 1 & & 1 & & 1 & 3 & & & 1 \\
i & & & & & 1 & 1 & & & 2 & 1 & \\
j & & & & & & 1 & & & 1 & 1 & \\
k & 1 & & 2 & 1 & 2 & 3 & 1 & 1 & & & 4
\end{array}$$

As it may be seen from the diagonal and the off-diagonal entries of these two matrices, with the radio system the stations will have a greater number of direct and alternative two-step outlets to other stations than with the cable system.

The comparative degrees of flexibility of the two systems, as obtained from the above matrices, are as follows:

	Direct contacts between stations	*Two-step contacts between stations*
Cable system network	22	28
Radio system network	30	70

Acknowledgment

My thanks are due to my former doctoral advisor, Prof. S. B. Littauer and to Prof. L. A. Zadeh, both of Columbia University, for their valuable council which led to my interest in this subject. Thanks are also due to my son, David J. Prihar, for his help in checking the nume ic il calculations of the matrices.

IRE Standards on Letter Symbols for Semiconductor Devices, 1956*

56 IRE 28. S1

COMMITTEE PERSONNEL

Subcommittee on Semiconductor—Definitions, 1954–1956

S. J. Angello, *Chairman*

J. M. Early
S. K. Ghandhi
M. F. Lamorte
B. J. Rothlein
J. S. Schaffner
K. Uhler

Committee on Semiconductor Devices, 1955–1956

J. M. Early, *Chairman*

J. B. Angell
S. J. Angello
R. L. Bright
A. C. Clarke
A. Coblenz
W. H. Lapham
R. M. LeLacheur
B. R. Lester
L. T. MacGill
H. T. Mooers
C. W. Mueller
R. L. Pritchard
K. A. Pullen, Jr.
B. J. Rothlein
J. Saby
H. N. Sachar
A. C. Sheckler
A. P. Stern
W. J. Mayo-Wells

Committee on Solid State Devices, 1955–1956

R. R. Law, *Vice-Chairman*
H. L. Owens, *Chairman*
V. P. Mathis, *Secretary*

A. E. Anderson
J. B. Angell
S. J. Angello
A. Coblenz
L. Davis, Jr.
J. M. Early
J. J. Ebers
H. Epstein
R. S. Fallows
J. R. Flegal
H. Goldberg
J. R. Hyneman
J. P. Jordan
N. R. Kornfield
A. W. Lampe
J. R. MacDonald
L. T. MacGill
W. J. Mayo-Wells
C. W. Mueller
C. F. Spitzer
W. J. Pietenpol
R. L. Pritchard
J. R. Roeder
C. A. Rosen
B. J. Rothlein
R. M. Ryder
J. Saby
B. R. Shepard
S. Sherr

Standards Committee, 1955–1956

E. Weber, *Chairman*
R. F. Shea, *Vice-Chairman*
M. W. Baldwin, Jr., *Vice-Chairman*
L. G. Cumming, *Vice-Chairman*

W. R. Bennett
J. G. Brainerd
P. S. Carter
P. S. Christaldi
A. G. Clavier
J. E. Eiselein
A. W. Friend
V. M. Graham
R. A. Hackbusch
H. C. Hardy
D. E. Harnett
P. J. Herbst
Hans Jaffe
Henry Jasik
A. G. Jensen
J. L. Jones
J. G. Kreer, Jr.
E. A. Laport
A. A. MacDonald
Wayne Mason
D. E. Maxwell
W. T. Wintringham
K. R. McConnell
H. R. Mimno
M. G. Morgan
G. A. Morton
H. L. Owens
P. A. Redhead
R. Serrell
R. M. Showers
H. R. Terhune
J. E. Ward

Measurements Coordinator

R. F. Shea

* Reprints of this Standard, 56 IRE 28. S1 may be purchased while available from the Institute of Radio Engineers, 1 East 79th Street, New York 21, N. Y. at $0.50 per copy. A 20 per cent discount will be allowed for 100 or more copies mailed to one address.

Introduction

These Standards are supplementary to the IRE Standards on Abbreviations, Graphical Symbols, Letter Symbols, and Mathematical Signs—1948, Section 1. The usage conforms to Section 101, General Principles of Letter Symbol Standardization. This Standard provides a uniform system of letter symbols for electrical quantities and parameters as applied to semiconductor devices in the same way that Section 102 provides symbols for electron tubes. The Standard has been divided into three Sections:

1) Electrical quantities, dealing primarily with voltage, current, and time quantities.
2) Electrical parameters, dealing with the relationship between specific electrical quantities.
3) List of letter symbols in alphabetical order.

Electrical quantities at the device terminals are defined in Section 1. The electrical parameters of Section 2 are ratios of the terminal electrical quantities; *i.e.*, they are two terminal-pair open- and short-circuit ratios. Letter subscripts are used for these ratios throughout this Standard; numeric subscripts following the matrix convention may be used when convenient, especially in the analysis of electric circuits.

1. Electrical Quantities

1.1 Quantity Symbols

1.1.1 Instantaneous values of current, voltage, and power, which vary with time, are represented by the lower case letter of the proper symbol.
Examples: i, v, i_e, v_{EB}

1.1.2 Maximum, average (dc), and root-mean-square values are represented by the upper case letter of the proper symbol.
Examples: I, V, I_e, V_{EB}

1.2 Subscripts for Quantity Symbols

1.2.1 DC values and instantaneous total values are indicated by upper case subscripts.
Examples: i_C, I_C, v_{EB}, V_{EB}, p_C, P_C

1.2.2 Varying component values are indicated by lower case subscripts.
Examples: i_c, I_c, v_{cb}, V_{eb}, p_c, P_c

1.2.3 If necessary to distinguish between maximum, average, or root-mean-square values; maximum or average values may be represented by the addition of a subscript *m* or *av*.
Examples: i_{cm}, I_{cm}, I_{CM}, I_{cav}, i_{CAV}

1.2.4 Abbreviations to be used as subscripts. (For example, see Fig. 1 and Basic Symbols Chart 1.2.5.)

E, e = emitter electrode
B, b = base electrode
C, c = collector electrode
J, j = electrode, general
X, x = circuit node
M, m = maximum value
AV, av = average value
Q = average (dc) value with signal applied.

1.2.5 Basic Symbols Chart (Table I)

TABLE I

		Symbols	
		i, v, p	I, V, P
Subscripts	e b c j	Instantaneous Varying Component Value	RMS or Effective Varying Component Value
	E B C J	Instantaneous Total Value	Average (dc) Value

1.3 The Subscript Sequence Conforms to the Mathematical Convention for Writing Determinants from a Set of Fundamental Kirchoff's Equations

1.3.1 The first subscript designates the electrode at which the current is measured, or where the electrode potential is measured with respect to the reference electrode, or circuit node, designated by the second subscript. (Conventional current flow into the electrode from the external circuit is positive.) When the reference electrode or circuit node is understood, the second subscript may be omitted, where its use is not required to preserve the meaning of the symbol.

1.3.2 Supply voltage may be indicated by repeating the electrode subscript. The reference electrode may then be designated by the third subscript.
Examples: V_{EE}, V_{CC}, V_{BB}, V_{EEB}, V_{CCB}, V_{BBC}.

1.3.3 In devices having more than one electrode of the same type, the electrode subscripts are modified by adding a number following the subscript and on the same line.
Example: *B2*
In multiple unit devices the electrode subscripts are modified by a number preceding the electrode subscript.
Example: *2B*
Wherever ambiguity might arise the complete electrode designations are separated by hyphens or commas.
Example: $V_1C_{1-2}C_1$

1.3.4 When necessary to distinguish between components of current or voltage the symbols may be used as shown in Fig. 1. The illustration shows a case where a small varying component is developed in the collector circuit of a transistor.

2. Electrical Parameters

2.1 Parameter Symbols

2.1.1 Values of four-pole matrix parameters, or other resistances, impedances, admittances, *etc.*, inherent in the device, may be represented by the lower case symbol with the proper subscripts.
Examples: h_{ib}, z_{fb}, y_{oe}, α_{fb}, h_{IB}, α_{FB}

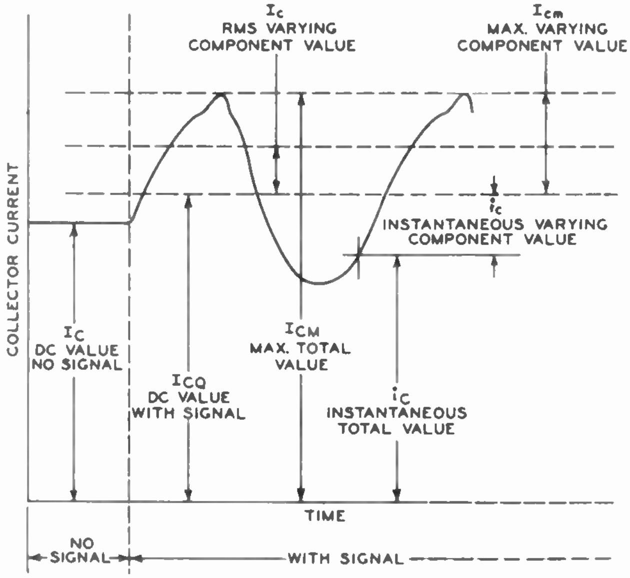

Fig. 1—Illustration of proper symbol usage.

2.1.2 Values of four pole matrix parameters or other resistances, impedances, admittances, etc., in the external circuits, may be represented by the upper case symbols with the appropriate subscripts.

2.2 Subscript for Parameter Symbols

2.2.1 Static[1] values of parameters are indicated by the upper case subscript.
Examples: r_B, h_{IB}, α_{FB}

2.2.2 Small-signal values of parameters are indicated by the lower case subscript.
Examples: r_b, y_c, h_{ib}, z_{ob}, α_{fb}

2.2.3 The first subscript or subscript pair in matrix notation, identifies the element of the four-pole matrix.

i or 11 = input
o or 22 = output
f or 21 = forward transfer
r or 12 = reverse transfer

Examples: $V_i = h_i I_i + h_r V_o$ $\quad V_1 = h_{11} I_1 + h_{12} V_2$
$I_o = h_f I_i + h_o V_o$ $\quad I_2 = h_{21} I_1 + h_{22} V_2$

Note: Voltage and current symbols in matrix notation are designated with a single digit subscript. The subscript 1 = input. The subscript 2 = output.

2.2.4 The second subscript or the subscript following the numeric pair identifies the circuit configuration. When the common electrode is understood, the second subscript may be omitted.

e = common emitter
b = common base
c = common collector
j = common electrode, general.

Examples: (common base)
$I_i = y_{ib} V_{ib} + y_{rb} V_{ob}$ $\quad I_1 = y_{11b} V_{1b} + y_{12b} V_{2b}$
$I_o = y_{fb} V_{ib} + y_{ob} V_{ob}$ $\quad I_2 = y_{21b} V_{1b} + y_{22b} V_{2b}$

[1] The static value is the slope of the line from the origin to the operating point on the appropriate characteristic curve.

2.2.5 Electrical parameters characterizing the behavior of a device with associated circuitry are designated by upper case symbols with an appropriate subscript; *e.g.*, Z_i, Z_o. The termination may be indicated by an additional subscript such as: o = ac open circuit termination; s = ac short-circuit termination; a or other appropriate subscript for other terminations. This additional subscript may be omitted.
Examples: Z_{io}, Z_{is}, Z_{ia}, $Z_{i\ \mathrm{match}}$

3. Letter Symbols in Alphabetical Order

The following list has been compiled according to the conventions set forth in Sections 1 and 2 of this Standard.

In general, the first symbol given for each electrical quantity or parameter illustrates the basic symbol with the subscript which designates the reference electrode or common electrode. (See Sections 1.3.1 and 2.2.5.) The transfer ratio of the current generator shunting the collector branch low-frequency equivalent circuit is shown in Fig. 2.

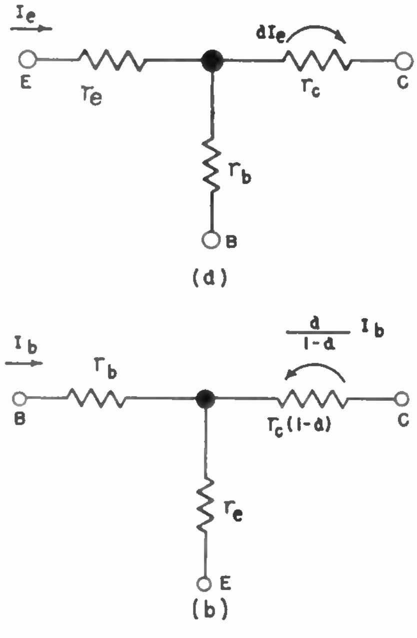

Fig. 2—Low frequency T equivalent circuit. (a) base common; (b) emitter common.

α_F, α_{FB}, α_{FC}, α_{FE},—The static value of the short-circuit forward current transfer ratio.[2]

α_f, α_{fb}, α_{fc}, α_{fe},—The small-signal short-circuit forward current transfer ratio.[2]

α_R, α_{RB}, α_{RC}, α_{RE},—The static value of the short-circuit reverse current transfer ratio.[2]

α_r, α_{rb}, α_{rc}, α_{re},—The small-signal short-circuit reverse current transfer ratio.[2]

[2] The algebraic sign of α for the common base configuration is taken as positive in accordance with established usage, therefore $\alpha_{fb} = -h_{fb} = -h_{21b}$.

Reference Data for Radio Engineers

Fourth Edition

Considerable time is spent by radio engineers in finding data needed to solve the wide variety of problems that arise from day to day. While much of this information is readily available, it is often necessary to search through several textbooks before the particular equation, curve, table, or nomograph is found.

Reference Data for Radio Engineers is presented as a one-book source of this basic material. In this single volume has been packed a tremendous quantity of data often needed in radio and electronic engineering.

The selection and preparation of the material contained in *Reference Data for Radio Engineers* have been the responsibility of a large group of practical engineers, each contributing in his particular field of specialization. The book in its entirety has been submitted for critical review to a group of engineers having collectively an extremely broad background of experience in radio, electronics, telephony, and telegraphy.

More than 150,000 copies of the first three editions of *Reference Data for Radio Engineers* have been distributed, with the sale of the third edition far surpassing that of its two predecessors. This fact is indicative of the increasingly widespread acceptance of the book.

Its usefulness has not been restricted to the practicing radio and electronic engineer for whom it was originally prepared—instead, it has also reached into the realm of the engineer-in-training. *Reference Data for Radio Engineers* has been accepted for classroom use in over 200 of the leading colleges in the United States. Students are encouraged to develop early in their engineering careers the habit of saving time through the use of this handy compilation of reference data.

Here is the wide range of subjects covered in Reference Data for Radio Engineers and the number of pages devoted to each:

	Number of Pages
Frequency data	22
Units, constants, and conversion factors	12
Properties of materials	35
Components	36
Fundamentals of networks	52
Filters, image-parameter design	23
Filters, modern-network-theory design	49
Filters, simple bandpass design	11
Attenuators	16
Bridges and impedance measurements	8
Iron-core transformers and reactors	34
Rectifiers and filters	18
Magnetic amplifiers	21
Feedback control systems	23
Electron tubes	65
Electron-tube circuits	46
Semiconductors and transistors	21
Transistor circuits	28
Modulation	22
Transmission lines	68
Waveguides and resonators	27
Scattering matrixes	18
Antennas	48
Radio-wave propagation	52
Radio noise and interference	16
Broadcasting	22
Radar fundamentals	16
Wire transmission	34
Electroacoustics	29
Digital computors	9
Nuclear physics	32
Miscellaneous data	44
Information theory	17
Probability and statistics	21
Fourier waveform analysis	23
Maxwell's equations	6
Mathematical formulas	67
Mathematical tables	23

International Telephone and Telegraph Corporation

Publication Department • 67 Broad Street • New York 4, N. Y.

UNIT CONVERSION TABLE

quantity	symbol	equation in mks(r) units	mks(r) (rationalized) unit	equivalent number of: mks(nr) units	pract units	esu	emu	mks(nr) (nonrational-ized) unit	equivalent number of: pract units	esu	emu	practical (cgs) unit	equivalent number of: esu	emu	esu	equivalent number of emu units	emu
length	l		meter (m)	1	10^2	10^2	10^2	meter (m)	10^2	10^2	10^2	centimeter (cm)	1	1	centimeter (cm) (G)	1	centimeter (cm)
mass	m		kilogram	1	10^3	10^3	10^3	kilogram	10^3	10^3	10^3	gram	1	1	gram (G)	1	gram
time	t		second	1	1	1	1	second	1	1	1	second	1	1	second (G)	1	second
force	F	$F = ma$	newton	1	10^5	10^5	10^5	newton	10^5	10^5	10^5	dyne	1	1	dyne (G)	1	dyne
work, energy	W	$W = Fl$	joule	1	1	10^7	10^7	joule	1	10^7	10^7	joule	10^7	10^7	erg (G)	1	erg
power	P	$P = W/t$	watt	1	1	10^7	10^7	watt	1	10^7	10^7	watt	10^7	10^7	erg/second (G)	1	erg/second
electric charge	q		coulomb	1	1	3×10^9	10^{-1}	coulomb	1	3×10^9	10^{-1}	coulomb	3×10^9	10^{-1}	statcoulomb (G)	$10^{-10}/3$	abcoulomb
volume charge density	ρ	$\rho = q/v$	coulomb/m^3	1	10^{-6}	3×10^3	10^{-7}	coulomb/m^3	10^{-6}	3×10^3	10^{-7}	coulomb/cm^3	3×10^9	10^{-1}	statcoulomb/cm^3 (G)	$10^{-10}/3$	abcoulomb/cm^3
surface charge density	σ	$\sigma = q/A$	coulomb/m^2	1	10^{-4}	3×10^5	10^{-5}	coulomb/m^2	10^{-4}	3×10^5	10^{-5}	coulomb/cm^2	3×10^9	10^{-1}	statcoulomb/cm^2 (G)	$10^{-10}/3$	abcoulomb/cm^2
electric dipole moment	p	$p = ql$	coulomb-meter	1	10^2	3×10^{11}	10	coulomb-meter	10^2	3×10^{11}	10	coulomb-cm	3×10^9	10^{-1}	statcoulomb-cm (G)	$10^{-10}/3$	abcoulomb-cm
polarization	P	$P = p/v$	coulomb/m^2	1	10^{-4}	3×10^5	10^{-5}	coulomb/m^2	10^{-4}	3×10^5	10^{-5}	coulomb/cm^2	3×10^9	10^{-1}	statcoulomb/cm^2 (G)	$10^{-10}/3$	abcoulomb/cm^2
electric field intensity	E	$E = F/q$	volt/m	1	10^{-2}	$10^{-4}/3$	10^6	volt/m	10^{-2}	$10^{-4}/3$	10^6	volt/cm	$10^{-2}/3$	10^8	statvolt/cm (G)	3×10^{10}	abvolt/cm
permittivity	ϵ	$F = q^2/4\pi\epsilon l^2$	farad/m	4π	$4\pi\times10^{-9}$	$36\pi\times10^9$	$4\pi\times10^{-11}$		10^{-9}	9×10^9	10^{-11}		9×10^{18}	10^{-2}	(G)	$10^{-20}/9$	
displacement	D	$D = \epsilon E$	coulomb/m^2	4π	$4\pi\times10^{-4}$	$12\pi\times10^5$	$4\pi\times10^{-5}$		10^{-4}	3×10^5	10^{-5}		3×10^9	10^{-1}	(G)	$10^{-10}/3$	
displacement flux	Ψ	$\Psi = DA$	coulomb	4π	4π	$12\pi\times10^9$	$4\pi\times10^{-1}$		1	3×10^9	10^{-1}		3×10^9	10^{-1}	(G)	$10^{-10}/3$	
emf, electric potential	V	$V = El$	volt	1	1	$10^{-2}/3$	10^8	volt	1	$10^{-2}/3$	10^8	volt	$10^{-2}/3$	10^8	statvolt (G)	3×10^{10}	abvolt
current	I	$I = q/t$	ampere	1	1	3×10^9	10^{-1}	ampere	1	3×10^9	10^{-1}	ampere	3×10^9	10^{-1}	statampere (G)	$10^{-10}/3$	abampere
volume current density	J	$J = I/A$	ampere/m^2	1	10^{-4}	3×10^5	10^{-5}	ampere/m^2	10^{-4}	3×10^5	10^{-5}	ampere/cm^2	3×10^9	10^{-1}	statampere/cm^2 (G)	$10^{-10}/3$	abampere/cm^2
surface current density	K	$K = I/l$	ampere/m	1	10^{-2}	3×10^7	10^{-3}	ampere/m	10^{-2}	3×10^7	10^{-3}	ampere/cm	3×10^9	10^{-1}	statampere/cm (G)	$10^{-10}/3$	abampere/cm
resistance	R	$R = V/I$	ohm	1	1	$10^{-11}/9$	10^9	ohm	1	$10^{-11}/9$	10^9	ohm	$10^{-11}/9$	10^9	statohm (G)	9×10^{20}	abohm
conductance	G	$G = 1/R$	mho	1	1	9×10^{11}	10^{-9}	mho	1	9×10^{11}	10^{-9}	mho	9×10^{11}	10^{-9}	statmho (G)	$10^{-20}/9$	abmho
resistivity	ρ	$\rho = RA/l$	ohm-meter	1	10^2	$10^{-9}/9$	10^{11}	ohm-meter	10^2	$10^{-9}/9$	10^{11}	ohm-cm	$10^{-11}/9$	10^9	statohm-cm (G)	9×10^{20}	abohm-cm
conductivity	γ	$\gamma = 1/\rho$	mho/meter	1	10^{-2}	9×10^9	10^{-11}	mho/meter	10^{-2}	9×10^9	10^{-11}	mho/cm	9×10^{11}	10^{-9}	statmho/cm (G)	$10^{-20}/9$	abmho/cm
capacitance	C	$C = q/V$	farad	1	1	9×10^{11}	10^{-9}	farad	1	9×10^{11}	10^{-9}	farad	9×10^{11}	10^{-9}	statfarad (cm) (G)	$10^{-20}/9$	abfarad
elastance	S	$S = 1/C$	daraf	1	1	$10^{-11}/9$	10^9	daraf	1	$10^{-11}/9$	10^9	daraf	$10^{-11}/9$	10^9	statdaraf (G)	9×10^{20}	abdaraf
magnetic charge	m		weber	$1/4\pi$	$10^8/4\pi$	$10^{-2}/12\pi$	$10^8/4\pi$		10^8	$10^{-2}/3$	10^8		$10^{-10}/3$	1		3×10^{10}	unit pole (G)
magnetic dipole moment	m	$m = ml$	weber-meter	$1/4\pi$	$10^{10}/4\pi$	$1/12\pi$	$10^{10}/4\pi$		10^{10}	$1/3$	10^{10}		$10^{-10}/3$	1		3×10^{10}	pole-cm (G)
magnetization	M	$M = m/v$	weber/m^2	$1/4\pi$	$10^4/4\pi$	$10^{-6}/12\pi$	$10^4/4\pi$		10^4	$10^{-6}/3$	10^4		$10^{-10}/3$	1		3×10^{10}	pole/cm^2 (G)
magnetic field intensity	H	$H = nI/l$	ampere-turn/m	4π	$4\pi\times10^{-3}$	$12\pi\times10^7$	$4\pi\times10^{-3}$		10^{-3}	3×10^7	10^{-3}	oersted	3×10^{10}	1		$10^{-10}/3$	oersted (G)
permeability	μ	$F = m^2/4\pi\mu l^2$	henry/m	$1/4\pi$	$10^7/4\pi$	$10^{-13}/36\pi$	$10^7/4\pi$		10^7	$10^{-13}/9$	10^7	gauss/oersted	$10^{-20}/9$	1		9×10^{20}	gauss/oersted (G)
induction	B	$B = \mu H$	weber/m^2	1	10^4	$10^{-6}/3$	10^4	weber/m^2	10^4	$10^{-6}/3$	10^4	gauss	$10^{-10}/3$	1		3×10^{10}	gauss (G)
induction flux	Φ	$\Phi = BA$	weber	1	10^8	$10^{-2}/3$	10^8	weber	10^8	$10^{-2}/3$	10^8	maxwell (line)	$10^{-10}/3$	1		3×10^{10}	maxwell (line) (G)
mmf, magnetic potential	M	$M = Hl$	ampere-turn	4π	$4\pi\times10^{-1}$	$12\pi\times10^9$	$4\pi\times10^{-1}$		10^{-1}	3×10^9	10^{-1}	gilbert	3×10^{10}	1		$10^{-10}/3$	gilbert (G)
reluctance	$\mathcal{R}$	$\mathcal{R} = M/\Phi$	amp-turn/weber	4π	$4\pi\times10^{-9}$	$36\pi\times10^{11}$	$4\pi\times10^{-9}$		10^{-9}	9×10^{11}	10^{-9}	gilbert/maxwell	9×10^{20}	1		$10^{-20}/9$	gilbert/maxwell (G)
permeance	$\mathcal{P}$	$\mathcal{P} = 1/\mathcal{R}$	weber/amp-turn	$1/4\pi$	$10^9/4\pi$	$10^{-11}/36\pi$	$10^9/4\pi$		10^9	$10^{-11}/9$	10^9	maxwell/gilbert	$10^{-20}/9$	1		9×10^{20}	maxwell/gilbert (G)
inductance	L	$L = \Phi/I$	henry	1	1	$10^{-11}/9$	10^9	henry	1	$10^{-11}/9$	10^9	henry	$10^{-11}/9$	10^9	stathenry (G)	9×10^{20}	abhenry (cm) (G)

Compiled by J. R. Ragazzini and L. A. Zadeh, Columbia University, New York.

The velocity of light was taken as 3×10^{10} centimeters/second in computing the conversion factors.

G = Gaussian unit.

Equations in the second column are for dimensional purposes only.

Reprinted from the Fourth edition of the Reference Data for Radio Engineers

Published by INTERNATIONAL TELEPHONE AND TELEGRAPH CORPORATION

Reference Data for Radio Engineers

Fourth Edition

Considerable time is spent by radio engineers in finding data needed to solve the wide variety of problems that arise from day to day. While much of this information is readily available, it is often necessary to search through several textbooks before the particular equation, curve, table, or nomograph is found.

Reference Data for Radio Engineers is presented as a one-book source of this basic material. In this single volume has been packed a tremendous quantity of data often needed in radio and electronic engineering.

The selection and preparation of the material contained in *Reference Data for Radio Engineers* have been the responsibility of a large group of practical engineers, each contributing in his particular field of specialization. The book in its entirety has been submitted for critical review to a group of engineers having collectively an extremely broad background of experience in radio, electronics, telephony, and telegraphy.

More than 150,000 copies of the first three editions of *Reference Data for Radio Engineers* have been distributed, with the sale of the third edition far surpassing that of its two predecessors. This fact is indicative of the increasingly widespread acceptance of the book.

Its usefulness has not been restricted to the practicing radio and electronic engineer for whom it was originally prepared—instead, it has also reached into the realm of the engineer-in-training. *Reference Data for Radio Engineers* has been accepted for classroom use in over 200 of the leading colleges in the United States. Students are encouraged to develop early in their engineering careers the habit of saving time through the use of this handy compilation of reference data.

The fourth edition is almost twice the size of the third edition. It has 1121 pages and a 29-page cross index. It may be ordered from International Telephone and Telegraph Corporation, Publication Department, 67 Broad Street, New York 4, N. Y., at $6.00 per copy or in lots of 12 or more to a single address at $4.80 each, postpaid.

Here is the wide range of subjects covered in Reference Data for Radio Engineers and the number of pages devoted to each:

International Telephone and Telegraph Corporation
Publication Department • 67 Broad Street • New York 4, N. Y.

C_o, C_{ob}, C_{oc}, C_{oe}—The capacitance measured across the output terminals with the input open-circuited to ac.

f_α, $f_{\alpha b}$, $f_{\alpha c}$, $f_{\alpha e}$—The frequency at which the magnitude of the small-signal short-circuit forward current transfer ratio is 0.707 of the low-frequency value.

h_F, h_{FB}, h_{FC}, h_{FE}—The static value of the short-circuit forward current transfer ratio.

h_f, h_{fb}, h_{fc}, h_{fe}, h_{21}, h_{21b}, h_{21c}, h_{21e}—The small-signal short-circuit forward current transfer ratio.

h_I, h_{IB}, h_{IC}, h_{IE}—The static value of the short-circuit input resistance.

h_i, h_{ib}, h_{ic}, h_{ie}, h_{11}, h_{11b}, h_{11c}, h_{11e}—The small-signal value of the short-circuit input impedance.

h_O, h_{OB}, h_{OC}, h_{OE}—The static value of the open-circuit output conductance.

h_o, h_{ob}, h_{oc}, h_{oe}, h_{22}, h_{22b}, h_{22c}, h_{22e}—The small-signal value of the open-circuit output admittance.

h_R, h_{RB}, h_{RC}, h_{RE}—The static value of the open-circuit reverse voltage transfer ratio.

h_r, h_{rb}, h_{rc}, h_{re}, h_{12}, h_{12b}, h_{12c}, h_{12e}—The small-signal value of the open-circuit reverse voltage transfer ratio.

I_{BO}, I_{BEO}, I_{BCO}—The base current when the base is biased in the reverse (high resistance) direction with respect to the reference electrode and the other electrode(s) is dc open-circuited (to the reference electrode).

I_{BS}, I_{BES}, I_{BCS}—The base current when the base is biased in the reverse (high resistance) direction with respect to the reference electrode and the other electrode(s) is dc short-circuited (to the reference electrode).

I_{CO}, I_{CEO}, I_{CBO}—The collector current when the collector is biased in the reverse (high resistance) direction with respect to the reference electrode and the other electrode(s) is dc open-circuited (to the reference electrode).

I_{CS}, I_{CES}, I_{CBS}—The collector current when the collector is biased in the reverse (high resistance) direction with respect to the reference electrode and the other electrode(s) is dc short-circuited (to the reference electrode).

I_{EO}, I_{EBO}, I_{ECO}—The emitter current when the emitter is biased in the reverse (high resistance) direction with respect to the reference electrode and the other electrode(s) is dc open-circuited (to the reference electrode).

I_{ES}, I_{EBS}, I_{ECS}—The emitter current when the emitter is biased in the reverse (high resistance) direction with respect to the reference electrode and the other electrode(s) is dc short-circuited (to the reference electrode).

r_b—Resistance of the base branch of the low-frequency equivalent circuit shown in Fig. 2.

r_c—Resistance of the collector branch of the low-frequency equivalent circuit shown in Fig. 2.

r_e—Resistance of the emitter branch of the low-frequency equivalent circuit shown in Fig. 2.

r_m—The product of a and r_c of the low-frequency equivalent circuit shown in Fig. 2.

t_d—The ohmic delay time is the time interval between the rise of a pulse applied at the input terminals and the rise of the minority-carrier-generated pulse appearing at the output terminals.

t_s—The storage time is the time interval between the fall of a pulse applied to the input terminals and the fall of the carrier-generated pulse at the output terminals.

V_{CF}, V_{CBF}, V_{EF}, V_{EBF}, V_{CEF}, V_{ECF}, V_{BF}, V_{BEF}, V_{BCF}—The dc open-circuit voltage (floating potential) between the electrode indicated by the first subscript and the reference electrode when the other electrode is biased in the reverse (high resistance) direction with respect to the reference electrode.

BV_{CO}, BV_{CBO}, BV_{CEO}, BV_{EO}, BV_{EBO}, BV_{ECO}, BV_{BO}, BV_{BEO}, BV_{BCO}—The breakdown voltage between the electrode indicated by the first subscript when it is biased in the reverse (high resistance) direction with respect to the reference electrode and the other electrode is open-circuited.

μ_f, μ_{fb}, μ_{fc}, μ_{fe}—The small-signal open-circuit forward voltage-transfer ratio.

μ_r, μ_{rb}, μ_{rc}, μ_{re}—The small-signal open-circuit reverse voltage-transfer ratio.

μ_F, μ_{FB}, μ_{FC}, μ_{FE}—The static value of the open-circuit forward voltage-transfer ratio.

μ_R, μ_{RB}, μ_{RC}, μ_{RE}—The static value of the open-circuit reverse voltage-transfer ratio.

y_f, y_{fb}, y_{fc}, y_{fe}, y_{21}, y_{21b}, y_{21c}, y_{21e}—The small-signal short-circuit forward transfer admittance.

y_i, y_{ib}, y_{ic}, y_{ie}, y_{11}, y_{11b}, y_{11c}, y_{11e}—The small-signal short-circuit input admittance.

y_o, y_{ob}, y_{oc}, y_{oe}, y_{22}, y_{22b}, y_{22c}, y_{22e}—The small-signal short-circuit output admittance.

y_r, y_{rb}, y_{rc}, y_{re}, y_{12}, y_{12b}, y_{12c}, y_{12e}—The small-signal short-circuit reverse transfer admittance.

z_f, z_{fb}, z_{fo}, z_{fbo}, z_{21}, z_{21b}, z_{21ce}, z_{21bce}—The small-signal open-circuit forward transfer impedance.

z_i, z_{ib}, z_{io}, z_{ibo}, z_{11}, z_{11b}, z_{11ce}, z_{11bce}—The small-signal open-circuit input impedance.

z_o, z_{ob}, z_{oo}, z_{obo}, z_{22}, z_{22b}, z_{22ce}, z_{22bce}—The small-signal open-circuit output impedance.

z_r, z_{rb}, z_{ro}, z_{rbo}, z_{12}, z_{12b}, z_{12ce}, z_{12bce}—The small-signal open-circuit reverse transfer impedance.

z_{fs}, z_{fbs}, z_{fcs}, z_{fes}—(The reciprocal of y_f.) The small-signal short-circuit forward transfer impedance.

z_{is}, z_{ibs}, z_{ics}, z_{ies}—The small-signal short-circuit input impedance.

z_{os}, z_{obs}, z_{ocs}, z_{oes}—The small-signal short-circuit output impedance.

z_{rs}, z_{rbs}, z_{rcs}, z_{res}—The small-signal short-circuit reverse transfer impedance (the reciprocal of y_r).

Correspondence

A Dip in the Minimum Noise Figure of Beam-Type Microwave Amplifiers*

With the aid of theories of random numbers and a high-speed computer, it is possible to calculate numerically certain complicated noise phenomena occurring in electron-dynamics, which otherwise are difficult to treat because of the multivelocity and nonlinear nature of the problem. A calculation of this sort, generally known as the MONTE CARLO method, is used here to evaluate current and velocity fluctuations at the potential minimum of a specific diode. The diode considered has a cathode to anode spacing of 0.01852 cm and is assumed shorted for ac. The dc potential across the diode is 10 volts; the average emission and anode current densities are respectively 1.5 and 0.3 amperes/cm².

The calculation is based on a one-dimensional model and may be described briefly as follows. The time is divided into small and equal intervals (2×10^{-12} seconds). For each time-interval, random numbers are generated to determine the number of electrons emitted in this interval, the exact times these electrons are emitted, and the initial velocities of the electrons. These electrons are added to the other electrons in the diode and the actual space charge field distribution is calculated. The new positions and velocities of electrons at the end of the time-interval are then computed. During the computation, electrons returned to the cathode or collected by the anode are automatically erased, and those passing the potential-minimum are recorded. The computer finally tabulates the velocity and current fluctuations at the potential-minimum, and thus completes one cycle of computation. The same procedure is repeated for the next time-interval and the computation proceeds until enough data have been accumulated.

* Received by the IRE, February 20, 1956.

The computation described has been carried out in cooperation with J. Moshman of the Mathematics Department, for 3,000 time-intervals, using the "UNIVAC I" of the Remington Rand Corporation in New York. The results obtained indicate that, within the accuracy of the calculation, the velocity fluctuation is not smoothed and the current and velocity fluctuations are not correlated. The reduction in current fluctuation is shown in Fig. 1 in the form of the cumulative auto-correlation function.

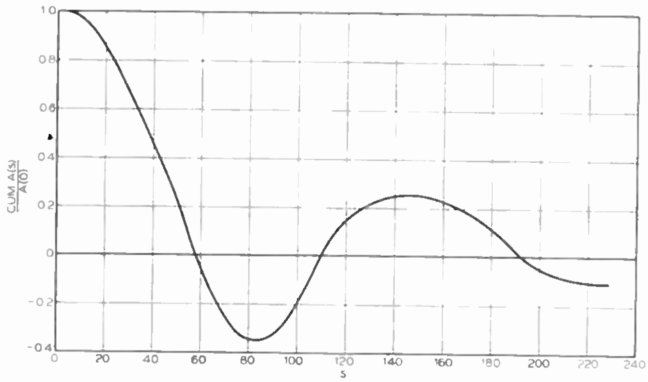

Fig. 1.—Normalized cumulative auto-correlation function of the current fluctuation.

The cumulative auto-correlation function shown in Fig. 1 is defined as

$$\text{Cum. } A(s) = \sum_{s=-R}^{+R} A(s)$$

and

$$A(s) = \frac{1}{2R} \sum_{t=-R}^{+R} \tilde{i}(t)\tilde{i}(t+s),$$

where $A(s)$ is the auto-correlation function,[1] and $\tilde{i}(t)$ and $\tilde{i}(t+s)$ are respectively the current fluctuations at the potential minimum at the t-th and $(t+s)$-th time-intervals. $2R$ is the number of time-intervals over which the statistical process is investigated. If $A(O)$ is considered as the noise power associated with a disturbance in current observed at the plane of the potential-minimum, $A(s)$ is that associated with the compensation current at the same plane, which flows s time-intervals after the disturbance. Therefore, if Cum. $A(s)$ is zero, the sum of the compensation charges is just equal to the disturbance charges. A negative Cum. $A(s)$ means over-compensation. Thus Fig. 1 is essentially a picture of the noise-smoothing process.

The over-compensation phenomenon and the damped oscillatory characteristic exhibited by the curve of Cum. $A(s)$ agrees qualitatively with the results obtained by Whinnery,[2] and may be better understood from a physical picture. As a disturbance in emission occurs, a compensation current flows because of the resultant potential perturbation. The compensation current however will continue to flow even when the disturbance charges are temporary balanced by the sum of the compensation charges. This happens because of electron inertia; current cannot change abruptly and it takes times to build up or to stop the compensation current.

The power spectrum of the current fluctuation can be computed from Fig. 1. This then leads to the calculation of the minimum noise figure of traveling-wave amplifiers,[3] which has been shown by Haus[1] to be common to all beam-type amplifiers. The minimum noise figure thus computed is shown in Fig. 2. The curve shows a sharp dip down to less than 2 decibels around 2,500 megacycles, a fact which may be important in practical applications. It also shows a peak of 7.5 db near 4,000 megacycles. The electron plasma frequency at the potential-minimum of this diode is 3,784 megacycles. At low frequencies the noise figure is small and agrees with the existing low-frequency theory.[4] At very high frequencies, it approaches the figure for full shot noise of 6.3 decibels. The details of the calculation will be presented in a forthcoming paper.

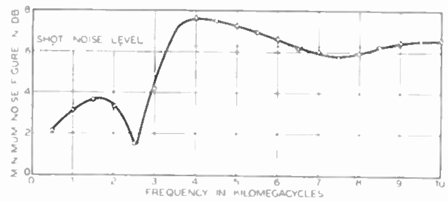

Fig. 2—The minimum noise figure of a typical traveling-wave amplifier.

P. K. Tien
Bell Telephone Labs., Inc.
Murray Hill, N. J.

[1] H. A. Haus, "Noise in one-dimensional beams," *J. Appl. Phys.*, vol. 26, p. 560; May, 1955.
[2] J. R. Whinnery, "Noise phenomena in the region of the potential minimum," Trans. IRE, vol. ED-1, pp. 221–237; December, 1954.
[3] D. A. Watkins, "Noise at the potential minimum in the high-frequency diode," *J. Appl. Phys.*, vol. 26, p. 622; May, 1955.
[4] B. J. Thompson, D. O. North, and W. A. Harris, "Fluctuations in space-charge limited currents at moderately high frequencies," *RCA Rev.*, vol. 4, p. 269, and vol. 5, p. 106; April and July, 1940.

Microphonism Due to Transistor Leads*

The transistor is usually considered to be a nonmicrophonic device.[1] However, a source of microphonic voltage has been

* Received by the IRE, March 14, 1956.

[1] J. A. Morton, "Present status of transistor development," Proc. IRE, vol. 40, p. 1323; November, 1952.

found which is traceable to the transistor leads and case rather than to the device itself. This effect was first noticed while testing a high-gain audio amplifier employing germanium alloy junction transistors. The transistors were mounted by leads approximately one and one-half inches long. The input transistor was mechanically driven by a phonograph recording head and needle with sinusoidal motion at any single frequency. The frequency range covered was from 100 to 10,000 cps. The input was purely mechanical; there was no electrical input. Various resonant frequencies were observed in this range. For example, at 1,200 cps about 10 microvolts of equivalent input voltage was generated. When an external magnet was brought near the leads the output increased markedly. The same effect could be observed with shorter leads except that there were fewer observable resonances.

Further tests confirmed the fact that the leads were mechanically resonant and generated a voltage as they vibrated in the magnetic field. This conclusion in itself is not surprising. The interesting point is that the case and leads of the particular transistor used are made of magnetic materials which can produce a local magnetic field. Relative motion between the leads and these local magnetic fields arising in the leads and the case can generate a voltage input.

We would like to acknowledge the help and suggestions of Edward Ramos and J. E. Vineski.

C. W. Durieux and T. A. Prugh
Diamond Ordnance Fuze Laboratories
Washington, D. C.

On the Effective Noise Temperature of Gas Discharge Noise Generators*

Gas discharge lamps are widely used at present as standard sources of random noise at microwave frequencies. The correlation between the electron temperature of the positive column of the discharge and the microwave noise temperature available from a network to which the discharge is coupled has been well-established.[1,2] If there is no resistive loss in the network with the lamp "off" and a very large resistive loss with the lamp "on," the available noise temperature of the network is the same as the electron temperature. However, the available noise temperature of the network is less than the electron temperature if there is resistive loss in the network with the lamp "off" and/or the resistive loss with the lamp "on" is not very large.

If the device is treated as a four-terminal network, it is necessary to measure only the available insertion loss in the lamp "on" and "off" conditions to determine the reduction in available noise temperature. An expression for obtaining this reduction, which is correct only when the loss in the lamp "off" condition is zero, has been given in the literature.[3] The following derivation gives an exact expression for the case where the resistive losses in the lamp "on" and "off" conditions are uniformly distributed in the network, and the characteristic impedance of the network is the same in both conditions. These assumptions are valid for a gas discharge noise generator of coaxial-helix construction, such as the AIL Type 70A. For a waveguide noise generator, where the gas discharge lamp is inserted at a small angle through the broad faces of the guide, the expression obtained is also valid, provided that the diameter of the lamp is small compared with the guide width, the lamp "off" loss is primarily determined by losses in the glass of the lamp envelope, and there is negligible power transferred from the guide to the junctions through which the lamp is inserted into the guide. These conditions are obtained in most well-designed waveguide noise generators.

Consider the noise generator to be composed of infinitesimal sections of length dl and terminated in its characteristic impedance z_0 as shown in Fig. 1. Alternate

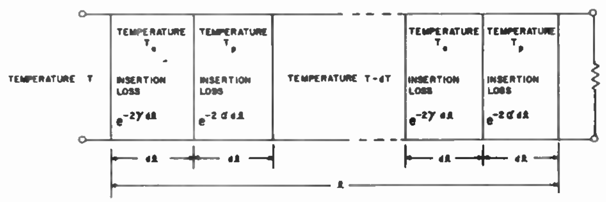

Fig. 1

sections represent losses in the generator with no gas discharge present and have a characteristic impedance z_0. The real part of their propagation constant is α. Intervening sections represent losses in the gas discharge, and also have a characteristic impedance z_0. The real part of their propagation constant is γ. Thus the total real part of the propagation constant of the noise generator with the discharge present is $\alpha+\gamma$. Let the physical temperature of the network be T_p and the electron temperature of the discharge be T_e. Then the available noise temperature T at the input terminals of the noise generator can be written as

$$T = (T - dT)e^{-2(\alpha+\gamma)dl} + T_e(1 - e^{-2\gamma dl}) + T_p(1 - e^{-2\alpha dl})e^{-2\gamma dl} \quad (1)$$

where $T-dT$ is the available noise temperature at the output terminals of the first pair of sections. Expanding (1) and neglecting higher powers of dl, which vanish in the limit as dl approaches zero, the differential equation for the available noise temperature of the generator becomes

$$\frac{dT}{dl} + 2(\alpha+\gamma)T = T_p(2\alpha) + T_e(2\gamma). \quad (2)$$

The solution of (2) can be written as

$$T = \frac{T_p\alpha + T_e\gamma}{\alpha+\gamma} + \left[T_0 - \frac{T_p\alpha + T_e\gamma}{\alpha+\gamma}\right]e^{-2(\alpha+\gamma)l} \quad (3)$$

where T_0 is the temperature of the terminating impedance of the network, and l is the distance from the termination to the input terminals of the noise generator.

Let L, the insertion loss of the noise generator, be defined as the ratio of available input power at one set of terminals to available output power at the other set of terminals. In particular let L_h be the insertion loss of the noise generator with the discharge present, and L_c be the insertion loss with no discharge present. Then $d_h = 10 \operatorname{Log} L_h$ is the insertion loss of the generator in db with the discharge present, and $d_c = 10 \operatorname{Log} L_c$ is the insertion loss of the generator in db with no discharge present. Then

$$e^{-2\alpha l} = \frac{1}{L_c} = 10^{-d_c/10}$$

$$e^{-2(\alpha+\gamma)l} = \frac{1}{L_h} = 10^{-d_h/10},$$

from which

$$2\alpha = \frac{d_c}{10l}\ln 10, \text{ and } 2\gamma = \left(\frac{d_h - d_c}{10l}\right)\ln 10.$$

Substituting these terms in (3) and simplifying, T can be written as

$$T = T_p\frac{d_c}{d_h} + T_e\left(1 - \frac{d_c}{d_h}\right) + \left[T_0 - T_p\frac{d_c}{d_h} - T_e\left(1 - \frac{d_c}{d_h}\right)\right]\frac{1}{L_h}. \quad (4)$$

The relative excess value of the available noise temperature T can be written as

$$\left(\frac{T}{T_0} - 1\right) = \left[\left(\frac{T_e}{T_0} - 1\right) - \frac{d_c}{d_h}\left[\frac{T_e}{T_0} - \frac{T_p}{T_0}\right]\right]\left(1 - \frac{1}{L_h}\right), \quad (5)$$

where the reference temperature T_0 is that of the terminating impedance. If T_0 is not 290°K (5) becomes

$$\left(\frac{T}{290} - 1\right) = \left[\left(\frac{T_e}{290} - 1\right) - \frac{d_c}{d_h}\left(\frac{T_e}{290} - \frac{T_p}{290}\right)\right]\left(1 - \frac{1}{L_h}\right) + \left(\frac{T_0}{290} - 1\right)\frac{1}{L_h}. \quad (6)$$

Eqs. (5) or (6) gives the relative excess noise temperature available from the noise generator.

W. D. White and J. G. Greene
Airborne Instruments Lab.
Mineola, N. Y.

* Received by the IRE, March 16, 1956.

[1] M. A. Easley and W. W. Mumford, "Electron temperature and noise temperature in low pressure mercury-argon discharges," *J. Appl. Phys.*, vol. 22, pp. 846, 847; June, 1951.

[2] K. S. Knol, "Determination of the electron temperature in gas discharges by noise measurements," *Philips Research Reports*, vol. 6, pp. 288–302; 1951.

[3] W. H. Spencer and P. D. Strum, "Broadband uhf and vhf noise generators," Trans. IRE, vol. PGI-4, pp. 47–50; October, 1955.

"Geophysical Prospection of Underground Water in the Desert by Means of Electromagnetic Interference Fringes"*

I read with great interest the above paper[1] by M. A. H. El-Said on a radio frequency water prospecting method. The technique applied represents an interesting approach to a difficult task. The unexplained absence of the attenuation constant in the propagation equation seems to be a serious oversight in this study. The exact phase velocity term as derived from Stratton[2] using mks units is

$$v = \frac{\omega}{\alpha} = \left[\frac{\mu\epsilon}{2}\left(\sqrt{1+\frac{\sigma^2}{\epsilon^2\omega^2}}+1\right)\right]^{-1/2}.$$

The associated attenuation constant is

$$\beta = \omega\left[\frac{\mu\epsilon}{2}\left(\sqrt{1+\frac{\sigma^2}{\epsilon^2\omega^2}}-1\right)\right]^{1/2}.$$

The assumption of unity magnetic permeability is warranted for the bulk of earth materials. The term $\sigma/\epsilon\omega$ must be examined to determine the validity of the simplification $v=1/\sqrt{\epsilon}=c/\sqrt{K_\epsilon}$. For most earth materials the dielectric constant is approximately 10, and for extremely arid regions and some igneous rocks the conductivity σ may be as high as 10^{-4} mhos/meter. This results in a value of $\sigma/\epsilon\omega$ which is smaller than 0.1 for most of the frequencies used, and the velocity becomes $v=1/\sqrt{\epsilon}$. The attendant attenuation constant reduces to $\beta=\sigma/2\sqrt{\epsilon}=188.3\sigma/\sqrt{K_\epsilon}$. Expressed in terms of the napier depth, or "skin depth," $\delta=1/\beta=\sqrt{K_\epsilon}/188.3\sigma$ where the plane wave is attenuated to $1/e$ of its initial value or by 8.7 db.

For the field tests cited the reflected signal traveled along a path of 10.4 to 11 napier depths, hence suffering an attenuation not less than 90 db or signal strength reduction of 3×10^4. The reflected path is always greater than the direct path by a ratio of 1.38 and the spreading geometry of the wave fronts further reduces the reflected signal not less than the square of the ratio. Hence, in order to detect the reflected signal, the signal strength measurements must be made with an accuracy well in excess of 1 part in 10^5. This was not the case for the measurements cited, and we must either conclude that the propagation and attenuation data presented herein are incorrect or an invalid geological interpretation has been derived from the data obtained. These propagation data are based upon Maxwell's equations and for the range of frequencies involved in this discussion have been verified by various investigators in this country in connection with the evaluation of radio frequency oil prospecting methods. Some of the references citing field tests are McGehee,[3] Pritchett,[4] and Silverman and Sheffet.[5] In the event that a new mode of propagation is involved in this water prospecting method more complete information on this theory should be reported since this would be of far reaching importance to the geophysical industry in general.

It might also be noted that the infinite reflection coefficient assumption used is valid only for water of relatively high conductivity and hence high mineral content. This is usually the case for ground water, but for fresh water of 10^{-2} mhos/meter the reflection coefficient will not exceed 7 and will be much less if the earth conductivity is greater than 10^{-4} mhos/meter, and the reflected signal would be reduced to even greater insignificance. Earth conductivities greater than 10^{-4} mhos/meter would necessitate consideration of the conductivity term in the velocity expression for the frequencies used. The conductivity of the earth cannot be lightly considered in electromagnetic propagation since this is the predominant term in the attenuation equation. The conductivity also determines the velocity at low frequencies and consideration of conductivity versus dielectric constant determined the frequency at which transition occurs.

G. L. Brown
Development and Research Dept.
Continental Oil Co.
Ponca City, Okla.

* Received by the IRE, March 14, 1956.

[1] Proc. IRE, vol. 44; pp. 24–30; January, 1956.

[2] J. A. Stratton, "Electromagnetic Theory," McGraw-Hill Book Co., Inc., New York, p. 276, 1941.

[3] F. M. McGehee, "Propagation of radio frequency energy through the earth," *Geophysics*, vol. 19, pp. 459–478; July, 1954.

[4] W. C. Pritchett, "Attenuation of radio frequency waves through the earth," *Geophysics*, vol. 17, pp. 193–218; April, 1952.

[5] D. Silverman and D. Sheffet, "Note on transmission of radio waves through the earth," *Geophysics*, vol. 7, pp. 406–414; October, 1942.

Rebuttal[6]

The question of attenuation was not oversighted. In fact, attenuation was the major factor behind this research until the time came when the first interference patterns at Baharya Road were obtained. Prior to this time, enlightening laboratory work was done by Dr. H. Lowy under Professor H. Mahmoud's supervision at Cairo University, for determining the degree of transparency of Egyptian Desert material to electromagnetic waves. The results of this work were published.[7] The authors state that: "According to F. E. Terman's 'Radio Engineers Handbook,' earth resistivities of the order of 10^5 ohm cm must be considered as very high.[8] In contradiction to this, the resistivities of 59 different sandstone discs, as indicated for frequency 100 kc in Tables II and III, are more than 10 to 1,000 times greater than the maximum earth resistivity, according to Terman."

For the sake of clarity, Fig. 1 shows calculated curves for the attenuation factor F_a vs distance x in a homogeneous lossy dielectric having $\sqrt{\epsilon}=2.5$ and $\mu=1$ for various values of resistivity ρ between 5×10^5 and 5×10^6 ohm cm. The values between 1×10^6 and 2×10^6 ohm cm are, in my opinion representing the average prevailing resistivity range of the underground material in the Egyptian Deserts during summer time. These values are less than those anticipated by Dr. Lowy, but considerably greater than those quoted by Terman. With this range

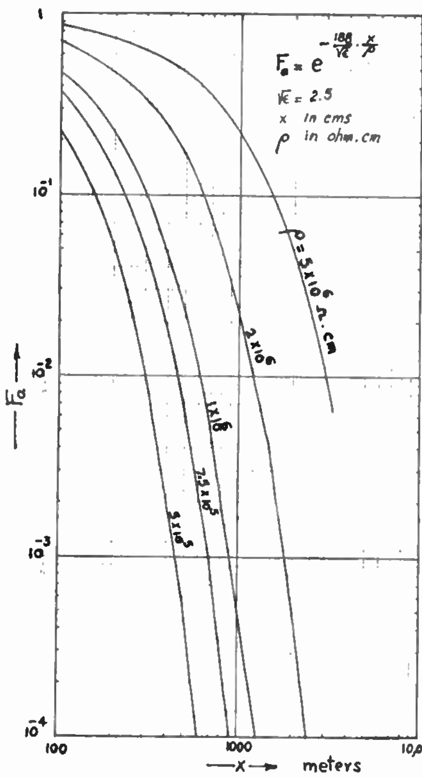

Fig. 1

of resistivity, it was inferred that the Egyptian Desert material is reasonably transparent to electromagnetic waves.

Moreover, the mode of propagation and techniques described in my prospecting work, depended largely upon the proper choice of optimum condition which would result in the reflected and surface rays being of same order of magnitudes at the receiver site. Undoubtedly, both rays suffer consiberadle attenuation. The surface ray is sometimes even more attenuated than the ground ray since it is bound by the surface layer which is usually more conducting than the interior of the earth. The merit of the prospecting technique described in the paper under discussion is actually in the choice of the favorable frequency range and distances which would enable the engineer to correctly apply ordinary instrumentation for the successful detection of electromagnetic interference fringes. Particular emphasis was also given to beneficial choice of a frequency interval small compared to the order of magnitude of the operating frequencies.

Mr. Brown's conclusion is in my opinion unjustified. It seems also that Mr. Brown is using a slightly unconventional definition of the term "reflection coefficient" which can never exceed unity in any case. It is also worth mentioning that reflections occurring at the water-rock interface are due to the large change in dielectric constant and that water conductivity is immaterial. In the case of oil-rock interface, the change in dielectric constant is small and the reflections are poor.

Dr. M. A. H. El-Said
Faculty of Engineering
University of Cairo
Giza, Egypt

[6] Received by the IRE, April 3, 1956.

[7] H. Mahmoud and H. Lowy, "Electric constants of desert rocks," *Extrit du Bulletin De L'Institut D'Egypt*, TXXXIII, Session 1950–1951.

[8] *Op. cit.*, p. 708.

Maximum Efficiency of Four-Terminal Networks*

In contributions to this column Mathis[1] and Altschuler[2] have, respectively, shown geometric constructions for finding the input impedance Z_a (reflection coefficient Γ_a) and the maximum efficiency η_{max} of an arbitrary two-port network which is terminated in its conjugate-image impedance match. The constructions are shown in Fig. 1. The purpose of this paper is to give simple geometric explanations for the constructions.

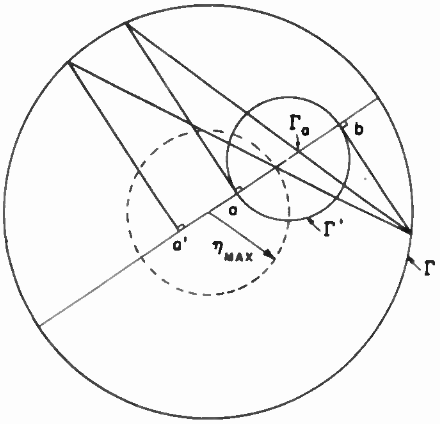

Fig. 1—The constructions by Mathis and Altschuler for determining Γ_a and η_{max}.

Several authors[3-5] have found that the reflection coefficient Γ_a is the limit point of a pencil of circles of which the circles Γ and Γ' in Fig. 1 are members. If the limit point is moved to the center of the circle Γ, the radius of the new Γ'-circle equals the maximum efficiency η_{max}.[5]

Let us assume that the Γ-circle in Fig. 1 is the absolute curve of a Poincaré model of a hyperbolic geometry.[6-8] In this model the pencil mentioned above is composed of coaxial circles having Γ_a as common center. To find Γ_a we thus have to divide the distance ab into two equal hyperbolic distances. This can be done by a simple butterfly-shaped figure shown in Fig. 2(a). Two lines of the figure are non-Euclidean perpendicular to the line through a and b. The hyperbolic distances ac and cb are equal, because the cross-ratios $(uacv)$ and $(ucbv)$ are equal, and the hyperbolic distance is by definition proportional to the logarithm of the cross-ratio of the endpoints and the two points cut out on the absolute curve. The butterfly figure was introduced in network theory by Van Slooten.[6] It can be thought of as forming part of a complete quadrangle. The division of ab in Fig. 2(a) can be performed completely inside the circle Γ if the butterfly figure is centered around a diameter as shown in Fig. 2(b). A simple use of the butterfly figure is the transformation $\mathcal{B}(\mathcal{B}^{-1})$ used by Deschamps[7,8] in transforming the Poincaré model into the Cayley-Klein diagram (called "the projective plane" by Deschamps), and vice versa.

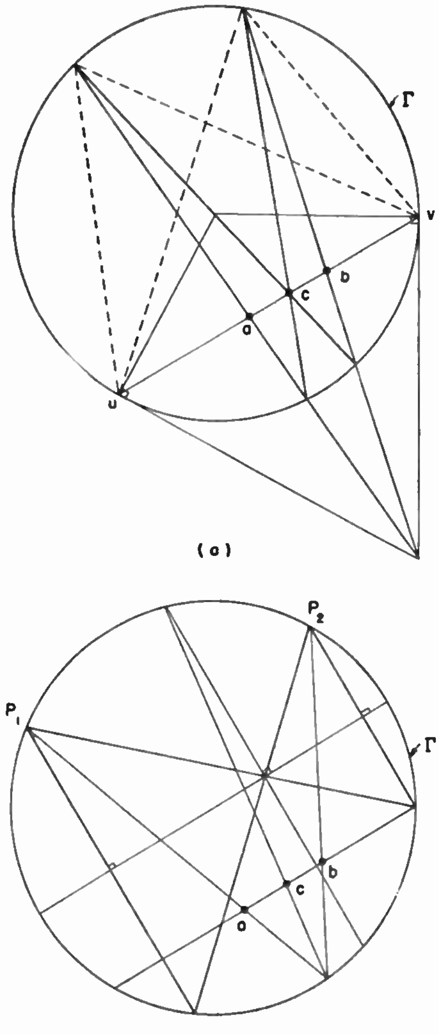

Fig. 2—Division of a hyperbolic distance into two equal parts.

A hyperbolic distance ab can be displaced along a straight line to cd by an analogous construction shown in Fig. 3 in which one of the points P_1 or P_2 can be selected arbitrarily. Another butterfly figure is obtained.

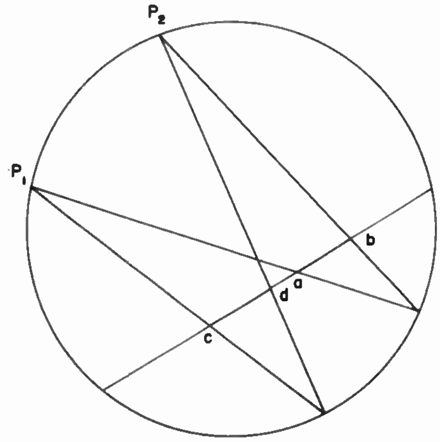

Fig. 3—Displacement of a hyperbolic distance along a straight line.

Figs. 2 and 3 give simple geometric explanations of the constructions by Mathis and Altschuler; also see Fig. 4(a). From this figure it is evident why Altschuler starts out from the point a' at the same distance as a from the center of Γ and opposite the point a. Fig. 4(b), finally, shows a more symmetric construction for moving the circle Γ' to the center of the circle Γ.

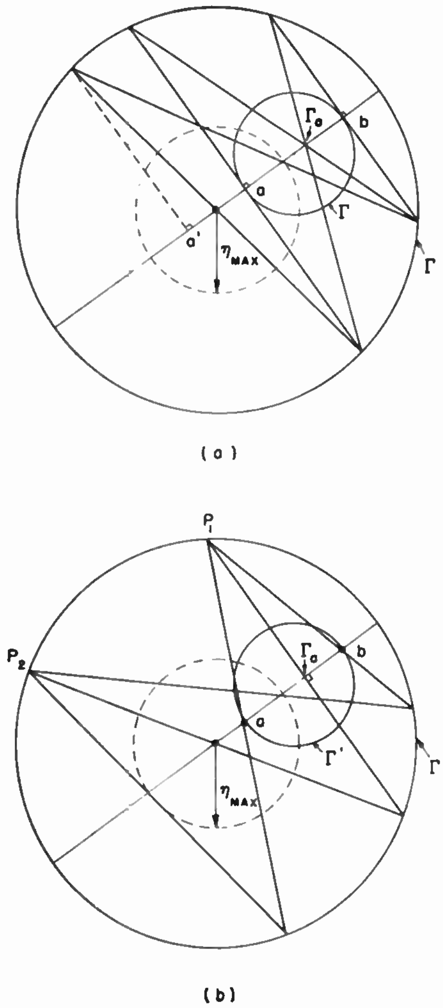

Fig. 4—Use of the butterfly figure for determining Γ_a and η_{max}.

If a copy of the ingenious hyperbolic protractor invented by Deschamps[7,8] is available, it can, of course, be used directly for determining Γ_a and η_{max}.

E. F. Bolinder
Res. Lab. of Electronics
Mass. Inst. Tech.
Cambridge, Mass.
(Formerly at Royal Inst. Tech.
Div. of Radio Engrg.
Stockholm, Sweden.)

* Received by the IRE, April 9, 1956. This work was supported in part by the Army (Signal Corps), the Air Force (Office of Scientific Research, Air Research and Development Command), and the Navy (Office of Naval Research).

[1] H. F. Mathis, "Maximum efficiency of four-terminal networks," Proc. IRE, vol. 43, pp. 229–230; February, 1955.

[2] H. M. Altschuler, "Maximum efficiency of four-terminal networks," Proc. IRE, vol. 43, p. 1016; August, 1955.

[3] A. Weissfloch, "Die Wirkleistungsverluste in linearen Vierpolen in Abhängigkeit vom Wert des transfermierten Scheinwiderstandes," *ENT*, vol. 19, pp. 259–265; December, 1942.

[4] W. Altar, "Q-circles," Proc. IRE, vol. 35, pp. 355–361; April, 1947, and pp. 478–484; May, 1947.

[5] H. A. Wheeler and D. Dettinger, "Measuring the efficiency of a superheterodyne converter by the input impedance circle diagram," Wheeler Monographs, No. 9; March, 1949.

[6] J. Van Slooten, "Meetkundige Beschouwingen in Verband met de Theorie der Electrische Vierpolen," W. D. Meinema, Delft, 1946.

[7] G. A. Deschamps, "New chart for the solution of transmission-line and polarization problems," Trans. IRE, vol. MTT-1, pp. 5–13; March, 1953; Elec. Commun., vol. 30, pp. 247–254; September, 1953.

[8] G. A. Deschamps, "A hyperbolic protractor for microwave impedance measurements and other purposes," Federal Telecommun. Labs.; 1953.

Contributors

George R. Brewer (A'43–M'49–SM'54) was born in New Albany, Ind., on September 10, 1922. He received the B.E.E. degree in Electrical Engineering from the University of Louisville in 1943, the M.S.E. in Electrical Engineering in 1948, the M.S. degree in Physics in 1949, and the Ph.D. degree in Electrical Engineering in 1952 from the University of Michigan.

G. R. Brewer

Dr. Brewer has been engaged principally in research and development of electron tubes; from 1943 to 1944 at the Radiation Laboratory, M.I.T., from 1944 to 1947 at the Naval Research Laboratory, and from 1947 to 1951 at the Engineering Research Institute of the University of Michigan. He is now in the Electron Tube Laboratory of Hughes Research and Development Laboratories.

He is a member of the American Physical Society, Sigma Xi, and Phi Kappa Phi.

❖

Benjamin J. Dasher (A'41) received the degrees of B.S. and M.S. in E.E. from Georgia Tech in 1935 and 1945, respectively, and the Sc.D. in E.E. from M.I.T. in 1952. From 1940 to 1946 he taught Electrical Engineering at Georgia Tech, and from 1946 to 1951 he was first Instructor and then Assistant Professor of Electrical Communications at M.I.T. From 1949 to 1951 he was also a Group Leader of the Telemetering and Instrumentation Group, Project Meteor, Research Laboratory of Electronics, M.I.T. Dr. Dasher returned to Georgia Tech in 1951 and was appointed Director of the School of Electrical Engineering in 1954. His fields of special interest include advanced network theory, vacuum tube electronics (circuit design and analysis), applied mathematics, and communication theory.

B. J. Dasher

❖

J. H. Dellinger (F'23) was born on July 3, 1886 in Cleveland, Ohio. He attended Western Reserve University in Cleveland, and George Washington University in Washington, D. C. from which he received the A.B. degree in 1908 and the Sc.D. degree in 1932. In 1913 he received the Ph.D. degree from Princeton University.

Dr. Dellinger was a physicist for the National Bureau of Standards from 1907 to 1948, serving as Chief of the Radio Section from 1919 to 1946, and Chief of the Radio Propagation Laboratory from 1946 to 1948. For one year, 1928–1929, he was Chief Engineer for the Federal Radio Commission on loan from NBS.

J. H. Dellinger

From 1922 to 1948, he was a representative of the Department of Commerce on the Interdepartment Radio Advisory Committee. He has also represented the United States at numerous international radio conferences since 1921. Dr. Dellinger has held the chairmanship of the Radio Technical Commission for Aeronautics since 1941, the Radio Technical Commission for Marine Services since 1947, and, presently, of Study Group VI, Ionospheric Propagation, International Radio Consultative Committee. He is honorary president of the International Scientific Radio Union, and Chairman of the General Arrangements Committee of the 1957 General Assembly. He was president of the IRE in 1925.

❖

Donald A. Dunn (S'46–A'52) was born on December 31, 1925, in Los Angeles, Calif. He received the B.S. degree from California Institute of Technology in 1946, the M.S. degree from Stanford University in 1947, the degree of Engineer from Stanford in 1950, and the L.L.B. degree from Stanford in 1951. He was a Research Assistant from 1947 to 1950 and has been a Research Associate from 1951 to the present at the Electronics Research Laboratory at Stanford University, where he has been doing research on traveling-wave tubes. Since 1953 he has been a group leader and lecturer. From 1951 to 1953 he was with the firm of Flehr and Swain as a patent attorney.

D. A. Dunn

Mr. Dunn is a member of the bar of the State of California and has been admitted to practice before the U. S. patent office. He is a member of Sigma Xi.

❖

Lester M. Field (M'48–F'52) received the B.S. degree from Purdue University in 1939, the Ph.D. degree from Stanford in 1943, and then became a member of the Electron Dynamics Group of the Physical Research Department at Bell Telephone Laboratories from 1943 until 1946. In 1946 he returned to Stanford University, and in 1951 became a full professor. In 1953 he went to the California Institute of Technology as a professor and there established a tube research activity and an associated graduate teaching program. In July, 1955 he became head of the Electron Tube Laboratory and has recently been appointed Associate Director of the Research Laboratories of the Hughes Aircraft Co.

L. M. Field

In 1949 he received an Eta Kappa Nu award. He is a member of the American Association of University Professors and the American Physical Society.

❖

Ward A. Harman (S'46–A'49–M'55) was born on July 3, 1922, in Seattle, Wash. He received the B.S. degree in Electrical Engineering from the University of Washington in 1946. From 1943 to 1946 he served with the U. S. Army Signal Corps where he was involved in the operation and maintenance of communications equipment. He was engaged in graduate study at Stanford University from 1946 to 1948 and received the degree of Engineer in 1948. From 1948 to 1950 he was employed at the Aerophysics Laboratory of North American Aviation, Inc., Downey, Calif., as a Research Engineer. In 1950 he resumed studies at Stanford University and received the Ph.D. degree in 1954. Dr. Harman continued his research activities at the Stanford Electronics Research Laboratory until December, 1954 at which time he joined the General Electric Co. He is currently a member of the technical staff at the G. E. Microwave Laboratory at Stanford where he is engaged in microwave tube research.

W. A. Harman

Dr. Harman is a member of Tau Beta Pi and Sigma Xi.

❖

Gordon S. Kino (S'52–A'54) was born on June 15, 1928, in Melbourne, Australia. He received the B.Sc. degree in Mathematics in

1948 and the M.Sc. degree in Mathematics in 1950 from London University. In 1955, he received the Ph.D. degree in Electrical Engineering from Stanford University.

G. S. Kino

He joined the Mullard Radio Valve Co., Salfords, Surrey, England, in 1947 as a managerial apprentice. In 1948, he became a member of the Mullard Vacuum Physics Laboratory, where he was engaged in research on microwave triodes, traveling-wave tubes, and klystrons.

From 1951 to 1955, he was employed as a Research Assistant of the Electronics Research Laboratory of Stanford University, where he carried out research on traveling-wave tubes and electromagnetic theory. He then worked as a Research Associate of the Microwave Laboratory, Stanford University, on electromagnetic theory.

At present, he is a member of the Technical Staff of the Bell Telephone Laboratories, Murray Hill, N. J., where he is associated with the Electron Tube Development Department, and is carrying out research on magnetrons.

Dr. Kino is a member of Sigma Xi.

❖

Jack M. Manley (A'43–SM'49) was born in Farmington, Mo. on March 9, 1909. He received the B.Sc. degree in Electrical Engineering from the University of Missouri in 1930. Since 1930 he has been a member of the technical staff of Bell Telephone Laboratories. For a number of years, he was concerned mainly with studies of nonlinear electric circuits. More recently, he has been working on new multiplex methods for communication systems.

J. M. Manley

Mr. Manley is a member of Tau Beta Pi and the American Institute of Electrical Engineers and an associate member of Sigma Xi.

❖

For a photograph and biography of Samuel J. Mason, see page 821 of the June, 1956 issue of Proceedings.

❖

D. A. McLean was born in Golden, Colo., on July 15, 1905. Since graduation from the University of Colorado in 1929 with the degree of B.S. in chemical engineering, he has been a member of the technical staff of Bell Telephone Laboratories. He has been primarily concerned with the chemical aspects of electrical insulation with particular reference to capacitor dielectrics. In this field he has a number of patents and other publications. Recently, his work has emphasized miniaturization of capacitors, resistors, and other passive components.

D. A. McLean

Mr. McLean is a member of the American Chemical Society, Sigma Xi, and Tau Beta Pi.

❖

Florence S. Power was born in Denver, Colo., October 9, 1898. She received the A.B. and M.A. degrees from the University of Denver in 1919 and 1920, and then taught Physics and Chemistry in Rocky Ford High School for two years.

F. S. Power

From 1922 to 1925, she studied at the University of Illinois and received the Ph.D. degree in Organic Chemistry in 1925, working on anthraquinone derivatives. She was Assistant and then Associate Professor of Chemistry at Lawrence College, Appleton, Wis. from 1925 to 1929. As a Research Chemist she worked with Scott and Bowne and Food Research Laboratories from 1929 to 1933, becoming director of research at Scott and Bowne from 1932 to 1933. Her work there was concerned with cod liver oil therapy for pretubercular children, stabilization of vitamins in cod liver oil, and X ray vitamin estimation in rachitic bones of white rats. Mrs. Power joined Bell Telephone Laboratories in 1951 and is a member of the Technical Staff.

She is a member of the American Chemical Society, Sigma Xi, and Iota Sigma Pi.

❖

Zvi Prihar (SM'51) was born in Austria in 1903. He received the degree of Ing.ITN in engineering from the University of Caen, France, in 1928, and the degree of Doctor of Engineering Science from Columbia University in 1954.

Zvi Prihar

From 1928 to 1931, he was with Bell Telephone Manufacturing Co., Antwerp, Belgium, as transmission engineer, engaged in long-distance transmission projects, and working in the Transmission Laboratory. He worked for Palestine Electric Corp. from 1931 to 1933 on telecommunication problems and as assistant to the Chief Engineer. From 1934 to 1948, he was with Iraq Petroleum Co. as communication engineer and later as transmission engineer on planning and operation of telecommunication systems. He also acted as advisor on telecommunication planning and operation to several Middle East countries and to the British military authorities during World War II, holding a commission in the Reserve of Officers of the British Army. From 1948 to 1951, he was responsible for the organization of postal, telecommunication, and radio services in Israel. Since January, 1953, he has been full-time consulting engineer with RCA International Division, New York.

Dr. Prihar is a member of the Institution of Electrical Engineers, London.

❖

Harrison E. Rowe (S'49–A'53) was born in Chicago, Ill. on January 29, 1927. He received the B.S. degree in 1948, the M.S. degree in 1950, and the Doctor of Science degree in 1952, all from the Massachusetts Institute of Technology. From 1948 to 1952, he also served as a research assistant in the storage tube and microwave tube laboratories at M.I.T.

H. E. Rowe

Mr. Rowe joined the technical staff of Bell Telephone Laboratories in 1952. He is a member of the Radio Research Department at Holmdel, N. J., where he is associated with a group engaged in systems research. Since joining the Laboratories, he has specialized in systems problems connected with regenerative repeaters.

He is a member of Sigma Xi, Tau Beta Pi, and Eta Kappa Nu.

❖

Kendall L. Su was born in Nanping, Fukien, China, on July 10, 1926. He received his B.S. degree in electrical and mechanical engineering from the National University of Amoy, Amoy, China, in 1947, and the M.S. and Ph.D. degrees in electrical engineering from the Georgia Institute of Technology in 1949 and 1954 respectively.

K. L. Su

From 1947 to 1948 he was a junior engineer with the Taiwan Power Co. in Formosa. From 1949 to 1950 he was a research fellow with the Engineering Experiment Station of the University of Washington. Dr. Su is at present a member of the faculty of the School of Electrical Engineering at the Georgia Institute of Technology.

He is a member of Eta Kappa Nu and Sigma Xi.

IRE News and Radio Notes

Calendar of Coming Events

National Telemetering Conference, Biltmore Hotel, Los Angeles, Calif., Aug. 20–21

IRA-West Coast Electronic Manufacturers' Association, WESCON, Pan Pacific Auditorium and Ambassador Hotel, Los Angeles, Calif., Aug. 21–24

Annual Summer Seminar, Emporium Section, Emporium, Pa., Aug. 24–26

Symposium on Information Theory, Cambridge, Mass., Sept. 10–12

Second RETMA Conference on Reliable Electrical Connections, U. of Pa., Philadelphia, Pa., Sept. 11–12

PGBTS Sixth Annual Fall Symposium, Pittsburgh, Pa., Sept. 14–15

Conference on Communications, Roosevelt Hotel, Cedar Rapids, Iowa, Sept. 14–15

Transistor Reliability Symposium, New York City, Sept. 17–18

Instrument-Automation Conference & Exhibit, Coliseum, New York City, Sept. 17–21

Symposium on Radio-Wave Propagation, Paris, France, Sept. 17–22

Industrial Electronics Symposium, Manger Hotel, Cleveland, Ohio, Sept. 24–25

National Electronics Conference, Chicago, Ill., Oct. 1–3

Canadian IRE Convention & Exposition, Automotive Bldg., Exhibition Park, Toronto, Can., Oct. 1–3

Second Annual Symposium on Aeronautical Communications, Hotel Utica, Utica, N. Y., Oct. 8–9

IRE-RETMA Radio Fall Meeting, Hotel Syracuse, Syracuse, N. Y., Oct. 15–17

Conference on Magnetism & Magnetic Materials, Hotel Statler, Boston, Mass., Oct. 16–18

PGED Annual Technical Meeting, Shoreham Hotel, Washington, D. C., Oct. 25–26

East Coast Conference on Aeronautical & Navigational Electronics, Fifth Regiment Armory, Baltimore, Md., Oct. 29–30

Convention on Ferrites, Institute of Electrical Engineers, London, England, Oct. 29–Nov. 2

Conference on Electrical Techniques in Medicine and Biology, Governor Clinton Hotel, N. Y., Nov. 7–9

Kansas City IRE Technical Conference, Town House Hotel, Kansas City, Kan., Nov. 8–9

Symposium on Applications of Optical Principles to Microwaves, Washington, D. C., Nov. 14–16

PGVC National Meeting, Fort Shelby Hotel, Detroit, Mich., Nov. 29–30

1957 Officers Are Nominated

At its May 11, 1956 meeting, the IRE Board of Directors received the recommendations of the Nominations Committee and the reports of the Regional Committees for officers and directors for 1957. They are:

President, 1957—J. T. Henderson

Vice-President, 1957—Y. Niwa

Director-at-Large, 1957–1959 (two to be elected)—J. H. DeWitt, Jr., G. L. Haller, D. E. Noble, Samuel Seely, A. W. Straiton

Regional Directors, 1957–1958 (one to be elected in each Region)

Region 2—R. D. Chipp, F. A. Polkinghorn

Region 4—W. P. Caywood, H. R. Hegbar, George Rappaport

Region 6—Kenneth Newton

Region 8—A. B. Oxley, B. R. Tupper

According to Article VI, Section 1 of the IRE Constitution, nominations by petition for any of the above offices may be made by letter to the Board of Directors, giving name of proposed candidate and office for which it is desired he be nominated. For acceptance a letter of petition must reach the executive office before noon on August 14, 1956, and shall be signed by at least one hundred voting members qualified to vote for the office of the candidate nominated.

IRE Extends Greetings to Zenneck on His 85th Birthday

Jonathan A. W. Zenneck, a professor, now retired, of the Experimental Physics Laboratory, Institute of Technology, Munich, Germany, recently was sent a telegram by Haraden Pratt, IRE Secretary. The telegram read: "On behalf of the Board of Directors of the IRE may I extend congratulations and best wishes on the occasion of your eighty-fifth birthday."

An IRE Fellow, Dr. Zenneck was awarded the Medal of Honor in 1928, "for his contributions to original research on radio circuit performance and for his scientific and educational contributions to the literature of the pioneer radio art," and subsequently, numerous German awards. He served on the Standardization Committee in 1915–1917 and 1927. In 1933 he was an IRE Director and Vice-President.

Rosenberg Wins Abrams Award for Paper on Photogrammetry

The American Society of Photogrammetry has given the Talbert Abrams Award to Paul Rosenberg, president of Paul Rosenberg Associates, consulting physicists, Mt. Vernon, New York.

Paul Rosenberg

The award was made in recognition of Dr. Rosenberg's research paper on "Information Theory and Electronic Photogrammetry" appearing in *Photogrammetric Engineering*, in which he reported new applications of electronics to the automation of photogrammetry (the science of mapping the earth's surface by aerial photography).

For the past eleven years, Dr. Rosenberg has directed his firm's activities of consultation, research, and development in the industrial and military applications of physics and related sciences. Prior to World War II, he lectured in physics at Columbia University. During the war he served as staff member of the Radiation Laboratory of NRDC at the Massachusetts Institute of Technology, where he did research and development in radar, ultrasonics, and synthetic trainers.

Dr. Rosenberg is past president of the Institute of Navigation. He was general chairman of the 1950 Joint Electronics Conference of the Radio Technical Commission for Aeronautics, the Radio Technical Commission for Marine Service, and the ION.

He is a fellow of the American Association for Advancement of Science, and a member of the American Physical Society, the Institute of Aeronautical Sciences, the New York Academy of Sciences, Sigma Xi, the American Chemical Society, the Acoustical Society of America, and the Armed Forces Communications and Electronics Association. He is a Senior Member of the IRE.

The Newest Foreign IRE Section: Tokyo, Japan

The Tokyo Section held a meeting and dinner recently as part of the Japanese Electrical Communication Joint Annual Meeting. Shown are (*left to right*): Fumio Minozuma, Yasujuro Niwa, Hidetsugu Yagi and Issac Koga.

New York's Coliseum Will Hold Instrument-Automation Conference Sept. 17–21

The Instrument Society of America will sponsor the eleventh annual Instrument-Automation Conference and Exhibit at the Coliseum in New York City, Sept. 17–21. Hotel headquarters for the conference will be at the Statler and New Yorker Hotels.

Technical sessions will offer information concerning design, manufacture, application and operation of instruments and automatic controls. Typical types of instruments and systems will be presented for every application ranging from atomic reactors to sanitation and soap processing.

The opening session of the conference will feature a series of papers concerning instrumentation of the earth satellite and the International Geophysical Year. The three sessions on this subject will be sponsored by ISA, the American Rocket Society and the U. S. National Committee on the IGY.

One-and-a-half days will be allotted to the data handling workshop, and clinics on instrument maintenance and analytical instruments are also scheduled. A symposium on industrial computers will be held Thursday, Sept. 20.

Running concurrently with the other conference activities will be the exhibits of more than five hundred equipment manufacturers. Engineering schools will also display projects for applying measurement and control instruments to scientific and technological research.

Shown (*left to right*) are: O. C. Haycock, Conference Chairman, A. V. Loughren, C. F. Wolcott, Director of Region Seven, and J. M. Pettit, former Director of Region Seven and one of the speakers at the session on transistor circuitry. IRE President A. V. Loughren attended the conference and gave the opening address, in which he discussed the growth and future of the IRE. Over four hundred persons attended the regional conference.

Region Seven Conference Inaugurates Student Award

The Seventh Region Technical Conference for 1956 was held in Salt Lake City, Utah, April 11–13. The technical program included sessions on electronic systems and devices, circuit theory, nuclear science and instrumentation, transistors and transistor circuitry, antennas and propagation, and broadcast transmission systems. In addition, a trade show was held on the roof garden of the Hotel Utah.

Highlight of the conference was the talk by Simon Ramo on the subject *The Guided Missile—Its Impact on Radio Engineering*. Dr. Ramo brought a note of optimism into the arms race by recognizing the peacetime and peaceful applications of electronic developments associated with national defense. Dr. Ramo stressed that in the next few years the scientific advance of greatest significance would be the development of a three-dimensional society, with ramifications in all technical fields.

On the night of April 11 the student paper competition for the Seventh Region was held in conjunction with the conference. Seven schools were represented this year in the final competition. K. D. Baker, of the University of Utah, won first place with a paper entitled *Efficiency of Aerobee Rocket Antennas*, and Warren Shelton, University of Nevada, took second place with a paper entitled *An Electronic RMS Voltmeter*. This inaugurates a student prize paper award to be made every year. The winning student wins a cash prize for himself and a plaque for his school. A bar with his name engraved on it will be placed on the plaque and remain with the school. Future winners from the school will also have an engraved bar added. Each school will win only one plaque and it will remain with the school and become a permanent record of that school's competition record.

Among the ladies' activities was a very pleasant afternoon spent at Brighton Resort high in the Wasatch Mountains.

Technical inspection trips were made to the Kennecott Copper Corporation's Bingham open pit mine and electrolytic refinery, a transmitting tube plant, and the United States Steel Company's Geneva plant's open hearth and rolling mill.

Conference chairmen were: O. C. Haycock, *General Conference Chairman;* A. L. Gunderson, *Section Chairman;* V. E. Clayton, *Vice-Chairman;* S. B. Hammond, *Secretary-Treasurer;* Larry Cole, *Technical Program;* A. L. Gunderson, *Exhibits;* J. S. Hooper, *Publicity and Publications;* E. F. Pound, *Facilities;* Clay Westlund, *Registration and Hospitality;* F. Y. Gates, *Entertainment;* R. O. Evans, *Technical Inspection Trips;* Mrs. A. L. Gunderson, *Women's Activities;* Kay Baker and Moylen Heslop, *Student Activities*.

A. C. Beer, A. E. Middleton, H. Q. North and G. K. Teal were session chairmen at the recent Fourth Annual Semiconductor Symposium of the Electrochemical Society. J. W. Faust, Jr. headed the program, and other speakers were H. Y. Fan, F. J. Biondi and E. M. Clarke.

A. C. Beer, Semiconducting Alloys and Compounds

A. E. Middleton, Surface Controlled Phenomena

H. Q. North, Process Technology

J. W. Faust, Jr., Program Chairman

G. K. Teal, Elemental Semiconductors

ACTIVITIES OF IRE SECTIONS AND PROFESSIONAL GROUPS

Cedar Rapids Section officers for 1956 are (*left to right*): Stuart Morrison, Treasurer; Arthur Wulfsberg, Chairman; Warren Bruene, Secretary; and Emil Martin, Vice-Chairman. The picture was taken at the Section's annual dinner dance.

At the Fellow award meeting and cocktail party of the Long Island Section, Herre Rinia from the Netherlands (*center*) chats with J. N. Dyer, IRE Director of Region Two (*left*), and A. V. Loughren, IRE President. Lothar Rohde of Germany was another guest.

B. B. Young (*right*) glances at an AC network calculator as S. Charp of the Science and Electronics Technical Division of A.I.E.E. points out some interesting features. Mr. Young, Chief of the Power and Control Section of the Franklin Institute, spoke at a joint meeting of the Philadelphia Sections of the IRE and A.I.E.E., and the PG on Electronic Computers.

Several Fellow awards were presented at a recent Los Angeles Section dinner meeting. W. E. Peterson, Section Chairman, presents B. F. Miller (*left*) with an award and congratulates him while others applaud.

C. P. Bean holds a model used to demonstrate domain wall effects at the April Symposium on Microwave Properties and Applications of Ferrites while J. H. Van Vleck (*left*), C. L. Hogan (*second from right*), and M. T. Weiss (*extreme right*) look on. The symposium met at Harvard.

Nonlinear Circuit Symposium Recently Was Held by PIB

The Polytechnic Institute of Brooklyn, in cooperation with the Professional Group on Circuit Theory and with the co-sponsorship of the Signal Corps, the Office of Naval Research and the Air Force Office of Scientific Research, held a three-day Symposium on Nonlinear Circuit Analysis April 25–27 in New York City. This, sixth in a series of annual international symposia organized by Polytechnic Microwave Research Institute, was attended by over three hundred persons.

The symposium opened with addresses by H. S. Rogers, President of the Polytechnic Institute of Brooklyn, A. V. Loughren, President of the IRE, and Ernst Weber, Director of the Microwave Research Institute. Brig. General E. F. Cook, Captain B. J. Wade and W. J. Otting represented the co-sponsoring agencies.

Twenty-four papers were delivered by scientists from the United States, Europe and Japan, covering the basic methods and recent advances in the analysis and design of nonlinear networks and emphasizing the use of nonlinear network theory in the study of oscillators, feedback systems, switching and discontinuous systems and nonlinear systems with random inputs. Fundamental mathematical methods of analysis were correlated with applications in such fields as automatic control to illustrate such nonlinear phenomena as subharmonic generation, parametric damping, jump resonance and stabilized oscillation.

The last afternoon of the meeting was devoted to a round-table discussion, in which a panel representing both engineers, interested in different types of nonlinear systems, and applied mathematicians, who have worked extensively with various methods of analysis, attempted to arrive at a practical evaluation of methods in nonlinear circuit theory.

The *Proceedings of the Symposium on Nonlinear Circuit Analysis, Volume VI of the M.R.I. Symposia Series*, will be published in October, 1956 by the Polytechnic Institute of Brooklyn. IRE-PGCT members may purchase this volume at a reduced rate.

Advisory Board Is Formed for Third RQC Symposium

The third National Symposium on Reliability and Quality Control in Electronics, which is sponsored jointly by the IRE Professional Group on Reliability and Quality Control, the American Society for Quality Control and RETMA, will be held at the Hotel Statler, Washington, D. C., January 14–15, 1957.

The Advisory Board for the symposium consists of M. C. Batsel, Radio Corporation of America; Capt. Henry Bernstein, U. S. Navy Electronics Laboratory; J. M. Bridges, Office of Assistant Secretary of Defense; M. B. Carlton, Magnavox Company; L. M. Clement, Crosley Division of AVCO; R. D. Huntoon, National Bureau of Standards; L. A. Hyland, Hughes Aircraft Company; J. E. Keto, Wright Air Development Center; W. H. Martin, Office of Assistant Secretary of Defense; J. W. McRae, Sandia Corporation; and J. K. Sprague, Sprague Electric Co.

FCC Engineer Addressed Tenth Spring TV Conference

The Tenth Anniversary Spring Television Conference, held on April 13th and 14th at the Engineering Society of Cincinnati Building, Cincinnati, Ohio, attracted over 300 persons to the exhibits and technical sessions. The annual conference was sponsored this year by the Cincinnati Section of the Institute of Radio Engineers in cooperation with the IRE Professional Groups on Broadcast and Television Receivers and Broadcast Transmission Systems.

At the conference banquet on Friday evening, an address entitled "Television 1946–1956–1966?" was given by E. W. Allen, Chief Engineer of the Federal Communications Commission. Mr. Allen traced the growth of the television industry since 1946. He described the problems of local outlets vs larger stations and complete national coverage vs the need for competitive outlets in large population centers. These problems and others have been brought about by a growth from six stations and 10,000 receivers in 1946 to 466 stations and 37 million receivers in 1956.

D. W. Martin, Chairman of the Cincinnati Section, opened the technical sessions on Saturday. IRE President A. V. Loughren extended greetings and felicitations.

Nine papers covering the latest engineering achievements in the television field were presented. Included among the speakers were John Wentworth of RCA, and Kurt Schlesinger, Motorola, Inc.

November 2 Deadline for 1957 IRE Convention Papers

Original papers only shall be submitted, not published or presented prior to the 1957 IRE National Convention.

Prospective authors are requested to submit *all* of the following information: (1) 100-word abstract *in triplicate*, title of paper, name and address; (2) 500-word summary *in triplicate*, title of paper, name and address; (3) indicate the technical field in which your paper falls: Aeronautical & Navigational Electronics, Antennas & Propagation, Audio, Automatic Control, Broadcast & Television Receivers, Broadcast Transmission Systems, Circuit Theory, Communications Systems, Component Parts, Electron Devices, Electronic Computers, Engineering Management, Industrial Electronics Information Theory, Instrumentation, Medical Electronics, Microwave Theory & Techniques, Military Electronics, Nuclear Science, Production Techniques, Reliability & Quality Control, Telemetry & Remote Control, Ultrasonics Engineering, Vehicular Communications.

Address all material to: Ben Warriner, Chairman, 1957 Technical Program Committee, The Institute of Radio Engineers, Inc., 1 East 79 Street, New York 21, N. Y.

Joined in one of the many discussions that animated the Nonlinear Circuit Symposium were (*left to right*): T. E. Stern, M.I.T., H. P. Thielman, Battelle Memorial Institute, T. Kikuchi, Tohoku University, Japan, Brig. Gen. E. F. Cook, Commanding Officer of the Signal Corps Engineering Laboratories, Fort Monmouth, N. J., and Ernst Weber, Director of the Microwave Research Institute, Polytechnic Institute of Brooklyn.

Professional Group News

PGBTS Outlines Program for Sixth Fall Symposium at Pittsburgh September 14–15

The Sixth Annual Fall Symposium of the the Professional Group on Broadcast Transmission Systems will be held in Pittsburgh, Pennsylvania on Friday and Saturday, September 14 and 15. The technical sessions will be held in the Mellon Institute Auditorium. The host hotel will be the Webster Hall located in the area of the auditorium. Sessions will feature speakers in the area of television measurements, television studio development, and broadcast facilities and operation.

Included in the area of television measurements will be field strength, and studio-transmitter equipment proof-of-performance measurements. A speaker from the Federal Communications Commission will present a paper on the television monitoring mobile unit developed for the broadcast service by this regulatory agency. Color equipment test measurements featuring a demonstration will be presented by J. R. Popkin-Clurman of Telechrome. Field strength measurement techniques for television will be treated by Robert Crotinger of WHIO-TV and Robert Kirby, electronic scientist with the Central Radio Propagation Laboratory of the National Bureau of Standards, Boulder, Colorado.

The development of modern television studio facilities will be treated by a panel including J. B. Epperson, Chief Engineer, WEWS, Scripps-Howard Radio, Inc., Cleveland, Ohio and Duane Weise, Chief engineer of Chicago's Educational Television Station WTTW. The latter presentation will include a description of new model studios now in operation at the Chicago Museum of Science and Industry.

The session on broadcast facilities and operation will include papers on the remote control of directional antennas, installation of non-rigid transmission lines, an arrangement for aural transmitter standby facilities, automatic gain control in video circuitry and Conelrad.

Material on video tape recording and the newest automatic techniques in the industry practice will also be available.

The symposium banquet will feature G. H. Brown as toastmaster. Registration forms will be mailed to Group members August 1. Registration, including banquet reservation and cocktail party, will be $8.00. Scott Helt is serving as Program Chairman and Oscar Reed, Jr., is serving as Publicity Chairman. Non-members of PGBTS may obtain further information by addressing PGBTS, 1735 De Sales Street, N.W., Washington, D. C.

PG on Electronic Computers Gives Three Papers Awards

The Professional Group on Electronic Computers has awarded three prizes for papers written during 1955. *Surface-Barrier Transistor Switching Circuits* by R. H. Beter, W. E. Bradley, R. B. Brown and Morris Rubinoff was chosen as the most significant contribution to the electronic computer field during 1955. H. Epstein and F. Innes won the award for the most original contribution to the electronic computer field for their paper on electrographic recording technique. A. S. Robinson's paper, *An Electronic Analog Computing Technique for the Solution of Trigonometric Problems,* was adjudged the most clearly written paper on a topic of significance in the computer field.

A token gift of $50 accompanied each award.

Three New Chapters Approved

The IRE Executive Committee, at its meeting of May 9, approved the formation of the following chapters: PG's on Military Electronics, Buffalo-Niagara and Chicago Sections, and PG on Engineering Management, Rome-Utica Section.

OBITUARY

Arthur S. McDonald (M'23-F'41) died recently. He had been Chief Engineer of the Overseas Telecommunication Commission (Australia) in Sydney, Australia.

A. S. McDonald

Born March 6, 1890 at Castle Donnington, Victoria, Australia, he had received his education at the public school of Victoria and the Melbourne Technical School.

In 1912 he became construction engineer in charge of the erection of radio stations in Australia. From 1914 to 1920 he was a radio design engineer responsible for the construction of radio gear used by the Australian Navy Department. For two years afterward he was a radio engineer responsible for the design and construction of radio stations in Australia. He then became chief engineer of the Amalgamated Wireless Australasia Ltd., where he became engaged in the reorganization of radio services in Australasia, including the Australia transoceans scheme. In 1947 the company assumed its present name of the Overseas Telecommunication Commission (Australia).

Mr. McDonald had been an IRE Vice-President and Director in 1949.

Technical Committee Notes

The **Antennas and Waveguides** Committee met at IRE Headquarters on April 11 with Chairman Henry Jasik presiding. The committee discussed the problem of reactivating the West Coast Subcommittee. After discussion it was decided that (a) the West Coast Subcommittee will not be reactivated next year, (b) West Coast members will be kept on the main committee roster and eventually be assigned temporary tasks. The chairman discussed plans for next year. After finishing Method of Measurement of Waveguide Components, the committee will review Definitions of Antennas Terms and Methods of Testing Antennas. The remainder of the meeting was devoted to reviewing the Proposed Standard on Antennas and Waveguides: Method of Measurement of Waveguide Components.

Vice-Chairman Iden Kerney presided at a meeting of the **Audio Techniques** Committee on April 24 at IRE Headquarters. The major portion of the meeting was devoted to the review of the Proposed Standard on Audio Techniques: Definitions of Terms. Portions of this proposed standard are still in preparation in Subcommittee 3.1 on Audio Definitions under the chairmanship of L. D. Runkle.

The **Electron Tubes** Committee met at IRE Headquarters on April 13 with Chairman P. A. Redhead presiding. Mr. Redhead announced that the Gas Tube Definitions and the TR and ATR Tube Definitions were approved at the April 12 meeting of the Standards Committee. The Cathode Ray Tube Definitions and the Non-Transit Time Tube Definitions were considered at the May Standards Committee meeting.

The committee discussed, amended and unanimously approved the following proposed standards: Proposed Standard on Electron Tubes: Definitions of Terms Related to Camera Tubes; Proposed Standards on Electron Tubes: Definitions of Terms Related to Phototubes; Proposed Standards on Electron Tubes: Physical Electronics Definitions.

Chairman K. R. McConnell presided at a meeting of the **Facsimile** Committee on April 13 at the Times Building. The committee discussed at length the IRE Facsimile Test Chart, which is to be distributed by RETMA. The remainder of the meeting was devoted to the discussion of the revision of the 1943 Facsimile Test Standards.

The **Information Theory and Modulation Systems** Committee met at IRE Headquarters on April 17 with Chairman J. G. Kreer presiding. The entire meeting was devoted to the discussion of the proposed information theory definitions.

Chairman Ernst Weber presided at a meeting of the **Standards** Committee on April 12 at IRE Headquarters. After discussion it was unanimously approved on motion by R. Serrell and seconded by J. G. Kreer that the Standards Committee is in favor of the establishment of a Technical Committee on Medical Electronics, and recommends W. E. Tolles as chairman. Subsequently Dr. Tolles will be requested to submit a proposed scope and suggested membership. This motion will be sent to the Executive Committee for approval.

The Proposed Supplement to IRE Standard 54 IRE 17. S1 (Standards on Receivers: Methods of Measurement of Interference Output of Television Receivers in the Range of 300 to 10,000 kc, 1954) was unanimously approved.

The following proposed standards were discussed, amended and unanimously approved as IRE Standards: Proposed Standards on Electron Tubes: Definitions of Terms Related to Gas Tubes; Proposed Standards on Electron Devices: TR and ATR Tube Definitions.

Professional Groups†

Areonautical & Navigational Electronics—James L. Dennis, General Technical Films, 3005 Shroyer, Dayton, Ohio.

Antennas & Propagation—H. G. Booker, School of Physics and Elec. Engrg., Cornell Univ., Ithaca, N. Y.

Audio—D. W. Martin, The Baldwin Piano Company, 1801 Gilbert Ave., Cincinnati 2, Ohio.

Automatic Control—Robert B. Wilcox, Raytheon Manufacturing Co., 148 California St., Newton 58, Mass.

Broadcast & Television Receivers—L. R. Fink, Research Lab., General Electric Company, Schenectady, N. Y.

Broadcast Transmission Systems—O. W. B. Reed, Jr., Jansky & Bailey, 1735 DeSales St., N.W., Washington, D. C.

Circuit Theory—H. J. Carlin, Microwave Res. Inst., Polytechnic Inst. of Brooklyn, 55 Johnson St., Brooklyn 1, N. Y.

† Names listed are Group Chairmen.

Communications Systems—F. M. Ryan, American Telephone and Telegraph Co., 195 Broadway, New York 7, N. Y.

Component Parts—R. M. Soria, American Phenolic Corp., 1830 S. 54 Ave., Chicago 50, Ill.

Electron Devices—R. R. Law, CBS-Hytron, Danvers, Mass.

Electron Computers—J. D. Noe, Div. of Engineering Research, Stanford Research Institute, Stanford, Calif.

Engineering Management—Rear Adm. C. F. Horne, Jr., Convair, Pomona, Calif.

Industrial Electronics—C. E. Smith, Consulting Engineer, 4900 Euclid Ave., Cleveland 3, Ohio.

Information Theory—M. J. Di Toro, Polytech. Research & Dev. Corp., 200 Tillary St., Brooklyn, N. Y.

Instrumentation—F. G. Marble, Boonton Radio Corporation, Intervale Road, Boonton, N. J.

Medical Electronics—V. K. Zworykin, RCA Labs., Princeton, N. J.

Microwave Theory and Techniques—H. F. Englemann, Federal Telecommunication Labs., Nutley, N. J.

Military Electronics—C. L. Engleman, 2480 16 St., N.W., Washington 9, D. C.

Nuclear Science—W. E. Shoupp, Westinghouse Atomic Power Div., Box 1468, Pittsburgh, Pa.

Production Techniques—R. R. Batcher, 240-02—42nd Ave., Douglaston, L. I., N. Y.

Reliability and Quality Control—Victor Wouk, Beta Electric Corp., 333 E. 103rd St., New York 29, N. Y.

Telemetry and Remote Control—C. H. Hoeppner, Stavid Engineering, Plainfield, N. J.

Ultrasonics Engineering—J. F. Herrick, Mayo Foundation, Univ. of Minnesota, Rochester, Minn.

Vehicular Communication—Newton Monk, Bell Labs., 463 West St., N. Y., N. Y.

Sections*

Akron (4)—H. L. Flowers, 2029—19 St., Cuyahoga Falls, Ohio; H. F. Lanier, 49 West Lowell Ave., Akron, Ohio.

Alberta (8)—J. W. Porteous, Alberta Univ., Edmonton, Alta., Canada; J. G. Leitch, 13024—123A Ave., Edmonton, Alta., Canada.

Albuquerque-Los Alamos (7)—T. G. Banks, Jr., 1124 Monroe St., S.E., Albuquerque, N. Mex.; G. A. Fowler, 3333—49 Loop, Sandia Base, Albuquerque, N. Mex.

Atlanta (3)—M. D. Prince, 3821 Stoland Dr., Chamblee, Ga.; P. C. Toole, 605 Morningside Dr., Marietta, Ga.

Baltimore (3)—C. F. Miller, Johns Hopkins University, 307 Ames Hall, Baltimore 18, Md.; H. R. Hyder, 3rd, Route 2, Owings Mills, Md.

Bay of Quinte (8)—J. C. R. Punchard, Elec. Div., Northern Elec. Co. Ltd., Sydney St., Belleville, Ont., Canada; M. J. Waller, R.R. 1, Foxboro, Ont., Canada.

Beaumont-Port Arthur (6)—W. W. Eckles, Jr., Sun Oil Company, Prod. Laboratory, 1096 Calder Ave., Beaumont, Tex.; E. D. Coburn, Box 1527, Beaumont, Tex.

Binghamton (4)—O. T. Ling, 100 Henry Street, Binghamton, N. Y.; Arthur Hamburgen, 926 Glendale Dr., Endicott, N. Y.

Boston (1)—T. P. Cheatham, Jr., Hosmer St., Marlborough, Mass.; R. A. Waters, 4 Gordon St., Waltham, Mass.

Buenos Aires—J. M. Rubio, Ayachucho 1147, Buenos Aires, Argentina; J. L. Blon, Transradio Internacional, San Martin 379, Buenos Aires, Argentina.

Buffalo-Niagara (1)—D. P. Welch, 859 Highland Ave., Buffalo 23, N. Y.; W. S. Holmes, 1961 Ellicot Rd., West Falls, N.Y.

Cedar Rapids (5)—A. H. Wulfsberg, 3235—14 Ave., S.E., Cedar Rapids, Iowa; W. B. Bruene, 2769 Franklin Ave., N.E., Cedar Rapids, Iowa.

Central Florida (3)—K. A. West, 1345 Indian River Dr., Eau Gallie, Fla.; J. M. Kaeser, 1453 Thomas Barbour Dr., Loveridge Heights, Eau Gallie, Fla.

* Numerals in parentheses following Section Designate Region number. First name designates Chairman, second name, Secretary.

Chicago (5)—J. S. Brown, 9829 S. Hoyne Ave., Chicago 43, Ill.; D. G. Haines, 17 West 121 Oak Lane, Bensenville, Ill.

China Lake (7)—B. B. Jackson, 54-B Rowe St., China Lake, Calif.; H. W. Rosenberg, 217-B Fowler St., N.O.T.S., China Lake, Calif.

Cincinnati (4)—D. W. Martin, The Baldwin Company, 1801 Gilbert, Cincinnati 2, Ohio; F. L. Wedig, Jr., 3819 Davenant Ave., Cincinnati 13, Ohio.

Cleveland (4)—R. H. DeLany, 5000 Euclid Ave., Cleveland 3, Ohio; J. F. Keithley, 22775 Douglas Rd., Shaker Heights 22, Ohio.

Columbus (4)—W. E. Rife, 6762 Rings Rd., Amlin, Ohio; R. L. Cosgriff, 2200 Homestead Dr., Columbus, Ohio.

Connecticut Valley (1)—P. F. Ordung, Dunham Laboratory, Yale University, New Haven, Conn.; H. M. Lucal, Box U-37, University of Connecticut, Storrs, Conn.

Dallas (6)—M. W. Bullock, 6805 Northwood Rd., Dallas 25, Texas; C. F. Seay, Jr., Collins Radio Company, 1930 Hi-Line Dr., Dallas, Texas

Dayton (4)—M. A. McLennan, 304 Schenck Ave., Dayton 9, Ohio; N. A. Nelson, 408 Lewiston Road, Dayton 9, Ohio

Denver (6)—J. W. Herbstreit, 2000 E. Ninth Ave., Boulder, Colo; R. S. Kirby, 455 Hawthorne Ave., Boulder, Colo.

Des-Moines-Ames (5)—A. D. Parrott, 1515—45 St., Des Moines 11, Iowa; W. L. Hughes, E. E. Department, Iowa State College, Ames, Iowa.

Detroit (4)—M. B. Scherba, 5635 Forman Dr., Birmingham, Mich.; R. H. Reust, 20078 Westbrook, Detroit 19, Mich.

Egypt—H. M. Mahmoud, Faculty of Engineering, Fouad I University, Giza, Cairo, Egypt; E. I. El Kashlan, Main E.S.B. Stations, 4, Sherifein, Cairo, Egypt.

Elmira-Corning (1)—R. A. White, 920 Grand Central Ave., Horseheads, N. Y.; R. G. Larson, 220 Lynhurst Ave., Windsor Gardens, Horseheads, N. Y.

El Paso (6)—J. C. Nook, 1126 Cimarron St., El Paso, Texas; J. H. Maury, 3519 For, Blvd., El Paso, Texas.

Emporium (4)—D. A. Dander, 22 S. Cherry St., Emporium, Pa.; R. J. Bisso, 99 Meadow Rd., Emporium, Pa.

Evansville-Owensboro (5)—E. C. Gregory, 1120 S.E. First St., Evansville, Ind.; A. K. Miegl, 904 Kelsey Ave., Evansville, Ind.

Fort Worth (6)—G. C. Sumner, 3900 Spurgeon, Fort Worth, Texas; C. W. Macune, 3132 Forest Park Blvd., Fort Worth, Texas.

Fort Wayne (5)—C. L. Hardwick, 2905 Chestnut St., Fort Wayne 4, Ind.; Paul Rudnick, Farnsworth Electronics Company, Fort Wayne 1, Ind.

Hamilton (8)—G. F. Beaumont, 6 Tallman Ave., Burlington, Ont., Canada; C. N. Chapman, 40 Dundas St., Waterdown, Ont., Canada.

Hawaii (7)—H. E. Turner, 44-271 Mikiola Dr., Kaneohe, Hawaii; G. H. Hunter, Box 265, Lanikai, Oahu, T. H.

Houston (6)—L. W. Erath, 2831 Post Oak Rd., Houston, Texas; R. W. Olson, Box 6027, Houston 6, Texas.

Huntsville (3)—A. L. Bratcher, 308 E. Holmes St., Huntsville, Ala.; W. O. Frost, Box 694, Huntsville, Ala.

Indianapolis (5)—A. J. Schultz, 908 E. Michigan St., Indianapolis, Ind.; H. L. Wisner, 5418 Rosslyn Ave., Indianapolis 20, Ind.

Israel—Franz Ollendorf, Box 910, Hebrew Inst. of Technology, Haifa, Israel; A. A. Wulkan, P.O. B. 1, Kiryat Motzkin, Haifa, Israel.

Ithaca (1)—Benjamin Nichols, School of Electrical Engineering, Cornell University, Ithaca, N. Y.; H. L. Heydt, General Electric Advanced Electronics Center, Cornell University Airport, Ithaca, N. Y.

Kansas City (6)—Richard W. Fetter, 8111 W. 87 St., Overland Park, Kan.; Mrs. G. L. Curtis, Radio Industries, Inc., 1307 Central Ave., Kansas City 2, Kan.

(Sections cont'd)

Little Rock (6)—J. E. Wylie, 2701 N. Pierce, Little Rock, Ark.; D. L. Winn, Tenth and Springs Sts., Little Rock, Ark.

London (8)—C. F. MacDonald, 328 St James St., London, Ont., Canada; J. D. B. Moore, 27 McClary Ave., London, Ont., Canada.

Long Island (2)—Paul G. Hansel, Addison Lane, Greenvale, L. I., N. Y.; W. P. Frantz, Sperry Gyroscope Co., Great Neck, L. I., N. Y.

Los Angeles (7)—Walter E. Peterson, 4016 Via Cardelina, Palos Verdes Estates, Calif.; John K. Gossland, 318 E. Calaveras St., Altadena, Calif.

Louisville (5)- O. W. Towner, WHAS Inc., 525 W. Broadway, Louisville 2, Ky.; L. A. Miller, 314 Republic Bldg., Louisville, Ky.

Lubbock (6)—H. A. Spuhler, Electrical Engineering Department, Texas Technological College, Lubbock, Texas; J. W. Dean, 1903—49 St., Lubbock, Texas.

Miami (3)—C. S. Clemans, Station WSWN, Belle Glade, Fla.; H. F. Bernard, 1641 S.W. 82 Place, Miami, Fla.

Milwaukee (5)—Alex Paalu, 1334 N. 29 St., Milwaukee 8, Wis.; J. E. Jacobs, 6230 S. 116 St., Hales Corner, Wis.

Montreal (8)—Sydney Bonneville, Room 1427, 1050 Beaver Hall Hill, Montreal, Que., Canada; R. E. Penton, 2090 Claremont Ave., N.D.G., Montreal, Que., Canada.

Newfoundland (8)—E. D. Witherstone, 6 Cornell Heights, St. John's, Newfoundland, Canada; R. H. Bunt, Box H-182, St. John's, Newfoundland, Canada.

New Orleans (6)—J. A. Cronvich, Dept. of Electrical Engineering, Tulane University, New Orleans 18, La.; N. R. Landry, 620 Carol Dr., New Orleans 21, La.

New York (2)—A. C. Beck, Box 107, Red Bank, N. J.; J. S. Smith, 506 East 24 St., Brooklyn 10, N. Y.

North-Carolina-Virginia (3)—J. C. Mace, 1616 Jefferson Park Ave., Charlottesville, Va.; A. L. Comstock, 1404 Hampton Drive, Newport News, Va.

Northern New Jersey (2)—P. S. Christaldi, Box 111, Clifton, N. J.; W. C. Moore, 130 Laurel Hill Rd., Mount. Lakes, N. J.

Northwest Florida (3)—B. H. Overton, Box 115, Shalimar, Fla.; G. C. Fleming, 579 E. Gardner Dr., Ft. Walton Beach, Fla.

Oklahoma City (6)—A. P. Challenner, University of Oklahoma, Norman, Oklahoma; Frank Herrmann, 1913 N.W. 21 St., Oklahoma City, Okla.

Omaha-Lincoln (5)—M. L. McGowan, 5544 Mason St., Omaha 6, Neb.; C. W. Rook, Dept. of Electrical Engineering, University of Nebraska, Lincoln 8, Neb.

Ottawa (8)—George Glinski, 36 Granville Ave., Ottawa, Ont., Canada; C. F. Pattenson, 3 Braemar, Ottawa 2, Ont., Canada.

Philadelphia (3)—C. R. Kraus, Bell Telephone Co. of Pa., 1835 Arch St., 16 Floor, Philadelphia 3, Pa.; Nels Johnson, Philco Corp., 4700 Wissahickon Ave., Philadelphia 44, Pa.

Phoenix (7)—W. R. Saxon, 641 E. Missouri, Phoenix, Ariz.; G. L. McClanathan, 509 East San Juan Cove, Phoenix, Ariz.

Pittsburgh (4)—J. N. Grace, 112 Heather Dr., Pittsburgh 34, Pa.; J. B. Woodford, Jr., Box 369, Carnegie Tech. P.O., Pittsburgh 13, Pa.

Portland (7)—J. M. Roberts, 4325 N.E. 77, Portland 13, Ore.; D. C. Strain, 7325 S.W. 35 Ave., Portland 19, Ore.

Princeton (2)—G. C. Sziklai, Box 3, Princeton, N. J.; L. L. Burns, Jr., R.C.A. Labs., Princeton, N. J.

Rochester (1)—G. H. Haupt, 48 Van Voorhis Ave., Rochester 17, N. Y.; B. L. McArdle, Box 54, Brighton Sta., Rochester 10, N. Y.

Rome-Utica (1)—H. F. Mayer, 60 Fountain St., Clinton, N. Y.; R. S. Grisetti, 67 Root St., New Hartford, N. Y.

Sacramento (7)—R. C. Bennett, 3401 Chenu Ave., Sacramento 21, Calif.; R. A. Poucher, Jr., 3021 Mountain View Ave., Sacramento 21, Calif.

St. Louis (6)—F. A. Fillmore, 5758 Itaska St., St. Louis 9, Mo.; Christopher Efthim, 1016 Louisville Ave., St. Louis 10, Mo.

Salt Lake City (7)—A. L. Gunderson, 3906 Parkview Dr., Salt Lake City, Utah; S. B. Hammond, Engineering Hall, Univ. of Utah, Salt Lake City 1, Utah.

San Antonio (6)—Paul Tarrodaychik, 215 Christine Dr., San Antonio 10, Texas; J. B. Porter, 647 McIlvaine St., San Antonio 1, Texas.

San Diego (7)—R. A. Kirkman, 3681 El Canto Dr., Spring Valley, Calif.; A. H Drayner, 4520—62 St., San Diego, Calif.

San Francisco (7)—B. M. Oliver, 275 Page Mill Rd., Palo Alto, Calif.; Wilson Pritchett, Div. of Electrical Engineering, University of California, Berkeley 4, Calif.

Schenectady (1)—C. C. Allen, 2064 Baker Ave., Schenectady 9, N. Y.; A. E. Rankin, 833 Whitney Dr., Schenectady, N. Y.

Seattle (7)—W. C. Galloway, 5215 Pritchard St., Seattle 6, Wash.; J. M. Scovill, 7347—58 Ave., N.E., Seattle 15, Wash.

Syracuse (1)—G. M. Glasford, Electrical Engineering Dept., Syracuse University, Syracuse 10, N. Y. (Secretary).

Tokyo—Hidetsugu Yagi, Musashi Kogyo Daigaku, 2334 Tamagawa Todoroki 1, Setagayaku, Tokyo, Japan; Fumio Minozuma, 16 Ohara-Machi, Meguro-Ku, Tokyo, Japan.

Toledo (4)—L. R. Klopfenstein, Portage, Ohio; D. F. Cameron, 1619 Milburn Ave., Toledo 6, Ohio.

Toronto (8)—A. P. H. Barclay, 2 Pine Ridge Dr., Toronto 13, Ont., Canada; H. W. Jackson, 352 Laird Dr., Toronto 17, Ont., Canada.

Tulsa (6)—Glen Peterson, 502 S. 83 East Ave., Tulsa, Okla.; D. G. Egan, Research Laboratory, Carter Oil Company, Box 801, Tulsa 2, Okla.

Twin Cities (5)—N. B. Coil, 1664 Thomas Ave., St. Paul 4, Minn.; A. W. Sear, 5801 York Ave. S., Minneapolis 10, Minn.

Vancouver (8)—J. E. Breeze, 5591 Toronto Rd., Vancouver 8, B. C., Canada; R. A. Marsh, 3873 W. 23 Ave., Vancouver, B. C., Canada.

Washington (3)—H. I. Metz, U. S. Government Dept. of Commerce, CAA, Room 2076, T-4 Bldg., Washington 25, D. C.; R. M. Page, 5400 Branch Ave., Washington 23, D. C.

Williamsport (4)—G. B. Amey, 968 N. Market St., Williamsport, Pa.; W. H. Bresee, 818 Park Ave., Williamsport, Pa.

Winnipeg (8)—R. M. Simister, 179 Renfrew St., Winnipeg, Man., Canada; G. R. Wallace, 400 Smithfield Ave., Winnipeg, Man., Canada.

Subsections

Berkshire (1)—Gilbert Devey, Sprague Electric Company, Marshall St., Bldg. 1, North Adams, Mass.; R. P. Sheehan, Ballou Lane, Williamstown, Mass.

Buenaventura (7)—W. O. Bradford, 301 East Elm St., Oxnard, Calif.; M. H. Fields, 430 Roderick St., Oxnard, Calif.

Centre County (4)—W. L. Baker, 1184 Omeida, St., State College, Pa.; W. J. Leiss, 1173 S. Atherton St., State College, Pa.

Charleston (3)—W. L. Schachte, 152 Grove St., Charleston 22, S. C.; Arthur Jonas, 21 Madden Dr., Dorchester Terr., Charleston Heights, S. C.

East Bay (7)—J. M. Rosenberg, 1134 Norwood Ave., Oakland 10, Calif.; C. W. Park, 6035 Chabolyn Terrace, Oakland, Calif.

Erie (1)—R. S. Page, 1224 Idaho Ave., Erie 10, Pa.; R. H. Tuznik, 905 E. 25 St., Erie, Pa.

Fort Huachuca (7)—B. V. Blom, Box 682, Benson, Ariz.; J. H. Homsy, Box 123, San Jose Branch, Bisbee, Ariz.

Lancaster (3)—R. B. Janes, Radio Corporation of America, Tube Dept., Lancaster, Pa.; H. F. Kazanowski, 108 Mackin Ave., Lancaster, Pa.

Mid-Hudson (2)—R. E. Merwin, 13 S. Randolph Ave., Poughkeepsie, N. Y.; P. A. Bunyar, 10 Morris St., Saugerties, N. Y.

Monmouth (2)—G. F. Senn, Orchard Rd.-River Plaza, Red Bank, N. J.; C. A. Borgeson, 82 Garden Rd., Little Silver, N. J.

Orange Belt (7)—F. D. Craig, 215 San Rafael, Pomona, Calif.; C. R. Lundquist, 6686 De Anza Ave., Riverside, Calif.

Palo Alto (7)—W. W. Harman, Electronics Research Laboratory, Stanford University, Stanford, Calif.; W. G. Abraham, 611 Hansen Way, c/o Varian Associates, Palo Alto, Calif.

Pasadena (7)—H. A. Curtis, 5193 La Canada Blvd., La Canada, Calif.; Jennings David, 585 Rim Rd., Pasadena 8, Calif.

Piedmont—Officers to be elected.

Quebec (8)—Maurice Boisvert, 1340 De Buisson, Sillery, P. Q., Canada; G. J. E. Fortin, 57 Fraser St., Quebec 6, P. Q., Canada.

Richland (7)—R. G. Clark, 1732 Howell, Richland, Washington; R. E. Connally, 515 Cottonwood Dr., Richland, Wis.

Tucson (7)—R. C. Eddy, 5211 E. 20 St., Tucson, Ariz.; P. E. Russell, Elect. Eng. Dept., Univ. Ariz., Tucson, Ariz.

USAFIT (5)—J. J. Gallagher, Box 3482 USAFIT, Wright-Patterson AFB, Ohio (Secretary).

Westchester County (2)—Joseph Reed, 52 Hillcrest Ave., New Rochelle, N. Y.; D. S. Kellogg, 9 Bradley Farms, Chappaqua, N. Y.

Wichita (6)—M. E. Dunlap, 548 S. Lorraine Ave., Wichita 16, Kan.; English Piper, 1838 S. Parkwood Lane, Wichita, Kan.

Books

Ultrasonic Engineering by A. E. Crawford

Published (1955) by Academic Press Inc., 125 E. 23 St., N. Y. 10, N. Y. 338 pages+6 page index+x pages. 222 figures. $8\frac{3}{4}\times5\frac{1}{2}$. $8.00.

Ultrasonics and some of its spectacular effects have aroused the interest of physicists and engineers, ever since Wood and Loomis' paper on the effects of high intensity ultrasonics appeared in 1927. During the last couple of years, however, the literature on the technology of ultrasound has grown tremendously. This may be best illustrated by the number of references in succeeding editions of Ludwig Bergmann's well known book on the subject, *Der Ultraschall*, (*Ultrasonics and its Application in Science and Technology*, Hirzel, Stuttgart, 1954). The 3rd (1937), 5th (1949), and 6th (1954) German editions present 1069, 2322 and 5162 references respectively. With more and more industrial applications becoming commercially important, the lack of appropriate presentation of the technology of ultrasonics (and for that matter also of sonics) in book form is quite obvious. No wonder, therefore, that during the last five years physicists[1-3] and engineers[4,5] have covered different aspects of the subject in books. Most recently A. E. Crawford has made his contribution to this list. The author states, "The objective of this book is to collect together and correlate the mass of data on applications and effects of ultrasonic waves, and to cover the basic methods of generations."

The book comprises three parts: "Theory" (2 chapters, 46 pages), "Generation" (4 chapters, 108 pages), and "Applications" (7 chapters, 184 pages). The first chapter, "Ultrasonic Waves," deals with wave types, propagation, absorption, visualization, energy and frequency measurement of sound. Unfortunately, the treatment is rather casual and inaccurate, and a reader who is not yet familiar with the subject may only be confused by statements like "Longitudinal waves . . . travel at high velocity, so that their wavelength is short, in most media" (p. 3), or "The alternating pressure is determined by the formula $J=0.5\ c(\omega A^2)=0.5\ Pu$ where J is the intensity per cm^2 in unit time, . . . , A is the maximum amplitude of the vibration particle . . . " (p. 18). The second chapter is on ultrasonically induced cavitation, a very important phenomenon indeed in high intensity ultrasonic processing applications. The outstanding work of the late G. W. Willard is referred to in detail (7 figures).

Under "Generation," piezoelectric transducers, magnetostrictive transducers, jet generators, and electromagnetic transducers are described and illustrated by numerous figures. Although the formulas given in the text will hardly enable anyone to design such generators, they may help the reader to get some general idea about the subject. The same holds true for the third and main part, entitled "Applications." A wealth of descriptive material is presented with chapters on "Precipitation and Agglomeration," "Emulsification and Dispersion" (including ultrasonic cleaning), "Chemical Applications," "Metallurgical Applications," "Casting of Metals," "Biological and Medical Applications," and "Ultrasonic Instruments and Control Gear."

The author discusses all the better known applications, sometimes heavily borrowing from other reviewers' texts without proper reference.

The main objective of a book on ultrasonic engineering should be to help the designer of ultrasonic equipment in his particular field of application. The engineer, therefore, would appreciate a clear presentation of the basic design principles, illustrated by examples of well-designed equipment; such a presentation already has been achieved by Hueter-Bolt's excellent book *Sonics*.

In spite of the foregoing criticism, the reviewer believes that the reader will find much useful information in Mr. Crawford's book, which is very well illustrated with photographs and diagrams of currently used ultrasonic equipment.

O. E. MATTIAT
Clevite Research Center
Cleveland, Ohio

[1] W. P. Mason, "Piezoelectric Crystals and Their Application to Ultrasonics," Van Nostrand, New York, 1950.

[2] P. Vigoureux, "Ultrasonics," Wiley & Sons, New York, 1951.

[3] E. G. Richardson, "Ultrasonic Physics," Elsevier, New York, 1952.

[4] B. Carlin, "Ultrasonics," McGraw-Hill, New York, 1949.

[5] T. F. Hueter and R. H. Bolt, "Sonics, Techniques for the Use of Sound and Ultrasound in Engineering and Science," Wiley & Sons, New York, 1955.

Scattering and Diffraction of Radio Waves by J. R. Mentzer

Published (1955) by Pergamon Press Inc., 122 East 55 Street, N. Y. 22, N. Y. 130 pages+2 index pages+1 page appendix+viii pages. 34 figures. $5\frac{1}{2}\times8\frac{3}{4}$. $4.50.

In this monograph on scattering and diffraction the author purports "to bring up to date those readers who have a good background in electromagnetic theory. . . ." It is to be questioned whether full justice is done to this noteworthy goal. The presentation is of relatively narrow scope, being restricted almost exclusively to the radar cross-section problem, and appears to be more a variation on a classical theme than an up-to-date account of the advances of the last decade or so.

Approximately half the book is devoted to an introduction on integral equation and Green's function techniques in the formulation of vector electromagnetic problems, and on variational and physical optics techniques for their solution. There are subsequent applications to the separable problems of the perfectly conducting cylinders, half-plane, sphere and cone and the nonseparable finite cylinder, circular hole, paraboloid of revolution, etc. A few pages on the measurement of radar cross sections are also appended.

This book will appeal to those interested in acquainting themselves with some of the theoretical and experimental work on scattering problems having radar applications. Its shortcomings of omission, not unexpected for a brief monograph, in a rapidly expanding field, should not detract from the readability and interest of the material it contains.

NATHAN MARCUVITZ
Polytechnic Inst. of Brooklyn
Brooklyn, N. Y.

Spheroidal Wave Functions by J. A. Stratton et al

Published (1956) by The Technology Press of Massachusetts Institute of Technology and John Wiley & Sons, 440 Fourth Ave., N. Y. 16, N. Y. 63 pages+548 pages of tables+xiii pages. $8\frac{3}{8}\times11\frac{3}{8}$. $12.50.

On the jacket of this book we find the statement, "This volume makes it possible for the electrical engineer and physicist to handle wave problems in spheroidal coordinates with approximately the same degree of facility as has been possible previously for rectangular, circular, cylindrical, and spherical coordinates." This is probably the work of an over-enthusiastic representative of the publishers; it reflects no discredit on the authors to point out that this promise is not fulfilled, because it cannot be. Spheroidal coordinates are basically more complicated than the aforementioned ones, and there is no help for it. In order to show the reason for this, and also to describe just what this volume does contain, let us look at a few details.

The scalar wave equation $\nabla^2\psi+k^2\psi=0$ admits a separation of variables in a prolate spheroidal coordinate system (ξ, η, ϕ) related to the cartesian (x, y, z) by $x+iy=a(\xi^2-1)^{1/2}(1-\eta^2)^{1/2}\exp(i\phi)$, $z=a\xi\eta$, where the foci are at $z=\pm a$. In this process two independent separation constants are needed, and in addition the expressions involve the continuously variable parameter $h=ka$. Thus, a wave function takes the form

$$\psi = J_{ml}(h, \xi)S_{ml}(h, \eta)\exp(im\phi)$$

where m and l are integers. Now, it would be very nice to have a "Jahnke-Emde" in which the various forms of the functions J and S are tabulated, with graphs indicating their behavior on the real axis and in the complex plane, their zeroes, maxima and minima, roots of equations that arise in fitting boundary conditions, etc., as we have available for the Bessel and Legendre functions, and which make the solution of the simpler cylindrical and spherical boundary-value problems almost as easy as using a dictionary. However, when one considers the amount of space necessary to tabulate the various Bessel functions, which contain only a single discrete parameter, it is apparent that the size of tables for a function with three parameters, two discrete and one continuous, would be, as the authors say, "quite large."

In the face of this difficulty, they have done the next best thing. Rapidly convergent expansions of the spheroidal functions in terms of spheroidal Bessel functions and Legendre functions are known; two examples are:

$$J_{ml}(h, \xi) = (1-\xi^{-2})^{m/2}\sum_n a_n(h, ml)j_{n+m}(h\xi)$$

$$S_{ml}(h, \eta) = \sum_n d_n(h, ml)P_{n+m}{}^m(\eta).$$

It is the coefficients $a_n(h, m, l)$, $d_n(h, m, l)$, and others for similar expansions that this book tabulates to seven figures. In order to obtain numerical values of the J and S functions, one needs in addition to this book, three volumes of the NBS Mathematical Tables Project; *Tables of Associated Legendre Functions*, Columbia University Press, New York (1945), and *Tables of Spherical Bessel Functions*, Vols. I and II, Columbia University Press, New York (1947). In most cases the expansions converge rapidly enough so that four-figure accuracy is attained with three or four terms; ultimate six to seven-figure accuracy is possible.

In addition to the numerical tables, and a nine-page introduction to them which should be read first, although it is not in the front of the book, the volume contains a reprint of a paper "Elliptic and Spheroidal Wave Functions," by L. J. Chu and J. A. Stratton, which appeared earlier in the *Journal of Mathematics and Physics*, Vol. XX, No. 3 (1941). This paper discusses various analytical properties of the functions and the basis of the above expansions.

In addition to their great value for various problems of applied mathematics, these tables are of interest for the way in which they were prepared. Punched paper tapes, prepared from the output of the MIT Whirlwind I Computer, operated automatic typewriters that produced the final page layout, ready for photo-offset reproduction. Thus there was no human copying or proofreading.

E. T. Jaynes
Microwave Laboratory
Stanford, Calif.

Atlas of Ground-Wave Propagation Curves for Frequencies Between 30 MC and 300 MC by Balth. van der Pol

Published (1955) by Publications Dept., International Telecommunication Union, Palais Wilson, Geneva, Switzerland. xxxv pages+174 diagrams. 8½×12. $8.55.

The seventh Plenary Assembly of the CCIR asked the director of this international body, Balth. van der Pol, to prepare an atlas of curves describing propagation of radio waves from a half wave transmitting dipole in the presence of the earth. The curves were to neglect all ionospheric effects, refer to propagation over a spherical earth, take into account only standard atmospheric refraction, and neglect all incoherent scattering phenomena. This atlas of curves has now been published in a form that is extremely convenient to use. The transmitting and receiving antennas are supposed to be oriented both horizontally, or both vertically. The electrical ground constants are given by a dielectric constant of 80 and a conductivity of 4 mhos per meter for sea water, and by a dielectric constant of 10 and a conductivity of 10^{-2} mhos per meter for land. The curves refer to an effective earth's radius 4/3 times the actual earth's radius, and the other parameters are as follows: (a) frequencies of 30, 60, 100, 150, 200, and 300 megacycles per second; (b) heights of the transmitting antenna above the ground of 20, 50, 100, 200, 500, and 1000 meters; (c) heights of the receiving antenna above the ground 0, 2, 5, 10, 20, 50, 100, 200, 500, 1000 meters. This atlas of propagation curves is the best information at present available concerning propagation over a spherical earth allowing for standard atmospheric refraction. The curves are preceded by a convenient outline of the theoretical formulae upon which the calculations have been based.

H. G. Booker
Cornell University
Ithaca, New York

IRE Abstracts of Transactions

The following issues of "Transactions" have recently been published, and are now available from the Institute of Radio Engineers, Inc., 1 East 79th Street, New York, N. Y. at the following prices. The contents of each issue and, where available, abstracts of technical papers are given below.

Sponsoring Group	Publication	Group Members	IRE Members	Non-Members*
Circuit Theory	Vol. CT-3, No. 1	$2.00	$3.00	$6.00
Communication Systems	Vol. CS-4, No. 2	2.90	4.35	8.70
Electron Devices	Vol. ED-3, No. 2	1.10	1.65	3.30
Information Theory	Vol. IT-2, No. 1	1.60	2.40	4.80
Microwave Theory & Techniques	Vol. MTT-4, No. 2	1.70	2.55	5.10
Reliability & Quality Control	PGRQC-7	1.10	1.65	3.30

*** Public libraries and colleges may purchase copies at IRE Member rates.**

Circuit Theory

Vol. CT-3, No. 1, March, 1956

Abstracts of Papers in This Issue

Preface to the Transistor-Circuits Papers—J. G. Linvill, A. W. Lo, J. C. Logue, and A. P. Stern

Electric-Network Representation of Transistors—A Survey—R. L. Pritchard

In this survey paper the various methods used to describe the electric-circuit properties of a transistor are reviewed. After a brief introduction and discussion of the low-frequency characterization of transistors and of the representation used for point-contact transistors, the remainder of the paper is devoted to the subject of high-frequency representation for junction transistors. The more popular equivalent circuits are described, and relations between parameters of different equivalent circuits are given. The alternative procedure of characterizing a transistor by its quadripole parameters (or matrix elements) as a function of frequency also is described, and advantages of this procedure are indicated. Throughout the paper a distinction is made between *device* parameters, or electrical parameters that can be related to the structure of the transistor as a device, independent of its circuit configuration, and *circuit*, or terminal, parameters, which correspond to relations between terminal voltages and currents. Included are references to approximately ninety papers representing the work of sixty authors.

Application Aspects of the Germanium Diffused Base Transistor—D. E. Thomas and G. C. Dacey

This paper briefly considers some of the improvements in transistor circuit performance made possible by the diffused base germanium transistor developed at the Bell Telephone Laboratories. The paper points out the advantage of the diffusion process for the fabrication of the thin base layers required for very high frequency transistors. The basic steps in the fabrication of a germanium transistor with a base-layer thickness of 1.5×10^{-4} centimeters and an alpha-cutoff frequency of 500 megacycles per second are given. The electrical equivalent circuit of this transistor and the current gain frequency characteristics in both the common emitter and common base connections are presented and discussed. The potential of this type transistor for performing various circuit functions in both the common emitter and common base connections are then briefly discussed. The various application possibilities discussed are based on both the measured electrical characteristics of the transistor and the actual performance characteristics of research and advanced development models of diffused base transistors in exploratory circuits. The greater universality of application of the diffused base transistor as compared to earlier transistors is briefly discussed.

Two-Terminal Analysis of Junction Transistor Multivibrators—J. J. Suran and F. A. Reibert

The basic junction-transistor multivibrator circuit is analyzed from the point of view of a circuit designer who wishes to know: (a) how to predict the performance of a particular configuration, and (b) how to synthesize a multivibrator circuit, which may be either astable, bistable, or monostable, from a given set of specifications.

The analytical method consists of breaking the multivibrator circuit (two basic, well-known configurations are treated) at a suitable point and using the two terminals thus obtained as a driving-point pair to derive a useful V-I characteristic. In part I of the paper, the static driving-point resistance characteristics are derived theoretically and compared to experimental measurements. In part II, transient and high-frequency effects are considered and the two-terminal analysis is extended to derive a prediction of the maximum frequency, or pulse repetition rate, at which the regenerative mode of operation can take place. Part III of the paper treats the problem of circuit synthesis. Using the results of parts I and II, straightforward methods are developed which permit the circuit designer to uniquely determine the seven circuit parameters which must be specified in the design of symmetrical multivibrators. Several design examples of astable, monostable, and bistable configurations are given.

Stable Transistor Oscillator—E. Keonjian

Frequency stability is an essential requirement for most transistor oscillators as for many other oscillators. However, unlike vacuum tube oscillators, transistor oscillators usually suffer a great change in frequency with variation in operating characteristics. The most serious causes of frequency instability are the effect of temperature on parameters of transistors and the variation of supply voltage. By using certain circuit arrangements and a crystal as frequency-controlled element, a high degree of stability could be achieved over a wide range of temperature and supply voltages. As a practical example, a simple crystal controlled 100 kc oscillator is described, capable to deliver 3 volts rms, from supply voltage 12 volts. The frequency stability of the oscillator is better than 10 parts per million per 1 volt supply voltage, and two parts per million per degree centigrade, for a wide range of load resistance, ranging from a few ohms to 100,000 ohms. At a frequency of 1 mc, a stability better than 5 parts per ten million per 1 volt supply voltage and one part per ten million per degree centigrade was obtained.

An N-Stage, Series Transistor Circuit—K. H. Beck

A description is given of some of the characteristics of a circuit wherein a number of transistors are connected so that the sum of their collector to emitter voltages appears across a common load. This circuit permits large output voltage swings to be obtained and provides a means for adding the power outputs of a number of units

The circuit is analyzed as a cascade of common base stages with added base resistors. The contribution of the individual stages to the total output is determined by the manner in which the base resistances are selected. Three cases are treated: equal division of voltage, equal power increase per stage, and equal power output per transistor.

The Emitter-Coupled Differential Amplifier—D. W. Slaughter

The transistor emitter-coupled differential amplifier is analogous to the cathode-coupled differential amplifier and gives promise of excellent utility in transistorized circuitry. Expressions are given for 1) the circuit voltage gain, current gain, and input impedance, 2) the common-mode rejection when the circuit is used as a differencing amplifier, and 3) the signal unbalance when the circuit is employed as a single-ended-to-push-pull amplifier or phase inverter. When the circuit is used as a dc amplifier, drift generated by variations in the temperature-sensitive parameters cancels to a satisfactory degree.

Solution of a Transistor Transient Response Problem—J. R. MacDonald

The transient response of the exact current transfer function, $\alpha(\omega)$, of a grounded-base junction transistor operating in the short-circuited output condition is compared with the transient response derived from the conventional approximate form for $\alpha(\omega)$. The response to both a unit impulse and a unit step is calculated, and it is shown how the results may be readily adapted to yield a rapid oscilloscope method of determining the α cutoff frequency and several of the transistor material and dimensional constants.

Transistor Superregenerative Detection—W. F. Chow

This paper presents the results of an analytical and experimental study of the principles and mechanism of superregenerative detection using junction transistors.

The analysis is based on the study of a transistor oscillator, the criterion of oscillation, and the build-up and decay of oscillation.

Due to the dependence of transistor parameters on the operating points, the loop gain of a transistor oscillator can be controlled by changing the emitter current (I_e) and/or the collector voltage (V_c). This property makes the control of a transistor oscillator by an external quenching signal possible. Either the linear mode or the logarithmic mode of detection can be obtained.

Self-quenched superregenerative detection also can be obtained. The circuit design and the bias of the transistor have to be such that the initial emitter current (I_e) is small, but the loop gain of the oscillator is sufficient to start oscillations. Then the bias point of the transistor should be able to change corresponding to the amplitude of oscillation.

Typical properties of a superregenerative detector, such as high gain and noise, are characteristic of both vacuum tube and transistor circuits.

An Eighty-Volt-Output Transistor Video Amplifier—V. Grinich

A three-transistor video amplifier is described that has sufficient dynamic range and bandwidth to drive a standard television picture tube. Sufficient drive is obtained by means of a common-base stage (having a voltage gain of two) with a dynamic range of output voltage that is twice the collector breakdown voltage of the transistor used. Adequate high-frequency response and linearity are obtained by resistive degenerative feedback.

Two Representations for a Junction Transistor in the Common-Collector Configuration—V. H. Grinich

Two small-signal circuit representations are given for the common-collector configuration. The representations contain no internal generators nor do they contain any negative resistances. Instead, the active nature of the device is accounted for by impedance transformations (that are a function of frequency) on either the input or output network. The factors used in the impedance transformation are determined from two transistor parameters—the current gain and the alpha cutoff frequency. Because the common-collector configuration has a large amount of internal feedback, the representation given here is simpler than other representations that have been proposed.

An Unsymmetrical Square-Wave Power Oscillator—D. A. Paynter

A dc converter which utilizes a single power transistor connected into an unsymmetrical square-wave oscillator circuit is described. High power output coupled with excellent over-all efficiency can be obtained. The power output is comparable with that of the two power transistor converter for the case when the converter supply voltage is small as compared with the power transistor inverse voltage rating.

Transistor DC Amplifiers—J. W. Stanton

The problems that face the designer of transistorized dc amplifiers are discussed. The design of a specific transistorized dc amplifier is described and the extension of this design is given for several other amplifier circuits. Particular emphasis is placed on overcoming the difficulties associated with ambient temperature changes. The results obtained on experimental models show that reliable transistorized dc amplifiers may be built. Sensitivities in the microampere and milli-microampere range have been obtained even when the ambient temperature is varied over a wide range. Experimental models have been built which perform satisfactorily in ambient temperatures of from 0°C to 60°C.

A Transistorized IF Amplifier-Limiter—J. A. A. Raper

A transistorized IF amplifier designed to provide limiting presents several difficulties, in particular, instability due to the presence of tuned circuits at input and output. A circuit is described which utilizes a junction diode for limiting in conjunction with a transistor amplifier. The storage effects of the junction diode are used, the diode presenting very low impedance in both directions. The effect is similar to that obtained by using two diodes connected in opposite polarity across a signal source. The low limiting level may be controlled with a small bias in either the forward or reverse direction.

Micropower Audio Amplifier—E. Keonjian

A reduction of power requirements in transistor circuitry is very desirable, since it would enable the design of subminiature equipments using self-contained batteries and operating continuously for several years without maintenance. In the course of an investigation of silicon transistors in the micropower region, an audio amplifier consisting of two directly coupled common emitter stages was developed. The total power gain of the amplifier is 38 db. The input impedance was chosen 30 *k* ohms and the output impedance is 600 ohms. The frequency response from 20 to 20,000 cps is flat within ±3 db. The dynamic range is of the order of 54 db with an equivalent input noise voltage of approximately 3 μv. The amplifier is compensated against variations of the ambient temperature by means of a thermistor and a characteristic shaping network. The total variation of the gain is 1.2 db in the temperature range from −25°C to +75°C. A miniature 1.35 v cell is used as power supply, the total current drain being less than 70μa, which permits continuous use of this amplifier for over three years.

Logarithmic Attenuators Using Silicon Junction Diodes—T. P. Sylvan

Two types of logarithmic attenuator circuits are described and their relative advantages and disadvantages are compared. The first type of circuit discussed makes use of the inherent logarithmic characteristics of forward-biased silicon junction diodes. Deviation of the characteristics from the ideal logarithmic response are discussed and corrective circuits are given. It is shown that while very good characteristics may be obtained over four decades of input current, the variations between diodes and the variations with temperature present serious problems of compensation for mass-produced circuits. The second type of circuit makes use of the switching property of silicon junction diodes and permits selection of diodes on the basis of their inverse current at elevated temperatures alone. This circuit uses diodes in conjunction with an easily calculated resistor network to provide the logarithmic response by a series of linear approximations. Circuit operation at temperatures up to 100°C and over current ranges of 10^{-7} to 10^{-1} amperes with accuracies of better than ±1 per cent is possible. The problems of using this attenuator in conjunction with transistor dc amplifiers are discussed briefly.

A Note on the Admittance and Impedance Matrices of an *N*-Terminal Network—T. H. Puckett

The indefinite admittance matrix as discussed by Shekel, and the corresponding indefinite impedance matrix, represent the two most natural and widely used methods of specifying a given *n*-terminal network of the "black box" type, where the internal physical composition of the network is unknown. Either of these two matrices completely specify the network, so there must be a relationship between them. This relationship is discussed, and procedures developed for obtaining either matrix from the other.

Reviews of Current Literature—New Methods of Driving-Point and Transfer-Function Synthesis—R. H. Pantell . . . *Reviewed by W. H. Kautz*

Recent Russian Publications on Switching Theory . . . *Reviewed by V. Belevitch*

Correspondence

PGCT News

IRE Transactions on Circuit Theory—Index to Volumes CT-1—1954 and CT-2—1955

Communications Systems

Vol. CS-4, No. 2, May, 1956

A 1 KW Amplifier for the Military UHF Band—D. H. Peckham and W. E. Phillips

Reliability Measurement and Prediction—C. M. Ryerson

Various measures of reliability are summarized with emphasis given to the mean life or mean time to failure of equipment. Methods for making this measurement and its interpretation are described.

Calculation and prediction methods are presented based on equipment life characteristics under service conditions. Application procedures are described, and practical hints for reliable design and procurement are presented. Related aspects of the RCA Program for Reliability Control are described.

The Role of Telecommunication in Air Transport—J. S. Anderson

Air/Ground Communications in Air Traffic Control—F. J. Cervenka

Aviation Communications Facilities for the Next Ten Years—R. G. Brown

The object of this program has been to recommend, for domestic civil aeronautical communications, both point/point and air /ground (excluding tower), a systems and implementations plan which will best satisfy anticipated requirements for the next 10 years.

The program started with a study of current aeronautical communications to identify specific functional, economic and frequency-utilization requirements and problems—both existing and anticipated. The next step was to forecast total air traffic and scheduled carrier-passenger volumes and characteristics, and to determine their probable effects on communication requirements over the next 10 years. In projecting communication trends, we considered probable revisions in traffic control and airline policies and procedures.

Next, we devised specific requirements for control and operational communication networks. Alternate radio networks and directly associated point/point networks were set up and evaluated in terms of these requirements. The systems required to implement these networks provided bases for evaluations of investment, operating costs and frequency requirements of the alternate networks. Network and system recommendations were then formulated.

These conclusions are derived from ranges of probable increases in air-carrier passenger volume and aircraft traffic. In addition, other communication-influencing factors, such as aircraft seating capacities, speeds and altitudes were considered.

Air Traffic Control in the Jet Age—D. R. Kirshner

An effective forward step in terminal area air traffic control has been accomplished by development and installation of Radar Approach Control (RAPCON) Center and control tower prototype facilities described. Esoteric complexes detailed provide airport and approach controllers with radar and communication implementation of manual aids to jet and propeller driven traffic control procedures and techniques. Equipment reported also serves as manual backup and override facilities capable of eventual expansion to fully automatic air traffic control system operation dictated by high-speed jet performance characteristics.

Air-Ground Communications—The ANDB System Development Plan—B. E. Montgomery

The Air Navigation Development Board recently established its System Engineering Advisory Team to aid the Director in formulating and carrying out a unified program of research and development for the common system of air navigation and traffic control. This group began its work in the summer of 1955.

The goal of ANDB is to secure a system design of air navigation and traffic control that permits a free movement of all types of aircraft as desired by their operators. In this program, the communications system is treated as a tool of air traffic control and its characteristics are dependent on basic air traffic control principles and practices.

The program is divided into two broad phases: short term and long term. The short term portion is aimed at achieving a system design based on currently available equipment and techniques. The long term goal is directed toward the design of a system capable of completely automatic operation.

When an advanced system design has been achieved, it is essential that a carefully planned evolutionary transition be available to permit going from the old to the new. As far as can be seen in the future, the ATC system, both in the air and on the ground, will be heterogeneous in nature. That is, old and new equipment must operate compatibly together in the system.

There is a considerable history of communications planning in post-war aeronautical studies. Several authoritative plans for air-ground communications systems are contrasted to show a need for better coordination and consistency in planning.

Consideration of Mechanical and LC Type Filters—G. H. DeWitz

Consideration of Mechanical and LC Type Filters—Part II—Two Criteria for the Comparison of Filters—R. I. Ścibor-Marchocki

A Novel Decoder for Digital Communication—R. K. Walker

An Air Force Single Sideband System—G. E. Brunette and D. E. Le Brun

An Airborne Single Sideband Transceiver—E. W. Pappenfus

A High Power Linear Amplifier for Single Sideband Applications—F. B. Gunter

The design of a high power linear amplifier intended for use as a power amplifier for Single Sideband transmitters is discussed. The availability of new components and a new concept of pi type tank circuits permit avoiding difficulties experienced in previous designs.

This new linear amplifier provides up to 30 KW output in the frequency spectrum from 4.0 to 26.5 mc with low distortion products on two tone tests. This performance is accomplished with a material reduction not only in the complexity of the apparatus but also with a reduction of complete installed size to a length of 8 ft. Air cooled components utilizing high velocity, low volume air circulation enables installation with minimum difficulty at altitudes up to 8000 feet. A discussion of the electrical and mechanical characteristics will be presented with emphasis on the simplified tuning system which allows rapid change of frequency.

The Communications Picture in 1965—J. F. Taylor, Jr.

The communications capacity required of the Common System for the year 1965 is projected from figures of fix postings for 1946 and 1954. In 1946, 8,800,000 fixes were reported; in 1954, 16,900,000 fixes were recorded. If this trend continues, the forecast for 1965 is 1,100,000 instrument approaches, and 32 million fix postings! Additionally, there are new requirements to be considered for the 1965 communications system. These are airport surface detection equipment and expanded helicopter service making short distance flights between cities and from airports to urban heliports, plus the ever increasing tendency for all flights to be controlled similarly to IFR flights.

Studies on improving communications, conducted in the Boston area, have indicated the pattern for future work to be undertaken. One finding was the excessive amount of time spent by the controller communicating rather than controlling. The possibility of using codes for routine communications to eliminate repetition of messages between pilot and controller was suggested by this study.

The Common System Beacon, under development primarily for radar reinforcement and flight identity, with the addition of altitude information would lend itself well to coding, with a subsequent saving in voice communications time.

In the investigation of a communications system for the Common System of Air Navigation and Traffic Control, the goal should be for one of limitless communications capacity. This is the challenge for the communications engineer.

The Reduction of Radio Interference in Aeronautical Communications Systems—A. L. Albin and H. M. Sachs

Radio interference suppression must be considered in early design stages for maximum effectiveness. The chief sources of interference to communication systems are spurious and harmonic radiations, corona and precipitation static, and co-channel and adjacent-channel interference. Other interference sources such as ignition systems, rotating machinery and contacting devices are not included in the scope of this paper. Interference may render some equipments inoperative or produce distortion in others. Most types of interference can be successfully eliminated by the reduction of transmitter spurious radiation, reduction of receiver susceptibility, antenna design to reduce mutual coupling, and judicious frequency assignments.

The Place of the Submarine Cable in Aeronautical Communication—J. J. Gilbert

Difficulty in satisfying increased requirements for aeronautical communication channels appears to justify investigating the potentialities of various means of submarine cable communication as a means of easing the burden on long radio links. Relief might be found by using submarine cables to connect strategic and widely separated land stations and thus materially reduce the length of radio links required. As a first step in this direction, the paper discusses the capabilities of conventional types of cable now in use for telegraph, voice and carrier frequency transmission. Submerged repeaters are now being used for increasing the range of telegraph and telephone cables, and the fundamental principles involved in their design and installation are described.

Information Rates in Remoted Radar Systems—E. A. Mechler

Air traffic information collected by long range radars is available to the CAA at the radar sites. This information will be remoted to the air route traffic control center. A theoretical study is made here of resolving power and the information rate inherent in the air traffic, radar video signals, displays, and various transmission techniques. Air traffic provides the basic information and radar video establishes the maximum information rate for the system. On the other hand, a display can show only a limited amount of this information. But if the display magnifies a small area, it can show all the information the radar collects. Between the radar and the presentation, the information may be transmitted by a wide band communication channel that transmits all the radar video information or it may be compressed by analog, digital or manual methods so that it can be transmitted over a much narrower communication channel. The final choice of system components will be decided by the requirements of the basic problem for resolution, off-centered displays and the needs of the traffic controller.

A Servomechanism Approach to the Problem of Communication for Aircraft Control—S. J. O'Neil

The traffic-handling capability of a communication system used for aircraft control during Airport Traffic Control, Ground-Controlled Approach, and Ground-Controlled Landing is studied. The system is treated as a multi-loop servomechanism which includes both ground and airborne equipment. The factors which affect the location of the communication link in the system are discussed. These include message rate, airborne equipment or ground measurements necessary, flight geometry and flight safety. It is shown that the minimum message rate is possible if the quantity transmitted is the same as the flight motion desired. Several methods are presented for increasing the traffic-handling capability by reducing the message rate. One of these introduces controlled blacklash into the outermost feedback loop and automatically determines the minimum message rate while navigating to a point. A dynamic analysis is used to determine the limitations of the method. The methods presented are illustrated by showing their application to automatic flight control during Ground-Controlled Approach and Ground-Controlled Landing.

Microwave Relay System Between Saint John and Halifax—H. C. Sheffield

A microwave relay system employing time-division multiplex has been constructed to provide toll telephone circuits for the New Brunswick Telephone Company and the Maritime Telegraph and Telephone Company. This system links Saint John in New Brunswick and Halifax in Nova Scotia via five intermediate unattended repeaters and yields 46 four-wire circuits of toll quality that provide out-of-province connections to Montreal, Toronto, Boston, and New York. This system has been in partial use since December, 1952, and the complete system has been in continuous service since December, 1954. A description of the radio relay link is given primarily from the system-planning aspects. Performance figures are outlined.

Disaster Planning in the Field of Communications—H. R. Hampton

In the past the telephone company has been confronted with many emergencies due to fires, floods, hurricanes, etc., which have required prompt action to establish, maintain and restore communications. Throughout the years, a vast amount of experience has been gained and a well-trained organization established. Planning for major disasters in the Washington area, including recent construction activities and new programs, both local and nationwide, is described.

Communication Equipment for Aircraft Rescue Operations (Abstract)—L. M. Glantz and T. C. Nehrbas

Radio Set AN/ARC=44—The First Army Airborne FM Communication Set (Abstract)—P. B. Petersen and T. J. Sueta

The Aeronautical Radio Installations of a Large Aircraft Manufacturer (Abstract)—R. A. Spiker and C. F. W. Anderson

Investigation of Transistor Parameters and Power Gain As a Function of Both Temperature and Frequency (Abstract)—A. B. Glenn

Speech Communications in Aircraft (Abstract)—M. E. Hawley

IRE Professional Group on Communications Systems Membership Directory

Electron Devices

Vol. ED-3, No. 2, April, 1956

A Memo from the Editor

Equivalence of Llewellyn and Space Charge Wave Equations—C. K.

The Llewellyn equations are shown to yield results identical with the space charge wave equations when the Llewellyn matrix is iterated over very many very short regions approximating a nearly constant average electron velocity.

High-Frequency Silicon Alloy Transistor—A. D. Rittmann and T. J. Miles

The silicon alloy transistor is a high-frequency, *p-n-p* type transistor capable of operation at high temperatures. Its temperature characteristic, derived principally from the use of silicon as the semiconductor, permits operation from $-70°C$ to $150°C$. It achieves its high-frequency characteristic through accurate control of the base geometry. The *n*-type base of silicon is accurately machined by jet electrochemical techniques. Alloy contacts of aluminum are fused into the bottoms of the etch pits without producing appreciable change in base geometry. The depth of alloy is limited by the thickness of the aluminum, by the temperature, and by the length of time for alloying. Lead wires are soldered to the aluminum contacts and the transistor hermetically sealed in glass-metal containers.

The electrical characteristics of typical silicon alloy transistors include an I_{co} of 0.005 μa, a common emitter forward current gain of 12, and an alpha-cutoff frequency of 12 mc.

High Gain Traveling-Wave Amplifiers—E. D. Denman and P. M. Lally

Modern techniques make it possible to built traveling-wave amplifiers with stable gains as high as 60 or 70 db. Such tubes can have relatively flat frequency response, and high gain over frequency ranges well in excess of two to one. In design it is necessary to pay strict attention to adequate isolation of the input and output so that spurious feedback paths do not cause oscillation or excessive variation of gain with frequency. In many practical applications, such tubes are required to operate with source and load impedances which produce large reflections of energy. Special design techniques result in tubes which are stable under such conditions. Another feature which can be achieved in modern tubes is a high ratio of backward loss to forward gain, so that the amplifier can very effectively isolate an oscillator.

The recent design trend is toward higher currents and lower voltages, which is of direct benefit to the equipment designer, since it results in shorter tubes as well as simpler power supply designs. With the use of highly convergent electron beams, cathode current density can be kept quite low, and ion bombardment effects minimized, so that excellent life is achieved.

Traveling-wave amplifiers may be readily phase modulated since small variations in the beam voltage yield large phase excursions. This characteristic is used for high level mixing. By proper gun design, it is possible to obtain good mixer action with modulation frequencies as high as a few hundred megacycles.

The problems involved in obtaining the above characteristics and typical experimental results are illustrated by data on the STS-69, a half-watt twt for the 2 to 4 kmc frequency range.

Design Theory and Experiments for Abrupt Hemispherical *P-N* Junction Diodes—H. L. Armstrong, E. D. Metz and I. Weiman

The gold-bonded germanium diode offers a practical example of a hemispherical *p-n* junction. In this discussion, a theory is given for the parameters of interest in design for such a junction, *i.e.*, the breakdown voltage, forward current, and transient effects.

It is shown that voltage breakdown differs from that for a planar junction due to the concentration of the field by the geometry, this effect leading to lower breakdown voltages. The forward current and reverse transient dependence on the radius of the junction, bulk properties, and the thickness of the semiconductor, are shown. The nature of the back contact to the semiconductor is also discussed.

Since this is a design theory, rigor is sacrificed in some cases for simplicity. Despite this, comparison of the theoretical predictions with experimental results usually shows good agreement. The possibility of applying the results to other hemispherical geometries, such as point contact diodes, is considered briefly.

The Use of Titanium Metal in Vacuum Devices—J. E. Beggs

The excellent gettering and gas retention properties of titanium metal make it highly suitable for use in vacuum devices. Tiny receiving tubes made with titanium parts are described which are capable of operating at high cathode emission densities. These high densities reduce the electron transit times and give better high-frequency performance. They permit the use of small electrodes and reduced heater and plate input powers. Vacuum devices made with titanium and ceramic parts can be operated for long periods of time at temperatures up to 700°C.

A Method of Determining Impurity Diffusion Coefficients and Surface Concentrations of Drift Transistors—L. S. Greenberg, Z. A. Martowska and W. W. Happ

In order to control the electrical parameters of drift transistors, it was found necessary to control the impurity concentration gradient in the base. An extension of the space charge widening theory provides a method of calculating this gradient, the surface concentration, and the diffusion coefficient. By this method, the diffusion coefficient of arsenic into germanium at 725°C was found to be 3.1×10^{-12} cm^2/second and the initial surface concentration was of the order of 10^{20} atoms/cm^3. Universal graphs for design calculations and rapid reference are presented.

Studies on Grid Emission—G. A. Espersen and J. W. Rogers

This paper is concerned only with the study of primary grid emission of various types of grid materials resulting from the evaporation products of *L*, impregnated, oxide-coated, and thoriated tungsten cathodes. The factors contributing to grid emission are analyzed. A detailed discussion of the performance of titanium, which exhibits excellent grid emission inhibiting properties, is included.

In our investigation a planar triode construction was used, the grids of which consisted of a two-terminal loop of 0.010 inch diameter wire. In the assembly and processing utmost precautions were taken to insure minimum contamination of the various elements. The methods of assembly and processing are fully described in the paper.

These tubes were tested using pulsed and dc techniques, and a discussion of the testing methods is included.

The work function of a tungsten grid exposed to the evaporation products of the L, impregnated, and oxide-coated cathodes varies from 1.2 to 2.0 ev, the final value depending upon the past history of the cathodes, namely, the nature of the surface of the grid and the temperature and length of exposure to the cathodes.

Program of the First Annual Technical Meeting on Electron Devices

Information Theory

Vol. IT-2, No. 1, March, 1956

Preliminary Announcement—Symposium on Information Theory

Annual ACM Meeting

Claude E. Shannon

The Bandwagon—C. E. Shannon

The Probability Distribution for the Filtered Output of a Multiplier Whose Inputs are Correlated, Stationary, Gaussian Time-Series—D. G. Lampard

In this paper the techniques used by Kac and Siegert and by Emerson for evaluating the probability distribution for the filtered output of a square-law device with a stationary, Gaussian input, have been extended to the case of a multiplier whose inputs are a pair of correlated, stationary, Gaussian time-series. It is shown that in this case the probability distribution is determined by the eigenvalues of a pair of simultaneous, linear, homogeneous, integral equations whose kernels involve only the correlation functions of the inputs and the impulse response of the postmultiplier filter.

Explicit solutions for the eigenvalues of these integral equations are obtained both for the case of no postmultiplier filtering and for a simple example system using RC filters. Using these solutions the corresponding probability distributions are discussed and in particular, the way in which the probability distribution of the output tends to Gaussian as the postmultiplier filter time constant is increased, is demonstrated.

Interpolation and Extrapolation of Sampled Data—A. B. Lees

This paper is essentially an extension of the optimum filtering theory of Zadeh and Ragazzini to the case where the time function to be operated upon is available only at a sequence of sample instants. As in the latter paper the signal is taken to consist of two parts, one being a polynomial $p(t)$ with unknown coefficients and known maximum degree n, and the other being a stationary random component $M(t)$ with known autocorrelation function. It is assumed that the signal has been contaminated before filtering by the addition of stationary random noise, also of known autocorrelation function, and that the input to the filter consists of a sequence of impulse functions of constant repetition period T, each impulse being of area equal to the sample value of the signal plus noise at the time of occurrence of the impulse. This paper shows how to find the weighting function $W(t)$, of a linear filter which will convert the sequence of impulse functions into a smoothed output subject to the following conditions: the weighting function $W(t)$ is only nonzero over a finite range; in the absence of random components, the interpolation or extrapolation is error-free; in the presence of any random signal the approximation at the output follows a least squares law. The weighting function of the optimum filter is shown to be piece-wise continuous in the intervals $\{rT\leq t\leq(r+1)E;\ r=0,\ 1,\ 2,\cdots N\}$ and the paper concludes with a discussion of a simple example illustrating the practical application of the solution.

The Third London Symposium on Information Theory—N. M. Blachman

Some Optimal Signals for Time Measurement—Herbert Sherman

Some optimal transmitted signals are given for communications systems in which the time of occurrence of a signal is desired in the presence of additive Gaussian noise. These signals are of two classes: those in which bipolar signal excursions are permitted and those in which only unipolar signal excursions are permissible.

Some bipolar codes used by R. H. Barker are supplemented when conditions permit unlimited negative excursions of the optimally correlated signal output. Other constraints, such as limiting the positive and negative excursions of the optimally correlated signal output, except at the proper phase, will lead to different codes.

When only unipolar codes are permitted, optimum repetitive and nonrepetitive codes (embedded in zeros) are given for various code lengths. The minimum length of such codes is given. A mathematical resemblance is indicated to a frequency allocation problem in which third-order intermodulation products must be avoided.

The closely related concepts of error-detecting and correcting codes and optimally correlated signals are illustrated in the derivation of these codes. The problem of generating such codes by other than trial and error is not solved and remains as a provocative problem.

An Analysis of Signal Detection and Location by Digital Methods—G. P. Dinneen and I. S. Reed

An analysis of the detection and location of repetitive signals in noise by digital techniques is made. The problem of location of the center of signals, herein denoted as beam-splitting, is explored. A Monte Carlo method employing a high speed digital computer was used to obtain quantitative results for a variety of digital detectors. A method of mathematical analysis is described and used to check computed results. The work described differs from much of the previous literature on detection or statistical decision theory in that an estimate of signal location is demanded.

Inverse Probability in Angular-Tracking Radars—B. J. Duwaldt

An angular-tracking radar of the pulsed type is analyzed for targets whose signal-return in the video follows a Rayleigh distribution. The pulse amplitudes are assumed independent from pulse-to-pulse but closely correlated for the duration of a pulse width. White Gaussian noise is introduced into the input of the receiver. It is assumed that rf phase information is lost. The method of inverse probability is used to find the most probable direction of the target from the scan axis. It is found that interference may be reduced by synchronizing transmissions in the scan cycle, by transmitting pulses in pairs simultaneously or nearly simultaneously, and by increasing the number of pulses integrated.

Contributors

Correspondence

Microwave Theory & Techniques

VOL. MTT-4, NO. 2, APRIL, 1956

H. A. Wheeler

Microwave Engineering—Is It Specialization or Diversification?—H. A. Wheeler

Report of Advances in Microwave Theory and Techniques—1955—D. D. King

Coupled-Strip-Transmission-Line Filters and Directional Couplers—E. M. T. Jones and J. T. Bolljahn

This paper describes the theory of operation of coupled strip line filters and directional couplers, and presents information from which these components may be easily designed. Low-pass, band-pass, all-pass, and all-stop filter characteristics are obtained from these coupled lines either by placing open or short circuits at two of the four available terminal pairs, or by interconnecting two of the terminal pairs. Directional couplers having perfect directivity and constant input impedance at all frequencies, and for all degrees of coupling, are obtained by placing equal resistive loads at each of the four terminal pairs.

Absolute Measurement of Receiver Noise Figures at UHF—E. Maxwell and B. J. Leon

Absolute measurements of noise-figures in the uhf range are described, using hot and cold thermal sources as standards. It was found that the noise temperature of the T-5 6 watt fluorescent tube is 16.1 ± 0.6 db above $kT\Delta v$. Noise diodes were found to be in error at these frequencies by approximately 1 db.

Design and Development of Strip-Line Filters—E. H. Bradley

Strip transmission lines offer an alternate medium in which microwave filters can be realized. Since bandpass filters designed in waveguide or coaxial lines would necessarily be large at ultra-high frequencies, strip lines provide a practical means of realizing filters which are simply fabricated and which represent an appreciable saving in size and weight.

Design techniques which were formerly employed in the realization of waveguide and coaxial filters have been applied in the synthesis of strip-line filters having "maximally-flat" and Tchebycheff response characteristics. In this paper, these techniques as well as those for realizing the required circuit parameters in strip line will be described. Using engraving techniques instead of the more commonly employed photo-etching techniques, strip-line filters can be fabricated with such precision that tuning screws are generally not required to align the filters to a desired center frequency. Bandpass filters having a 10 per cent bandwidth at S-band have been developed with a mid-band insertion loss of less than 1 db and a rejection of greater than 50 db at frequencies 9 per cent from the center frequency. The effect of temperature variations on the filter performance has been evaluated and will be discussed. Techniques will also be presented for eliminating spurious responses in filters required to operate over a frequency range of several octaves.

The application of strip-line techniques in the development of multiplexers and other microwave components, such as detector mounts, attenuators, and loads, will be discussed.

Measurement of Crystal Impedances at Low Levels—H. N. Dawirs and E. K. Damon

It is very important to know the impedances of crystal diodes when constructing circuits such as mixers and detectors in which the crystals are used. It is always difficult to measure these impedances due to the nonlinear characteristics of the crystals but it is most difficult to make the measurements at minimum levels at which the crystals operate, since with such methods as the slotted line, the detector must operate at a still lower level to obtain the required probe decoupling. Thus, since the load whose impedance is being measured is itself a crystal operating at its minimum level, it is practically impossible to obtain a detector with sufficient sensitivity to make the measurement.

Crystal impedances at these minimum levels are of utmost importance as it is here that optimum matching is essential for maximum sensitivity.

This paper describes practical techniques which use only standard equipment to measure crystal impedances at low levels. The detector used is a crystal of the same type as that being measured. The method is capable of precise results and good measurements can be obtained at low levels with little more effort than is normally required in making careful impedance measurements.

Long-Line Effect and Pulsed Magnetrons—W. L. Pritchard

A simplified theory of long-line effect is developed leading to expressions for maximum tolerable line length and vswr. The theory is verified experimentally and photographic evidence of the deleterious effect of long-line behavior is presented. The prevention of long-line effect by various methods, including decoupling the magnetron, attenuation, phase shifter, and ferrite isolators, is discussed.

The Use of Non-Euclidean Geometry in Measurements of Periodically Loaded Transmission Lines—R. L. Kyhl

The propagation characteristics of periodically loaded transmission lines can be deduced from impedance measurements taken with a series of different terminating configurations in a manner analogous to the "nodal shift" method of measuring microwave junction characteristics. The non-Euclidean properties of impedance transformations form a particularly simple approach for analyzing measurements in the case of the loaded line.

A New Microwave Frequency Standard by Quenching Oscillator Control—N. Sawazaki and T. Honma

This paper shows that in this new frequency standard system the multiplication is made by synchronizing oscillation, which is achieved by quenching a microwave oscillator with a standard quartz-crystal oscillator. The output frequency spectrum of this synchronizing oscillator includes only integral multiple frequencies of a quartz-crystal oscillator. Each spectrum can be utilized as standard frequencies. Theoretical calculations and experimental results are also described here. And to avoid the influence of noise voltage on the build-up of the quenching control microwave oscillator, the double modulation system is used, controlled and intermitted simultaneously by both f_1 voltage (output of the low frequency standard) and n_1f_1 voltage (n_1 is an integer).

By this double modulation method we can understand that the build-up and the stop of the microwave oscillation are exactly controlled by the constant phase of the waves from the standard generator, and also the experimental results of this are described. As an application of this new system, a method of precise frequency measurement is also described.

Determining Attenuation of Waveguide from Electrical Measurements on Short Samples—A. F. Pomeroy and E. M. Suárez

An improved method for accurately determining the attenuation of waveguide from measurements on very short samples is presented. First, two samples are measured separately and then in tandem. When the measurements are properly made, the sum of the attenuations when the samples are measured separately agrees with the attenuation when measured in tandem at each frequency of measurement. Second, the average effective resistivity is found over a band of frequencies. Using the average effective resistivity, the attenuation at any frequency in the band can be determined. Results for WR159 copper waveguide are shown

correspondence
contributors

Reliability & Quality Control

PGRQC-7, April, 1956

A New Life-Quality Measure for Electron Tubes—J. H. K. Kao

Since the Military Standard MIL-E-1B replaced JAN-1A specifications, the tube industry and tube users have been searching for a common satisfactory measure for the life quality of electron tubes. This paper proposes a new measure, incorporating the information in the electron tube failure-age distribution for replacement of the obsolete Average Life Percentage originally specified in JAN-1A. A Weibull distribution with a fixed shape parameter was found appropriate for describing the failure age of electron tubes under a wide variety of application. Hence, a single measure, the scale parameter, will characterize the life quality of electron tubes. Secondary life-quality measures, such as mean life, median life and the recently introduced "reliability," hazard rate, etc., can all be expressed in terms of the proposed measure. Some numerical examples are given at the end of the paper.

(Abstracts of Papers Presented at the Radio Fall Meeting, Syracuse, New York, October, 1955)

Simple Production Methods for Dynamic Testing of Horizontal-Deflection Tubes—M. B. Knight

Type Testing to Insure TV Performance Reliability—Carl Quirk

Electron Tube Life and Reliability—Built-in Tube Reliability—M. A. Acheson

The relationship between reliability and performance ability of tubes, as both are affected by design factors, can be stated with considerable accuracy. For example, a tube with double the mutual conductance of another tube has grid-cathode spacing all other dimensions in the grid vicinity reduced to 59.5 per cent, which may adversely affect microphonic response by a factor of eight. Over the fifteen years from 1930 to 1945, the G_m of tubes was increased at a remarkably uniform rateof 2.18 times (a multiplying factor) every five years; it dropped to 1.19 times for the next five years, and since 1950 there has been no multiplying factor. The reasons for this change of trend in tube design are analyzed as related to fundamental design factors. It has shown that the current practice of using high performance tubes almost exclusively has all but brought about the disappearance of lower performance tubes. Equipment designers could enjoy a considerable increase in built-in tube reliability if the newer materials and techniques that have been developed for the high-performance tubes were incorporated in more conservatively designed, lower performance tubes. As affected by design, built-in reliability of a tube decreases much more rapidly than built-in performance increases. The need for better electron tube life and reliability increases in importance year by year. Although effort on reliability development also increases at a rapid pace, the need for even more such development remains a step ahead of the results obtained. This situation is due to the ever-increasing complexity of electronic equipments. In fact, each accomplishment of a higher degree of reliability extends tube usage into even more demanding applications. The reliability program is thus a dynamic one, and has no presently definable objective level.

Quality and the Television Production Engineer—H. H. Mahuron

Abstracts and References

Compiled by the Radio Research Organization of the Department of Scientific and Industrial Research, London, England, and Published by Arrangement with that Department and the *Wireless Engineer*, London, England

NOTE: The Institute of Radio Engineers does not have available copies of the publications mentioned in these pages, nor does it have reprints of the articles abstracted. Correspondence regarding these articles and requests for their procurement should be addressed to the individual publications, not to the IRE.

The Index to the Abstracts and References published in the PROC. IRE from February, 1955 through January, 1956 is published by the PROC. IRE, June, 1956, Part II. It is also published by *Wireless Engineer* and included in the March, 1956 issue of that journal. Included with the Index is a selected list of journals scanned for abstracting with publishers' addresses.

The number in heavy type at the upper left of each Abstract is its Universal Decimal Classification number and is not to be confused with the Decimal Classification used by the United States National Bureau of Standards. The number in heavy type at the top right is the serial number of the Abstract. DC numbers marked with a dagger (†) must be regarded as provisional.

ACOUSTICS AND AUDIO FREQUENCIES

534.213 1601
The Transmission of a Plane [acoustic] Wave between Parallel Plates—I. D. Campbell. (*Acustica*, vol. 5, pp. 298–302; 1955.) Analysis is presented taking account of viscosity and thermal conduction. An approximate method is used which allows the attenuation and phase velocity to be deduced for all frequencies. Results are compared with measured values.

534.232–14–8:534.133 1602
The Performance of a Quartz Oscillator in Liquids—S. Parthasarathy and V. Narasimhan. (*Z. Phys.*, vol. 143, pp. 300–311; December 12, 1955 and pp. 623–631; January 10, 1956. In English.) The ultrasonic output was determined by a calorimetric method. The efficiency of conversion was investigated in various liquids at frequencies of 2.8, 4.9, 8.7 and 14.7 mc.

534.6–8 1603
A Reverberation Method for the Measurement of the Absorption of Ultrasonics in Liquids—L. E. Lawley and R. D. C. Reed. (*Acustica*, vol. 5, pp. 316–322; 1955.)

534.79 1604
Loudness of Steady Noises—E. Zwicker and R. Feldtkeller. (*Acustica*, vol. 5, pp. 303–316; 1955. In German.) A method of determining the loudness of sustained noises is described based on subjectively derived equal-loudness contours, the measured bandwidth of the frequency groups into which the ear analyzes the noise, and the mutual reduction effect of the adjacent groups.

534.846.4 1605
Sound Amplification in Reverberant Spaces—A. F. B. Nickson. (*Aust. J. appl. Sci.*, vol. 6, pp. 476–485; December, 1955.) A system of vertical columns of loudspeakers, as proposed by Parkin and Taylor (1506 of 1952), is considered best. Three practical cases of improvements thus effected are described, and curves are given showing correct dimensions and positioning of columns for halls of various lengths.

534.86:621.375.2.029.3 1606
Phase Shift and Sound Quality—J. Moir. (*Wireless World*, vol. 62, pp. 165–168; April, 1956.) Experiments on the toleration of phase shifts in af amplifiers are reported. Results indicate that phase shifts introduced by typical domestic amplifiers are of little practical importance.

621.395.612.4 1607
The Design of a Ribbon Type Pressure-Gradient Microphone for Broadcast Transmission—D. E. L. Shorter and H. D. Harwood. (*B.B.C. Engng. Div. Monographs*, No. 4, pp. 1–22; December, 1955.) Detailed account of development work leading to the production of microphone Type PGS, with reduced size and weight and improved response.

621.395.623.5 1608
The Natural Frequencies of Horns—T. Lange. (*Acustica*, vol. 5, pp. 323–330; 1955. In German.) Calculations and measurements have been made of the input impedance of a system comprising a pressure chamber, a cylindrical connection, and a hyperbolic or catenoidal horn. In the general case, the combined effects of the pressure chamber and the horn shape produce inharmonic resonances, but the two effects can be balanced to produce harmonic resonances.

621.395.625.3:534.76 1609
Design of Magnetic Recording and Reproducing Equipment for Domestic Use with Special Reference to Stereophonic Reproduction—M. B. Martin and D. L. A. Smith. (*J. Brit. IRE*, vol. 16, pp. 65–77; February, 1956. Discussion, pp. 77–79.)

681.84:534.851 1610
Sapphire and Diamond Needles for reproducing Gramophone Disks—P. H. Werner. (*Tech. Mitt. schweiz. Telegr.-TelephVerw.*, vol. 33, pp. 504–511; December 1, 1955. In French.) Tests are reported to determine the playing time of both sapphire and diamond needles before quality of reproduction deteriorates noticeably. Photographs of unused and used needles are reproduced. The higher cost of the diamond needles is out of proportion to their longer service except for professional users. Where diamond needles are used, special precautions must be taken in respect of their finish.

ANTENNAS AND TRANSMISSION LINES

621.372.029.6 1611
Symposium on Microwave Strip Circuits—(TRANS. IRE, vol. MTT-3, pp. 1–177; March, 1955.) The text is given of 22 papers presented at a symposium held in October, 1954; strip-line, microstrip and triplate lines, and components using them are described. Abstracts of all the papers are given in PROC. IRE, vol. 43, pp. 894–895; July, 1955.

621.372.2:621.385.029.6 1612
Coupled Helices—J. S. Cook, R. Kompfner, and C. F. Quate. (*Bell Syst. Tech. J.*, vol. 35, pp. 127–178; January, 1956.) An analysis of coupled helices is presented, based on transmission-line and field theory. Applications based on the presence of one and of both normal modes of propagation are described, and curves and equations useful in the design of traveling-wave tubes and other microwave equipment are presented.

621.372.2.012 1613
New Diagram for solving Impedance Transformations—R. Guillien. (*Onde élect.*, vol. 35, pp. 1164–1170; December, 1955.) If the reflection coefficient of a transmission line is represented by its logarithm, the standard Smith chart may be replaced by a logarithmic chart of orthogonal curves on which impedance transformations may be effected by simple translation, avoiding the rotations required on the Smith chart.

621.372.22:621.372.51 1614
Nonuniform Transmission Lines as Impedance Transformers—J. Willis and N. K. Sinha. *Proc. IEE*, Part B, vol. 103, pp. 166–172; March, 1956.) "The equation for the reflection coefficient at one end of a nonuniform transmission line matched at the other end is considered, and an approximate form of solution is suggested which enables such lines to be designed for optimum performance as matching sections. A number of examples are calculated, and the results are compared with lines previously described in literature." See also 664 of 1956.

621.372.8:621.318.134 1615
Energy Concentration Effects in Ferrite-Loaded Waveguides—J. L. Melchor, W. P. Ayres, and P. H. Vartanian. (*J. appl. Phys.*, vol. 27, pp. 72–77; January, 1956.) The influence of geometric factors on the microwave transmission characteristics for the two circularly polarized waves in a circular waveguide

with an axially mounted ferrite rod are studied. The results support the prediction by Fox and Weiss (*Rev. mod. Phys.*, vol. 25, pp. 262–263; January, 1953), made in a comment on a paper by Hogan (*ibid.*, pp. 253–262), that the energy concentration within the ferrite is greater for one of the circularly polarized waves than for the other.

621.396.67 1616
Folded Unipole Antennas—J. Leonhard R. D. Mattuck, and A. J. Poté. (TRANS. IRE, vol. AP-3, pp. 111–116; July, 1955.) Analysis for folded unipoles less than $\lambda/4$ in length as input impedance transformers is presented and verified by experiment. Practical applications are proposed.

621.396.67 1617
A New Interpretation of the Integral-Equation Formulation of Cylindrical Antennas—C. T. Tai. (TRANS. IRE, vol. AP-3, pp. 125–127; July, 1955.) The conventional solution, based on an approximate integral equation, is verified by a method using the exact equation for a cylindrical shell; the new method is applicable to relatively thick antennas.

621.396.67:621.315.62 1618
A New Type of Aerial Insulator for High Voltages and High Tensile Stresses—W. Peters. (*Nachrichtentech. Z.*, vol. 8, pp. 632–635; December, 1955.) An insulator for use in stays of mast antennas is described; the optimum distribution of the insulators along the stays is indicated.

621.396.67:621.396.969 1619
Reflection of Electromagnetic Waves from Thin Metal Strips (Passive Antennae)—Lindroth. (See 1731.)

621.396.677.3 1620
Use of Folded Monopoles in Antenna Arrays—J. B. Lewis. (TRANS. IRE, vol. AP-3, pp. 122–124; July, 1955.) "A method of calculating the driving point impedances from the self and mutual impedances of related unfolded elements is given."

621.396.677.45 1621
Ground-to-Air Antenna uses Helical Array—V. J. Zanella. (*Electronics*, vol. 29, pp. 161–163; March, 1956.) An uhf antenna producing vertical polarization and consisting of a multi-element appropriately phased helical array gave a beam width at half-power points of 20° in the vertical plane and 45° in the horizontal plane. Constructional features for keeping the wind loading low are described.

621.396.677.51:621.318.134:621.396.93 1622
Ferrite Aerials for Goniometer Direction Finders—G. Ziehm. (*Telefunken Ztg*, vol. 28, pp. 227–234; December, 1955. English summary, p. 265.) A discussion of the design of df antennas for aircraft. The numerical calculations refer to a frequency of 300 kc and a magnetic field strength of 0.15 A/m. Arrangements of parallel rods offer advantages.

621.396.677.71 1623
The Radiation Field produced by a Slot in a Large Circular Cylinder—L. L. Bailin. (TRANS. IRE, vol. AP-3, pp. 128–137; July, 1955.) The results obtained by Silver and Saunders (1588 of 1950) are used in the computation of tables giving the magnitude and phase of the principal component of the far-zone electric field for $\lambda/2$ slots.

621.396.677.81.012.12 1624
Radiation of Electric Vibrators located near an Ideally Conducting Elliptic Cylinder—G. N. Kocherzhevski. (*Zh. tekh. Fiz.*, vol. 25, pp. 1140–1154; June, 1955.) Polar diagrams of the vibrators are calculated by determining the total field as a sum of the fields of incident (plane) and diffracted waves and then applying the principle of reciprocity. The cases of longitudinal, transverse, and radial vibrators are considered separately and a study is made of the effects of the shape and size of the cylinder and of the position of the vibrator. A comparison is made between the theoretical and experimental polar diagrams; under certain conditions good agreement is obtained.

621.396.677.833 1625
Effect of Arbitrary Phase Errors on the Gain and Beamwidth Characteristics of Radiation Pattern—D. K. Cheng. (TRANS. IRE, vol. AP-3, pp. 145–147; July, 1955.) Expressions applicable to microwave parabolic reflectors are derived giving the maximum reduction of gain and the maximum change in main-lobe beam-width when the peak value of the aperture phase deviation and the amplitude distribution function are known.

621.396.677.833 1626
Design and Construction of Double-Curvature Reflectors—L. Thourel. (*Onde élect.*, vol. 35, pp. 1153–1163; December, 1955.) A practical method for calculating the contours of a surface with given reflecting properties is presented and the effect on the radiation pattern of varying the position of the primary source is examined. Diffraction is taken into account. Calculated patterns agree with experimental results.

621.396.677.833.1 1627
Parabolic Cylinder Aerials—K. Foster. (*Wireless Engr.*, vol. 33, pp. 59–65; March, 1956.) For cm-λ antennas the ratios of whose beam widths in two orthogonal planes are greater than about 8:1, parabolic cylinders are more practicable than paraboloidal reflectors. The radiation pattern of the parabolic cylinder is studied theoretically and design criteria are established. Comparison with performance figures given by Kiely (1572 of 1951) indicates that the theory is accurate enough for practical purposes.

621.396.677.85:537.226 1628
Study of the Diffraction of Electromagnetic Waves by an Array of Perforated Plates—G. Broussaud. (*Ann. Radioélect.*, vol. 10, pp. 42–63; January, 1955.) Artificial dielectrics comprising stacked metal plates with holes arranged in regular lines are investigated. The phenomena involved are conveniently represented as a series of guided propagations. With oblique incidence, the coupling between the individual guides provides an explanation of the refraction process. The critical angle at which incident energy is entirely absorbed is related simply to the hole spacing. Application of the results to the design of microwave lenses is indicated.

AUTOMATIC COMPUTERS

681.142 1629
Electronic Computers—(*Elektronische Rundschau*, vol. 9, October, 1955.) The main part of this issue is devoted to a series of papers on digital computers, with titles as follows:
Programme-Controlled Computers—H. J. Dreyer, (pp. 341–343).
From the Punched-Card Computer to the EDPM [electronic data-processing machine]—O. Schröter, (pp. 344–348).
Micro-program Control Mechanism—H. Billing and W. Hopmann, (pp. 349–353).
The Parallel Adding Mechanism of the PERM [programm-gesteuerte elektronische Rechenanlage München]—W. E. Proebster, (pp. 353–359).
Printing the Results from Electronic Computers—G. Overhoff, (pp. 360–361).
Use of the Electronic Computer "GAMMA 3" for solving Complicated Mathematical Problems—H. Päsler, (pp. 362–365).
Technical Problems in the Development of Magnetic-Drum Stores—H. O. Leilich, (pp. 365–368).
Store Resonator Circuit and Data Input and Output for the BULL Electronic Computer "GAMMA 3"—R. Machery, (pp. 369–370).
Assessment of Quality of Rectangular [-loop] Ferrites for Electronic Computers—O. Eckert, E. Weides, and K. Wallenfang, (pp. 371–374).
Development of Resistances for Electronic Apparatus—H. Loth, (pp. 375–376).
Transistors in Computer Technique—A. Krösa and K. Ganzhorn, (pp. 377–380).
Properties required in Germanium Diodes for Electronic Computers—W. Bühler, (pp. 381–382).

681.142 1630
The Design, Construction and Applications of Electronic Digital Computers—E. Grundy and H. McG. Ross. (*Trans. S. Afr. IEE*, vol. 46, Part 10, pp. 261–294; October, 1955.) A survey of the whole field, with a comprehensive bibliography; a wide range of actual and projected applications in science and industry is discussed, including process control and data analysis.

681.142:621.314.7 1631
A Transistor Digital Fast Multiplier with Magnetostrictive Storage—G. B. B. Chaplin, R. E. Hayes, and A. R. Owens. (*Proc. IEE*, Part B, vol. 103, pp. 121–124; March, 1956.) Discussion on 3170 of 1955.

681.142:621.374.3 1632
An Electrostatic Pulse Generator—W. Woods-Hill. (*Electronic Engng.*, vol. 28, pp. 122–123; March, 1956.) Pulse patterns required in electronic computers are generated by presenting a probe feeding a tuned amplifier to a suitably figured track on an insulated rotating drum carrying a rf voltage.

CIRCUITS AND CIRCUIT ELEMENTS

621.3:061.3/.4 1633
1954 Western Electronic Show and Convention, Los Angeles, California—(TRANS. IRE, vol. PGCP-2, pp. 1–118; September, 1954.) The full text or an abstract is given of papers on various components, equipment and techniques presented at the Convention. Abstracts of all the papers are published in PROC. IRE, vol. 42, pp. 1819–1820; December, 1954.

621.3.011.22 1634
The Resistance of Sheets, Strips, Wires, Tubes and Coils of Various Materials at Frequencies between 10 c/s and 100 kMc/s—J. Bachel, K. L. Lenz, and O. Zinke. (*Frequenz*, vol. 9, pp. 401–406; December, 1955.) A method of calculation applicable to materials with widely different conductivities, ranging from Ag to Ge, is presented. The values of the resistance per square are found from sets of curves for material thicknesses of 0.1, 0.3 and 1 mm. Because of skin effect at high frequencies, the curves for these thicknesses cover all requirements.

621.318.4 1635
Oscillations of Coupled Windings—P. A. Abetti, G. E. Adams, and F. J. Maginniss. (*Elect. Engng., N. Y.*, vol. 74, p. 1002; November, 1955.) Digest of paper in *Trans. AIEE*, Part III, *Power Apparatus and Systems*, vol. 74, pp. 12–21; April, 1955. By using the mutual-inductance function, the integral-equation method of determining the natural frequencies [3483 of 1954 (Abetti and Maginniss)] is extended to take account of the effect of a transformer secondary winding.

621.318.57:621.3.042 1636
The Transfluxor—J. A. Rajchman and A. W. Lo. PROC. IRE, vol. 44, pp. 321–332; March, 1956. See 3509 of 1955.

621.316.82 1637
Concavity of Resistance Functions—C. E.

Shannon and D. W. Hagelbarger. (*J. appl. Phys.*, vol. 27, pp. 42–43; January, 1956.) "It is proved that any network of linearly wound potentiometers and fixed resistors has a curve of resistance vs shaft angle which is concave downward."

621.372.029.6 1638
Symposium on Microwave Strip Circuits—(See 1611.)

621.372.412 1639
Variation with Temperature of Quartz Resonator Characteristics—R. Bechmann and V. Durana. (PROC. IRE, vol. 44, p. 377; March, 1956.) Calculations based on the temperature variation of the piezoelectric constants of AT-, BT-, CT-, DT-, and X-cut quartz resonators indicate that the AT- and DT-cut resonators are particularly suitable for use; *e.g.*, in filters, at temperatures as high as 250°C. or over.

621.372.413 1640
Theory of Electromagnetic Resonators of Almost Conical Shape—A. S. Kompaneets and Yu. S. Sayasov. (*Zh. tekh. Fiz.*, vol. 25, pp. 1124–1131; June, 1955.) A mathematical investigation is carried out of *E*-mode oscillations in a resonator formed by a spheroid and a confocal two-sheet hyperboloid, for the case of a small ratio between the focal distance and the wavelength. Perturbation theory is modified to take into account the large deviation of the field from that in a resonator formed by a sphere and two coaxial cones.

621.372.413:621.396.67 1641
Theory of Thin Aerials in Cavity Resonators—A. V. Gaponov. (*Zh. tekh. Fiz.*, vol. 25, pp. 1069–1084; June, 1955.) Free oscillations in a cavity resonator containing thin metallic antennas or having narrow slots in its walls are considered. Formulas are derived for the natural frequency and eigenfunctions of such a system and for the decrement and *Q* of the resonator. The results are used in a discussion of the excitation of a cavity resonator by thin antennas. The problem is reduced to the excitation of the resonator by given external electric or magnetic currents. Several examples are considered in detail. The analysis is continued in the following paper (*ibid.*, pp. 1085–1099); both tuned and untuned antennas are considered.

621.372.5 1642
A Matrix Method in the Solution of Cascaded Four-Terminal Networks—R. E. Vowels. (*Aust. J. appl. Sci.*, vol. 6, pp. 427–441; December, 1955.)

621.372.5 1643
The Geometrical Representation of the Parallel and the Series Reactance as a Loss-Free "Parabolic" Quadripole—J. de Buhr. (*Nachrichtentech. Z.*, vol. 8, pp. 636–641; December, 1955.) Further application of the method described previously (349 of 1956 and back references).

621.372.5:621.396.822 1644
Calculations with Noise Voltages: Part 2—Passage of Noise Voltages through Nonlinear Elements—G. Bosse. (*Frequenz*, vol. 9, pp. 407–413; December 1955.) The correlation function is used to calculate the modification suffered by a noise spectrum on passing through a quadripole with nonlinear elements. The method is based on that of Rice (440, 2168 and 2169 of 1945). The quadripole characteristic is represented as an integral; the relation between the correlation functions for input and output voltages is in the form of a double integral which can be expanded in a power series. Simple expressions are obtained when the quadripole characteristic comprises a sum of Hermite polynomials. An introduction to the various parameters used is given in Part 1, *ibid.*, vol. 9, pp. 258–264; August, 1955.

621.372.54.029.6:621.372.8 1645
Design of [waveguide] Microwave Filters with Quarter-Wave Couplings—G. Craven and L. Lewin. (*Proc. IEE*, Part B, vol. 103, pp. 173–177; March, 1956.) "Resonator diaphragms are constructed from triplets of inductive posts, whose spacings and radii are chosen to prevent the generation of the first five nonpropagating modes. This is sufficient to insure negligible coupling at quarter-wave separation. Measurements on filters at 4,000 mc indicate a satisfactory performance."

621.372.542.2 1646
Normalized Filter Design—S. D. Bedrosian and R. McCoy, Jr. (*Electronics*, vol. 29, pp. 200–202, 204; March, 1956.) The design chart presented for composite low-pass filters permits predetermining the attenuation characteristic from trial design. Six normalized designs are presented as examples to cover a practical range of stop-band loss.

621.372.56.029.63/.64:538.569.3 1647
R. F. Attenuators and Load Materials—D. Lichtman. (*Tele-Tech and Electronic Ind.*, vol. 14, Section 1, pp. 88, 126, 129; November, 1955.) The preparation of iron-araldite mixtures with ratios of 1:1 to 8:1 by weight is described and results of loss measurements in the frequency range 1.5–7.5 kmc are reported. The results are presented graphically.

621.373:621.396.822 1648
A Comparison of the Noise, and Random Frequency and Amplitude Fluctuations in Different Types of Oscillator—R. L. Beurle. (*Proc. IEE*, Part B, vol. 103, pp. 182–189; March, 1956.) "The nature of the random fluctuation in the output is dependent on the form of feedback employed and the method by which the output amplitude is controlled. The frequency band over which the output power is distributed depends, however, on the relative magnitudes of signal and noise in the circuit rather than on the particular circuit employed. The conclusion is that an oscillator should be operated at as high a level as possible consistent with stability and constancy of the circuit components."

621.373.4:621.396.822:621.376.3 1649
Frequency Modulation Noise in Oscillators—J. L. Stewart. (PROC. IRE, vol. 44, pp. 372–376; March, 1956.) The discussion is confined to noise due to the discrete nature of the electron and the random motion of the electrons in the oscillator tube; the spectrum ranges from zero to hundreds of mc. The effect of the usual band-pass filter on the noise modulation is determined and the power spectrum of the oscillator output is evaluated. The theory is applied to several types of oscillator.

621.373.421:621.376.32 1650
A Wide-Band Frequency-Modulated System with Asymmetrical 3-Phase Oscillator—P. Kundu. (*Indian J. Phys.*, vol. 29, pp. 151–160; March, 1955.) An analytical investigation is made of the operation of the 3-phase RC oscillator; symmetrical and asymmetrica arrangements are compared as regards linearl ity of modulation, modulation sensitivity, and frequency stability in a fm system.

621.373.43 1651
A Phase-Controlled Oscillator—P. G. Davis. (*Electronic Engng.*, vol. 28, pp. 101–105; March, 1956.) Description of an oscillator whose frequency is an exact multiple of the mains frequency; the phase relation is maintained constant by a feedback loop and phase comparator.

621.373.43 1652
A Particular Mode of Relaxation Oscillation in a Triode Valve—R. Bedos and P. Jean. (*C. R. Acad. Sci., Paris*, vol. 242, pp. 234–236; January, 1956.) Operation of an arrangement with a very high resistance between the grid and the point of application of grid voltage is discussed. The I_a/V_g characteristic is two-valued, giving rise to relaxation oscillations. See also 3172 of 1954 (Jean.)

621.373.431.2:621.314.7 1653
Junction Transistors with Alpha Greater than Unity—Schenkel and Statz. (See 1893.)

621.373.52:621.314.7 1654
Transistorizing Meacham-Bridge Oscillators—S. N. Witt, Jr. (*Electronics*, vol. 29, pp. 193–195; March, 1956.) 1955 National Electronics Conference paper. Highly stable circuits using either point-contact or junction transistors are described, for operation at a frequency of 1 mc.

621.374.3 1655
Experiments on the Regeneration of Binary Microwave Pulses—O. E. DeLange. (*Bell Syst. Tech. J.*, vol. 35, pp. 67–90; January, 1956.) A device consisting of a waveguide hybrid junction with a Si crystal diode in each arm, working at signal frequency (4 kmc), gives sufficient regeneration to permit transmission of signals over a long chain of repeaters, providing that the rms signal/noise ratio at each repeater is >20 db.

621.374.32:621.314.7 1656
High-Speed Counter uses Surface-Barrier Transistor—E. Gott. (*Electronics*, vol. 29, pp. 174–178; March, 1956.) The complete circuit is given of a four-stage reversible binary counter used for decoding pcm signals. The high α-cutoff frequency of the surface-barrier transistors employed permits the attainment of a counting rate of 6×10^6 pulses per second.

621.374.4:621.396.91 1657
Time-Signal Generator employing Decade-Counting Tubes—Y. Suguri, T. Ichida, and K. Harada. (*J. Radio Res. Labs, Japan*, vol. 2, pp. 235–238; July, 1955.) In a frequency-dividing circuit operated in conjunction with a frequency standard and using two decade counters to effect the last stages of division from 100 cps to 1 cps, fluctuation of delay time for the leading edge of the seconds output pulse is 3.5 μs, and for the trailing edge 0.1 μs or better.

621.375.2+621.373.4+621.317.3].029.6 1658
Disc-Seal Circuit Techniques—J. Swift. (*J. Brit. IRE*, vol. 15, pp. 607–622; December, 1955 and vol. 16, pp. 95–111; February, 1956.) Reprint. See 3541 of 1955.

621.375.23:621.314.222 1659
Stability Problems with Low-Frequency Amplifiers with Transformers in the Feedback Path—W. Langsdorff. (*Frequenz*, vol. 9, pp. 369–379; November and pp. 422–428; December, 1955.) Measurements were made of the attenuation and phase variation of typical push-pull output transformers over the frequency band 20–200 kc, outside the low-frequency band; the phase variation was compared with that of a minimum-phase-rotation network with the same attenuation variation. The results indicate the possibility of simplifying the stability testing of the amplifier circuit by treating the transformer as a minimum-phase-rotation network.

621.375.3:621-526 1660
Self-Balancing Magnetic Servo Amplifier—W. A. Geyger. (*Electronics*, vol. 29, pp. 196–199; March, 1956.) "Positive magnetic and negative electric feedback improve performance of single-stage magnetic servo amplifier driving two-phase 400-cps induction motor and standard position servomechanism."

621.375.3:621.318.57 1661
Magnetic Amplifiers in Bistable Operation

—L. A. Finzi and G. C. Feth. (*Elect. Engng., N. Y.*, vol. 74, p. 1008; November, 1955.) Digest of paper in *Trans. AIEE*, Part I, *Communication and Electronics*, vol. 74, 1955. Flip-flop operation can be achieved by overregenerative feedback. The relation of the switching cycle to the steady-state transfer characteristic is examined.

621.375.4:621.314.7 1662

A Study of Transistors connected in Parallel—A. N. Daw. (*Indian J. Phys.*, vol. 29, pp. 121–130; March, 1955.) The performance of the parallel combination of transistors is studied in terms of a single equivalent transistor whose parameters are related in a simple manner to those of the individual transistors. Expressions are derived for the gain and the input and output impedances for the three basic modes of operation. Results of experiments with both point-contact and junction types are in good agreement with the theoretical results.

621.375.4:621.376.22:621.314.63 1663

A Silicon Junction Diode Modulator—N. F. Moody. (*Electronic Engng.*, vol. 28, pp. 94–100; March, 1956.) By the use of biased diodes in a specially designed bridge circuit, dc is converted to ac over a range from audio frequencies to at least 100 kc, with a zero stability of better than 10^{-10} w at room temperature and 10^{-8} w at 80°C.

621.376.23:538.569.4 1664

Theory of the Autodyne Detector for Paramagnetic Resonance—F. Bruin and F. M. Schimmel. (*Physics*, vol. 21, pp. 867–876; November, 1955. In French.)

GENERAL PHYSICS

53.081.4 1665

Use of Logarithmic Notation in Science and Engineering—S. Devons. (*Nature, Lond.*, vol. 177, pp. 373–374; February 25, 1956.) A unit for general logarithmic systems is proposed, termed the "jot;" the notation used is: $x = (\text{unit} \pm xyz \cdot ab)$ jot, but the word "jot" is normally omitted. Advantages of the system are simplicity of calculation, economy of notation, simplification of units, and simplification of representation of errors. Examples of use of the notation are given.

535.1 1666

Correlation between Photons in Two Coherent Beams of Light—R. H. Brown and R. Q. Twiss. (*Nature, Lond.*, vol. 177, pp. 27–29; January 7, 1956.) Principles used in the radio interferometer described previously (103 of 1955) are applicable to the measurement of the angular diameter of visual stars if the two antennas are replaced by mirrors and the rf detectors by photocells. For operation of such a system it is essential that the time of arrival of photons at the two photocathodes should be correlated when the light beams incident on the two mirrors are coherent; a laboratory experiment demonstrating the existence of this effect is described.

535.13 1667

Asymptotic Solutions of Maxwell's Equations involving Fractional Powers of the Frequency—M. Kline. (*Commun. pure appl. Math.*, vol. 8, pp. 595–614; November, 1955.) The principal theorem derived indicates the method of obtaining steady-state solutions, provided that the behavior of the corresponding pulse solutions in the neighborhood of the singularities is known.

535.231:536.7 1668

Mathematical Study of Boltzmann's Equation—S. Marquet. (*C. R. Acad. Sci., Paris*, vol. 242, pp. 615–617; January 30, 1956.)

535.42:538.566 1669

Diffraction by a Plane Aperture with Variable Contour. General Formulae—O. Costa de Beauregard. (*C. R. Acad. Sci., Paris*, vol. 242, pp. 347–350; January 16, 1956.) Four-dimensional extension of the formulas of classical diffraction theory [2909 of 1954 (Bouwkamp)].

537.211 1670

Some Theoretical and Practical Considerations of the Johnsen-Rahbek Effect—A. D. Stuckes. (*Proc. IEE*, Part B, vol. 103, pp. 125–131; March, 1956.) The Johnsen-Rahbek effect which is observed when a voltage is applied between metal and semiconductor surfaces in "contact" with one another is explained as due to the es force across the gap, which exists at all points except a few where contact is actually made. The force increases with the voltage until the latter reaches the critical value causing field emission. Experiments with a clutch based on this effect are described; the results indicate that such a device would be too unreliable for practical purposes; the effect might be used in relays and gas-flow tubes.

537.226 1671

Dielectric Properties of a Lattice of Anisotropic Particles—Z. A. Kaprielian. (*J. appl. Phys.*, vol. 27, pp. 24–32; January 1956.) Analysis is presented for a uniform lattice of similarly oriented particles of arbitrary shape and material. The packing density is assumed to be such that interaction between particles must be considered but the induced fields can still be regarded as simple dipole fields. Two particular casea are examined: a) a cubic array of ferrite spheres, and b) a tetragonal array of disks; in the latter case the calculated values of dielectric constant are in good agreement with experimental results reported by [El-]Kharadly and Jackson (2902 of 1953.)

537.311.31:535.215 1672

Electronic Interaction between Adsorbed Gas Molecules and Metal Surfaces—R. Suhrmann. (*Z. Metallkde*, vol. 46, pp. 780–786; November, 1955.) The interaction is discussed in terms of the structure of the gas molecules and the work function of the metal. Experimental investigations based on the variation of photoelectric sensitivity and resistance of thin films of the metal on adsorption of the gas are described. Metals used were Ni and Pt, gases were O, H, N, CO_2, N_2O, water vapor and benzene vapor. The investigation is relevant to the problem of conduction at the surface of semiconductors.

537.5 1673

The Diffusion of Electrons in a Gas at Low Temperatures—B. I. H. Hall. (*Aust. J. Phys.*, vol. 8, pp. 551–554; December, 1955.) Laboratory measurements were made of electron agitation energy Q as a function of Z/n and Q_0, where Z is an applied electric field, n the concentration of gas molecules and Q_0 the mean agitation energy of the molecules. The gases used were N_2 and H_2.

537.52 1674

International Symposium on Electrical Discharges in Gases—(*Appl. sci. Res.*, vol. B5, pp. 1–344; 1955.) The text is given of 66 papers presented at the Symposium held at Delft in April, 1955. The subjects discussed included a) fundamental processes in gas discharges, b) instabilities and oscillations in gas discharges, c) high-frequency discharges and the dependence of breakdown on frequency and on the product of pressure and electrode separation, d) methods of measurement, e) arc discharges, and f) spark discharges.

537.525 1675

Study of the Induced Electric Discharge in Rare Gases—F. Cabannes. (*Ann. Phys., Paris*, vol. 10, pp. 1026–1078; November/December, 1955.) Experiments were performed using a tube of a few centimeters diameter and a frequency of 1 mc. Aspects investigated included the conditions for starting the discharge and the radiation from the discharge. Theory is developed giving a quantitative explanation of the experimental results. See also 2915 of 1954 and *Appl. sci. Res.*, vol. B5, pp. 318–320; 1955.

537.533/.534 1676

Penetration of Electrons and Ions in Aluminium—J. R. Young. (*J. appl. Phys.*, vol. 27, pp. 1–4; January, 1956.) "The depth of penetration of 0.5- to 11-kev electrons and 1- to 25-kev H^+, H_2^+, and He^+ ions in aluminium has been measured. It has been found that the Thompson-Whiddington law for electrons does not hold for electrons having energies less than 10 kev. The practical range-energy relation obtained for electrons in aluminium was found to be $R = KE^{1.3}$, where K is 0.042 if E is expressed in kev and R in microns. The practical range-energy relation for light ions in aluminium was found to be $R = KE^{0.83}$ where $K = 0.020$ for H^+, $K = 0.021$ for He^+, and $K = 0.015$ for H_2^+. Results are compared with those obtained by previous observers."

537.533 1677

Use of the Knife-Edge Method to determine Aberrations of Deflected Electron Beams—H. Grümm. (*Optik, Stuttgart*, vol. 12, pp. 544–553; 1955.) The beam is caused to throw a shadow of a knife-edge or wire on a distant plane. Theory is given and selected shadow pictures are reproduced.

537.533.7 1678

Collective Oscillations and Characteristic Electron-Energy Losses—D. Gabor. (*Phil. Mag.*, vol. 1, pp. 1–18; January, 1956.) An attempt is made to give a simple theory of the interaction of fast electrons with thin films of solids, adequate for interpreting results of past experiments and for suggesting new, crucial tests.

537.533.8:546.45 1679

Secondary Electron Emission from Thin Layers of Be: Part 2—I. M. Bronshtein and T. A. Smorodina. (*Zh. eksp. teor. Fiz.*, vol. 29 pp. 495–499; October, 1955.) An experimental investigation is reported of the secondary-electron emission coefficient σ and the variation of secondary-electron energy distribution with the thickness of thin layers of Be. For approximately monatomic layers of Be on Ni or Ag and constant primary electron energy, the secondary electron energy, E_v, at which the maximum of the $d\sigma/dE_v$ vs E_v curve occurs is a minimum. Part 1: 684 of 1955.

537.533.8:546.57 1680

Secondary Electron Emission from Thin Layers of Silver—I. M. Bronshtein and T. A. Smorodina. (*Zh. eksp. teor. Fiz.*, vol. 29 (10), pp. 500–506; October, 1955.) An experimental investigation of Ag films on Ni or Be base. See also 1679 above.

537.56:538.56:537.311.33 1681

Plasma Oscillations at Extremely High Frequencies—M. A. Lampert. (*J. appl. Phys.*, vol. 27, pp. 5–11; January, 1956.) The analysis presented is applicable to plasmas in impurity semiconductors as well as those in gas discharges. The design of mm-λ generators based on standing waves in such plasmas is considered; electron densities of the order of $10^{15}/\text{cm}^3$ are required. In a system discussed, an electron beam is shot into the plasma, which is confined between two parallel reflecting surfaces; these may be the faces of a wafer of semiconductor whose thickness determines the natural oscillation frequency. Problems introduced by the slowing-up of the electron beam in such a system are indicated.

538.1 1682
Magnetic Systems associated with Systems of Permanent Electric Currents and their Application to the Numerical Calculation of Fields—É. Durand. (*Ann. Phys., Paris*, vol. 10, pp. 883–907; November/December, 1955.) By superposing magnetic shells associated with the elementary tubes corresponding to an arbitrary distribution of currents, the associated magnetic systems are simply determined. In this way a scalar potential inside the currents can be defined. See also 3229 of 1955.

538.1 1683
Derivation of an Expression for the Scalar Potential of a Line Current in the Form of a Curvilinear Integral—É. Durand. (*C. R. Acad. Sci., Paris*, vol. 242, pp. 78–81; January 4, 1956.)

538.13 1684
Calculating the Distance between Equivalent Poles of a Bar Magnet—J. R. Boggs. (*Trans. Amer. geophys. Union*, vol. 36, pp. 487–488; June, 1955.)

538.221 1685
The Barkhausen Effect—R. S. Tebble. (*Proc. phys. Soc.*, vol. 68, pp. 1017–1032; December 1, 1955.) The only feasible mechanism to account for the phenomena associated with the Barkhausen effect is one in which the movement of a limited section of a 180° domain boundary is delayed by a nonmagnetic inclusion whose cross sectional dimensions lie within the range $1-2\times10^{-5}$ cm. Hysteresis losses in ferromagnetic materials may be reduced by the selective reduction of the number of inclusions whose size is within this critical range.

538.221 1686
Temperature Dependence of Ferromagnetic Anisotropy in Cubic Crystals—F. Keffer. (*Phys. Rev.*, vol. 100, pp. 1692–1698; December 15, 1955.) Theories advanced by Zener and by Van Vleck are reconciled; they afford respectively, low- and high-temperature approximations to the same physical picture, namely, an anisotropy decreasing with rising temperature, due to statistical fluctuations from alignment of anisotropically coupled neighbor spins.

538.3:52 1687
A Discussion on Magneto-hydrodynamics—(*Proc. roy. Soc. A*, vol. 233, pp. 289–406; December 29, 1955.) The text is given of papers presented at the discussion noted previously [3577 of 1955 (Ferraro)].

538.3:537.56 1688
Some Exact Solutions of the Lorentz Invariant Problem of the Motion of Two Electric F uids—J. J. Gibbons. (*Canad. J. Phys.*, vol. 33, pp. 819–823; December, 1955.)

538.566:535.42 1689
Some Problems on Obstacles placed in the Path of Electromagnetic Radiation—M. Bouix. (*Ann. Télécommun.*, vol. 10, pp. 243–251; November and pp. 254–260; December, 1955.) The relations between the incident, reflected and refracted fields at the surface separating two media are studied using vectorial analysis with a system of coordinates attached to the surface. Both media may be dielectrics or one may be conducting. The plane separating surface is discussed first and the analysis is extended to treat diffraction by a sphere; exact formulas are derived for the reradiation gain and the total diffusion surface.

538.566:535.43 1690
Tensor Scattering Matrix for the Electromagnetic Field—D. S. Saxon. (*Phys. Rev.*, vol. 100, pp. 1771–1775; December 15, 1955.) Theory presented previously 3105 of 1954 (Gerjuoy and Saxon) is extended to treat the vector field and to include absorption.

538.566:537.56 1691
Interaction of Centimetre Waves with a Plasma in the Presence of a Magnetic Field—F. Diamand, A. Gozzini, and T. Kahan. (*C. R. Acad. Sci., Paris*, vol. 242, pp. 90–93; January 4, 1956.) Experimental evidence of self-interaction was sought, using an AM wave of frequency 10 kmc in a circular waveguide containing a continuous discharge parallel to the direction of propagation and a transverse magnetic field. Absorption was observed, passing through a maximum at the field-strength value corresponding to the gyrofrequency. An expression for the modulation depth is derived in terms of carrier frequency, gyrofrequency and modulation frequency. The term "self-interaction" is preferred to "self-demodulation" since the modulation depth may be either increased or decreased, depending on the circumstances. Further experiments were made by transmitting an unmodulated 10-kmc wave through a plasma oscillating at low frequency in a neon tube of length 30 cm. The rf wave became strongly modulated, the form of the wave envelope was modified greatly by application of a magnetic field, while the modulation disappeared completely at the field strength corresponding to gyromagnetic resonance.

538.569.4 1692
Absorption of Microwaves and U.H.F. Radio Waves in Phenol, Cyclohexanol and 1-Bromo 2-Chloroethane—D. K. Ghosh. (*Indian J. Phys.*, vol. 29, pp. 161–166; April, 1955.)

538.569.4:535.33:546.171.1 1693
New Method for the Observation of Hyperfine Structure of NH_3 in a "Maser" Oscillator—K. Shimoda and T. C. Wang. (*Rev. sci. Instrum.*, vol. 26, pp. 1148–1149; December, 1955.)

538.569.4:539.15 1694
Nuclear Magnetic Resonance in Very Weak Fields—(*Helv. phys. Acta*, vol. 28, pp. 617–632; December 15, 1955. In French.)

Part 1—A Radio Spectroscope for Observation of Resonance between 15 and 2 kc—C. Manus, G. Béné, R. Extermann, and R. Mercier (pp. 617–625). The apparatus is described in detail. The signal/noise ratio is calculated and the result compared with values obtained experimentally.

Part 2—Study of Nuclear Magnetic Resonance between 2 and 0.5 Gauss—B. Cagnac, C. Manus, G. Béné, and R. Extermann (pp. 626–632). Proton-resonance experiments are described. Variation of resonance curves with hf amplitude and with the characteristics of the scanning field is investigated.

538.569.4:621.376.23 1695
Theory of the Autodyne Detector for Paramagnetic Resonance—F. Bruin and F. M. Schimmel. (*Physics*, vol. 21, pp. 867–876; November, 1955. In French.)

538.569.4.029.6:621.372.413 1696
Observation of Nuclear Quadrupole Resonances with a Coaxial-Cavity Spectrometer—S. Kojima, A. Shimauchi, S. Hagiwara, and Y. Abe. (*J. phys. Soc. Japan*, vol. 10, pp. 930–933; November, 1955.) A note on the construction of a spectrometer based on a two-cavity klystron oscillator, and its operation in the range 700 mc–1 kmc.

538.691 1697
The Stability of the Equilibrium Configuration of a Current-Carrying Wire in a Magnetic Field—C. Bernardini. (*R. C. Accad. naz. Lincei*, vol. 19, pp. 297–301; November, 1955.) The problem is considered in relation to the investigation of the trajectories of charged particles by the floating-wire method, as discussed by Loeb (78 of 1947). Analysis shows that in certain cases when the field has focusing properties the configuration of the wire is unstable. Application of the results to a betatron problem is briefly indicated.

GEOPHYSICAL AND EXTRATERRESTRIAL PHENOMENA

52:538.3 1698
A Discussion on Magneto-hydrodynamics—(See 1687.)

523:538.69 1699
Interplanetary Magnetic Fields and Cosmic Rays—L. Davis, Jr. (*Phys. Rev.*, vol. 100, pp. 1440–1444; December 1, 1955.) A discussion of the implications of the hypothesis that, as a result of solar corpuscular emission, a field-free region is produced round the sun, with a mean radius of the order of 200 times the distance between the sun and the earth.

523.16 1700
The Measurement of the Angular Diameter of Two Intense Radio Sources—R. C. Jennison and M. K. Das Gupta. (*Phil. Mag.*, vol. 1, pp. 55–75; January, 1956.) An interferometer using post-detector correlation is described and results of measurements of the diameter and structure of the radio stars Cygnus A and Cassiopeia A are given. The interferometer operates on 116.5, 125 or 132.5 mc and uses antennas spaced at up to 12 km, the remote antenna being connected via an 83-mc radio link to the correlator.

523.16 1701
Apparent Intensity Variations of the Radio Source Hydra-A—O. B. Slee. (*Aust. J. Phys.*, vol. 8, pp. 498–507; December, 1955.) Over a period of 12 months about 200 observations of the intensity of Hydra-A were compared with observations on other strong rf sources. The results indicate that Hydra-A is relatively much more variable, though no periodic changes have been detected. Possible mechanisms producing the intensity changes are considered.

523.16 1702
Rotation and other Motions of the Magellanic Clouds from Radio Observations—F. J. Kerr and G. de Vaucouleurs. (*Aust. J. Phys.*, vol. 8, pp. 508–522; December, 1955.) The motions have been studied by means of 21-cm-λ line radiation from interstellar hydrogen.

523.16 1703
The Angular Size of the Variable Radio Source Hydra-A—A. W. L. Carter. (*Aust. J. Phys.*, vol. 8, pp. 564–567; December, 1955.) Preliminary observations on 101 mc suggest that the size as well as the intensity of this source varies. See also 1701 above.

523.72+523.32]:538.56.029.6 1704
Observations of Solar and Lunar Radiation at 1.5 Millimeters—W. M. Sinton. (*J. opt. Soc. Amer.*, vol. 45, pp. 975–979; November, 1955.) Further observations have been made using the method described previously (3076 of 1952). Measured values of atmospheric absorption are greater than values of water-vapor absorption calculated by Van Vleck (3100 of 1947). The transmittances of some materials at 1.5 mm are tabulated.

523.72:551.593.5 1705
Investigation of Sky Brightness in the Spectral Region near 1μ during the Solar Eclipse of 30th June 1954—S. F. Rodionov and E. D. Sholokhova. (*C. R. Acad. Sci. U.R.S.S.*, vol. 105, pp. 676–679; December 1, 1955. In Russian.) The variation of the atmospheric infrared radiation excited by the incident solar ultraviolet radiation was investigated. Intensity variations observed at wavelengths of 1μ and 0.71μ indicate that the radiation from the

corona is richer in ultraviolet than the radiation from the sun as a whole.

523.72:621.396.822 **1706**

The Distribution of Radio Brightness over the Solar Disk at a Wavelength of 21 Centimetres: Part 3—The Quiet Sun—Two-Dimensional Observations—W. N. Christiansen and J. A. Warburton. (*Aust. J. Phys.*, vol. 8, pp. 474–486; December, 1955.) The observations reported in Part 2 (715 of 1954) are extended by using two multiple interferometers arranged at right angles, thus enabling the solar disk to be scanned in many different directions. From the data thus obtained the two-dimensional brightness distribution is reconstructed by a Fourier-analysis method. Marked limb-brightening in the equatorial zones is indicated, but none in the polar regions.

523.72:621.396.822 **1707**

Solar Brightness Distribution at a Wavelength of 60 Centimetres: Part 1—The Quiet Sun—G. Swarup and R. Parthasarathy. (*Aust. J. Phys.*, vol. 8, pp. 487–497, December, 1955.) Observations were made with a 32-element interferometer to check Stanier's results (1401 of 1950) obtained with a two-antenna interferometer. The observed limb-brightening is reasonably consistent with that reported by O'Brien and Tandberg-Hanssen (2607 of 1955), whereas Stanier found no limb-brightening. The divergencies may be related to actual differences consequent on the changing phase of the solar cycle.

550.385:523.7:523.165 **1708**

Correlation among Magnetic Storms, Solar Phenomena and Cosmic-Ray Storms—Y. Sekido, M. Wada, I. Kondoh, and K. Kawabata. (*Rep. Ionosphere Res. Japan*, vol. 9, pp. 174–180; September, 1955.)

551.510.535 **1709**

Movements in the Ionosphere—J. A. Ratcliffe. (*Nature Lond.*, vol. 177, pp. 307–308; February 18, 1956.) Report of Royal Astronomical Society discussion held in November, 1955. Methods of measuring the movements and results obtained are briefly indicated. An important piece of new information about the lower F region is that simultaneous observations on large-scale ripples and on the small-scale irregularities producing fading show that these two types of irregularity travel with the same speed.

551.510.535 **1710**

Movement of Sporadic-E Ionization—J. A. Harvey. (*Aust. J. Phys.*, vol. 8, pp. 523–534; December, 1955.) "The horizontal movement of patches of daytime sporadic E ionization has been observed by using a system of spaced pulse transmitters and a central recorder. The directions of movement are mainly towards the north and west, with speeds mainly between 40 and 80 m/second. These velocities differ in direction from the F region disturbances recorded at the same time and have only about half the speed."

551.510.535 **1711**

Electronic Collisional Frequency in the F-Region over Calcutta—S. Datta. (*Indian J. Phys.*, vol. 29, pp. 279–284; June, 1955.) Determinations of the collision frequency were made on the basis of Appleton's formula relating ionosphere reflection coefficient with the difference between the group and optical wave paths within the region. Values corresponding to different heights in the F layer are tabulated. The "most probable" value is 3.8×10^3 per second per electron.

551.510.535 **1712**

On the Influence of Electron-Ion Diffusion on the Electron Density and Height of the Nocturnal F_2 Layer (supplement)—T. Yonezawa. (*J. Radio Res. Labs., Japan*, vol. 2, pp. 281–291; July, 1955.) The influence of the earth's magnetic field on electron-ion diffusion will tend to reduce the atmospheric density in the F_2 region at night; a lower limit for the maximum density of 3×10^9 cm^{-3}, or 60 per cent of the value suggested in the earlier paper (751 of March), is possible. Other considerations tend to confirm the value of 5×10^9 cm^{-3} originally suggested, which agrees with extrapolations from rocket data if the true height of the F_2 layer is about 200 km.

551.510.535 **1713**

On the Occurrence of Spread Echoes in the F Region over Japan—I. Kasuya, S. Katano, and S. Taguchi. (*J. Radio Res. Labs., Japan*, vol. 2, pp. 329–339; July, 1955.) Analysis of published ionospheric data for Japan for the period 1949–1954, suggests that spread echoes occur more frequently in the north than in the south, chiefly at night, at the solstices and when solar activity is weak. Echoes of the most common type are attributed to reflections from irregularities in the upper regions of the F layer which are normally masked in daytime; others may be due to reflections from turbulences during magnetic storms, or to ionized clouds passing through the normal layer.

551.510.535 **1714**

Photoelectric Studies of the Night Sky Light: Part 4—M. Huruhata, H. Tanabe, and T. Nakamura. (*Rep. Ionosphere Res. Japan*, vol. 9, pp. 136–147; September, 1955.) An attempt is made to correlate variations of nightglow intensity with those of electron density in the F_2 layer; the results are inconclusive.

551.510.535:001.4 **1715**

Russian Ionosphere Terminology—G. F. Schultz. (PROC. IRE, vol. 44, p. 376; March, 1956.) Russian equivalents are given for about 30 English terms.

551.510.535:523.78:550.385 **1716**

Effect of the Solar Eclipse on the Lower Parts of the Ionosphere and the Geomagnetic Field—T. Nagata, Y. Nakata, T. Rikitake, and I. Yokoyama. (*Rep. Ionosphere Res. Japan*, vol. 9, pp. 121–135; September, 1955.) Changes in E-layer electron density observed at a number of stations during the solar eclipse of May 9, 1948 have been examined and the resulting changes in conductivity deduced. The effects are found to exist over a very much wider area than that eclipsed. The calculated modifications in the S_q current consequent upon the electron-density changes provide a satisfactory quantitative explanation of changes in the earth's magnetic field at the time of the eclipse.

551.510.535:525.624 **1717**

Lunar Tide in Sporadic E at Brisbane—J. A. Thomas and A. C. Svenson. (*Aust. J. Phys.*, vol. 8, pp. 554–556; December, 1955.) An analysis has been made of nighttime values of $h'E_s$ for the period December, 1952–November, 1953; results are tabulated and plotted on a 12-hour harmonic dial. The semidiurnal variation has a mean amplitude of 0.69 km and a mean phase of 6.7 hours. Results are compared with those of Martyn (1052 of 1949) and Matsushita (408 of 1954).

551.510.535:550.385 **1718**

The Electrical Conductivity of the Ionosphere and Disturbances of the Geomagnetic Field at Audio and Lower Frequencies—G. Grenet. (*C. R. Acad. Sci., Paris*, vol. 242, pp. 401–403; January 16, 1956.) On the basis of assumed values for collision frequency and maximum electron density for the E, F_1 and F_2 layers, values are calculated for the conductivity parallel and perpendicular to the magnetic field, and for periods corresponding to certain critical frequencies. The significance of the results is discussed in relation to the possibility of extraterrestrial origins for geomagnetic-field disturbances.

551.510.535:550.385 **1719**

Daily Variations of the Electrical Conductivity of the Upper Atmosphere as deduced from the Daily Variations of Geomagnetism: Part 1—Equatorial Zone—H. Maeda. (*Rep. Ionosphere Res. Japan*, vol. 9, pp. 148–165; September, 1955.)

551.510.535:550.385 **1720**

Studies on the Disturbances in F_2 Layer associated with Geomagnetic Disturbances—K. Sinno. (*Rep. Ionosphere Res. Japan*, vol. 9, pp. 166–173; September, 1955.) Reports on work published previously (3303 of 1953 and 3258 of 1955) are collected and discussed.

551.510.535:621.396.11 **1721**

Radio Observations of the Ionosphere at Oblique Incidence—Chapman, Davies, and Littlewood. (See 1850.)

551.594.5 **1722**

Preliminary Studies of the Distribution of Auroras in Alaska—C. T. Elvey, H. Leinbach, J. Hessler, and J. Noxon. (*Trans. Amer. Geophys. Union*, vol. 36, pp. 390–394; June, 1955.) "The analysis of auroral observations for 1951–53 from five stations spread over Alaska shows a zone at geomagnetic latitude 68° for which the incidence of auroras is independent of magnetic activity. At geomagnetic latitudes south of 67°, the incidence of auroras is markedly dependent upon magnetic activity."

551.594.5 **1723**

Auroral Heights over West-Central Canada—B. W. Currie. (*Canad. J. Phys.*, vol. 33, pp. 773–779; December, 1955.) Results of an analysis of parallactic photographs of auroras taken in 1933 at Chesterfield (63.3° N, 90.7° W) suggest that auroral heights in this region are slightly greater than those observed from Norway. There is no definite evidence of a change of height with time after sunset.

551.594.6 **1724**

Observations of Whistling Atmospherics at Geomagnetically Conjugate Points—M. G. Morgan, H. E. Dinger, and G. McK. Allcock. (*Nature, Lond.*, vol. 177, pp. 29–31; January 7, 1956.) Comparison of records obtained at points in N. America and in New Zealand appear to confirm Storey's theory (142 of 1954) that "whistlers" and "swishes" are produced as the atmospherics travel along the dispersive paths constituted by the geomagnetic flux lines between the northern and southern hemispheres.

LOCATION AND AIDS TO NAVIGATION

621.396.93:621.396.677.51:621.318.134 **1725**

Ferrite Aerials in Goniometer Direction Finders—Ziehm. (See 1622.)

621.396.96+621.396.93 **1726**

Symposium on Marine Communications and Navigation—(TRANS. IRE, vol. CS-3, pp. 1–72; March, 1955.) The full text is given of 24 papers presented at the symposium held at Boston, Mass., in October, 1954. The subjects discussed included electronic aids to the fishing industry, and the need for further developments and supplementary techniques in radar.

621.396.96 **1727**

A Radar System for Harbour Surveillance—A. Leconte. (*Onde élect.*, vol. 35, pp. 1147–1152; December, 1955.) Shore-based radar systems for harbor control are discussed and the installation at Dunkirk is described; the frequency used is between 9.345 and 9.410 kmc. Identification of ships by means of transponder beacons, either permanently installed or carried to the ship by the pilot, is suggested.

621.396.96 **1728**

Radar Warning Net uses Centralized Con-

trol—J. L. Lombardo. (*Electronics*, vol. 29, pp. 168–170; March, 1956.) Description of the SAGE (semiautomatic ground environment) system, which does not depend on voice communication or interpretation of tracks by individual operators. Computers are used to identify unknown objects by correlating radar tracks with flight plans.

621.396.96:551.578.1 1729
A Turnstile Polarizer for Rain Cancellation—P. A. Crandell. (TRANS. IRE, vol. MTT-3, pp. 10–15; January, 1955.)

621.396.963:628.972 1730
A Method of increasing the Ambient Illumination of Radar Operations Rooms without Reduction of Signal Detection Threshold—C. R. Barnard. (*Proc. IEE*, Part B, vol. 103, pp. 199–202; March, 1956.) A narrow-band optical filter is arranged on the face of the display cr tube, and the color of the illumination is chosen to be complementary to the response of the tube.

621.396.969:621.396.67 1731
Reflection of Electromagnetic Waves from Thin Metal Strips (Passive Antennae)—K. Lindroth. (*Kungl. tek. Högsk. Handl., Stockholm*, 62 pp.; 1955.) The accuracies of several previously described methods of calculating the current in the strips are compared.

621.396.969.32 1732
Microwave Vehicle-Speed Indicator—G. W. G. Court. (*Wireless Engr.*, vol. 33, pp. 66–74; March, 1956.) A Doppler-radar-type instrument developed at the New Zealand Dominion Physical Laboratory uses a hybrid waveguide junction to provide both transmitting and receiving channels, so that only a single antenna is required. Leakage from the klystron oscillator used as cw transmitter provides local-oscillator power for the homodyne detector. Ranges of several hundred yards are obtained on small cars. An estimate of the various possible errors is included.

MATERIALS AND SUBSIDIARY TECHNIQUES

533.583:539.16 1733
Use of Krypton-85 in measuring Gas Clean-up Rates—D. J. Harris and P. O. Hawkins. (*Nature, Lond.*, vol. 177, pp. 285–286; February 11, 1956.) Techniques for monitoring the cleanup rate in pre-tr tubes are briefly described. Radioactive krypton is more suitable than argon or xenon because of its long half-life and readily detectable radiation.

535.37+535.215]:537.311.33 1734
Cadmium Sulfide with Silver Activator—J. Lambe. (*Phys. Rev.*, vol. 100, pp. 1586–1588; December 15, 1955.) Further experiments are reported, the results of which are consistent with the model for CdS(Ag) suggested previously [3274 of 1955 (Lambe and Klick)].

535.37:546.472.21 1735
X-Ray Powder Diffraction Data for Hexagonal Zinc Sulphide—M. A. Short and E. G. Steward. (*Acta cryst.*, vol. 8, Part 11, pp. 733–734; November 10, 1955.)

535.376:546.472.21 1736
Electroluminescence in Disordered Zinc Sulphide—M. A. Short, E. G. Steward, and T. B. Tomlinson. (*Nature, Lond.*, vol. 177, pp. 240–241; February 4, 1956.) Experiments are briefly reported indicating that electroluminescence both in single crystals and in powders of Cu-activated ZnS may be associated with one-dimensional structural disorder.

537.226/.227 1737
Replacement of Ti in $BaTiO_3$ Ceramic by Si and Ge—K. W. Plessner and R. West. (*Proc. phys. Soc.*, vol. 68, pp. 1150–1152; December 1, 1955.) Permittivity/temperature curves are shown for $BaTiO_3$, $Ba(Ti_{0.9}Ge_{0.1})O_3$ and $Ba(Ti_{0.9}Si_{0.1})O_3$; the principal effect of introducing the Ge and Si is to reduce the peaks at the transitions at 120° and 10°C. Values of remanent polarization, coercive field and total permittivity are tabulated.

537.226/.227 1738
Very-Low-Temperature Study of the Dielectric Constant of Ferroelectric Alkaline Phosphates and Arsenates—S. Le Montagner, J. Le Bot, M. Hagene, F. Lasbleis, and M. Le Page. (*C. R. Acad. Sci., Paris*, vol. 242, pp. 475–478; January 23, 1956.) Anomalous variations corresponding to absorption maxima in the complex-dielectric-constant/temperature curves have been observed in the region of 60°–70°K at frequencies between 100 cps and 1 mc. Variation of the coercive force may be responsible for the effect, which is observed only in the ferroelectric phosphates and arsenates; *i.e.*, those of K, Rb and Cs.

537.226 1739
Dielectric Absorption in Dilute, Liquid, Polar Solutions: a New Approach—A. Fairweather. (*Proc. phys. Soc.*, vol. 68, pp. 1038–1042; December 1, 1955.) On the assumption that energy loss in a liquid polar dielectric is related to density rather than to viscosity, the relaxation time is shown to be proportional to $(a^6\rho/kT)^{1/2}$, where a is the molecular radius, ρ the density, k Boltzmann's constant and T the absolute temperature.

537.226:621.315.612.4:546.431.824–31 1740
Dependence of the Dielectric Properties of Ceramic $BaTiO_3$ for High Frequency Currents on the Technology of the Preparation of Samples—M. Jeżewski and T. Piech. (*Acta phys. polon.*, vol. 14, pp. 395–405; 1955.) Measurements were made on a series of samples prepared by grinding, pressing and resintering the previously prepared sample. The dielectric constant increases significantly with the amount of processing; the losses do not vary significantly.

537.226.2/.3.029.6 1741
Measurements of the Dielectric Constant and Loss Angle of Building Materials—M. Balachandran. (*Z. angew. Phys.*, vol. 7, pp. 588–593; December, 1955.) Measurements were made on brick, gypsum, cement, and various wood specimens at 10-cm λ, and on oak and beech also at 8.75- and 3.2-cm λ. The effects of water absorption are shown graphically.

537.227/.228:546.431.824–31 1742
Theory of Spontaneous [ferroelectric] Deformation of Barium Titanate—W. Kinase and H. Takahashi. (*J. phys. Soc. Japan*, vol. 10, pp. 942–952; November, 1955.)

537.227/.228.1:547.476.3 1743
Electrical After-Effects in Rochelle Salt—K. N. Karmen. (*Zh. eksp. teor. Fiz.*, vol. 29, pp. 533–534; October, 1955.) The observed changes of the charge/discharge characteristics following applicationf of a pulses electric field for various lengths of time are presented graphically and briefly discussed.

537.227:[546.32.882.5+546.33.882.5 1744
A Thermodynamic Treatment of Ferroelectricity and Antiferroelectricity in Pseudo-Cubic Dielectrics—L. E. Cross. (*Phil. Mag.*, vol. 1, pp. 76–92; January, 1956.) "The Kittel-Devonshire phenomenological treatment of antiferroelectricity is extended to the case of polarizations in three dimensions in a pseudo-cubic material. There are ten possible solutions of the proposed free energy equation, corresponding to nonpolar, ferroelectric, antiferroelectric and ferrielectric states, and expressions are derived for the polarization and dielectric stiffness coefficients in these forms." The theory is applied to $NaNbO_3$ and $KNbO_3$ and their solid solution $(NaK)NbO_3$.

537.227:546.431.824–31 1745
Dynamic Method for measuring the Pyroelectric Effect with Special Reference to Barium Titanate—A. G. Chynoweth. (*J. appl. Phys.*, vol. 27, pp. 78–84; January, 1956.) "Transient currents produced in single crystals of barium titanate when subjected to flashes of light are shown to be pyroelectric in origin. The illumination results in a small change in the temperature of the crystal which, in turn, causes the polarization to change. This change is recorded as a current in the external circuit. It is shown that from room temperature up to the Curie point, the pyroelectric current is consistent with the polarization as a function of temperature, as determined from hysteresis loop measurements. The technique proves to be a sensitive and nondestructive method for studying the state of polarization of a crystal. The technique is used to study the pyroelectric effect induced by applied static electric fields at temperatures above the Curie point. The results are consistent with Devonshire's theory of the ferroelectricity of $BaTiO_3$, and they confirm that the Curie point transition is of the first order."

537.311.33 1746
The Concept of the Hole in Semiconductors—J. L. Salpeter. (*Proc. IRE, Aust.*, vol. 16, pp. 427–442; December, 1955.) Use is made of the transmission line and wave-filter analogy to explain the concept of the hole. The behavior of semiconductors subjected to magnetic fields and mechanical forces and the thermoelectric power of semiconductors are discussed.

537.311.33 1747
Magnetic Susceptibility of Impurity-Trapped Electrons and Holes in Semiconductors—E. Mooser. (*Phys. Rev.*, vol. 100, pp. 1589–1592; December 15, 1955.) Calculations are made explicitly for donor impurities; similar reasoning holds for acceptors. At low temperatures there is an appreciable difference between the values of susceptibility of the electron gas with and without the impurities; this difference enables the presence of an impurity conduction band to be determined from magnetic measurements. Measurements on Si reported by Portis *et al.* (3342 of 1953) are interpreted in terms of the theory. A narrow donor band is found in Si containing 1.5×10^{18} P atoms/cm³, in agreement with Baltensperger's predictions (1451 of 1954).

537.311.33 1748
Impurity Band in Semiconductors with Small Effective Mass—F. Stern and R. M. Talley. (*Phys. Rev.*, vol. 100, pp. 1638–1643; December 15, 1955.) An approximate calculation of the energy states for the $1s$ band of metallic hydrogen is carried out for lattice constants smaller than those considered by Baltensperger (1451 of 1954). A simple transformation of the distance and energy scales makes the calculation applicable to impurities in a semiconductor. Optical measurements of the energy gap in InAs as a function of impurity content are reported. The effective carrier mass required to fit published optical data for InSb is about 0.03 m, as compared with 0.013 m found by cyclotron-resonance measurements.

537.311.33 1749
Interaction of Impurities and Mobile Carriers in Semiconductors—G. W. Lehman and H. M. James. (*Phys. Rev.*, vol. 100, pp. 1698–1712; December 15, 1955.) A comprehensive analysis is presented. The theory differs from others in predicting a marked temperature dependence of the activation energy; this results from the temperature dependence of the polarizability of the mobile carrier distribution.

537.311.33 1750
A Particular Form of the Equations govern-

ing the Propagation of Free Carriers in a Homogeneous Crystal Lattice of Junction Type in a Unidimensional System—A. Leblond. (*C R. Acad. Sci., Paris*, vol. 242, pp. 85–87; January 4, 1956.) Analysis is given for a semiconducter system comprising a number of parallel plane junctions. Equations permitting of solution by simple numerical integration are derived by choosing as unknown variables the numbers of free electrons and holes and the electric field strength; *I/V* characteristics can hence be deduced.

537.311.33 1751

Properties and Structures of Ternary Semiconducting Systems: Part 1—B. T. Kolomiets and N. A. Goryunova. (*Zh. tekh. Fiz.*, vol. 25, pp. 984–994; June, 1955.) An experimental investigation has shown that in the pseudobinary section $m\mathrm{Tl_2Se}\cdot n\mathrm{Sb_2Se_3}$ of the ternary system Tl-Sb-Se there is a compound $Tl_2Sb_2Se_4$ which is a typical *p*-type semiconductor. By altering the proportion of the constituents in the series $m\mathrm{Tl_2Se}\cdot n\mathrm{Sb_2Se_3}$ it is possible to obtain a large variety of semiconductors. Replacement of Sb by As in the system gives a new group of semiconductors of amorphous structure. It is suggested that a study of ternary systems should lead to the discovery of semiconductors with new basic properties.

537.311.33 1752

Bipolar Diffusion in Semiconductors at Heavy Currents—K. B. Tolpygo and I. G. Zaslavskaya. (*Zh. tekh. Fiz.*, vol. 25, pp. 955–977; June, 1955.) A solution is given of equations describing bipolar diffusion in a semiconductor in which there is an inversion of the sign of conductivity. The forward current is considered for a plane or hemispherical contact; in addition to "flooding" of the barrier layer by current carriers, the penetration of carriers of one sign into the region of opposite sign is of great importance. As a result, the total resistance of the system is much lower than that of a homogeneous semiconductor of the same thickness. Calculated voltage current characteristics for forward current are plotted.

537.311.33 1753

Electrical Properties of the Intermetallic Compounds Mg_2Si, Mg_2Ge, Mg_2Sn and Mg_2Pb—U. Winkler. (*Helv. phys. Acta*, vol. 28, pp. 633–666; December 15, 1955. In German.) Polycrystalline specimens were prepared by direct co-fusion of the ingredients. Measurements of conductivity, Hall constant and thermoelectric power over the temperature range 100°-1,100°K indicate that the compounds are true semiconductors; Mg_2Pb appears to be strongly degenerate.

537.311.33:535.215:546.289 1754

Negative Photoeffects in Semiconductors—F. Stöckmann. (*Z. Phys.*, vol. 143, pp. 348–356; December 12, 1955.) The observed decrease of conductivity on illuminating a Ge specimen which had previously been bombarded by fast electrons is discussed. This effect is due to the removal of minority carriers from impurity centers and their recombination with the majority carriers. The effect occurs most easily in semiconductors with doubly charged impurities in the lattice. A full account of the investigation is to be published in *Phys. Rev.*

537.311.33:536.2 1755

A New Method of measuring the Thermal Characteristics of Semiconductors—M. A. Chernyakova and A. F. Chudnovski. (*Zh. tekh. Fiz.*, vol. 25, pp. 1013–1018; June, 1955.) A single arrangement, based on a bridge circuit, is used to determine electrical conductivity σ, thermal conductivity γ, volume thermal capacity C, thermometric conductivity γ/C, and thermal admittance $\sqrt{\lambda C}$. The method is based on certain regularities of a nonstationary temperature field during the cooling (or heating) of a body; it is particularly convenient for obtaining thermal characteristics of thermistors.

537.311.33:538.63 1756

Experimental Investigation of Transverse Nernst-Ettingshausen Effect in Tellurium—I. V. Mochan. (*Zh. tekh. Fiz.*, vol. 25, pp. 1003–1012; June, 1955.)

537.311.33:538.632 1757

Theory of Hall Effect in Ionic Semiconductors—M. I. Klinger. (*Zh. eksp. teor. Fiz.*, vol. 29, pp. 439–448; October, 1955.) The Hall constant of ionic semiconductors is calculated using the method of steady states. The interaction between an electron and the polarization oscillations of the crystal is considered in the adiabatic and the weak-coupling approximations.

537.311.33:[546.28+546.289 1758

A Mathematical Analysis of Solute Redistribution during Solidification—V. G. Smith, W. A. Tiller, and J. W. Rutter. (*Canad. J. Phys.*, vol. 33, pp. 723–745; December, 1955.) It is shown and experimentally verified that *p-n* junctions may be produced during solidification in Ge and Si melts containing two suitable solutes; *e.g.*, Ga and Sb in Ge.

537.311.33:[546.28+546.289 1759

Statistica and Galvanomagnetic Effects in Germanium and Silicon with Warped Energy Surfaces—B. Lax and J. G. Mavroides. (*Phys. Rev.*, vol. 100, pp. 1650–1657; December 15, 1955.) Calculations based on the Boltzmann transport theory are applied to the warped energy surfaces which have been determined by the cyclotron-resonance experiments. Expressions are derived for the hole densities, conductivity, effective carrier masses, intrinsic carrier concentration, and Hall coefficient as a series expansion in terms of the anisotropy parameters of the warped surfaces.

537.311.33:546.28 1760

Exchange Effects in Spin Resonance of Impurity Atoms in Silicon—G. Feher, R. C. Fletcher, and E. A. Gere. (*Phys. Rev.*, vol. 100, pp. 1784–1786; December 15, 1955.) Observations lending support to Slichter's theory (151 of 1956) are reported.

537.311.33:546.289 1761

Observations of Dislocations along Grain Boundaries in Germanium Crystals—J. Okada. (*J. phys. Soc. Japan.* vol. 10, pp. 1018–1019; November, 1955.)

537.311.33:546.298 1762

On the Coupled Dislocations along a Grain Boundary—Y. Uemura. (*J. phys. Soc. Japan*, vol. 10, pp. 1020–1033; November, 1955.) Theoretical calculations are presented relevant to the observations of Okada (1761 above) and Oberly (745 of 1955.)

537.311.33:546.289 1763

Amphoteric Impurity Action in Germanium—W. C. Dunlap, Jr. (*Phys. Rev.*, vol. 100, pp. 1629–1633; December 15, 1955.) Impurities capable of acting either as donors or acceptors are discussed, gold being taken as an example: the effect depends on the presence of other impurities. The existence of a donor level at 0.05 ev above the valence band as well as two acceptor levels at 0.15 and 0.55 ev is confirmed.

537.311.33:546.289 1764

Carrier Capture Probabilities in Nickel-Doped Germanium—J. F. Battey and R. M. Baum. (*Phys. Rev.*, vol. 100, pp. 1634–1637; December 15, 1955.) "Nickel has been diffused into germanium in order to study the carrier capture probabilities of the two nickel acceptor levels. Measurements of minority carrier lifetime as a function of temperature show that the electron capture probability of low-resistivity *p*-type samples is temperature-independent. The electron capture probability of high-resistivity *p*-type samples increases exponentially with increasing temperature, as does the hole capture probability of high-resistivity *n*-type samples. Possible interpretations of the results are discussed."

537.311.33:546.289 1765

Thermal Acceptors in Vacuum Heat-Treated Germanium—R. L. Hopkins and E. N. Clarke. (*Phys. Rev.*, vol. 100, pp. 1786–1787; December 15, 1955.) An experiment is described which indicates that very few acceptor centers are introduced into Cu-free Ge by quenching from high temperatures provided care is taken to maintain the Ge surface free from impurities.

537.311.33:546.289 1766

Investigations of Surface Recombination Velocities on Germanium by the Photoelectromagnetic Method—T. M. Buck and W. H. Brattain. (*J. electrochem. Soc.*, vol. 102, pp. 636–640; November, 1955.) Ge specimens subjected to various surface treatments and to temperatures between 65° and 100°C were investigated using technique described by Moss *et al.* (748 of 1954). Results indicate that the method does not permit accurate calculation of surface recombination velocity.

537.311.33:546.289 1767

Surface States on Germanium—J. Lees and S. Walton. (*Proc. phys. Soc.*, vol. 68, pp. 1152–1153; December 1, 1955.) *I/V* characteristics of W contacts on *p*- and *n*-type Ge specimens with a range of resistivities are presented. The results are in agreement with Bardeen's surface-states theory (*Phys. Rev.*, vol. 71, pp. 717–727; May 15, 1947.)

537.311.33:546.289 1768

Modulation of the Surface Conductance of Germanium by Pulsed Electric Fields—G. G. E. Low. (*Proc. phys. Soc.*, vol. 68, pp. 1154–1157; December 1, 1955.) The effect found previously (2007 of 1955), that the free surface of *n*-type Ge is positive with respect to the bulk of the material in the presence of a pulsed negative field, is confirmed; it is explained as a capacitance effect resulting from the action of surface traps.

537.311.33:546.561-31 1769

Exciton Absorption in Cuprous Oxide—J. H. Apfel and L. N. Hadley. (*Phys. Rev.*, vol. 100, pp. 1689–1691; December 15, 1955.)

537.311.33:564.681.86 1770

Fast-Neutron Bombardment of GaSb—J. W. Cleland and J. H. Crawford, Jr. (*Phys. Rev.*, vol. 100, pp. 1614–1618; December 15, 1955.) Experimental results indicate that the charge-carrier concentration and mobility of *n*- and *p*-type GaSb decrease as a consequence of neutron bombardment. Effects obtainable by heat treatment subsequent to the bombardment are discussed.

537.311.33:564.682.19 1771

Pressure Dependence of the Resistivity, Hall Coefficient, and Energy Gap for InAs—J. H. Taylor. (*Phys. Rev.*, vol. 100, pp. 1593–1595; December 15, 1955.) Measurements have been made at pressures from 1 to 2,000 atm. Both resistivity and Hall constant increase exponentially over the range, the total resistivity increase being 19 per cent and the total Hall constant increase being 12 per cent at 201°C. The pressure coefficient of energy gap is deduced from the resistivity variation to be 8.8×10^{-6} ev/atm, and from the Hall constant variation to be 5.5×10^{-6} ev/atm; the latter value is considered the more accurate.

537.311.33:546.682.86 1772

Hall Effect and Conductivity of InSb—

H. J. Hrostowski, F. J. Morin, T. H. Geballe, and G. H. Wheatley. (*Phys. Rev.*, vol. 100, pp. 1672–1676; December 15, 1955.) The conductivity and Hall coefficient of high-purity single-crystal specimens of InSb have been measured over the temperature range 1.3°–700°K; semiconductor properties of the material are deduced.

537.311.33:546.682.86 1773
The Lifetime of Added Carriers in InSb—I. M. Mackintosh and J. W. Allen. (*Proc. phys. Soc.*, vol. 68, pp. 985–990; December 1, 1955.) Experimental optical-absorption curves of *n*-type and *p*-type samples of InSb are analyzed on the basis of the Roosbroeck-Shockley theory of radiative recombination (3258 of 1954), allowance being made for degeneracy. A decay time of 0.75 μs is indicated for a small disturbance in carrier concentration. The results suggest that the radiative process may be the predominant recombination mechanism in this material.

537.311.33:564.682.86 1774
Melting Patterns appearing on Single Crystals of InSb—M. F. Millea and C. T. Tomizuka. (*J. appl. Phys.*, vol. 27, pp. 96–97; January, 1956.)

537.311.33:669.046.54 1775
Electromagnetic Suspension of a Molten Zone—W. G. Pfann and D. W. Hagelbarger. (*J. appl. Phys.*, vol. 27, pp. 12–18; January, 1956.) A zone-melting method requiring no container is described. A rod of the material is held horizontally, clamped at both ends, and a direct current is passed through it. At the region where melting is to be effected a horizontal magnetic field is applied normal to the rod. The resulting vertical force on the rod balances the gravitational pull. Various applications are indicated, including the production of semiconductor junctions by the remelt or the rate-growing process.

537.311.62:546.811 1776
Surface Resistance of Tin in Superconducting State at a Frequency of 7.3×10^{10}c/s—P. A. Bezuglyi, A. A. Galkin, and G. Ya. Levin. (*C. R. Acad. Sci. U.R.S.S.*, vol. 105, pp. 683–684; December 1, 1955. In Russian.)

537.312.8:538.639:546.3-1-74-72 1777
Electrical Resistance of Iron-Nickel Alloys at Low Temperatures (14°–90°K) and its Change in a Strong Magnetic Field—E. Kondorski and I. Ozhigov. (*C. R. Acad. Sci. U.R.S.S.*, vol. 105, pp. 1200–1203; December 21, 1955. In Russian.) An experimental investigation of alloys containing between 40 per cent and 100 per cent Ni. The effect of heat treatment was also investigated. Results are presented graphically.

537.533:537.311.33 1778
Electron Bombardment Effects in Thin Dielectric Layers—W. E. Spear. (*Proc. phys. Soc.*, vol. 68, pp. 991–1000; December 1, 1955.) An investigation of primary- and secondary-electron currents is described for layers between 0.7 and 5 μ thick, of mica, pyrex, As_2S_3 and Sb_2S_3, using bombarding electron energies up to 50 kev and, in the case of mica, with fields up to 10^6 v/cm across the specimen. The values of primary and secondary currents for specimens of different thickness and material fall on common curves when plotted against a suitable independent variable. The secondary-current curves are interpreted in terms of the displacement of charge carriers in the space-charge field within the dielectric.

538.1:538.221 1779
Theory of Atomic Magnetic Moments in Ferromagnetic Materials—N. S. Akulov. (*C. R. Acad. Sci. U.R.S.S.*, vol. 105, pp. 935–938; December 11, 1955. In Russian.) Simple formulas are derived for elements and alloys on the basis of the zone theory.

538.221 1780
Ferromagnetic Domains in Permanent Magnet Materials—L. F. Bates. (*Research, Lond.*, vol. 8, pp. 462–472; December, 1955.) A general account is given of the domain concept and its application to ferromagnetic metals. Quantitative tests of contemporary theories by means of powder-pattern technique are described. Photographs and diagrams of powder patterns on alnico, columnar alcomax and other materials are reproduced.

538.221 1781
Technical Properties of Iron Powder Magnets—E. H. Carman. (*Brit. J. appl. Phys.*, vol. 6, pp. 426–429; December, 1955.) The coercive force, remanence and maximum energy product of compacts of iron prepared by hydrogen reduction of ferric oxide were measured as functions of the density of packing and the particle size. The results are presented graphically. The presence of a small percentage of oxide does not appreciably affect the quality of the magnets.

538.221 1782
Influence of Magnetic Field on the Precipitation Process of Ferromagnetic Phase in Cu-Co Alloy—T. Mitui and S. Miyahara. (*J. phys. Soc. Japan*, vol. 10, pp. 1023–1024; November, 1955.)

538.221:534.121.1 1783
[Mechanical] Damping in Iron-Nickel Alloys—R. Ochsenfeld. (*Z. Phys.*, vol. 143, pp. 357–373; December 12, 1955.) Apparatus for measuring the damping of flexural vibrations of the alloy strips is described. The vibrations, produced magnetically, were at frequencies between 200 and 1,300 cps. Results of measurements are discussed and compared with theoretical results; the contributions from magnetic and magnetomechanical hysteresis and from macroscopic and microscopic eddy currents are identified.

538.221:538.632 1784
Hall Effect, Spontaneous Magnetization and Temperature—E. A. Ascher. (*Helv. phys. Acta*, vol. 28, pp. 667–693; December 15, 1955. In French, with English summary.) Hall effect in ferromagnetic materials is studied on the basis of theory of spontaneous effects; a law is derived relating the spontaneous Hall effect to the spontaneous magnetization at a given temperature. Irreversible Fe-Ni alloys are used to permit the spontaneous magnetization to be varied without changing the temperature of the sample. See also 2337 of 1955 (Perrier and Ascher).

538.221:538.65 1785
The Magneto-elastic Properties of some Ferromagnetic Iron-Nickel Alloys—R. Ochsenfeld. (*Z. Phys.*, vol. 143, pp. 375–391; December 22, 1955.) An investigation of changes in elastic modulus with magnetization (ΔE effect) and with amplitude of vibration (δE effect) for 36 per cent and 60 per cent Ni strips. See also 1783 above.

538.221:538.652:546.74 1786
Residual Magnetization and Magnetostriction of Nickel Single Crystals—Y. Nakamura. (*J. phys. Soc. Japan*, vol. 10, pp. 937–941; November, 1955.) A report of measurements made on long cylindrical crystals at room temperature.

538.221:546.666 1787
Magnetic Properties of Erbium Metal—J. F. Elliott, S. Legvold, and F. H. Spedding. (*Phys. Rev.*, vol. 100, pp. 1595–1596; December 15, 1955.) Measurements indicate that the material becomes ferromagnetic at a temperature near 20°K.

538.221:621.318.124 1788
Mechanism by which Cobalt Ferrite heat-treats in a Magnetic Field—H. J. Williams, R. D. Heidenreich, and E. A. Nesbitt. (*J. appl. Phys.*, vol. 27, pp. 85–89; January, 1956.) Magnetic torque measurements and electron-diffraction observations on several Co and CoZn ferrites, interpreted in the light of previous work on Fe_2NiAl and alnico 5 [see *e.g.*, 172 of 1955 (Nesbitt *et al.*)], show that correlation between torque reversals and response to heat treatment in a magnetic field indicates the presence of fine precipitated particles of a second phase in the composition of the material.

538.221:621.318.134 1789
Paramagnetism of some Rare-Earth Ferrites—J. C. Barbier and R. Aléonard. (*C. R. Acad. Sci., Paris*, vol. 242, pp. 83–85; January 4, 1956.) Continuation of the investigation reported by Benoit (3319 of 1955.)

538.221:621.318.134 1790
Structure of Rare-Earth Ferrimagnetic Ferrites—F. Bertaut and F. Forrat. (*C. R. Acad. Sci., Paris*, vol. 242, pp. 382–384; January 16, 1956.) Discussion indicates that the spontaneous magnetization exhibited by these ferrites could not result from a perovskite structure but is consistent with a composition $Fe_5B_3O_{12}$ (B representing the rare earth) having the two-sublattice structure proposed by Néel (3275 of 1954.)

538.221:621.318.134:538.569.4 1791
Ferromagnetic Resonance in Manganese Ferrite Single Crystals—P. E. Tannenwald. (*Phys. Rev.*, vol. 100, pp. 1713–1719; December 15, 1955.) Two types of Mn ferrite were investigated at temperatures ranging from 4.2° to 300°K, using frequencies of 24, 9.1, 5.6, and 2.8 kmc. Resonance lines as narrow as 47 oersted were obtained; the width depends on crystal orientation, temperature and frequency. The anisotropy does not depend on frequency but increases rapidly at low temperature. Double resonances have been observed.

538.221:621.318.134:538.614 1792
Study of Magnetic Rotatory Polarization in Copper Ferrite at 10 kMc/s—F. Mayer. (*C. R. Acad. Sci., Paris*, vol. 242, pp. 81–83; January 4, 1956.) Measurements of the Faraday rotation are used to study the different properties of the cubic and quadratic crystal forms of Cu ferrite. The polarization-rotation-angle/magnetic-field characteristics are loops resembling the usual magnetization curves. Losses on introducing the two specimens in a waveguide are field-independent for the quadratic form and markedly field-dependent for the cubic form. Investigations of the polarization ellipticity indicate that the cubic form produces selective absorption.

538.221:621.385.833 1793
Depiction of Domains of a Ferromagnetic Material by an Electron-Optical Method—G. V. Spivak, N. G. Kanavina, I. S. Sbitnikova, and T. N. Dombrovskaya. (*C. R. Acad. Sci. U.R.S.S.*, vol. 105, pp. 706–708; December 1, 1955. In Russian.) Photographs of images (×50) obtained by the secondary-emission-microscope method [2739 of 1954 (Spivak *et al.*)] and by the powder-pattern method are compared.

538.221:621.385.833 1794
Magnetic Contrast in Electronic Mirrors and Observation of Domains in a Ferromagnetic Material—G. V. Spivak, I. N. Prilezhaeva, and V. K. Azovtsev. (*C. R. Acad. Sci. U.R.S.S.*, vol. 105, pp. 965–967; December 11, 1955. In Russian.) Further development of earlier work (1793 above) is reported. Microphotographs (×150) of electron-optical images of domain structures are shown.

538.569.3:621.372.56.029.63/.64 1795
R. F. Attenuators and Load Materials—Lichtman. (See 1647.)

546.3-1:541.57 1796
Covalent Alloys among the Intermetallic Compounds. The Compounds PrGe and CaGe—A. Iandelli. (*R. C. Accad. naz. Lincei*, vol. 19, pp. 307–313; November, 1955.)

621.319.2 1797
The Mechanism of some Electrets—K. Antenen. (*Z. angew. Math. Phys.*, vol. 6, pp. 478–484; November, 1955.) Measurements were made on carnauba-wax disks with thin silver electrodes on the faces and potential probes sealed at points round the circumference. The potential distribution through the disk was determined at temperatures of 35°, 50°, and 70°C. Charging and discharge currents exhibited the expected time variation. The results indicate that the electret effect in carnauba wax is due to the low conductivity of ions in the electric field.

MATHEMATICS

517 1798
Laplace Transformation—H. Goldenberg. (*Elect. Rev., Lond.*, vol. 157, pp. 1223–1224; December 23, 1955.) An elementary explanation of the Laplace transformation is given and illustrated by examples. The use of tables of Laplace transforms to find Heaviside pairs not easily obtainable by Heaviside calculus is demonstrated.

517:512.831 1799
The Solution of Linear Simultaneous Equations by Matrix Iteration—J. Guest. (*Aust. J. Phys.*, vol. 8, pp. 425–439; December, 1955.)

517.43 1800
Mikusiński's Operational Calculus—V. Doležal and J. Kurzweil. (*Slab. Obz., Prague*, vol. 16, pp. 582–592; November, 1955.) An introductory article which includes the fundamental theory of the calculus, its relation to the Laplace transform, and examples of its applications in circuit theory and the solution of ordinary differential equations with constant coefficients. The calculus is applicable in several cases where the Laplace transform method fails.

517.94:[535.13+538.561 1801
On Cauchy's Problem for Hyperbolic Equations and the Differentiability of Solutions of Elliptic Equations—P. D. Lax. (*Commun. pure appl. Math.*, vol. 8, pp. 615–633; November, 1955.) The Cauchy problem for symmetric hyperbolic systems of the first order is discussed; the class includes all equations in physics describing reversible time-dependent phenomena including Maxwell's equations, the equations of magnetohydrodynamics, etc. A theorem is presented on the differentiability of weak solutions of an elliptic equation of order $2m$.

517.948.3 1802
A New Method for solving Fredholm Integral Equations—C. Müller. (*Commun. pure appl. Math.*, vol. 8, pp. 635–640; November, 1955.)

519.283 1803
Statistical Techniques for reducing the Experiment Time in Reliability Studies—M. Sobel. (*Bell Syst. Tech. J.*, vol. 35, pp. 179–202; January, 1956.)

MEASUREMENTS AND TEST GEAR

535.24:535.37 1804
Direct Measurement of Quantity of Light in Rapidly Decaying Luminescence Processes—N. A. Tolstoi and I. A. Litvinenko. (*Zh. eksp. teor. Fiz.*, vol. 29, pp. 507–515; October, 1955.) An instrument for measuring the time integral of the light-quantum output in the rise and the decay of luminescence is described; circuit and block diagrams are given. The processes investigated have equivalent exponential-curve time-constants of between 10^{-6} and 10^{-1} seconds.

621.3:621.319.4:537.523.3 1805
The Detection of Corona Discharges in High-Voltage Air Capacitors—L. Medina. (*Aust. J. appl. Sci.*, vol. 6, pp. 453–457; December, 1955.) Corona discharge giving rise to increased power factor in capacitors used in ac bridges etc. may be detected by measurement of the direct component produced in the current through the capacitor.

621.3.018.4(083.74):621.385.029.6 1806
A Method of Forming a Broad-Band Microwave Frequency Spectrum—R. E. Wall, Jr, and A. E. Harrison. (TRANS. IRE, vol. MTT-3, pp. 4–10; January, 1955.) The beam-accelerating voltage of a klystron is modulated by two hf voltages, one frequency being an integral multiple of the other; the sidebands so produced are suitable for use as microwave frequency standards.

621.317:621.383.2 1807
The Photodianode: Modulation of the Differential Current by an Alternating Magnetic Field—Deloffre, Pierre, and Roig. (See 1895.)

621.317.3:621.374.3:621.372.8 1808
Waveguide Investigations with Millimicrosecond Pulses—A. C. Beck. (*Bell Syst. Tech. J.*, vol. 35, pp. 35–65; January, 1956.) Equipment for the generation, reception and display of 5-mμs pulses is described. Dominant-mode and multimode waveguide applications are considered. Resolution tests show the practicability with this technique of separating radar targets 4 feet apart. Pulses 70 db below the level of the outgoing pulse can be observed.

621.317.3:621.385.832.001.4 1809
Testing Cathode-Ray Tubes.—Nixon. (See 1919.)

621.317.3:621.397.6 1810
State of Standardization of Test and Measurement Methods for Television Transmission Technique—Müller. (See 1879.)

621.317.32:621.396.61 1811
A Method for the Direct Measurement of Spurious Emissions—S. Kurokawa, T. Takahashi, and M. Arai. (*J. Radio Res. Labs, Japan*, vol. 2, pp. 217–220; July, 1955.) Measurements in the frequency band 30–200 mc are effected by use of a directional coupler to connect a screened selective receiver and output meter to the feed line from the transmitter.

621.317.326:621.385.2:621.397.62 1812
The Response of Diode Circuits to Periodic Pulses—Suhrmann. (See 1883.)

621.317.33:621.384.622 1813
The Shunt Resistance of Linear Accelerators—W. Chahid. (*C. R. Acad. Sci., Paris*, vol. 242, pp. 244–247; January 9, 1956.) Application of the method of measuring cavity-resonator shunt resistance described previously (1324 of 1956). Results are compared with those obtained by the methods of Denis and Liot (1076 of 1948) and of Hall and Parzen (799 of 1954).

621.317.335 1814
Cell with Fixed Electrodes for Measurement of the Dielectric Constant of a Liquid—C. Abgrall. (*C. R. Acad. Sci., Paris*, vol. 242, pp. 76–78; January 4, 1956.) Details are given of the construction of a cell for use in the method described previously (1132 of 1954).

621.317.335.3.029.64 1815
The Measurement of Small Changes in Dielectric Constant by Means of a Cavity Wavemeter—E. S. Hotston and J. E. Houldin. (*J. sci. Instrum.*, vol. 32, pp. 484–485; December, 1955.) A modification of a cylindrical H_{01n} cavity-resonator design allows the dielectric constant to be determined from measurements including the length of the air-filled part of the resonator instead of the usual observation of the change of length of the resonator on insertion of the dielectric. At frequencies of about 9.6 kmc values obtained for dielectric constants of glass disks 0.08 inch thick were consistent to within one part in 750.

621.317.4:621.318.2 1816
Precision Apparatus for Investigations of Aging in Permanent Magnets—R. K. Tenzer. (*Arch. tech. Messen*, No. 239, pp. 285–288; December, 1955.) Apparatus developed in connection with the investigations described by Kronenberg (772 of 1954) is designed for ballistic measurements of induction using a compensation principle; the voltage pulse induced in the test coil when it is withdrawn from the permanent magnet is balanced against a pulse of known amplitude.

621.317.42.082.72 1817
A New Magnetic Flux Probe—J. E. Parton and G. D. Stairmand. (*J. sci. Instrum.*, vol. 32, pp. 464–467; December, 1955.) A differential-capacitance probe suitable for use in steady or transient fields of strength above 100 G is described. It comprises three parallel members, the middle one of which is current-carrying. This member is deflected by the magnetic field so that its capacitance to the earthed outer members changes. The change is detected by means of a bridge circuit.

621.317.7 1818
Electronic Measuring Instruments—E. H. W. Banner. (*Elect. Rev., Lond.*, vol. 157, pp. 1264–1267; December 30, 1955.) The different classes of commercially available voltmeter and testing set are indicated, and an example of each is briefly described.

621.317.729 1819
A Simple Equipment for solving Potential and other Field Problems—C. T. Murray and D. L. Hollway. (*J. sci. Instrum.*, vol. 32, pp. 481–483; December, 1955.) Two-dimensional field problems are solved by using, as an electrical analog, current flow in a sheet of ordinary paper, where pencil lines mark the electrode boundaries. Details of the circuit and construction of the equipment are given.

621.317.729 1820
An Electrolytic-Tank Equipment for the Determination of Electron Trajectories, Potential and Gradient—D. L. Hollway. (*Proc. IEE*, Part B, vol. 103, pp. 155–160; March, 1956. Discussion, pp. 163–165.) A description is given of equipment for testing either axially symmetric or two-dimensional systems; it can be switched to measure potentials, to mark equipotentials automatically, to measure potential gradients, and to trace electron trajectories. The accuracy is sufficient for most problems of electrode design.

621.317.729:538.691 1821
A Method of tracing Electron Trajectories in Crossed Electric and Magnetic Fields—D. L. Hollway. (*Proc. IEE*, Part B, vol. 103, pp. 161–163; March, 1956. Discussion, pp. 163–165.) An extension of Gabor's tangent method (*Nature, Lond.*, vol. 139, p. 373; February 27, 1937.) is used. Comparison of results with calculated paths for a trochoid indicates that the accuracy is satisfactory, being almost equal to that in purely electric fields.

621.317.73.029.64 1822
Automatic Plotter for Waveguide Impedance—H. L. Bachman. (*Electronics*, vol. 29,

pp. 184–187; March, 1956.) The input impedance of a waveguide component is automatically measured over the frequency range 8.5–9.6 kmc, the impedance locus in the reflection-coefficient plane being displayed on a cro screen. Comparison with slotted-line measurements indicates that the maximum errors in magnitude and phase of the reflection coefficient are 10 per cent and 5° respectively, occurring at the ends of the frequency band. See also TRANS. IRE, vol. MTT-3, pp. 22–30; January, 1955.

621.317.755 1823
A Multi-Trace Cathode-Ray-Tube Display—K. E. Wood and T. C. Keenan. (*Electronic Engng.*, vol. 28, pp. 105–107; March, 1956.) Equipment for displaying nine traces sequentially derives the switching waveform from a neon counter. Input frequencies up to 100 cps can be displayed.

621.317.755 1824
An Ultra-high-Speed Oscillograph—F. R. Connor. (*Proc. IEE*, Part B, vol. 103, pp. 178–181; March, 1956.) The instrument described has a linear sweep speed of 2.5 cm/mμs, with a full scan of 5 cm, and incorporates a cr tube with small plate systems. The Y-plate system is designed as a transmission line which can be either resonant or nonresonant, thus providing for narrow-band or wide-band matching. A coaxial-cable delay unit is included, and a calibrating circuit provides a 1.25-kmc timing waveform.

621.317.755 1825
Cathode-Ray Oscilloscope Intensity Modulator—R. F. Kemp. (*Rev. sci. Instrum.*, vol. 26, pp. 1120–1121; December, 1955.) A voltage derived by a push-pull differentiating amplifier from the vertical deflection signal is added to the brilliancy control voltage, thus preventing variation of trace brightness due to variation of writing speed.

621.317.755 1826
Equipment for the Vectorial Display of Alternating Voltages in the Frequency Range 5-215 kc/s—E. C. Pyatt. (*J. sci. Instrum.*, vol. 32, pp. 469–471; December, 1955.) A cro giving an Argand-diagram display is described; applications to measurements on electromechanical devices are indicated.

621.317.76 1827
Wavelength Measurement in the Millimeter Region—H. H. Theissing and J. McCue. (*Rev. sci. Instrum.*, vol. 26, pp. 1203–1204; December 1955.) Outline description of an interferometer arrangement using two nearly parallel semi-transparent metal films, interposed between source and detector.

621.317.761 1828
Electronic Device for measuring Reciprocal Time Intervals—E. F. MacNichol Jr. and J. A. H. Jacobs. (*Rev. sci. Instrum.*, vol. 26, pp. 1176–1180; December, 1955.) The device described, which is designed for the lower af range, converts a train of electrical pulses into a succession of hyperbolic waveforms of amplitude proportional to the interval between successive pulses. These waveforms are displayed on a cro; sudden changes in frequency are indicated immediately.

621.317.789.029.6 1829
A Film Radiometer for Centimetre Wavelengths—J. A. Lane. (*Nature, Lond.*, vol. 177, p. 392; February 25, 1956.) Preliminary experiments are briefly described on the development of a device affording the possibility of accurate substitution of dc power for cm-λ power. A narrow strip of resistive film is arranged transversely in a standard 3-cm-band waveguide, between the centers of the broad faces. With a reflecting plunger fixed at a distance $\lambda_g/4$ behind the strip, a voltage swr of 0.9 or better can be achieved over a 10 per cent bandwidth. The power can be determined by observing either the change of resistance or the rise in temperature.

621.318.4(083.74) 1830
A Standard of Mutual Inductance—J. T. Henderson and M. Romanowski. (*Canad. J. Phys.*, vol. 33, pp. 856–870; December, 1955.) The construction and measurement of a Campbell-type standard mutual inductor for the National Research Council of Canada is described. Its calculated value is 0.010 007 24_8 H, with an error $\ngtr$ 13 parts per million.

621.318.4(083.74) 1831
Considerations on the Primary Winding of the Campbell Standard Inductor—M. Romanowski and P. A. Fraser. (*Canad. J. Phys.*, vol. 33, pp. 871–885; December, 1955.) Estimates are made of the effect of the presence of the quartz cylinder and of the finite cross section of the primary wire on the value of the standard inductor described by Henderson and Romanowski (1830 above.)

OTHER APPLICATIONS OF RADIO AND ELECTRONICS

534–8 1832
Industrial Applications of Ultrasonics—E. G. Richardson. (*Brit. J. appl. Phys.*, vol. 6, pp. 413–415; December, 1955.) Modern techniques are described with particular reference to echo detecting, high-frequency agitation, and metallurgical applications. The possibilities and limitations of ultrasonics for these purposes are discussed.

538.566.029.6:541.126 1833
Microwave Observation of Detonation—J. L. Farrands and G. F. Cawsey. (*Nature, Lond.*, vol. 177, pp. 34–35; January 7, 1956.) A method of measuring the velocity of detonation of high explosives under contained conditions is described based on principles of microwave interferometry.

621–52:681.142 1834
Digital Methods in Control Systems—D. F. Nettell. (*Electronic Engng.*, vol. 28, pp. 108–114; March, 1956.) The application of digital computer techniques to factory automation is discussed, with special reference to the use of digital methods with existing analog installations.

621.317.39:531.71 1835
Noncontacting Gages for Nonferrous Metals—R. B. Colten. (*Electronics*, vol. 29, pp. 171–173; March, 1956.) Two gauges for Cu and Al from 0.003 to 0.5 inches thick are based on measurement of skin effect. Cu strip passing the pickup head is gauged and recorded at a rate of 300 feet per minute.

621.317.39:621.383.27 1836
Aerosoloscope counts Particles in Gas—E. S. Gordon, D. C. Maxwell, Jr., and N. E. Alexander. (*Electronics*, vol. 29, pp. 188–192; March, 1956.) Light scattered by an aerosol beam is received by a photomultiplier and the resulting random voltage pulses are analyzed in a pulse-height discriminator and counted in twelve groups, thus giving the number and size distribution of the particles. The instrument is accurate for particles of diameter 1–64 μ, and concentrations up to 10,000 particles/cm³ can be dealt with, at a maximum counting rate of 100 per second.

621.326.73 1837
A Uniform Blackbody Light Source excited by Radio Frequency—S. C. Peek. (*J. Soc. Mot. Pict. Telev. Engrs.*, vol. 64, pp. 671–673; December, 1955. Discussion, p. 673.) The lamp comprises a 5/16-inch tantalum carbide disk supported by a zirconium oxide rod and heated by rf induction. The lamp can be operated at a brightness of up to 50,000 candles per inch².

621.384.6:621.319.3 1838
An Electrostatic Particle Accelerator—D. R. Chick and D. P. R. Petrie. (*Proc. IEE*, Part B, vol. 103, pp. 132–145; March, 1956. Discussion, pp. 152–154.) Equipment combining a pressurized charged-belt es generator and a multisection ion-accelerator tube is described. Proton beams have been obtained with energy up to 3.25 mev and an energy resolution of 1 in 1,200.

621.384.612 1839
Synchrotron Oscillations in Strong-Focusing Accelerators—L. L. Goldin and D. G. Koškarev. (*Nuovo Cim.*, vol. 2, pp. 1251–1268; December, 1955. In English.) Linear theory is presented.

621.384.612 1840
Gas Scattering in a Strong-Focusing Electron Synchrotron—M. J. Moravcsik and J. M. Sellen, Jr. (*Rev. sci. Instrum.*, vol. 26, pp. 1158–1164; December 1955.)

621.385.833 1841
The EM 75 kV, an Electron Microscope of Simplified Construction—A. C. van Dorsten and J. B. Le Poole. (*Philips tech. Rev.*, vol. 17, pp. 47–59; August, 1955.) An instrument giving a resolving power of at least 100 Å has magnetic condenser, objective and projector lenses.

621.385.833 1842
The Testing of some Adjustable Permanent-Magnet Electron Lenses—G. Langner. (*Optik, Stuttgart*, vol. 12, pp. 554–562; 1955.)

621.385.833:538.221 1843
Magnetic Contrast in Electronic Mirrors and Observation of Domains in a Ferromagnetic Material—Spivak, Prilezhaeva, and Azovtsev. (See 1794.)

621.386:778.33:621.383.8:621.385.832 1844
X-Ray Images made Visible by Means of a Television Pickup Tube responding to X Rays—Keller and Ploke. (See 1901.)

621.387.422 1845
The Discharge Mechanism in an Argon-Filled Proportional Counter—K. Schütt. (*Z. Phys.* vol. 143, pp. 489–512; December 22, 1955.)

621.389 1846
Applications of the Optics of Electric Charges to Mass Spectrometry—R. Vauthier. (*Ann. Phys., Paris*, vol. 10, pp. 968–1025; November/December, 1955.)

621.9:537.523.4 1847
High-Frequency Electro-spark Machining of Hard Metals—(*Microtecnic*, vol. 9, pp. 267–271; 1955.) The technique discussed involves production of a nonoscillating spark discharge lasting a few microseconds, with current density of the order of 10⁵ A/mm². Some details are given of a machine with a spark frequency variable from 2,500 per second to tens of thousands per second.

PROPAGATION OF WAVES

621.396.11 1848
Propagation of Electromagnetic Waves over a Flat Earth across Two Boundaries separating Three Different Media—K. Furutsu. (*J. Radio Res. Labs, Japan*, vol. 2, pp. 239–279; July, 1955.) A theoretical paper. Formulas involving integrals are derived for field strength; calculated values are compared with observed values for several examples of propagation across a land/water boundary.

621.396.11:551.510.535 1849
Divergence Factor of the Wave reflected

from the Surface of the Ionosphere—H. Uyeda, T. Kitsunezaki, and Y. Arima. (*J. Radio Res. Labs, Japan*, vol. 2, pp. 311–327; July, 1955.) The effect of curvature of the surface of the ionosphere on the field strength of the reflected wave is discussed. A "divergence factor" expressing the energy loss on reflection from an infinitesimally small area is defined and a formula for it is deduced. The results for ellipsoidal and sinusoidal ionosphere surfaces are examined in detail.

621.396.11:551.510.535 1850

Radio Observations of the Ionosphere at Oblique Incidence—J. H. Chapman, K. Davies, and C. A. Littlewood. (*Canad. J. Phys.*, vol. 33, pp. 713–722; December, 1955.) Automatic vertical-incidence sounding equipment has been adapted for use in oblique-incidence measurements over the 2,355-km path between Ottawa and Saskatoon. Typical records are shown and discussed. Accepted theory relating vertical-incidence and oblique-incidence propagation is verified by comparison with vertical-incidence soundings taken at a station 200 km from the midpoint of the path. See also 1138 of 1955 (Cox and Davies).

621.396.11:621.396.674 1851

Propagation of Transient Fields from Dipoles near the Ground—H. Poritsky. (*Brit. J. appl. Phys.*, vol. 6, pp. 421–426; December, 1955.) The analysis presented is based on the resolution of a spherical wave into proper plane waves. A double-integral representation is obtained for the Hertz potential of the field. For a vertical dipole on the ground one of the integrations is carried out for the region above the ground and for a conical region underground, while the second integration is carried out for special directions and locations.

621.396.11.029.55 1852

Analysis of Sky-Wave Field Intensity—S. N. Mitra and R. B. L. Srivastava. (*Indian J. Phys.*, vol. 29, pp. 167–178; April, and pp. 227–242; May, 1955.) Measurements of the field strength of sw transmissions from Bombay, Calcutta and Madras made at Delhi over the period 1942–1952 are analyzed. The yearly, seasonal, and monthly variations and their correlation with sunspot numbers are shown graphically. An unexplained feature of the observations is the correlation of nighttime field strength with solar activity. The observations are compared with values calculated by the CRPL and SPIM methods; neither of these is strictly applicable to propagation conditions in India or in the tropics generally.

621.396.11.029.55 1853

Ionospheric Propagation of Decametre Waves and Form of Second-Marking Pulses in Standard Amplitude-Modulated Transmissions—J. Bouchard and A. Helaine. (*C. R. Acad. Sci., Paris*, vol. 242, pp. 480–482; January 23, 1956.) Continuation of the investigation reported previously by Bouchard (1783 of 1953.) Oscillograms of the time-signal pulses from WWV and WWVH have been recorded and examined in relation to propagation conditions at the relevant time. Various forms of distortion are observed.

621.396.11.029.55:551.510.535 1854

A Study of Ionospheric Propagation by means of Ground Back-Scatter—E. D. R. Shearman. (*Proc. IEE*, Part B, vol. 103, pp. 203–209; March, 1956. Discussion, pp. 232–235.) "The results of a year's observations in southern England of long-range back-scatter are analyzed. A pulse transmitter coupled to alternative directional antennas was used, and transmissions were made at noon each day on a number of frequencies between 10 and 27 mc. The echo patterns observed in winter were simple and were formed by echoes from the ground just beyond the skip distances for one- and two-hop F_2-layer propagation. In summer, however, ground echoes returning by way of the E_s, E and F_1 layers arrived nearly simultaneously and were difficult to distinguish. The marked increase in E_s ionization in summer could be seen clearly from the echo patterns. Examples of fixed frequency range-time recordings ($p't$) of back scatter are given. On one record echoes can be seen at ranges corresponding to each of the ground reflection points for four-hop F_2 propagation between England and Malaya. The application of the $p't$ technique to the direct measurement of maximum usable frequencies is described. To assess the accuracy of the back scatter technique of skip-distance measurement, comparisons were made between measured scatter ranges and ranges calculated from vertical-incidence ionosphere measurements. The measured ranges were consistently shorter than those calculated. It is uncertain whether this discrepancy arises from approximations in the theory used for the calculations from vertical-incidence data or from inadequate directivity in the antennas used in the scatter measurements. Comparisons of scatter ranges with direct measurements of muf over the same path are considered desirable to resolve this uncertainty."

621.396.11.029.55:551.510.535 1855

The Technique of Ionospheric Investigation using Ground Back-Scatter—E. D. R. Shearman. (*Proc. IEE*, Part B, vol. 103, pp. 210–223; March, 1956. Discussion, pp. 232–235.) "The skip distance in short-wave propagation is measured by observing the time delay of echoes scattered from the earth's surface beyond the skip distance. A theoretical study shows that the method should give good accuracy in determining skip distance, but can not yield unique values of the height and critical frequency of an ionospheric layer at a distant point. The radar equation is used to find the intensity of back scatter from the ground, and an approximate calculation indicates that the irregularities present on land and sea should be sufficient to explain the observed echo strength. The effect of ray focusing by the ionosphere is considered. Experimental results confirm the conclusions of other workers that the predominant sources of echoes are on the ground and not in the E region. An empirical correction for the effect of the earth's magnetic field shows that no error in the location of the sources is introduced by using no-field theory in the analysis of results."

621.396.11.029.55:551.519.535 1856

An Experiment to test the Reciprocal Radio Transmission Conditions over an Ionospheric Path of 740 km—R. W. Meadows. (*Proc. IEE*, Part B, vol. 103, pp. 224–226; March, 1956. Discussion, pp. 232–235.) "Two-way pulse transmissions made simultaneously on the same frequency (5.1 mc approximately) between Slough and Inverness (740 km) are described. An antenna common to transmitter and receiver was used at each terminal, and the fading patterns displayed at each end were compared visually: the Inverness display was relayed to Slough over a Post Office trunk line for this purpose. The fading of corresponding echoes was found to be nonreciprocal for about 1 per cent of the time during a total period of observation of about 15 daylight hours spread over 13 days in May, 1954. The precautions taken to ensure that the effects were ionospheric and not instrumental are outlined."

621.396.11.029.55:551.510.535 1857

An Experimental Test of Reciprocal Transmission over Two Long-Distance High-Frequency Radio Circuits—F. J. M. Laver and H. Stanesby. (*Proc. IEE*, Part B, vol. 103, pp. 227–232; March, 1956. Discussion, pp. 232–235.) "The results obtained both across the North Atlantic and between Australia and the United Kingdom show that at times the loss in both directions is substantially the same, and that at other times the loss difference can rise to values of the order of 5 or 10 db. Usually the loss differences were such that signals outwards from the United Kingdom suffered the greater attenuation, but without further evidence it would be unwise to assume that this tendency is permanent."

621.396.11.029.6:551.510.52 1858

On the Propagation of Ultra-short Waves beyond the Horizon—K. Tao. (*Japanese J. Geophys.*, vol. 1, pp. 27–79; May, 1954.) General analysis is presented for propagation in the diffraction region. The propagation modes are considered for a three-layer troposphere with the refractive index varying linearly with height in each layer. Refractive-index gradients are calculated from aerological data and standard propagation is studied by comparing calculated and observed values of field strength.

621.396.11.029.62 1859

Uses of Diffraction Effect of Mountains for V.H.F. Radiocommunication—T. Kono, M. Hirai, and Y. Uesugi. (*J. Radio Res. Labs., Japan*, vol. 2, pp. 293–309; July, 1955.) Results with a receiver placed in the diffraction field at a point where the received field strength is high and not critically dependent on location show that the field strength varies very little with time; reliable communication can be established over a distance of 300–400 km. See also 2093 of 1955 (Kono *et al.*).

621.396.11.029.62 1860

V.H.F. Propagation by Ionospheric Scattering and its Application to Long-Distance Communication—W. J. Bray, J. A. Saxton, R. W. White, and G. W. Luscombe. (*Proc. IEE*, Part B, vol. 103, pp. 236–257; March, 1956. Discussion, pp. 257–260.) "The paper describes an investigation of the propagation of vhf radio waves by scattering from the E-region of the ionosphere. The dependence of the characteristics of the received signal on frequency, distance and antenna directivity is examined, and observations are made on the diurnal and seasonal variations of the received signal strength; the results are discussed in relation to existing theories. Investigations are also described on the suitability of this form of propagation for the transmission of frequency-shift telegraphy signals, and for telephony signals transmitted by single-sideband amplitude modulation, and by phase modulation, of a carrier. A form of wave-angle diversity reception which yields a substantial improvement in the performance of a telegraphy system is described. The possible applications of vhf scatter propagation to commercial services are discussed."

RECEPTION

621.376.332:621.374.32 1861

Low-Distortion F.M. Discriminator—M. G. Scroggie. (*Wireless World*, vol. 62, pp. 158–162; April, 1956.) The operation of a resistance-coupled pulse-counting discriminator circuit is described. A circuit diagram of the limiter and discriminator and the characteristic curves are given.

621.396.812.3 1862

Diversity Reception with Correlated Signals—H. Staras. (*J. appl. Phys.*, vol. 27, pp. 93–94; January, 1956.) The variation of diversity advantage with degree of correlation of the signals at two spaced receivers is examined.

621.396.82 1863

Required Interference Protection Ratios for the Field Strengths of Two Medium-Wave Transmitters as a Function of their Frequency Separation—E. Belger and F. von Rautenfeld.

(*Tech. Hausmitt. NordwDtsch. Rdfunks*, vol. 7, pp. 235–237; 1955.) A preliminary report is presented of listener tests made on two simultaneous transmissions at frequencies in the region of 1 mc, using two commercially available broadcast receivers, one wide-band and the other narrow-band. The required interference protection ratios and the relative strengths of carrier and modulation interference effects are plotted as functions of frequency separation.

621.396.822:621.376.232.2 1864
On the Time Constants of Linear Detectors used in Radio Noise Measurements—K. Kawakami and H. Akima. (*J. Radio Res. Labs, Japan*, vol. 2, pp. 221–234; July, 1955.) The relations between output voltage and detector time constant are investigated for various types of radio noise and a method of waveform determination is deduced. Noise is classified according to the output characteristic obtained when the detector circuit constants are varied; a "sharpness factor" and a "fineness factor" are defined.

STATIONS AND COMMUNICATION SYSTEMS

621.39.001.11 1865
A Class of Binary Signaling Alphabets—D. Slepian. (*Bell Syst. tech. J.*, vol. 35, pp. 203–234; January, 1956.)

621.396.11.029.62 1866
V.H.F. Propagation by Ionospheric Scattering and its Application to Long-Distance Communication—Bray, Saxton, White, and Luscombe. (See 1860.)

621.396.41+621.395.43]:621.376.3 1867
An Extended Analysis of Echo Distortion in the F.M. Transmission of Frequency-Division Multiplex—R. G. Medhurst and G. F. Small. (*Proc. IEE*, Part B, vol. 103, pp. 190–198; March, 1956.) By a combination of analytical and semiempirical methods, Albersheim and Schafer's results (2022 of 1952) are extended to cover a wider range of cases. See also 247 of 1954 (Medhurst).

621.396.93+621.396.96 1868
Symposium on Marine Communications and Navigation—(See 1726.)

621.396.97:621.396.82 1869
Improvement of Reception in Shared-Channel Operation by means of Frequency Offset—E. Belger and F. von Rautenfeld. (*Tech. Hausmitt. NordwDtsch. Rdfunks*, vol. 7, pp. 232–234; 1955.) Listener tests indicate that the interference protection ratio required in a shared channel is increased if the carriers are separated by about 2 cps but is slightly reduced if the separation is about 15 cps. When the channel is shared by a number of transmitters two or three different frequencies may be used depending on the frequency constancy of the transmitters.

SUBSIDIARY APPARATUS

621.316.722.1 1870
Mains-Voltage Stabilizers—R. B. Stephens. (*Philips tech. Rev.*, vol. 17, pp. 1–9; July, 1955.) A fast-acting stabilizer is described combining features of the magnetic and feedback types. The voltage-sensitive element is a bridge containing an indirectly heated thermistor. A stability to within ±0.5 per cent over the temperature range 10–50°C. can be achieved for mains voltage fluctuations between 180 and 250 v, mains frequency variations between 47 and 51.5 cps, and load variations from no load to full load. Recovery time is 1–2 cycles.

621.35:539.169 1871
Nuclear Batteries: Types and Possible Uses—A. Thomas. (*Nucleonics*, vol. 13, pp. 129–133; November, 1955.)

621.352.32 1872
Depolarization of Electrochemical Cells containing Manganese Dioxide—J. Brenet, P. Malessan, and A. Grund. (*C. R. Acad. Sci., Paris*, vol. 242, pp. 111–112; January 4, 1956.)

621.355 1873
Recent Patents on Electrical Accumulators—L. Jumau. (*Rev. gén. Élect.*, vol. 64, pp. 537–554; November and pp. 602–616; December, 1955.) For previous review see 2230 of 1954.

TELEVISION AND PHOTOTELEGRAPHY

621.397.24 1874
Developments in Closed-Circuit Television—M. H Kraus. (*Elect. Engng., N. Y.*, vol. 74, pp. 974–979; November, 1955.) Multichannel distribution systems are discussed with particular reference to systems installed at Fort Monmouth and at the Case Institute of Technology. To be published in *Trans. AIEE*, Part I, *Communication and Electronics*, vol.74, 1955.

621.397.5 1875
American Colour Television: the Present State—D. C. Birkinshaw. (*J. Telev. Soc.*, vol. 7, pp. 509–515; October/December, 1955.) Report based on a survey made in April, 1955. It is concluded that premature launching of color television in Great Britain should be guarded against, that the picture tube is of paramount importance, and that a more sensitive camera is needed to make outside broadcasts satisfactory.

621.397.5:535.623 1876
Recent Developments in Colour Television—L. C. Jesty. (*J. Telev. Soc.*, vol. 7, pp. 488–508; October/December, 1955.) Text of a paper read to the Society in April, 1955. Various recent experiments in the USA and Great Britain are referred to. The importance of the picture tube is emphasized and possible alternatives to the tricolor-phosphor-dot shadow-mask type are mentioned, including flat constructions. Fundamental changes in television transmission systems by 1970 or 1980 are considered likely; for instance, a system in which each picture point is permanently associated with an individual channel would not be impossible.

621.397.6:535.623 1877
Fixing the Value of the Colour Carrier in a European Colour-Television System based on the N.T.S.C. System—F. Jaeschke. (*Tech. Hausmitt. NordwDtsch. Rdfunks*, vol. 7, pp. 224–228; 1955.) Investigations of the best method of adapting the NTSC system to the 625-line standards lead to the recommendation of a color-subcarrier frequency of 4.2109375 mc; a fixed phase relation between sound and color carriers is then possible. Combinations of frequency dividers, modulators and filters for effecting the necessary frequency conversions are described. See also 1878 below.

621.397.6:535.623 1878
The Position of the Colour Subcarrier in a Possible Adaptation of the N.T.S.C. System to the 625-Line C.C.I.R. Standard—F. Below and E. Schwartz. (*Tech. Hausmitt. NordwDtsch. Rdfunks*, vol. 7, pp. 229–232; 1955.) The frequency corresponding on the CCIR standard to the NTSC color-subcarrier frequency is about 4.26 mc. Reasons are given for choosing a lower frequency, particularly 4.1015625 mc; this is easier to divide than that recommended by Jaeschke (1877 above). A simple frequency-conversion arrangement is described. The final choice will be influenced by results of experiments in progress.

621.397.6:621.317.3 1879
State of Standardization of Test and Measurement Methods for Television Transmission Technique—J. Müller. (*Tech. Hausmitt. NordwDtsch. Rdfunks*, vol. 7, pp. 209–216; 1955.) Test methods recommended by the German authorities are discussed and compared with those used in other countries. See also 1489 of 1956 (Macek).

621.397.61 1880
Black-Level Control in Television Pick-Up Apparatus—W. Dillenburger. (*Tech. Hausmitt. NordwDtsch. Rdfunks*, vol. 7, pp. 217–223; 1955.) An examination is made of the extent to which the fly-back potential of different types of pickup apparatus bears a constant relation to picture black level. Clamp circuits are discussed; operation is facilitated by black-level control at the lowest brightness level. The control process is imperceptible with circuit time constants of 0.5–1 second. An improved automatic black-level control circuit is described.

621.397.62:535.623 1881
Color Television Receiver Design—a Review of Current Practice [in the U.S.A.]—R. G. Clapp, E. G. Clark, G. Howitt, H. E. Beste, E. E. Sanford, M. O. Pyle, and R. J. Farber. (PROC. IRE, vol. 44, pp. 297–321; March, 1956.) The review deals with the design of commercial receivers using shadow-mask picture tubes.

621.397.62:535.623 1882
Experimental Colour Receiver—H. A. Fairhurst. (*Wireless World*, vol. 62, pp. 112–118; March and pp. 183–187; April, 1956.) The design of a receiver for the British NTSC system (3095 of 1955) is described. A 21-inch RCA shadow-mask cr tube is used.

621.397.62+621.317.326]:621.385.2 1883
The Response of Diode Circuits to Periodic Pulses—R. Suhrmann. (*Nachrichtentech. Z.* vol. 8, pp. 659–665; December, 1955.) Analysis is presented relevant to the operation of diodes for restoring the dc component in television receivers and for peak-voltage measurements. Calculations are based on the initial exponential region of the diode characteristic. For practical purposes the resistance of the diode during the charging of the associated capacitor can be assumed constant; its value may be anything from 1 to 100 kΩ.

621.397.7 1884
The Marconi Television Centre—T. W. Pace. (*J. Telev. Soc.*, vol. 7, pp. 520–522; October/December, 1955.) Description of a studio in London, specially equipped for equipment testing and demonstrating and for personnel training.

621.397.813:621.397.611 1885
Television Vertical Aperture Compensation—A. C. Schroeder and W. G. Gibson. (*J. Soc. Mot. Pict. Telev. Engrs.*, vol. 64, pp. 660–670; December, 1955.) A method is described involving defocusing and refocusing at a rapid rate, thus yielding high- and low-resolution signals whose difference gives the aperture-compensated signal. A similar method using vertical-deflection wobble rather than focus wobble results in vertical aperture compensation only.

TRANSMISSION

621.396.61:621.317.32 1886
A Method for the Direct Measurement of Spurious Emissions—Kurokawa, Takahashi, and Arai. (See 1811.)

TUBES AND THERMIONICS

537.58:537.311.33 1887
Thermionic Constants of Semiconductors—K. S. Krishnan and S. C. Jain. (*Nature, Lond.*, vol. 177, p. 285; February 11, 1956.) The method of determining the constants described previously [3467 of 1952 (Jain and

Krishnan)] is used to investigate Ni ribbons coated with triple carbonates of Ba, Sr and Ca. The currents corresponding to zero field fitted Richardson's equation well, with $\phi=1.55$ ev and $A=48$ A. cm^{-2} deg^{-2}.

621.314.63 1888

Note on a Particular [semiconductor] Structure permitting Production of High-Frequency Oscillations—A. Leblond and R. Gentner. (*C. R. Acad. Sci., Paris*, vol. 242, pp. 621–623; January, 1956.) Experiments have been made with a *p-i* diode having metal electrodes making linear-resistance contacts. For thicknesses of the *i* region not greater than about a dozen microns, the low-temperature characteristic exhibits a negative-resistance region; stable relaxation oscillations at 35 mc have been observed.

621.314.632:537.311.33 1889

The Influence of Frequency on the Rectifying Properties of Semiconducting Diodes at Low Alternating Voltages—S. G. Kalashnikov and N. A. Penin. (*Zh. tekh. Fiz.*, vol. 25, pp. 1111–1123; June, 1955.) The frequency dependence of the rectified current is explained in terms of the capacitance of the *p-n* junction. This capacitance is due to the injection of carriers into the junction, and also to the displacement current. Simple expressions are derived for the limiting frequency and the frequency dependence of the rectified current under various operating conditions. The effects of the semi-conductor properties on the frequency characteristics are also discussed.

621.314.7 1890

Diffused Emitter and Base Silicon Transistors—M. Tanenbaum and D. E. Thomas. (*Bell Syst. Tech. J.*, vol. 35, pp. 1–22; January, 1956.) Techniques are described for making Si *n-p-n* transistors by diffusing impurities from the vapor phase. Base layers 3.8×10^{-4} cm thick have been produced. Characteristics are presented of a transistor for which $\alpha_0=0.97$ and cutoff frequency is 120 mc. The structure and design of these transistors are discussed. For a brief version see *Electronics*, vol. 29, pp. 137–139; February, 1956 (Carroll).

621.314.7 1891

A High-Frequency Diffused-Base Germanium Transistor—C. A. Lee. (*Bell Syst. Tech. J.*, vol. 35, pp. 23–34; January, 1956.) Techniques of impurity diffusion and alloying in Ge are discussed. Examples are given of Ge *p-n-p* junction transistors in which $\alpha_0=0.98$ and cutoff frequency is 500 mc. For a brief version see *Electronics*, vol. 29, pp. 137–139; February, 1956 (Carroll).

621.314.7:621.3.015.3 1892

Transfer Characteristic of Semiconductor Triodes—E. I. Adirovich and V. G. Kolotilova. (*C. R. Acad. Sci. U.R.S.S.*, vol. 105, pp. 709–712; December 1, 1955. In Russian.) An approximate expression is given for a function $g(t)$ in terms of parameters of the region between the emitter and collector, and the expression is used in deducing the effect of (*a*) a step and (*b*) a rectangular emitter current pulse.

621.314.7:621.373.431.2 1893

Junction Transistors with Alpha Greater than Unity—H. Schenkel and H. Statz. (Proc. IRE, vol. 44, pp. 360–371; March, 1956.) When the collector voltage of a junction transistor is raised to a level just below breakdown voltage, multiplication of charge carriers occurs and the alpha value rises above unity. The transistor characteristic corresponding to this condition of operation is investigated; the characteristic may be negative over a limited region. A free-running blocking oscillator using one transistor, operated in this condition, and no transformer is described.

621.314.7:621.396.822 1894

Measurements of Spontaneous Fluctuations in Currents with Different Carriers in Semiconductor Barrier Layers—W. Guggenbühl and M. J. O. Strutt. (*Helv. phys. Acta*, vol. 28, pp. 694–704; December 15, 1955. In German.) Measurements under "white-noise" conditions indicate that when current in *p-n* junctions is produced either by applied voltage or by spontaneous creation of carriers, the fluctuations are consistent with Schottky's equations. In some recently developed alloyed-junction transistors the junction superimposes no additional fluctuations on the injected current, so that noise factors as good as those of high-vacuum tubes can be obtained. See also 2778 and 3781 of 1955.

621.383.2:621.317 1895

The Photodianode: Modulation of the Differential Current by an Alternating Magnetic Field—L. Deloffre, É. Pierre, and J. Roig. (*C. R. Acad. Sci., Paris*, vol. 242, pp. 98–100; January 4, 1956.) The device described previously (1737 of 1955 and back references) can conveniently be operated with a magnetic field of the order of 30 oersted applied parallel to the anodes. Frequencies up to 75 kc have been used.

621.383.27 1896

High-Speed Electron Multiplication by Transmission Secondary Electron Emission—E. J. Sternglass. (*Rev. sci. Instrum.*, vol. 26, p. 1202; December, 1955.) Electron multipliers based on secondary emission from the rear sides of a series of plane-parallel insulating films is suggested. Tests on an experimental seven-stage device gave a delay in the response of $(3\pm1)\times10^{-9}$ second, with a pulse rise time of 10^{-9} second. The results are discussed in relation to the use of such devices for resolving short time intervals.

621.383.4:535.371.07 1897

Solid-State Image Intensifiers—G. Diemer, H. A. Klasens, and J. G. van Santen. (*Philips Res. Rep.*, vol. 10, pp. 401–424; December, 1955.) "A theory is given of the characteristics of solid-state image-intensifying screens consisting of a photoconducting and an electroluminescent layer, including the influence of positive internal feedback and negative electrical feedback. The possibilities of brightness as well as contrast amplification are discussed. With intermittent irradiation it is possible to increase the amplification factor by storage, due to the decay, or by triggering of a feedback amplifying-screen. In the latter case the gradation need not be lost. The dimensioning of the parameters with regard to specific applications (*e.g.*, radar, X-ray images, television) is discussed. Preliminary experimental results are in agreement with theory. With X rays a brightness-amplification factor of 30 was obtained with respect to a normal fluorescent X-ray screen."

621.383.42 1898

Modifications of the Spectral Sensitivity Curve of Selenium Photocells under the Influence of Temperature Variations—G. Blet. (*C. R. Acad. Sci., Paris*, vol. 242, pp. 95–98; January 4, 1956.) Measurements were made on cells of various types, at temperatures down to that of liquid helium. Complex variations of a generally similar nature were observed in all cases. Some results are shown graphically.

621.383.5:546.28:621.396.822 1899

Photovoltaic Noise in Silicon Broad Area *p-n* Junctions—U. F. Gianola. (*J. appl. Phys.*, vol. 27, pp. 51–54; January 4, 1956.) Photovoltaic cells of the type described by Fuller and Ditzenberger (1068 of 1955) exhibit a $1/f$ noise power spectrum under constant illumination. With varying illumination intensity the noise voltage exhibits a pronounced maximum. It is suggested that fluctuations in the primary photocurrent are produced as a result of traversing the junction; experimental evidence is presented in support of this view.

621.383.5:546.28:621.396.822 1900

Noise in Silicon *p-n* Junction Photocells—G. L. Pearson, H. C. Montgomery, and W. L. Feldmann. (*J. appl. Phys.*, vol. 27, pp.91–92; January, 1956.) "A silicon *p-n* junction photocell prepared by the gaseous diffusion process and biased in reverse showed no noise in excess of shot noise down to a frequency of 80 cps in a dry atmosphere. In a humid atmosphere the excess noise was a factor of 3×10^{6} above shot noise at 100 cps and showed the familiar $1/f$ spectrum."

621.383.8:621.385.832:621.386:778.33 1901

X-Ray Images made Visible by Means of a Television Pickup Tube responding to X Rays—M. Keller and M. Ploke. (*Z. angew. Phys.*, vol. 7, pp. 562–571; December, 1955.) An iconoscope tube with an amorphous selenium photosensitive screen is described. The Se layer is 150 μ thick, possesses good storage properties and is not affected by the atmosphere. By using this tube in a closed-circuit television system, high luminosity and high contrast X-ray images are obtainable.

621.385 1902

Irrotational Electron Beams—J. Coste and J. L. Delcroix. (*C. R. Acad. Sci., Paris*, vol. 242, pp. 236–238; January, 9 1956.) Theory presented by Gabor (362 of 1946) is extended to deal with relativistic beams. The general equation for monodromic irrotational beams is derived.

621.385.029.6 1903

Plasma Oscillations and Resonance Frequencies in a Magnetron in the Brillouin State—J. Coste and J. L. Delcroix. (*C. R. Acad. Sci., Paris*, vol. 242, pp. 87–90; January 4, 1956.) The system considered is a cylindrical whole-anode magnetron with the electrons describing circles round the axis. Analysis is based on a perturbation method. In general, the oscillations in the transverse plane comprise both radial and tangential components. Resonance frequencies are calculated by considering the anode/cathode system as a coaxial cavity.

621.385.029.6 1904

The O-Type Carcinotron Tube—P. Palluel and A. K. Goldberger. (Proc. IRE, vol. 44, pp. 333–345; March, 1956.) The O-type carcinotron is a backward-wave oscillator tube developed in France. Starting conditions deduced theoretically are compared with experimental results. The effects of reflections at the ends of the delay line are discussed and approximate expressions are derived for the efficiency and for frequency pushing. Design and performance data are given for a series of tubes in production; each type covers about one octave, the whole series covering the frequency range 1–12 kmc. The maximum beam voltage is 1.5 kv and the rf outputs range from 100 mw to 1 w.

621.385.029.6(083.7) 1905

I.R.E. Standards on Electron Devices: Definitions of Terms related to Microwave Tubes (Klystrons, Magnetrons, and Traveling Wave Tubes), 1956—(Proc. IRE, vol. 44, pp. 346–350; March, 1956.) Standard 56 IRE 7.S1.

621.385.029.6:537.533 1906

Growing Waves due to Transverse Velocities—J. R. Pierce and L. R. Walker. (*Bell Syst. Tech. J.*, vol. 35, pp. 109–125; January, 1956.) Conditions are derived for the propagation of antisymmetrical and symmetrical growing waves in neutralized electron beams in which all electrons have the same velocity in the direction of propagation, but in which there are streams of two or more velocities normal to the direction of propagation.

621.385.029.6:621.372.2 1907

Definition, Measurement and Character of the Phase Velocities in Systems with Periodic Structure—B. Epsztein and G. Mourier. (*Ann. Radioélect.*, vol. 10, pp. 64–73; January, 1955.) Analysis is presented elucidating the operation of lines with periodic structure in traveling-wave tubes.

621.385.029.6:621.372.2 1908

Investigation of an Interdigital Line operating in the Vicinity of the π Mode—A. Leblond. (*Ann. Radioélect.*, vol. 10, pp. 83–91; January, 1955.) The effect of radiation from the line is examined; though not in general negligible, it is not great enough to invalidate determinations of π-mode frequency and field distribution reported previously [1204 of 1955 (Leblond and Mourier)].

621.385.029.6:621.373.423 1909

Investigation of an Interdigital Line used as Anode Circuit for an U.H.F. Magnetron Oscillator. Distortions of the Electromagnetic Field—A. Leblond. (*Ann. Radioélect.*, vol. 10 pp. 20–41; January, 1955.) Continuation of earlier work (289 of 1954). Effects due to mismatch of the output circuit are studied; these include modifications of the field distribution as compared with the unloaded condition for the same mode, and frequency pulling. Analysis is based directly on Maxwell's equations, without any simplifying assumptions.

621.385.032.2 1910

Determination of the Shapes of Electrodes for Pierce-Type Electron Guns—R. Hechtel. (*Telefunken Ztg*, vol. 28, pp. 222–226; December, 1955. English summary, pp. 264–265.) A mathematical method is developed for obtaining a converging beam; its application is illustrated by the design of an electron gun with a semiaperture angle of 45°.

621.385.032.2:537.533 1911

New Points of View in the Design of Electron Guns for Cylindrical Beams of High Space Charge—M. Müller. (*J. Brit. IRE*, vol. 16, pp. 93–94; February, 1956.) English translation of paper abstracted in 2478 of 1955.

621.385.032.21:537.533 1912

Electron Emission from a Lattice Step on Clean Tungsten—J. K. Trolan, J. P. Barbour, E. E. Martin, and W. P. Dyke. (*Phys. Rev.*, vol. 100, pp. 1646–1649; December 15, 1955.) Experiments using pulsed T-F (temperature and field) emission are described; they afford the basis of technique for studying the transport of cathode material.

621.385.032.21:621.396.822 1913

The Influence of Cathode Standing Waves on Valve Stability—W. W. H. Clarke. (*Brit. J. appl. Phys.*, vol. 6, pp. 433–441; December, 1955.) Experimental results indicate that the changes in the space-charge patterns of the virtual cathode of a tube are determined by the local variations of emission properties and by the boundary conditions of the cathode. Each pattern is associated with a particular current characteristic, so that a tube can have several preferred emission levels for constant applied potentials, intermediate values of current being associated with patterns in a slightly unstable condition. The patterns change coherently and cause discrete current changes. The flicker effect may be related to these changes.

621.385.032.216 1914

Diffusion of Impurity Atoms in an Oxide Cathode through the Interface Layer—N. D. Morgulis and Yu. G. Ptushinski. (*Zh. tekh. Fiz.*, vol. 25, pp. 1157–1159; June, 1955.) The introduction of Si as an activator into the core of an oxide cathode results in the formation of Ba_2SiO_4 at the interface between the core and the oxide layer. This has a detrimental effect on the life of the cathode, possibly because with the growth of the Ba_2SiO_4 layer the diffusion of activating atoms from the core into the oxide layer becomes progressively more difficult. To verify this, an investigation was carried out using tracer atoms; the results are discussed.

621.385.032.216 1915

D.C. and Pulsed Emission from L-Cathodes—I. Brodie. (*Proc. phys. Soc.*, vol. 68, pp. 1146–1148; December 1, 1955.) The difference between pulsed and dc emission from oxide cathodes [2091 and 3590 of 1949 (Wright)] is found also, to a lesser degree, in L-type cathodes and in these is considered to be due to partial removal of Ba from the cathode surface by positive-ion or gas bombardment.

621.385.032.216 1916

A New Pressed Dispenser Cathode—P. P. Coppola and R. C. Hughes. (PROC. IRE, vol. 44, pp. 351–359; March, 1956.) Description of the development of a moulded cathode consisting of CaBa aluminate dispersed in a porous matrix of W-Mo alloy. This type of cathode is suitable for operation in the temperature range 1,000–1,200°C., and has an emission density of 10 A/cm² and a lifetime >5,000 h at an operating temperature of 1,130°C.

621.385.2.032.216 1917

Effect of the Cathode Work Function on the Space-Charge-Limited Characteristics of Plane Diodes—C. R. Crowell. (*J. appl. Phys.*, vol. 27, p. 93; January, 1956). An extension of Ferris' work (2099 of 1949.) The diode characteristic is shown to be independent of the cathode work function until the current drawn is an appreciable fraction of the saturation current.

621.385.832:621.397.6 1918

Resolving Power of the Image Converter with Uniform Electrostatic and Magnetic Fields—G. Wendt. (*Ann. Radioélect.*, vol. 10, pp. 74–82; January, 1955.) A calculation is made of the electron density distribution in the image point, taking the initial Maxwellian velocity distribution into account. The results are extended to the image of a line and a pattern of lines, and are compared with observations. Using a television test pattern, a definition of 100 lines/mm has been obtained on a screen of diameter 50 mm with an anode voltage of only 5 kv.

621.385.832.001.4:621.317.3 1919

Testing Cathode-Ray Tubes—R. D. Nixon. (*Elect. J.*, vol. 155, pp. 2011–2012; December 16, 1955.) Brief details are given of life tests carried out by a manufacturer.

621.387 1920

Impedance-Frequency Characteristics of Some Glow-Discharge Tubes—F. A. Benson and G. Mayo. (*Electronic Engng.*, vol. 28, pp. 124–126; March, 1956.) Measurements in the frequency range 20 cps–50 kc show that in every case the impedance of the tube increases considerably with frequency. The importance of ion inertia effects is emphasized.

621.387 1921

Ignition Sensitivity and Ignition Delay Time of Gas-Filled Triodes and Tetrodes—E. Knoop. (*Z. angew. Phys.*, vol. 7, pp. 575–582; December, 1955.) Results of a theoretical and experimental investigation indicate that for good sensitivity the tube should be designed for a high geometrical penetration coefficient and the gas chosen should have a large ionization cross section at not too low a pressure and at high ion velocity. The parameters and processes determining the delay time are discussed; the occurrence of maximum values of delay time is explained in relation to the adequacy of the supply of ions in the grid-anode space

621.387:537.56 1922

The Gas-Multiplier: a New Type of Electron Multiplier—C. H. Vincent. (*Nature Lond.*, vol. 177, pp. 391–392; February 25, 1956.) A multistage device based on use of the Townsend electron avalanche process is described; multiplication by the α process is permitted, while the accompanying processes which cause positive feedback by releasing further electrons in the input region are restricted. The electrodes dividing the chamber into stages are plane, parallel and equally spaced, and have small holes in a central area. Conditions for operational stability are discussed.

MISCELLANEOUS

621.3:061.3 1923

1956 I.R.E. National Convention Program—(PROC. IRE, vol. 44, pp. 382–417; March, 1956.) Includes abstracts of the papers presented.

621.3.002.2 1924

Making Photo-etched Circuits in Your Workshop—R. H. Dorf. (*Radio-Electronics*, vol. 26, pp. 56–58; December, 1955, and vol. 27, pp. 139, 148; January, 1956.) Simple instructions are given for preparing the circuit drawing, making the negative, sensitizing the laminated panel, exposing the panel, developing the image, and etching.

621.37+621.396]:519.2 1925

Some Problems of Fluctuation in Radio—J. C. Simon. (*Ann. Radioélect.*, vol. 10, pp. 3–19; January, 1955.) Statistical methods for summing vectors with random phase angles are discussed and the concept of correlation function is introduced. The theory is applied to an examination of various problems including multiple reflections on a transmission line, radiation from a large number of sources, fluctuations of a radar echo, influence of phase errors on antenna characteristics.

621.37/.39].004.6 1926

Prediction of Electronic Equipment Reliability—V. Harris and M. M. Tall. (*Elect. Engng., N. Y.*, vol. 74, pp. 994–997; November, 1955.) A method is described based on failure data collected by the US Navy.

621.385.832.002.2:621.397.621.2 1927

The Television Cathode-Ray-Tube Factory at Ulm [W. Germany]—C. F. Hühn. (*Telefunken Ztg*, vol. 28, pp. 215–222; December, 1955. English summary, p. 264.) A plant completed in 1955 with a planned output of 50,000 picture tubes per month is described. Photographs and a flow chart are presented.